Beach Profile Analysis Along the Delaware Atlantic Coastline

by

Kirk F. Bosma

and

Robert A. Dalrymple

RESEARCH REPORT NO. CACR-97-05

June, 1997

Center for Applied Coastal Research
Ocean Engineering Laboratory
University of Delaware
Newark, DE 19716

This study was sponsored by the Delaware Department of Natural Resources and Environmental Control.

TABLE OF CONTENTS

LIST OF FIGURES

LIST OF TABLES

ABSTRACT

Anytime there is a transition, the probability of a unique, and sometimes violent, reaction greatly increases. Mixing, turbulence, chemical reactions, shear, and countless other reactions all occur in areas of transition. The transition between the land and sea is no exception. The coastal zone, the area which divides land from sea, creates an environment of unmatched physical processes, including waves, currents, and chaotic turbulence. At this active intersection, many large cities and civilizations developed because of the ease of establishing trade routes. The coastlines across the world provided an important resource for commercial advance. As civilizations evolved, the value of the coastline was magnified by increased trade, industry, recreation, and tourism. Naturally, the advances resulted in a increasingly important conflict between the natural coastline processes and shoreline development.

The on-going battle to preserve the existing structures and beach area requires a comprehensive understanding of the processes at the shoreline. One of the keys to understanding a specific coast is the nature of changes in the beach profile. Over time, fewer and fewer measures of beach behavior have been taken. Many extensive monitoring programs have been eliminated due to a lack of financial support. However, without the historic beach profiles of the world's coasts, coastal scientists and engineers would have no knowledge of the adjustment and trends of the profile changes. The purpose of this work is to illustrate the importance of the beach profile as a coastal engineering tool, investigate the information they furnish, and encourage continued measurements along the coasts of the world.

Beach profile measurements are utilized to examine various reaches along the Delaware Atlantic coast. Various tools, such as shoreline change, volume change, sand budget, and even-odd analysis, are applied to the beach profiles. In addition to the standard analysis techniques, a statistical model, labelled complex principal component analysis (CPCA), is developed. The model is able to identify moving features within the coastal geometry, such as a fast moving sand wave. CPCA extracts the moving feature from the mean and is capable of distinguishing its direction, speed, amplitude, and frequency. The model can be utilized in either two dimensions, evaluating a specific alongshore or cross shore line, or in three dimensions, evaluating a bathymetric area.

Following a brief discussion of relevant coastal processes, beach profiles of particular sections along the Atlantic coast of Delaware are examined. Results are presented for the regions directly north and south of Indian River Inlet, beach nourishment monitoring at Dewey and Bethany beaches, and a general analysis for the entire Atlantic coast.

Chapter 1

INTRODUCTION

The Delaware Atlantic coastline, a sandy shore that spans approximately 24 miles, is an area of constant transformation. Significant littoral drift rates, man-made structures, remediation efforts, and occasional battering by large storms all effect the coastline. Thus, the beach profiles are 'dynamic' in character, changing continuously in both time and space. These resulting profile variations occur in both the subaqueous and subaerial elements of each profile, as wave energies constantly move sand on, off, or alongshore. These changes in profiles can reveal a vast amount of information, both long and short term, about the coastline. The constant changes in beach orientation are indeed natural and present no problem to uninhabited coasts. However, when communities develop and expand along a shoreline, and fixed structures are introduced into the natural system, these beach transformations become a concern. New dangers emerge as sea levels rise, shorelines retreat, and storm surges and large waves reach out and threaten previously safe communities.

The Atlantic coast of Delaware, which is located entirely in Sussex county, stretches from Cape Henlopen in the north to the Delaware/Maryland border in the south, as shown in Figure 1.1. Communities extend along the entire coastline, many which base their existence on the livelihood that the beaches supply. Areas such as Dewey Beach, Rehoboth Beach, and Bethany Beach thrive due to the popularity of their beaches and the income that the beaches generate. Thus, it is of utmost importance that the beaches along the Delaware Atlantic coast remain intact.

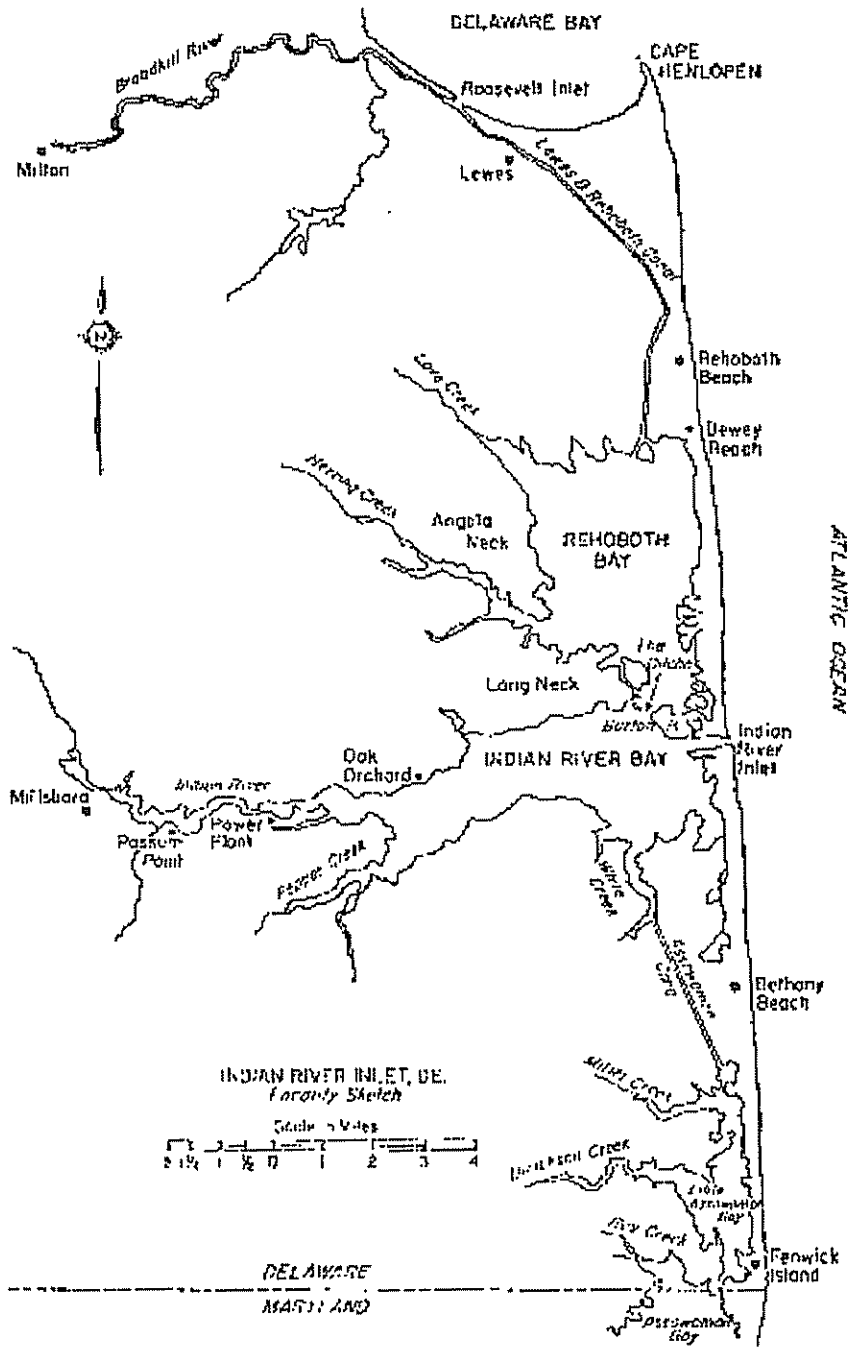

Figure 1.1: The Atlantic coast of Delaware (U.S. Army Corps of Engineers, 1996).

Most of the Delaware Atlantic coastline is in a state of erosion. Since 1972, the Department of Natural Resources and Environmental Control (DNREC), through its Beach Preservation Section, has had the responsibility for the enhancement, preservation, and protection of the beaches. DNREC attempts to control, repair, and prevent the beach erosion in a manner that is effective as well as both politically and economically sound. Various methods have been used by DNREC to stabilize the shoreline erosion; beach nourishments, dune stabilization, groins, and sand bypassing. DNREC has contracted with the Center for Applied Coastal Research to provide a comprehensive study of the entire Delaware Atlantic coastline (including i.e., sand bypassing performance, beach nourishment projects, shoreline changes, and volume changes). This report is the culmination of the study.

1.1 Previous Studies

Over the years, a number of studies and reports have been written describing various aspects of the Delaware coastline. Many of these studies and their results are referred to throughout this report. A description of some of the major studies is included in Table 1.1. Reports for the coast are not limited to these. There are numerous unpublished reports and documents as well as other various less related studies of the Delaware coast.

1.2 Project Purpose and Scope

The objective of the present study is to investigate many aspects of the beach profile through the use of the newest analytic methods and the most recent field data available. With the information that is extracted from profile surveying, an in-depth look is taken at the entire coastline. Although there are numerous previous studies, the data collected over the most recent decade has not been analyzed. First, a brief overview of the wave environment is presented. The study concentrates on how the profiles respond to an ever changing wave climate. Next, many unique areas along

the coast are focused upon. The study considers the effect of the jetty-stabilized Indian River Inlet on the coast, the performance of the sand bypassing plant, and the effectiveness of two of the major beach fill locations. Finally, the study undertakes a comprehensive exploration of the complete Atlantic coast of Delaware. For most of the areas, the study considers many standard analysis tools and also explores the use of a complex principal component analysis (CPCA), in both 2-mode and 3-mode versions, to evaluate propagating features that exist within the various bathymetries.

Table 1.1: Prior Studies and Reports

Report Title	Author	Date	Comments
Beach Erosion - Delaware Bay and Atlantic Ocean	Delaware State Highway Department	1956	25 year (1929-1954) averaged estimates of erosion based on plots of shoreline position.
Beach Erosion Control and Hurricane Protection along the Delaware Coast	U.S. Army Corps of Engineers	1968	Volumetric erosion calculations for the Delaware Atlantic coast using surveys from 1843-1964.
Coastal Engineering Assessment of Delaware's Beach Erosion	Dalrymple *et al.*	1976	Presents data from the 1956 State report and indicates that the area of highest erosion is at York Beach during 1929-1954.
Sediment Budget and Sand Bypassing System Parameters for Delaware's Atl. Coast	Coastal and Ocean Engineering and Research	1983	Average rate of change in sand volumes for the Delaware coast between 1964-1982. Depth of closure study.
Coastal Changes at Bethany Beach, Delaware	Dick and Dalrymple	1984	In-depth study of Bethany Beach, including EOF analysis.
A Coastal Engineering Assessment of Fenwick Island, DE.	Dalrymple and Mann	1985	Examines the erosion problems at Fenwick Island. Uses WIS data, EOF analysis & shoreline position.
Striking a Balance: A Guide to Coastal Process and Beach Management in DE.	Maurmeyer	1985	Considers general changes in the beach environment and the management aspects involved in retaining beaches.
A Probabilistic Prediction of Beach Nourishment Lifetime	Strine	1991	Examines the beach nourishment project in the early stages at Fenwick Island, DE.
Indian River Inlet and Bay	U.S. Army Corps of Engineers	1994	Study of Indian River Inlet, includes economic, engineering, and environmental aspects.
Rehoboth Beach/ Dewey Beach Interim Feasibility Study	U.S. Army Corps of Engineers	1996	Study to determine a solution to reduce storm damage for the beaches of Dewey and Rehoboth.

Chapter 2

RELEVANT COASTAL PROCESSES

The dimensions of a beach are in constant transition. Repeated measurements of the variations can give some indication of what is happening at the shoreline. The changes in beach profiles can be related to many factors, some of which are short-term, others long-term. This chapter takes a brief glance at some of the more important factors that contribute to these changes.

2.1 Relative Sea Level

Long-term coastal processes occur on the order of hundreds and thousands of years and are still active today (possibly to a greater or lesser extent). Although their effects may not be as apparent as other processes, an understanding of these forces that have shaped the shorelines is important. These "historic" phenomena provide a window to the past and a better comprehension of the characteristics of a particular section of shoreline.

Relative sea level change is a long-term on-going geological process that occurs due to either a change in the level of the sea or the subsidence or emergence of the land by geological processes. The factors that can effect sea level changes are numerous. The warming of the water, glacial melting, land movement, consolidation of the land, and a change in sediment supply can all effect the sea level. Since it is hard to determine which factor is causing rising (or sinking) with respect to the others, only the net change in sea level is important. Determining the historical relative sea level change is not an easy endeavor. Kraft and John (1976) use geological

evidence in the form of tidal marsh peat, among others, to determine historic sea levels. Utilizing radio-carbon dating, approximate dates of sea level elevation can be determined from old marshes originally formed at sea level. By matching the approximate date against the depth at which the sample was unearthed, a relative sea level rise curve was developed, as shown in Figure 2.1. The Delaware Atlantic coast is estimated to be sinking at approximately 1.0 foot per century and all evidence suggests that the trend will continue. As the sea continues to encroach upon the land, low-lying communities will experience increased flooding and damage from storm events.

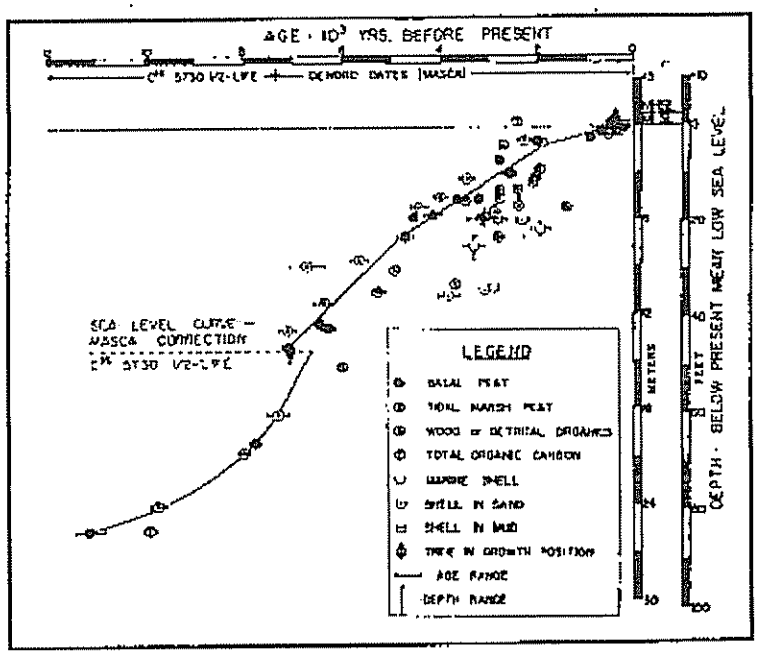

Figure 2.1: Relative sea level rise for the Delaware coast (Kraft and John, 1976).

2.2 Beach Migration

The relative sea level change causes the coast to re-adjust to the new sea level. Therefore, these processes can result in either erosion or accretion of the shoreline.

The Atlantic coast of Delaware lies within the geological province referred to as the Atlantic Coastal Plain province. The area is made up of essentially unconsolidated sediments and has both submerged (the continental shelf) and emerged sections, which are divided by the Atlantic coast. Most of this range of coast is characterized by the Atlantic barrier system, as shown in Figure 2.2. It is a continually transforming system of coastal marshes, tidal lagoons, and beach-dune complexes. The coastal barrier beach can be visualized as a constantly moving geomorphic form. As the sea level rises, the sandy beach of the ocean shore retreats and the shoreline must reform to a new equilibrium position. Hence, erosion occurs from the beach face and the eroded sediment is deposited landward across the barrier. The U.S. Army Corps of Engineers (1996) reports that this leading edge of marine transgression has advanced across approximately two-thirds of the Coastal Plain province in the past 15,000 years.

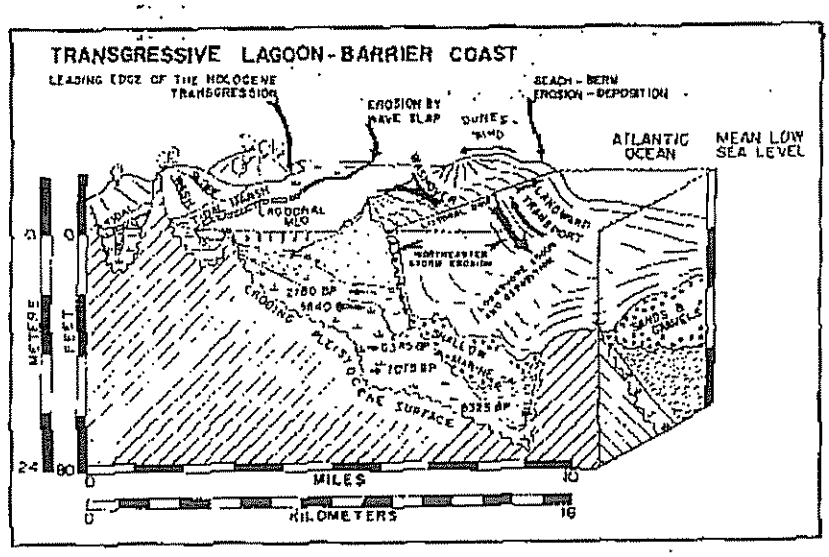

Figure 2.2: Transgressive Lagoon - Barrier Coast, adapted to the Delaware coast (Kraft and John, 1976).

In Delaware, the barrier beach migration usually occurs by the growth of flood tidal shoals or the overwash of storm waves transporting sand from the ocean side of the barrier. Inlets, including those no longer present, carry sediment from the ocean side of the barrier beach to the bay side. Marshes then grow on the tidal shoal sands and stabilize a new portion of the barrier system. Therefore, the land advances on the bay side while retreating on the ocean side. The barrier beach system can also migrate by overwash of large storm waves. During high storm events, like the northeaster of 1962, overwash transported a large quantity of sand across the land in the area north of Indian River Inlet. As stated above, most of the areas of the Delaware Atlantic coast are characterized by the barrier beach system. However, areas, such as Rehoboth and Bethany Beach, are beaches formed against headlands. Characterized by higher elevation and lack of lagoons, headland erosion occurs by sediment movement along and offshore, rather than by the overwash process.

2.3 Wave Environment

There are various factors that may influence the form of a beach profile: wind, sediment supply, and the influence of structures. No one factor, however (with the exception of gravity), is more dominant than the waves that constantly march against the coast. The energy they carry to the shoreline and the variety of currents and turbulence they generate play the leading role in the orientation of the beach. Waves produce both destructive and constructive factors when acting on the beach profile. For this reason, this section will briefly discuss the wave climate that exists in the Delaware region.

2.3.1 Wave Information Study

The Wave Information Study (WIS) provides the most accurate hindcast wave data for the Atlantic coast. The Coastal Engineering Research Center (CERC) developed the data base to accurately simulate nearshore wave conditions for specific

sites along the Atlantic coast. Though these are not actual measurements (and they do not include the effect of tropical storms), the simulation provides a large data set covering twenty years. Details on exactly how the data sets were generated can be found in Jensen (1983). Data are averaged over the twenty year interval (1956 to 1975) for the three relevant stations and presented in Table 2.1. A more complete description of the WIS wave data can be found in Dick and Dalrymple (1983) and Dalrymple and Mann (1985).

Table 2.1: Twenty-Year Averaged WIS Statistics

Station	Station 65	Station 66	Station 67
Location	Ocean City to Fenwick	Fenwick to Rehoboth	Rehoboth to Cape Henlopen
Mean Spectral Wave Height (m)	1.0	0.9	1.0
Mean Peak Period (sec)	6.4	6.1	6.6
St. Dev. of Wave Height (m)	0.6	0.6	0.6
St. Dev. of Wave Period (s)	2.6	2.5	2.5
Largest Mean Wave (m)	7.7	4.9	7.2

When waves attack the beach at an oblique angle, and they typically do, the erosional forces acting on the beach are composed of both cross-shore and longshore sediment transport. The on and offshore movement of sand is referred to as cross-shore sediment movement and is basically temporary (due to storms) or seasonal. Dick and Dalrymple (1983) found that for Delaware, during the winter seasons, the cross-shore transport is directed seaward. Conversely, in the summer and fall seasons, the cross-shore sediment transport is directed landward. The longshore sediment transport, or littoral drift, is the movement of sand along the beach. It is this transport that most significantly influences the amount of sediment entering or

leaving a given area. As expected, when the direction of wave approach varies, the direction of the littoral drift changes accordingly. Using the WIS data, Dalrymple and Mann (1985) presented potential net littoral drift values (shown in Table 2.2) for each WIS station.

Table 2.2: Potential Net Annual Sediment Transport for Delaware-Maryland Coast (Dalrymple and Mann, 1985)

Year	Station 65 (yd^3/yr)	Station 66 (yd^3/yr)	Station 67 (yd^3/yr)
1956	-63720	272426	1131544
1957	-113292	-40295	110485
1958	-176954	-450115	175900
1959	-172608	-175944	-43191
1960	-113479	67417	338391
1961	-96657	100242	245857
1962	-67646	584679	869985
1963	-130146	35547	153723
1964	-75295	-230978	229643
1965	-88862	83786	167369
1966	-191221	-20213	83561
1967	-47625	79274	143494
1968	-188871	44609	76025
1969	-119023	396041	798964
1970	-149771	-65215	187657
1971	-225432	-72666	134313
1972	-201196	126919	272020
1973	-420150	-160474	-210039
1974	-175128	-36368	-48388
1975	-243095	136825	666079
Mean	-153000	56900	274200
Standard Deviation	84530	217610	336178

Note: The negative sign (-) indicates littoral drift to the north.

Notice that the littoral drift values vary greatly from year to year. Since the values provided are only potential (remember WIS data is only an approximation

of the true wave climate), the actual value is of less importance than the amount of variance that is occurring from one year to the next. The fluctuations are so extreme, that for Stations 66 and 67 the standard deviations surpass the mean. The U.S. Army Corps (1996), using a 38 year WIS data set (1956-1993), also estimated littoral drift values for a stretch of Delaware's northern Atlantic coast. The results are calculated using a GENESIS support program, NSTRAN, and are limited by the use of one "representative" set of offshore wave conditions and one shoreline orientation. A summary of their results are shown in Table 2.3. The results are much higher than for other calculations of littoral drift in the area (approximately ten times higher!).

Table 2.3: Potential Sediment Transport Rates for Delaware Coast (U.S. Army Corps of Engineers, June 1996)

Year	North (yd^3/yr)	South (yd^3/yr)	Net (yd^3/yr)	Gross (yd^3/yr)
1956 - 1975	-470,900	115,100	-383,200	613,400
1976 - 1993	-1,215,100	167400	-1,051,100	1,382,500

Note: The negative sign (-) indicates littoral drift to the north.

It is important to remember that the basis for sediment transport along shorelines is still not fully developed. Even simple cases, such as the unidirectional sediment movement in rivers, are not completely quantifiable. Also, historical littoral drift values may or may not provide an indication of what can occur to a beach during any given year. The WIS data does not contain storm events, such as "northeasters," which are an important aspect of the environment of the Atlantic coast of Delaware. However, the results can provide a general idea of the direction of the moving sediment.

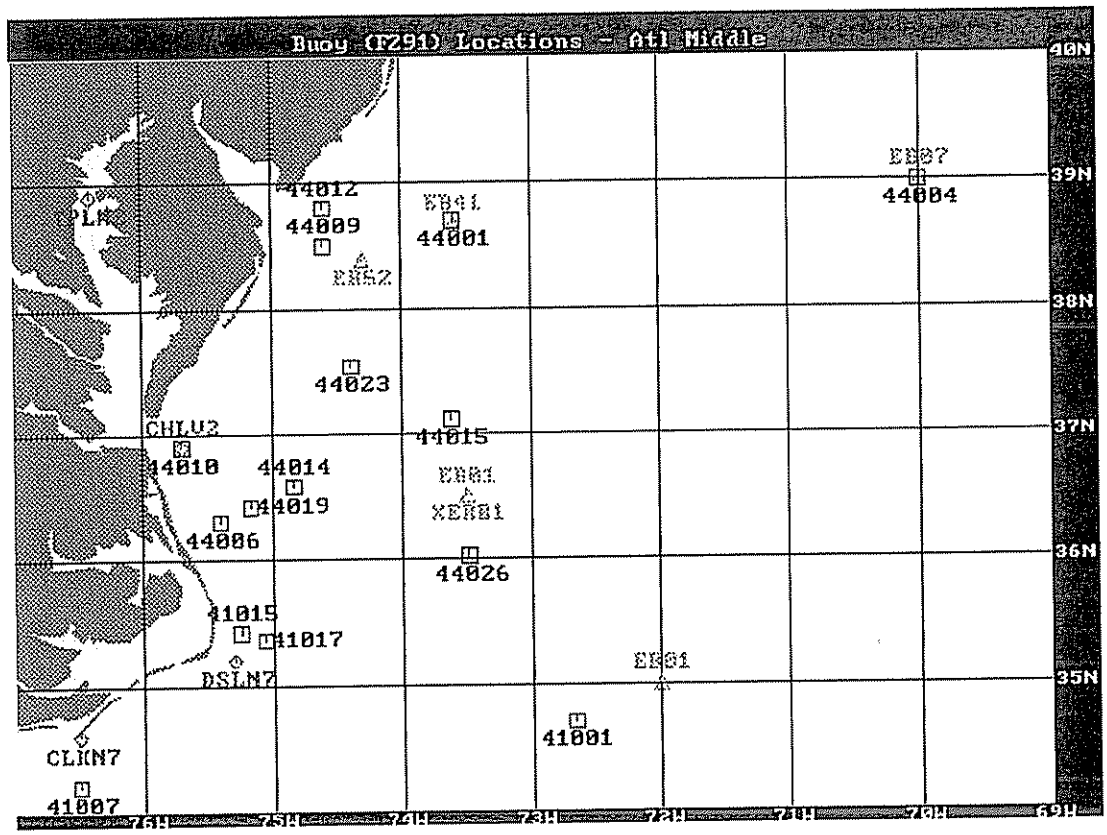

Figure 2.3: NOAA buoy locations in the Mid-Atlantic region (NOAA).

2.3.2 Offshore Buoy and Wave Gage Data

Recently, more field data have been collected in the Atlantic coast region. Although not as complete as the WIS data sets described in the previous section, the data are actual measurements of the wave climate, including storms. Wave data were recorded at three relevant locations along the Delaware coast. Waves at two sites (44009 and 44012, as shown in Figure 2.3) are measured by National Oceanic and Atmospheric Administration (NOAA) pitch and roll buoys. These buoys are located about 27 miles offshore, one in approximately 24 meters water depth and the other, about two miles south, in approximately 28 meters water depth. Buoy 44009 has gathered data from 1986 to 1994, while buoy 44012 has data from 1986

to 1992. A directional wave gage, installed by the U.S. Army Corps, was utilized at a third location to collect data from October of 1992 to May of 1995. The gage was located offshore of Dewey Beach in a water depth of approximately 10 meters. This section examines the basic statistical features of the wave climate for use in comparison of profile variations to extreme wave events and seasonal variability.

Daily and Monthly averages of significant wave height, dominant wave period, and wave power are computed at the three locations for all the available years. Wave power is determined by

$$P = \frac{1}{8} \rho \, g \, {H_s}^2 \, C_g \tag{2.1}$$

where: ρ = density of the water

g = gravity

H_s = significant wave height

C_g = group velocity

Figures 2.4 - 2.6 show the ensemble monthly mean and standard deviation results for buoy 44009, buoy 44012, and the Dewey Beach wave gage. Appendix A contains monthly time series for each year of data at all three locations.

Seasonal trends in the general wave climate are clearly exhibited in the figures. Significant wave height and wave power are larger during the late fall, winter, and early spring, whereas the dominant wave periods show no significant mean monthly variations. The significant wave height and wave power time series, as shown in Appendix A, are typically much less energetic in the summer months than at the other times throughout the year. The occurrence of random storms throughout the time series does lead to some interannual variations. The form of the data between locations is extremely consistent. All locations generally record the same increases in wave energy for active months. However, the Dewey Beach wave gage consistently experiences smaller significant wave height values than the offshore buoys. This is somewhat unexpected since the gauge is located in much

shallower water. Possible reasons for this occurrence are energy loss due to white capping, bottom friction, or, most likely, refraction effects. A basic summary of the wave climate, averaged over all locations and years, is provided in Table 2.4. There is a significant difference between the averaged statistical values in Table 2.4 and the averaged WIS statistics shown in Table 2.1. This is a direct result of the fact that the WIS data sets do not include storm episodes.

Table 2.4: Statistical Summary of Wave Climate

Season	Active May to Sep.	Mild Oct. to Apr.	Average
H_s (m)	1.287	0.978	1.158
T_p (sec)	8.793	8.667	8.741
St. Dev. of H_s (m)	0.198	0.130	0.170
St. Dev. of T_p (sec)	0.976	0.818	0.910

The most dominant features in the time series are the intermittent energetic months that occur during the active season. These extreme wave events (or months) are defined as periods when wave power exceeds approximately 40,000 Watts/m^2 and are listed in Table 2.5. Due to the aforementioned "gaps" in the data, the list may not include all extreme events during this time period. The occurrence of these events often result in important changes on the coastline.

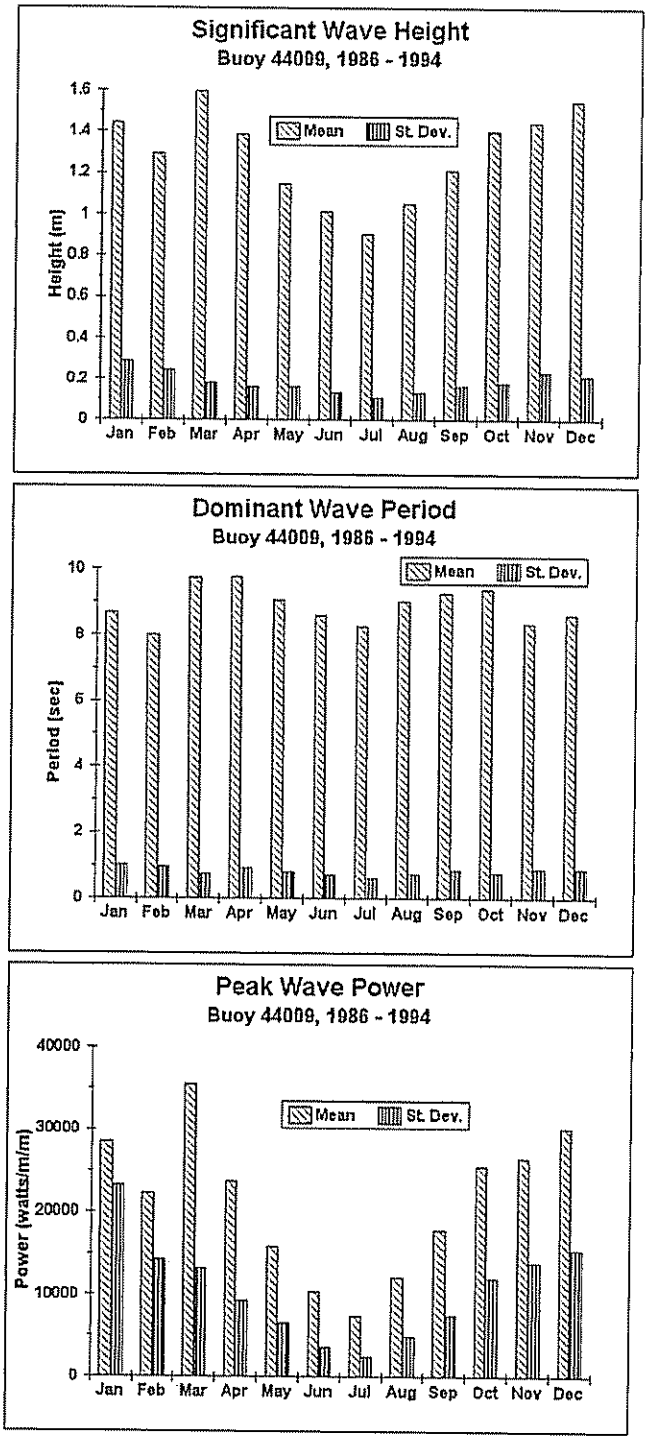

Figure 2.4: Histogram of monthly averaged mean and standard deviation offshore wave statistics for Buoy 44009: significant wave height (upper panel), dominant wave period (middle panel), and wave power (lower panel).

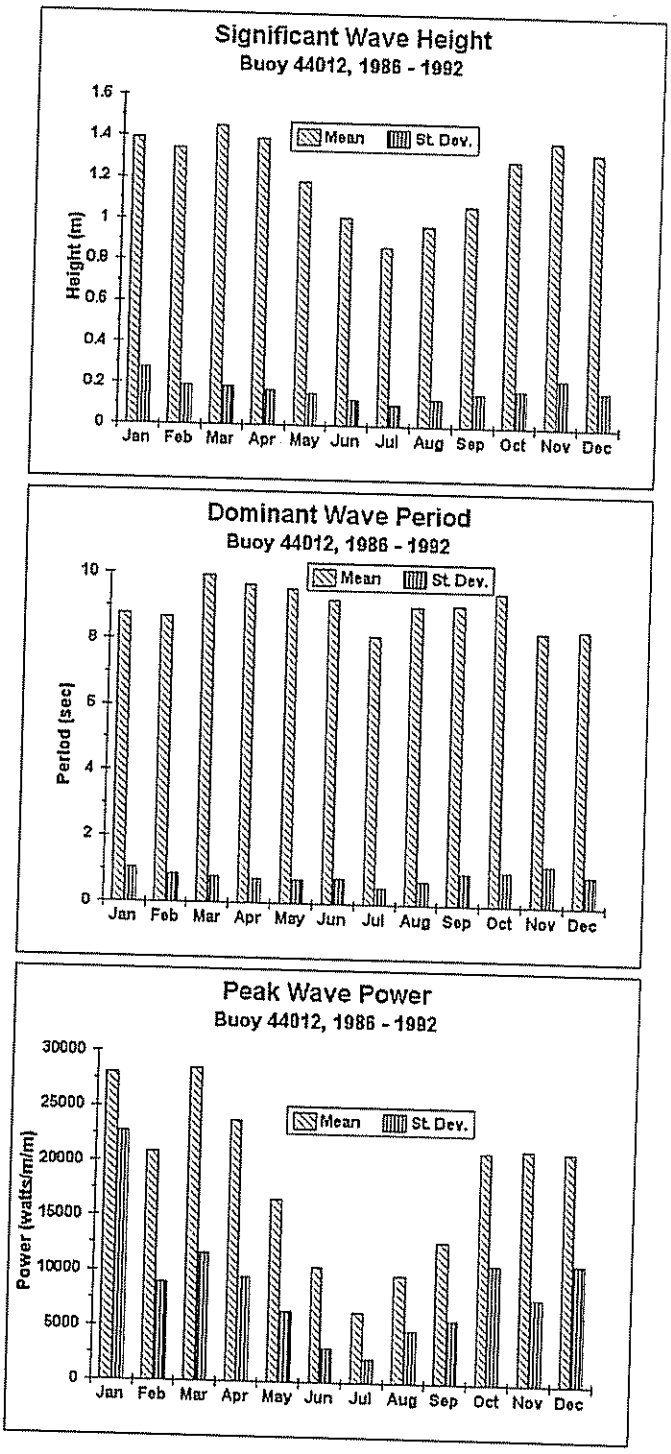

Figure 2.5: Histogram of monthly averaged mean and standard deviation offshore wave statistics for Buoy 44012: significant wave height (upper panel), dominant wave period (middle panel), and wave power (lower panel).

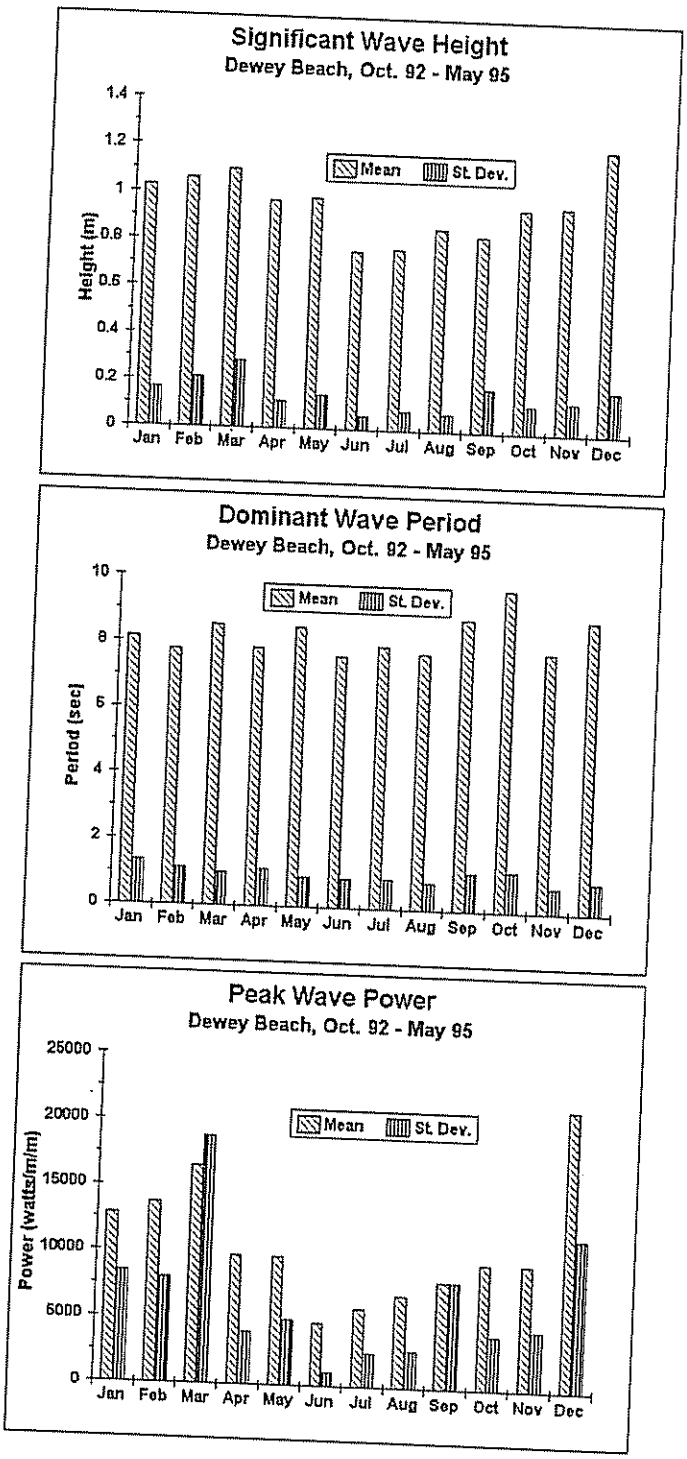

Figure 2.6: Histogram of monthly averaged mean and standard deviation offshore wave statistics for Dewey Beach wave gage: significant wave height (upper panel), dominant wave period (middle panel), and wave power (lower panel).

Table 2.5: Months with Extreme Wave Climates

Year	Month	Avg. H_s	Avg. T_p
1986	December	1.67	9.47
1987	January	1.70	8.10
	March	1.90	10.38
	April	1.86	10.16
1989	March	1.97	9.93
	September	1.76	10.59
1991	March	1.50	11.07
	October	1.71	10.66
1992	January	1.51	9.29
1994	November	1.79	8.58
	December	1.94	10.17

Chapter 3

COMPLEX PRINCIPAL COMPONENT ANALYSIS

This chapter investigates a powerful tool that can be applied to quantify changes in beach profiles. The chapter explores the development of principal component analysis (PCA), which is also referred to as empirical orthogonal function analysis (EOF), including the progression of the tool through 2-mode PCA, 2-mode complex principal component analysis (CPCA), and finally to a 3-mode model of both complex and non-complex varieties. Also, the theory behind both the 2-mode and 3-mode CPCA models is presented.

3.1 The History of Principal Component Analysis

Many geophysical phenomena derive from interactions between traveling waves of different spatial scales and temporal frequencies. Principal component analysis (PCA) was developed to explore these spatial and temporal relations with the primary advantage of its ability to express the complicated variability of data into the fewest possible number of modes. Thus, applying this idea to beach profiles, beach changes can be described by linear combinations of space and time functions through the breakdown of data into spatial and temporal dependence (e.g. Winant *et al.*, 1975; Aubrey, 1979). Winant *et al.* (1975) found that most of the variation in a profile configuration is accounted for by the first three eigenfunctions, which correspond to the "mean beach," "bar-berm," and "terrace" functions. PCA has also been used for determining cross-shore sediment movement by Medina *et al.* (1991). However, PCA detects standing oscillations only, such as the standing phenomena

of the shift from summer to winter profiles in seasonally sampled data (Winant *et al.*, 1975), not traveling waves. Therefore, PCA can not identify a coherent form moving through the data, such as a rapidly traveling bar as a sand wave alongshore.

Complex principal component analysis (CPCA) was developed for meteorological applications (e.g. Wallace and Dickinson, 1972; Barnett, 1983; Horel, 1984; Preisendorfer, 1988) and has been used to detect a fast moving sand bar by Liang and Seymour (1991). CPCA has also been shown to out-perform PCA by capturing more of the variance in fewer terms (Liang, White, and Seymour, 1992). CPCA has considerable potential for being widely used to detect propagating features, yet its use and possible limitations as an analysis technique have not been well explored.

Both of the methods discussed above account for only one spatial direction when evaluating the temporal changes in the data set. This assumes the movement is directed in one independent direction and therefore, the analysis is limited to looking at only individual cross-shore or alongshore "lines." However, what if there is two-dimensional movement of sand, as expected in response to a coastal structure or a beach nourishment? Then the two-dimensional analysis may be rendered inadequate. So, in a further expansion of PCA, the analysis was carried into a third dimension allowing the breakdown of data into three separate components. This so-called 3-mode PCA was started for mathematical psychology applications, such as the evaluation of multiple personality patients (Tucker, 1966; Kroonenberg and DeLeeuw, 1980). For the case of a coastal region, 3-mode PCA allows a bathymetric survey to be divided into two spatial directions (cross-shore and alongshore) and a temporal dependence. The technique was applied to a beach fill site in Spain by Medina *et al.* (1992) and the distribution of sediment by Losada *et al.* (1992).

In the next section, the 2-mode CPCA tool is explained and a 3-mode CPCA model is developed to examine movement occurring in multiple directions within a bathymetry. Through an example, CPCA is shown to not only detect moving forms

as well as standing forms, but also distinguish between them. In future chapters, both the 2-mode and 3-mode analysis are applied to specific bathymetries along the Delaware coast.

3.2 2-D Complex Principal Component Analysis

To apply CPCA, the data field, oriented so that each row of the data matrix represents a survey, must first be augmented in a manner such that propagating features within it may be detected. This is done by deriving a complex data matrix, where the real part is simply the original data field and the imaginary part is the Hilbert transform, which represents a filtering operation upon the data in which the amplitude of each spectral component is unchanged, but each component's phase is advanced by $\pi/2$. That is, if g(t) is a real-valued function of time, we can define an analytic function

$$z(t) = g(t) + ih(t) \tag{3.1}$$

where h(t) is the Hilbert transform of g(t) given as:

$$h(t) = \mathcal{H}(g(t)) = \frac{1}{\pi}\int_{-\infty}^{\infty}\frac{g(t')}{t-t'}dt' \tag{3.2}$$

This is usually implemented by applying the convolution theorem to arrive at

$$\mathcal{F}_h = \mathcal{F}_g\,\mathcal{F}\left(\frac{1}{\pi t}\right) \tag{3.3}$$

where F denotes the Fourier transform and

$$\mathcal{F}\left(\frac{1}{\pi t}\right) = -i\,\mathrm{sign}(\omega) = \begin{cases} -i & if\ \omega > 0 \\ i & if\ \omega < 0 \\ 0 & if\ \omega = 0 \end{cases} \tag{3.4}$$

Combining equation 3.3 and 3.4

$$\mathcal{F}_h = -i\,\mathrm{sign}(\omega)\mathcal{F}_g \tag{3.5}$$

for a two-sided frequency spectrum. Note that

$$-i\,\mathrm{sign}(\omega) = \begin{cases} e^{-i\pi/2} & if\ \omega > 0 \\ e^{i\pi/2} & if\ \omega < 0 \\ 0 & if\ \omega = 0 \end{cases} \tag{3.6}$$

which means that the Hilbert transform is equivalent to a phase shift of $\pm\ \pi/2$ in the Fourier domain.

From this point on, the analysis is exactly the same as standard PCA (although now with complex values). Using the complex data, we can compute complex eigenvectors (functional decompositions of the data) and eigenvalues (portions of the variation represented by each eigenvector). The goal is to expand the data, $z(x,t)$, into two dimensions (in this case offshore and time) as:

$$z(x,t) = \sum_{j=1}^{n} a_j\ g_j(t)\ e_j(x) \tag{3.7}$$

n=number of desired modes

a_j=normalizing factors

g_j=temporal eigenfunctions

e_j=spatial eigenfunctions

The normalizing factors are computed as:

$$a_j = (\lambda_j\ n_x\ n_t)^{1/2} \tag{3.8}$$

λ_j=the eigenvalue associated with the $j'th$ eigenfunction

n_x=the number of offshore grid points

n_t=the number of surveys used in the expansion

Expanding the data in this manner, it is evident that an infinite number of sets could be generated; for example, the usual Fourier series:

$$e(x)_j = \exp(2\pi i\ j\ x/L) \tag{3.9}$$

However, the strength of PCA is that a set of empirical eigenfunctions is selected so that the data is best fit in a least squares manner. This is done through computation of the correlation between the spatial locations to develop a complex correlation matrix as:

$$A_{ij} = \langle\, z(j,t)^* \cdot z(i,t) \,\rangle_{n_t} \tag{3.10}$$

where n_t is the total number of surveys and the large brackets denote a time average. The eigenvalues and eigenvectors are then determined from the complex correlation matrix, as could be done for any square matrix by:

$$A\ e(x)_j = \lambda_j\ e(x)_j \tag{3.11}$$

Similarly, we can define a complex correlation matrix between the temporal points as:

$$B_{ij} = \langle\, z(x,j)^* \cdot z(x,i) \,\rangle_{n_x} \tag{3.12}$$

where n_x is the number of offshore grid points. Again, as before, the eigenvalues and eigenfunctions are then determined from the square matrix. It should be noted that as an alternative, the normalized temporal eigenfunctions, $a_j\ g_j(t)$, can be computed by taking the dot product of the spatial eigenfunctions and the original data matrix.

3.2.1 Spatial and Temporal Phase Functions

As mentioned, the 2-mode CPCA has the ability to determine not only the standing phenomena (as standard PCA), but also moving features in the data set. Once the eigenvectors and eigenvalues have been determined, we are able to define both a spatial ($\theta_i(x)$) and temporal ($\phi_i(t)$) phase function as:

$$\theta_i(x) = \arctan\left[\frac{\mathcal{I}m(e_i(x))}{\mathcal{R}e(e_i(x))}\right] \qquad \phi_i(t) = \arctan\left[\frac{\mathcal{I}m(g_i(t))}{\mathcal{R}e(g_i(t))}\right] \tag{3.13}$$

These measures are no longer restricted to values between 0 and π as in standard PCA, but are now allowed to vary continuously between 0 and 2π. The spatial

derivative of the spatial phase function then provides a measure of the "local" wavenumber. Similarly, the time derivative of the temporal phase function is directly proportional to the "instantaneous" frequency. Therefore, CPCA not only allows us to identify a moving form, but also determine the direction, the frequency, and the rate at which it is moving.

3.2.2 Example of 2-D CPCA

To further clarify the application of CPCA, a brief example is presented in this section. Consider a progressive wave combined with a small amplitude standing wave as:

$$\eta = \cos\ \frac{\pi}{10}(x - 2t) + \frac{1}{10}\ \cos\left(\frac{\pi}{5}x\right)\ \sin\left(\frac{2\pi}{5}t\right) \tag{3.14}$$

The first three spatial eigenvectors from CPCA are shown in Figure 3.2.2. Each eigenvector is plotted in vector format where the real portion (magnitude) is indicated in the vertical direction and the imaginary portion (phase) is indicated in the horizontal direction. The numbers located next to each component correspond to the percent of variance explained by that eigenvector. The top panel shows the first eigenvector, which identifies the progressive wave and accounts for 99.4% of the total variance. The total variance is defined as the sum of all the eigenvalues,

$$\sigma = \sum_{j=1}^{n} \lambda_j \tag{3.15}$$

λ_j=the eigenvalue associated with the $j'th$ eigenfunction

n=the number of modes

σ=the total variance

Although somewhat difficult to see in this plot, the vectors are actually "spinning" and illustrate a progressive movement. Imagine the movement as a spinning motion indicated by the vectors "rotating" through space. The second eigenvector, shown in the middle panel, identifies the smaller amplitude standing wave and captures

0.5% of the variance. A standing feature is illustrated by all real values (or vectors that are all in the vertical direction). The example shows the ability of CPCA to separate the stationary motion from the progressive feature. The third eigenvector also detects a progressive feature, but since the amplitude and percent variance is so small this can be considered statistical noise.

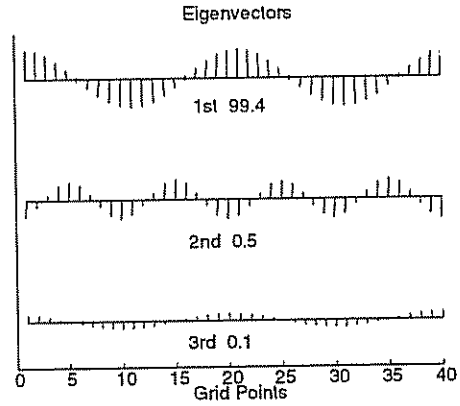

Figure 3.1: Example spatial eigenvectors for data generated by equation 3.14.

The spatial and temporal phase functions for the example are shown in Figure 3.2. The spatial phase function for the first component (solid line) correctly identifies the wavenumber of the progressive movement as $\pi/10$. What is the stair-stepping illustrated by the second component (dashed line)? Recall that a standing wave has no imaginary part. Therefore, the spatial phase function simply "jumps" in steps of π. The temporal phase function for the first component (solid line) also correctly produces the frequency of the progressive feature as $\pi/5$. The speed of the moving feature can then be calculated as

$$c = \frac{\sigma}{k} = \frac{0.6307}{0.3142} = 2.007 \text{ time steps/grid point}$$

which corresponds almost perfectly to the speed specified in Equation 3.14!

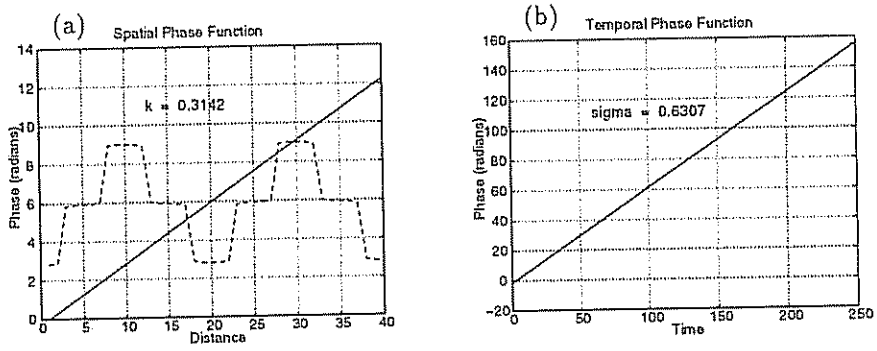

Figure 3.2: (a) Example spatial phase functions for data generated by Equation 3.14. The solid and dashed lines represent the spatial phase function for the first and second eigenvectors, respectively. The number indicates the wavenumber for the first component, which is approximately equal to $\pi/10$. (b) Example temporal phase functions for data generated by Equation 3.14. The solid line represents the temporal phase function for the first eigenvector. Since no movement is associated with the second and third eigenvectors, their corresponding functions are not shown. The number indicates the frequency for the first component, which is approximately equal to $\pi/5$.

3.3 3-D Complex Principal Component Analysis

The 2-mode CPCA appears to be very useful for many cases. However, as mentioned earlier, what if 2-dimensional movement of sediment is expected? In 3-mode CPCA, we begin with a set of data matrices or rather, a large 3 by 3 cube of data, which can be thought of as a collection of 2-mode matrices (Figure 3.3).

Again, after Hilbert transforming the data in time to generate a complex data set, we seek to expand the data in two spatial dimensions and time by:

$$z(x,y,t) = \sum_{m=1}^{s} \sum_{p=1}^{u} \sum_{q=1}^{v} e_m(x)\, f_p(y)\, g_q(t)\, C_{mpq} \tag{3.16}$$

s,u,v are the number of components in the 3 modes, respectively

e,f,g are the offshore, alongshore, and temporal eigenfunctions, and

C_{mpq} is the core matrix (normalizing factors)

As was the case with 2-mode analysis, the following analysis is similar to 3-mode PCA, with the exception that all variables are now complex. Rewriting equation 3.16 in matrix form we arrive at

$$Z(x \times yt) = E(x \times s)C(s \times uv)[F(y \times u)' \otimes G(t \times v)'] \tag{3.17}$$

where $\otimes$ denotes the Kronecker product and the dimension of the matrices Z and C are augmented to be two dimensional arrays. The core matrix, C, is no longer a simple diagonal matrix of eigenvalues as in 2-mode analysis, but a complex combination of elements that describe the basic relations that exist between the various collections of variables as expressed through their components (Kroonenberg and DeLeeuw, 1980).

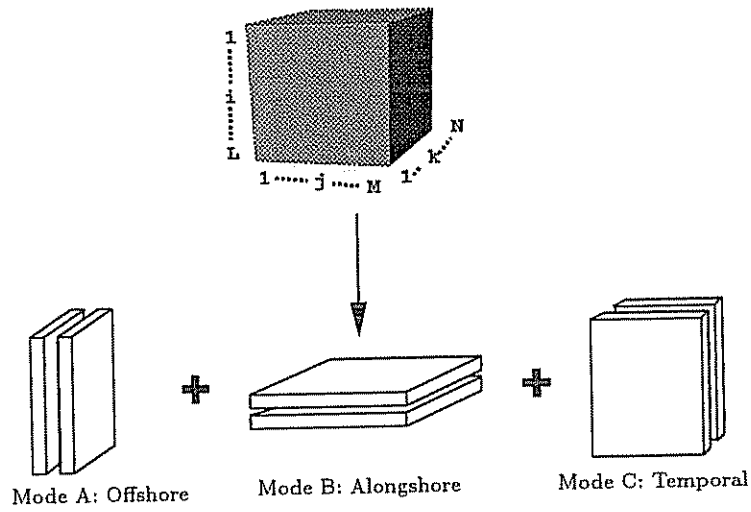

Figure 3.3: Schematic breakdown of a 3-mode data set into 2-mode submatrices.

The next step is to find E, F, G, and C such that the difference between the model and the data is minimized according to a mean squared loss function,

$$f(E, F, G, C) = \|Z - \tilde{Z}\|^2 = \|Z - EC(F' \otimes G')\|^2 \tag{3.18}$$

where the $\|\cdot\|$ denotes the Euclidean norm and $\tilde{Z}$ is an approximate factorization of the data based on the model. The restriction of this minimization problem is that E, F, and G must be columnwise orthonormal matrices. This minimization problem, along with the constraints, must be reduced before it can readily be solved (a brief summary of the reduction is shown here, for a complete proof see Kroonenberg and DeLeeuw, 1980). There is always some E, F, G, and C such that the function attains a global minimum. In fact, there exists a unique best C, called $\tilde{C}$, which for a fixed E, F, and G, minimizes the function, f.

$$\tilde{C} = E'Z(F \otimes G) \tag{3.19}$$

Thus, once we have E, F, and G, we can reconstruct $\tilde{C}$. Substituting Equation 3.19 into 3.18 and calling the rewritten function g, we attain

$$\begin{aligned} g(E,F,G) &= \|Z - EE'Z(F \otimes G)(F' \otimes G')\|^2 \\ &= \|Z - EE'Z(FF' \otimes GG')\|^2 \end{aligned} \tag{3.20}$$

In order to find the solution to this minimization problem, it is converted into a maximization problem by using traces (tr) instead of norms. Manipulating the terms to some degree we arrive at

$$\begin{aligned} g(E,F,G) &= \text{tr}[ZZ'] - 2\,\text{tr}[EE'Z(FF' \otimes GG')]Z' + \text{tr}[E'Z(FF' \otimes GG')Z'E] \\ &= \text{tr}[ZZ'] - \text{tr}[E'Z(FF' \otimes GG')Z'E] \end{aligned} \tag{3.21}$$

If we then define the function p as the the term on the right hand side of equation 3.21,

$$p(E,F,G) = \text{tr}[E'[Z(FF' \otimes GG')Z']E] \tag{3.22}$$

then clearly minimizing g is the same as maximizing p since both are bounded. Breaking down p a bit further;

$$p(E,F,G) = E'PE \tag{3.23}$$

where P is defined as

$$P(F,G) = Z(FF' \otimes GG')Z' \tag{3.24}$$

and contains the eigenvectors of E. Of course, we could also switch the variables in the Kronecker product term to obtain the eigenvectors of F and G.

$$Q(E,F,G) = \text{tr}[\text{F}'\text{QF}] \quad \text{Q(E, G)} = \text{Z(GG}' \otimes \text{EE}')\text{Z}' \tag{3.25}$$

$$R(E,F,G) = \text{tr}[\text{G}'\text{RG}] \quad \text{R(E, F)} = \text{Z(EE}' \otimes \text{FF}')\text{Z}' \tag{3.26}$$

where E is the eigenvector of matrix P, F of Q, and G of R. Therefore, we must solve these three equations simultaneously for E, F, and G in an iterative manner and then go back to solve C. This is done by utilizing the Bauer-Rutishauser method, an iterative scheme for solving eigenfunctions (Kroonenberg and DeLeeuw, 1980; Kroonenberg, 1985). This study uses the TUCKALS3 (Kroonenberg, 1985) computer program and modifies it to create a three-mode CPCA model.

Chapter 4

INDIAN RIVER INLET

The focus of this chapter is the profiles adjoining Indian River Inlet (as shown in Figure 4.1), which is one of the most unique features along the Atlantic coast of Delaware. After several failed attempts to keep Indian River Inlet open by dredging alone, a 500 foot wide inlet was constructed in the late 1930's. The goals were to establish a stable passage way from the inner bays (Rehoboth and Indian River) to the Atlantic Ocean, increase bay salinity, reduce stagnation, and increase the tide range (Thompson and Dalrymple, 1976).

The 500 foot wide inlet is stabilized by two parallel rubble mound jetties, originally extending a distance of 1550 feet (Figure 4.2). At the time of construction, 600 feet of this length extended seaward of the ocean shoreline. Significant problems with the engineered inlet have occurred over the years, including erosion of channel banks west of the jetties, accelerated scour along the jetties, and massive downdrift erosion, due to the predominant northward drift (Gebert *et al.*, 1992). The main concern related to the downdrift erosion is the threat it poses to the Route 1 highway located parallel to the shoreline. In fact, by 1954, a dune scarp had been created that was, in places, less than 200 feet from the roadway. From 1957 to 1990, mitigation of the beach erosion was accomplished by dredging of the inlet's flood tidal shoal and back barrier deposits. Close to 50,000 yd^3 of sand was placed on the north beach approximately every five years. Since February of 1990, however, a fixed sand bypassing system was constructed to pump sand from the southern shore and "slurry" it across the inlet to the northern shore.

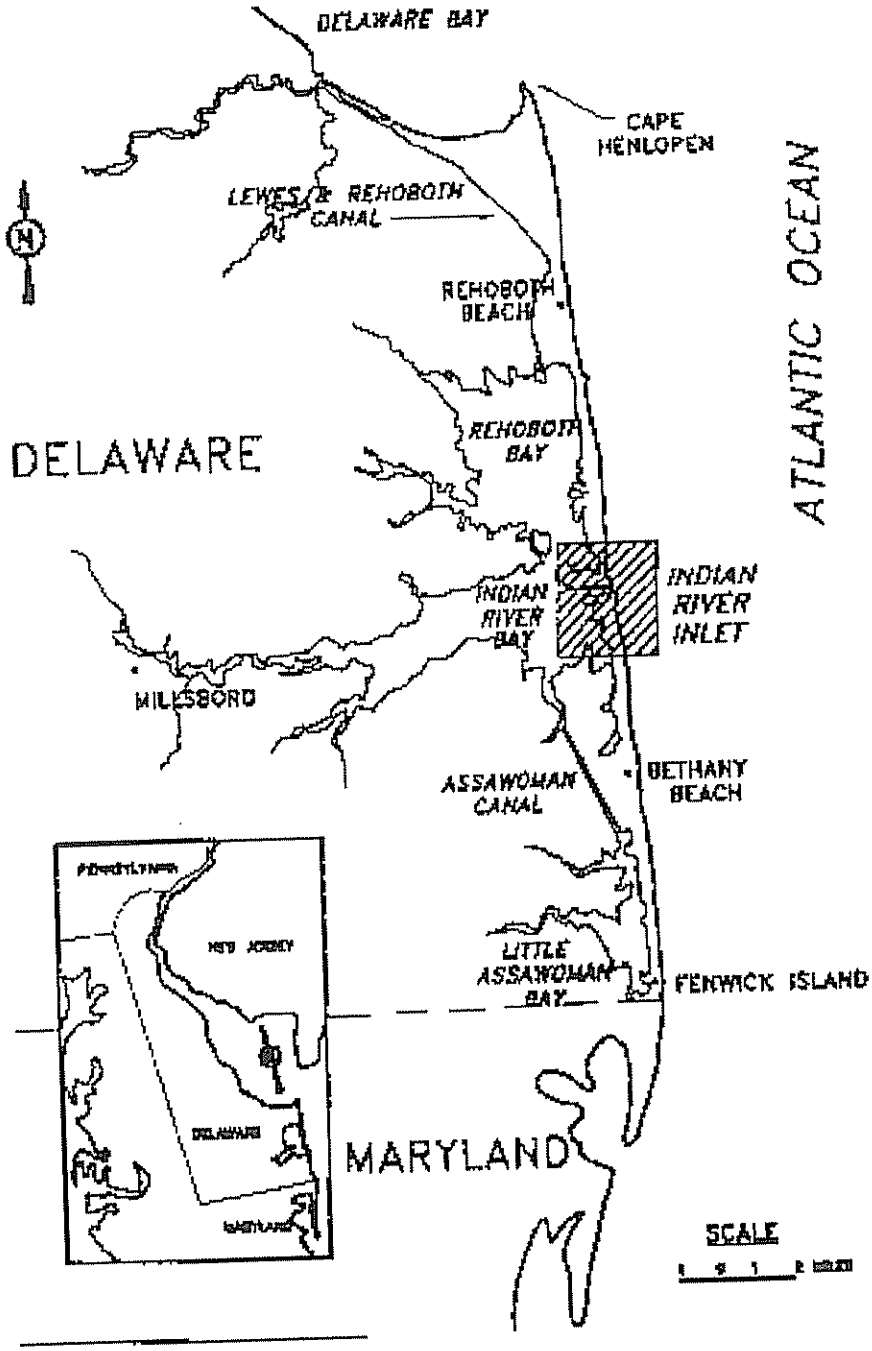

Figure 4.1: Location of Indian River Inlet on the Atlantic Coast of Delaware (U.S. Army Corps of Engineers, 1996).

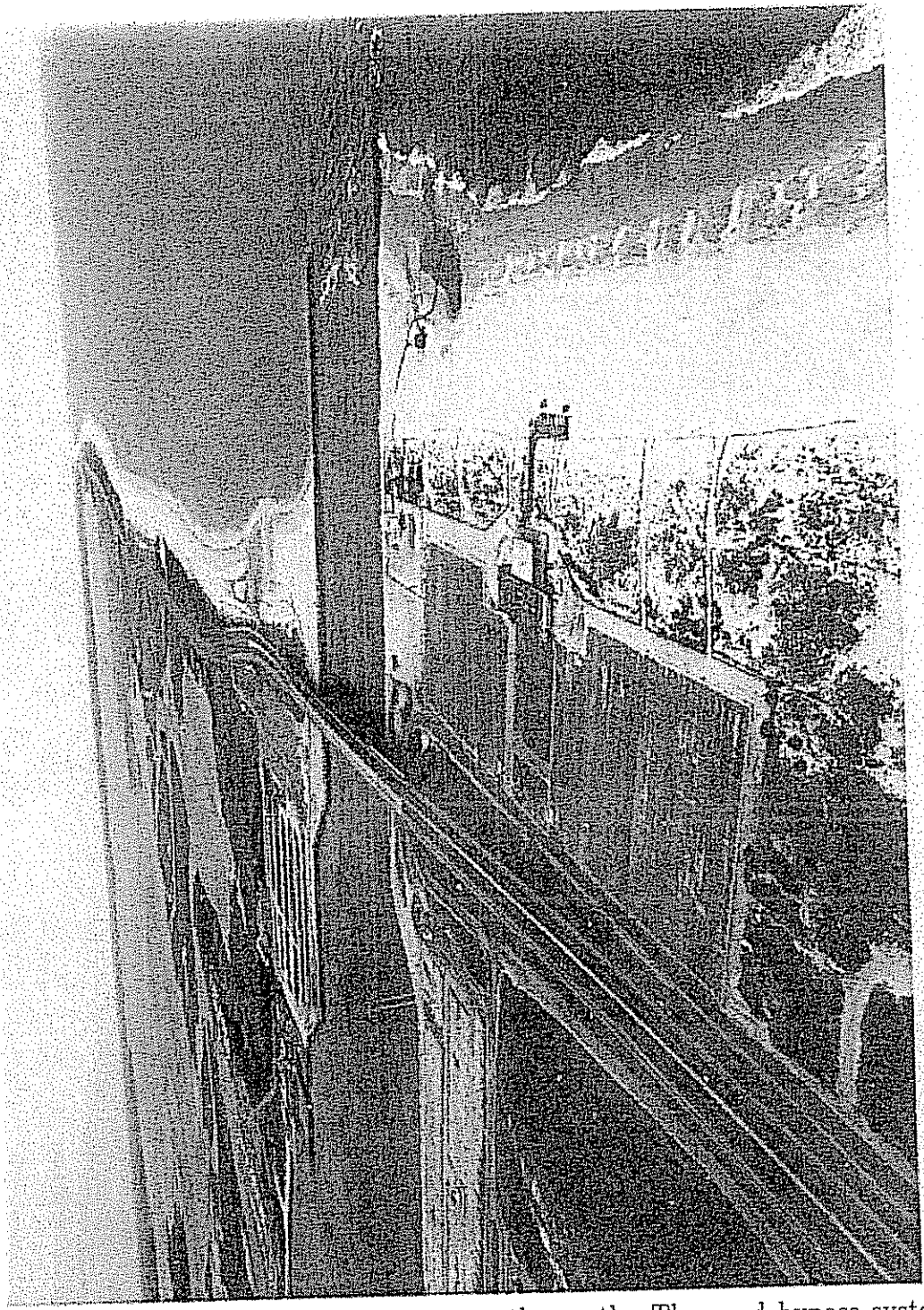

Figure 4.2: Indian River Inlet looking to the north. The sand bypass system is shown excavating a hole in the south fillet and discharging sand on the north side. (U.S. Army Corps of Engineers, 1996).

The system mines the updrift accretional fill by using an eduction unit deployed by a crane. Details on the system can be found in Clausner *et al.* (1992). Through May of 1995, approximately 456,000 yd^3 has been pumped across the inlet at a cost of \$1.62 per yd^3. Although the design rate of 100,000 yd^3/yr is not always attained, the system is performing well and is relatively inexpensive to run. The objective of the present section is to investigate many aspects of the beach profile at Indian River Inlet through the use of the most recent field data available. By using the profiles north and south of the inlet, we attempt to answer questions such as:

- What happens to the bypassed sand?
- Is enough sand being pumped?
- Can we identify moving forms or sand waves?

4.1 Field Data

Profile data sets for both the north and south side of Indian River Inlet have been collected by the U.S. Army Corps of Engineers, Philadelphia District. The profiling period spans from 1984 to 1994, with an average of two surveys per year. The survey dates and nomenclature are presented in Table 4.1.

A total of 28 profile lines were measured in the range from 5000 feet south of the inlet to 5000 feet north of the inlet, as shown in Figure 4.3. The northern portion of the study area contains 17 lines, while 11 are located in the south. As shown in Figure 4.3, some profile lines extend far offshore, while others only advance to the water line. The station numbers represent the distance in hundreds of feet from the respective jetty centerline (i.e. station 1+00N is 100 feet north of the northern jetty's centerline). Survey points were taken randomly during each survey, thus requiring linear interpolation in both the alongshore and cross-shore directions for much of the analysis. Examples of bathymetries north and south of the inlet are shown in Figure 4.4. The northern bathymetry reveals heavy erosion near the

Table 4.1: Survey Dates for Indian River Inlet

Survey Label	Date	Survey Label	Date
10	11/29/84	120	10/12/89
20	3/7/85	130	3/10/90
30	8/13/85	140	8/7/90
40	10/9/85	150	2/28/91
50	3/6/86	160	9/18/91
60	9/17/86	161	11/5/91
70	2/11/87	162	1/15/92
80	9/15/87	170	10/13/92
90	3/8/88	180	4/3/93
100	9/14/88	190	10/23/94
110	4/18/89		

shore as well as a scour hole that developed near the tip of the jetty. The remaining interpolated bathymetric surveys are presented in Appendix B.

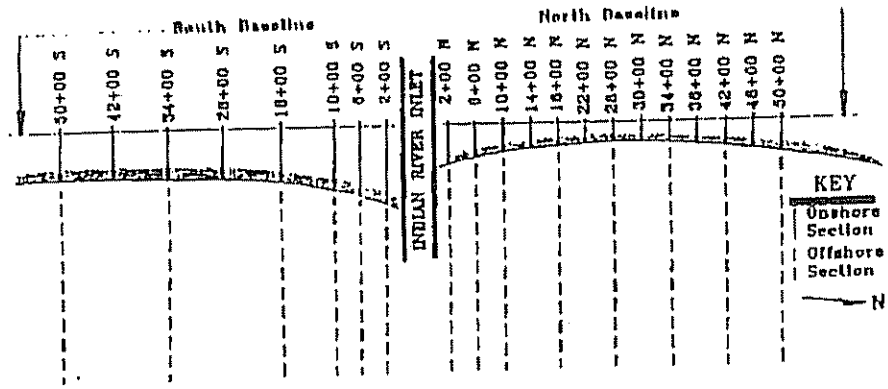

Figure 4.3: Profile lines north and south of Indian River Inlet

4.2 Shoreline Change

The simplest way to examine what is occurring in a given region along the coast is to evaluate the change in shoreline position. This 1-line analysis quantifies

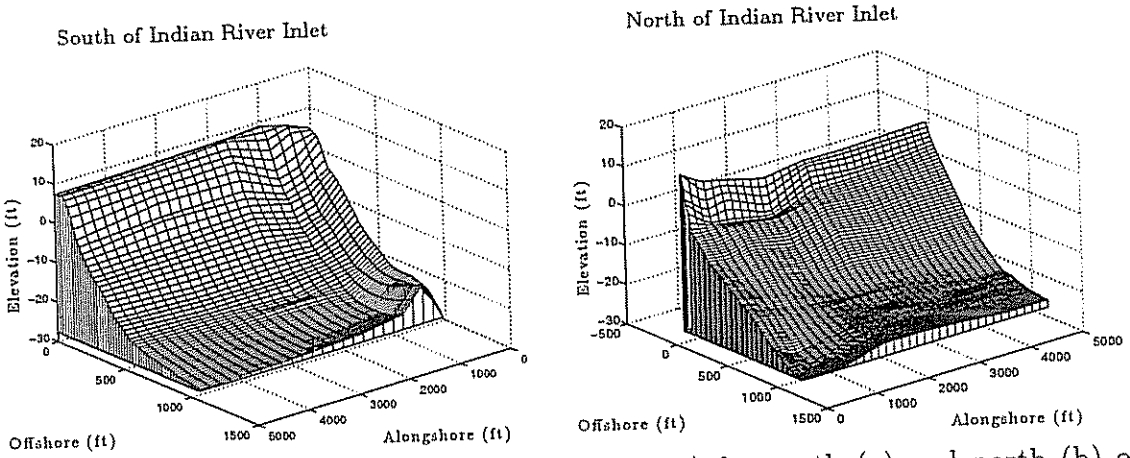

Figure 4.4: Sample bathymetries (October 1994) for south (a) and north (b) of Indian River Inlet.

beach behavior and allows for comparison of pre- and post-bypassing. The cumulative shoreline change plots for the four profile stations extending up to 1000 feet away from the inlet in both directions are shown in Figure 4.5. Similar plots for the profile stations ranging from 1800 to 5000 feet from the inlet are shown in Figure 4.6. The figures illustrate the shoreline behavior through time at the various stations. Watson *et al.* (1993) have computed similar results for a shorter interval of time. For this study, the pre-bypassing interval is from November 1984 to October 1989. The initial survey of November 1984 takes place after a large beach nourishment of 35,781 m^3 was placed between stations 0+00N to 30+00N. Surveys measured after October 1989 are considered post-bypassing. Since a minimal amount of data is available after bypassing initiation (four years), only the short-term performance of the system can be determined.

North of the inlet, the trend was progressive retreat, as expected due to the influence of the inlet and the northward littoral drift. Only once, during the winter season from September 1987 to March 1988, did a substantial shoreline advance occur. This is most likely due to the net reversal of littoral drift in the winter months (response to "northeasters") resulting in the impoundment of some sediment due to

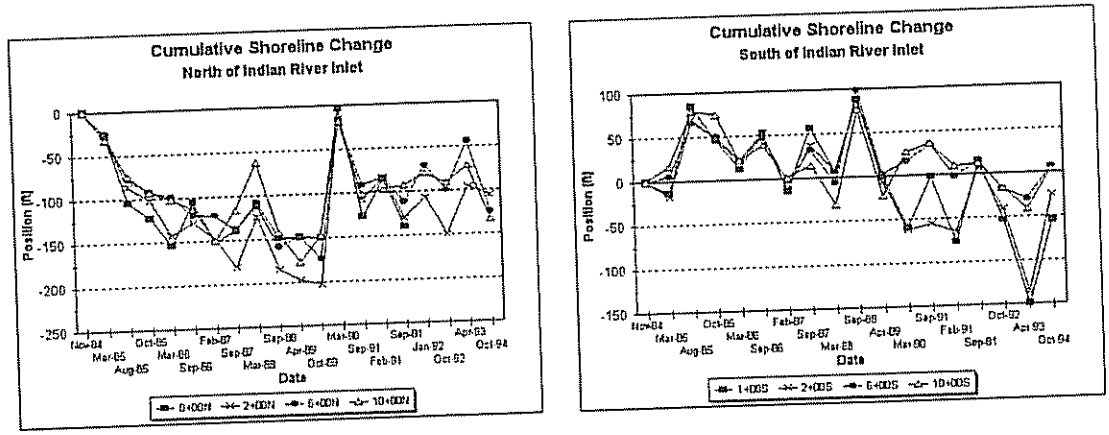

Figure 4.5: Cumulative shoreline for the first four profile stations both north and south of Indian River Inlet. Shoreline positions are shown relative to the shoreline position of November of 1984 for each station.

the southerly drift. The general shoreline retreat was evident until approximately 3400 feet from the jetty, as seen in Figure 4.6. At this distance, the effect of the inlet was lessened and larger seasonal variations tend to dominate. The bypassing operation was started with the aid of a 175,000 yd^3 fill (evident in the March 1990 survey) obtained from the flood shoal. The initial increase in beach width was not retained due to the spreading of the nourishment, but the shoreline for the stations just north of the inlet seem to have stabilized since bypassing initiation.

South of the inlet, pre-bypassing, the trend had been overall stability with some slight accretion. The accretion, if any, was at a much lower rate than the erosion to the north. Again, at around 3400 feet, the effect of the inlet seemed to be minimized as the overall change in beach width is small. After bypassing start-up, Stations 1+00S and 2+00S exhibited immediate effects of the sand mining. Proceeding southward, the next two stations (6+00S and 10+00S) showed a slight lag in the response to the mining and a smaller shoreline retreat. Notice as well that all stations recovered quickly from the effect of the mining. Sand bypassing influence was also typically seen to about 3400 feet south of the inlet. Therefore,

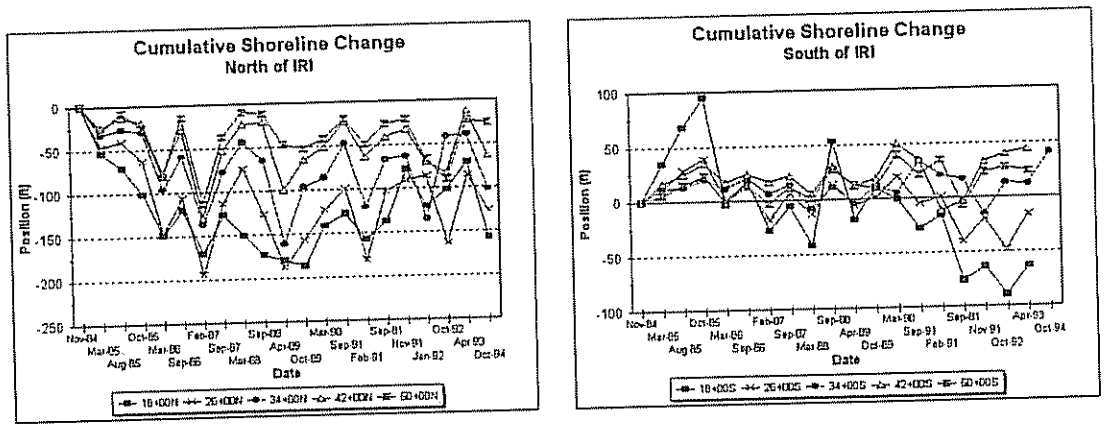

Figure 4.6: Cumulative shoreline plots for stations ranging 1800 to 5000 feet both north and south of Indian River Inlet. Shoreline positions are shown relative to the shoreline position of November of 1984 for each station.

it is reasonable to assume the effect of the inlet, as well as the bypassing system, extends approximately 3,500 feet in both directions.

4.3 Even-Odd Analysis

Another method to determine the effects of a coastal structure is called even-odd analysis (Berek and Dean, 1982). The goal of the analysis is to separate out the shoreline changes that are uniform along a coastline (the even function) from those that are due to a coastal structure or inlet (the odd function). The procedure can be applied to either shoreline or volumetric changes and separates them into a even and odd function about the alongshore origin of the structure or inlet. In this section, even-odd analysis is applied to the shoreline changes (Δs) centered around Indian River Inlet. The even function (Δs_e) can be interpreted as the background erosion or accretion which would be present in the absence of the inlet. The odd function (Δs_o) is then interpreted as the shoreline change which is attributed to the inlet alone. Defining y in the alongshore direction we have,

$$\Delta s(y) = \Delta s_e(y) + \Delta s_o(y) \tag{4.1}$$

and for negative values of y

$$\Delta s(-y) = \Delta s_e(-y) + \Delta s_o(-y) \tag{4.2}$$

Solving equations 4.1 and 4.2 produces the formulae for the even and odd functions

$$\Delta s_e(y) = \frac{1}{2}(\Delta s(y) + \Delta s(-y)) \tag{4.3}$$

$$\Delta s_o(y) = \frac{1}{2}(\Delta s(y) - \Delta s(-y)) \tag{4.4}$$

where the even function is symmetric about the alongshore direction and the odd function is anti-symmetric.

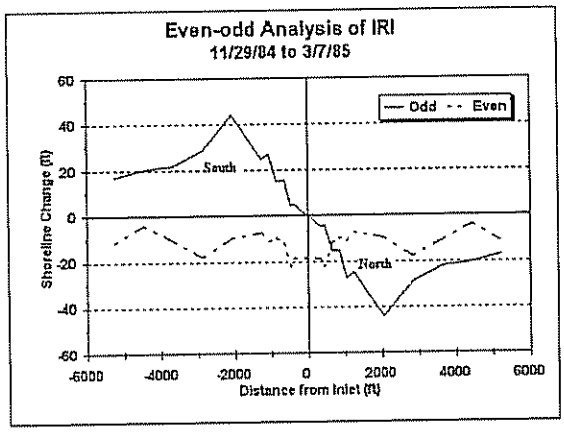

Figure 4.7: Even-odd analysis of Indian River Inlet during the winter season.

Figure 4.7 shows the results for the even-odd analysis for a period over the winter season, while Figure 4.8 shows the results for a period over the summer season. Both the time periods take place before bypassing was implemented. During the winter season the even function shows background erosion, while during the summer season the even function depicts accretion. The uniform changes along the coastline can be quantified by superimposing the two even functions and thus determining the dominant background phenomena. If the two functions cancel, then for this period no erosion or accretion would occur in the absence of the inlet. In this case,

the two seasonal even functions do not cancel. The summation of the winter and summer even functions (solid line) is presented in Figure 4.9 and compared to the even function representing the entire year (dashed line). The erosion indicated by the summation of the two seasonal even functions extends over most of the region. A definite background is also evident for the even function representing the entire year (November 1984 to October 1985). The addition of the spring and fall seasons enhance the erosion, even beyond the influence of the winter season alone.

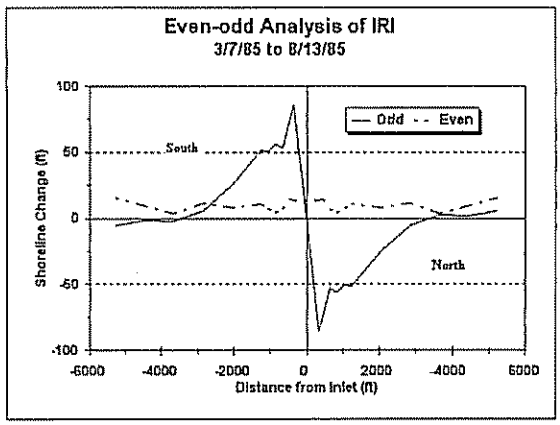

Figure 4.8: Even-odd analysis of Indian River Inlet during the summer season.

The odd function of both seasons indicate the effect the inlet has on the adjoining shorelines. Large erosion is evident in the north, while accretion occurs in the south. The inlet effect is more pronounced in the summer season, as the dominant northward drift heightens the effect close to the inlet. During the winter season however, the maximum changes occur further from the inlet due to the partial reversal of the littoral drift. The actual numbers of shoreline erosion/accretion may be inflated to some degree since the time period examined occurred after a beachfill placement in the northern region.

A more accurate representation of the even-odd analysis is obtained by examining a longer time period. Figure 4.10 shows the even and odd functions spanning

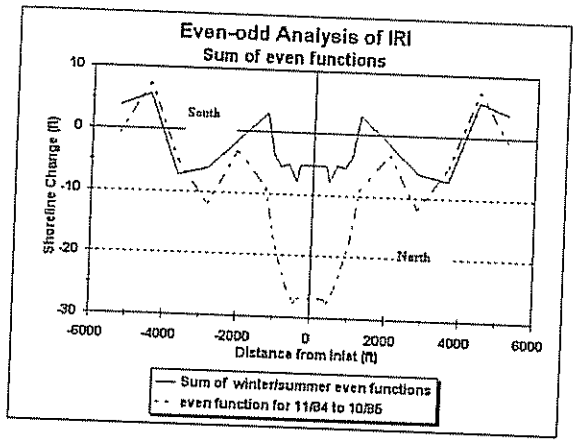

Figure 4.9: Summation of seasonal even functions, including a comparison to the even function spanning the entire year.

from 1984 to 1994. Again, the even function indicates a net erosion, while the odd function shows heavy erosion in the north and accretion in the south. The even function also must reflect a portion of the inlet effect since erosion is magnified near the inlet centerline. In all of the even-odd results, as was seen in the shoreline change plot, the inlet has an influence on the shoreline of $\pm$ 1 mile.

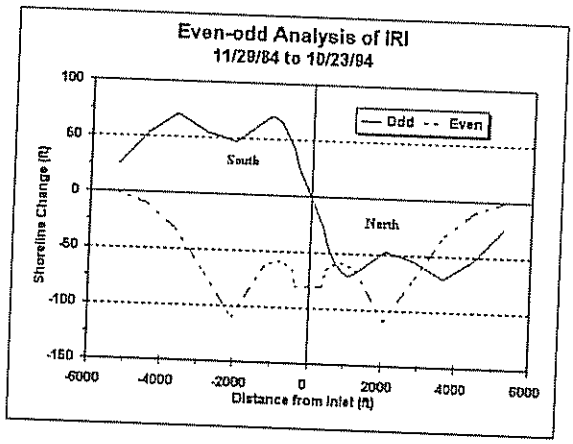

Figure 4.10: Even-odd analysis of Indian River Inlet from 1984 to 1994.

4.4 Volume Change and Sediment Budget

Next, volume changes for the areas between profile stations were computed. The net change in sand volume between the two profiles is equal to the increase in depth over the area or

$$\int\int \left(\frac{\partial h}{\partial t}\right) dx dy \Delta t \tag{4.5}$$

where,

h = depth

dx = width of vertical volume element

dy = alongshore volume element

A summary of the volume changes for the area north of the inlet is presented in Table 4.2. Similar results for the volume changes south of the inlet are shown in Table 4.3. Because of the random sampling of the data, many profile lines had to be discarded for various reasons (e.g. did not extend far enough offshore, a survey was missing, etc.). The value of the volume changes can only be as accurate as the surveys taken. Many of the profile lines north and south of the inlet never converged to a consistent depth of closure. For this reason, the trend of the volume changes is more important than the exact value.

Using the volume changes, a standard sand budget analysis is computed for the northern region by assuming that the only sediment entering the area was due to bypassing or beach nourishments. The results of this analysis, shown in Figure 4.11, yield a measure of the local transport rate. The littoral drift is found to be dominantly northward, as expected, at a rate of approximately 104,000 yd^3 per year. This value was found to be consistent with previous results computed by other methods (U.S. Army Corps of Engineers, 1984; Lanan and Dalrymple, 1977), but much less than the potential sediment transport rates calculated by the U.S. Army Corps of Engineers (1996) discussed earlier (on the order of 1,000,000 yd^3 per year).

Table 4.2: Volume Change Summary, Profiles North of Indian River Inlet

Survey Period	Profile 2+00 - 6+00	Profile 6+00 - 10+00	Profile 10+00 - 18+00	Profile 18+00 - 26+00	Profile 26+00 - 34+00	Profile 34+00 - 42+00	Profile 42+00 - 50+00
10-20	-20263	-15228	-45723	-37262	-216	7809	17280
20-30	-8339	-14037	-24760	-17305	-15597	-4473	11982
30-40	4221	14549	37496	35708	49155	41300	11842
40-50	-6358	-6578	-67124	-90841	-74242	-49735	-23043
50-60	-27785	-24237	31097	27047	-16369	-21110	92113
60-70	-28554	-19212	-68754	-42138	-14436	1264	-100887
70-80	24269	58536	114132	91455	79019	51749	38763
80-90	-6351	-42448	-71663	-54440	-50011	-31484	-28383
90-130	9760	6213	-11938	-57439	-40190	-38707	-41842
130-160	13909	10838	32349	86264	91883	69171	64236
160-170	-11420	-13971	-46850	-72551	-77813	-53114	-54305
170-180	7769	9625	29033	33819	13650	9397	7406
180-190	-21037	-29853	-39297	-5305	2043	-7506	26059

Note: All values are given in yd^3 where negative values (-) indicate erosion.

Likewise, a standard sand budget was calculated for the region south of the inlet. The analysis assumes that the southern jetty is sand tight (no sand gets through the jetty) and the only sediment that escapes the study region is that which is bypassed or extracted for a beach nourishment. The results, shown in Figure 4.12, yield a measure of the local transport rate in the southern region. The littoral drift was again found to be northward, but at a significantly smaller rate of approximately 48,000 yd^3 per year. The difference from the value calculated for the northern region is easily accounted for by the fact that the southern jetty, although assumed sand tight, is most certainly not. Sand is known to leak into the inlet and a great deal of sediment arriving in the southern region is lost to the outer shoal (Lanan and Dalrymple, 1977, U.S. Army Corps of Engineers, 1996).

Table 4.3: Volume Change Summary, Profiles South of Indian River Inlet

Survey Period	Profile 2+00 - 6+00	Profile 6+00 - 10+00	Profile 10+00 - 18+00	Profile 18+00 - 34+00	Profile 34+00 - 50+00
20-50	5706	22757	30182	15301	28304
50-60	2704	2013	27882	67481	110213
60-70	-40116	-26194	-79679	-179434	-162665
70-80	62135	45500	90719	219263	196107
80-90	-34266	-37835	-95840	-192431	-141104
90-130	-16378	-16489	16555	33274	-5788
130-160	35932	24551	23821	83056	124314
160-170	-24287	-38133	-96190	-146142	-91294
170-180	-7971	-1275	-15551	-29601	13135
180-190	6761	9343	15065	13304	2976

Note: All values are given in yd^3 where negative values (-) indicate erosion.

4.5 2-D CPCA Applied to North of Indian River Inlet

The 2-mode CPCA is used to look at alongshore profile lines north of Indian River Inlet in the hope of identifying migrating features. Again, because of the random sampling of the data, many profile lines had to be discarded for various reasons (e.g. did not extend far enough offshore, a survey was missing, etc.). The results shown are for an alongshore profile line located approximately 250 feet from the baseline, an offshore distance expected to show significant movement. The study period extends from November 1984 to October 1994. The complex correlation between the complex time series at given alongshore grid points are shown in Figure 4.13a. Each complex correlation is plotted in vector format such that a vector pointing upwards (downwards) indicates that the two time series are in-phase (out-of-phase). For example, a vector pointing to the right indicates a lag of 90 degrees. The complex correlation between the time series delineates the propagation of a moving "bump" through the domain. Figure 4.13b shows the resulting spatial eigenvectors for the alongshore line, plotted in vector format where the real portion

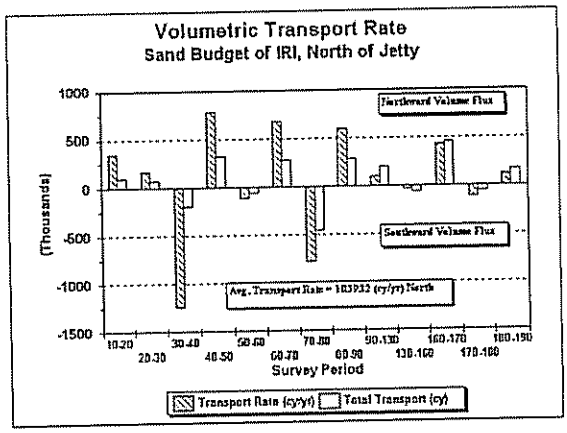

Figure 4.11: Local volumetric transport rate for north of Indian River Inlet.

(magnitude) is indicated in the vertical direction of the vector and the imaginary portion (phase) is indicated in the horizontal direction. The numbers correspond to the percent of variance retained by each eigenvector. The top panel shows the first eigenvector, which represents the mean alongshore profile and accounts for 98% of the variance. The eigenvector is almost entirely real valued, which signifies that no extensive movement is associated with it, and exhibits a depression in magnitude near the inlet entrance (corresponding to x=0). The second eigenvector identifies a definite progressive feature, which represents 1% of the total variance. The second eigenvector then represents a moving form that augments the mean alongshore profile. Similarly, the third eigenvector, which indicates no coherent movement, modifies the mean further.

The spatial and temporal phase functions for the same alongshore profile line, as presented in Figure 4.13, are shown in Figure 4.14. The numbers correspond to the approximate wavenumber and frequency of each eigenvector component. By using these values, the second eigenvector indicates a feature that is moving northward at the rate of approximately 5.5 feet per day. Therefore, over this time period, CPCA reveals that sand was relatively quickly moved out of the area to the north. Other

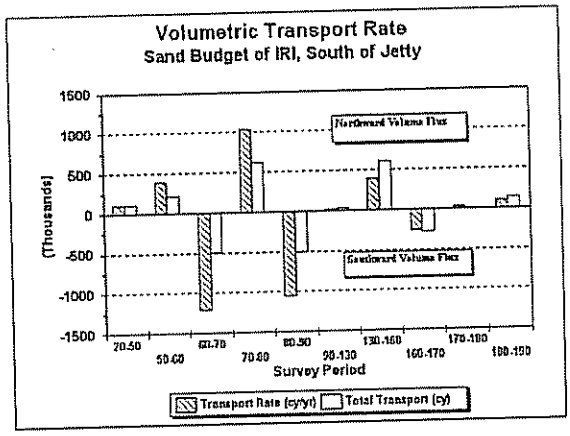

Figure 4.12: Local volumetric transport rate for south of Indian River Inlet.

alongshore profile lines evaluated north of the inlet revealed similar results. In fact, in the additional analysis, the second eigenvector approaches a maximum of 20% of the total variance. This maximum variance occurs in a shallow region near the shoreline and correspond to a moving bump with an amplitude of approximately 2.5 feet. Attempts to complete a similar analysis for the area south of the inlet were unsuccessful due to a lack of spatial and temporal resolution.

4.6 3-D CPCA Applied to Indian River Inlet Region

The 3-mode CPCA is applied to the nearshore region (approximately 400 feet offshore), where significant movement is occurring, for both north and south sides of the inlet. The analysis covers the same time span as in the previous section (November 1984 to October 1994). The cross-shore and alongshore eigenvectors for the region north of the inlet are presented in Figure 4.15. For simplicity, only the real part of each eigenvector is shown. To illustrate the relative importance between both the variables and components, the eigenvectors shown have been weighted. These eigenvectors can be thought of as the average form of all cross-shore or alongshore

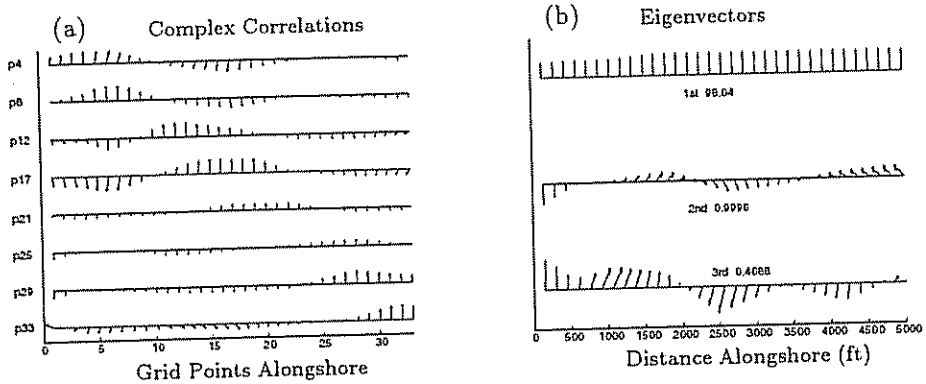

Figure 4.13: (a) Complex correlation between time series for alongshore grid points. Notice that the vector is normalized to one when a time series is correlated to itself; i.e. the time series of point 4 is perfectly related to itself as shown at point 4 on both axes. (b) Eigenvectors computed by CPCA for an alongshore profile line north of Indian River Inlet.

profile lines in the region. In the cross-shore direction, the mean is easily identifiable. The second component, typically referred to as the "bar-berm" function is significantly reduced in importance because of the larger fluctuations occurring in the alongshore direction. In the alongshore eigenvectors, the mean is characterized by a dramatic depression that occurs near the inlet (x=0). The second and third components highlight sizable changes in the alongshore direction.

The eigenvector components can also be combined to represent various features that may be hidden within a bathymetry. These *eigenvector combinations* are products of the different alongshore, cross-shore, and temporal components. Similar to a large puzzle, if three components are selected to represent each variable, then there are 27 combinations that make up a complete bathymetry. The three combinations that capture the highest amount of variance are shown in Figure 4.16. The percent variance captured by each eigenvector combination for each given temporal component (T1, T2, and T3) is also shown in Figure 4.16. The summation of these values is a measure of the importance of the combination. Since the analysis results

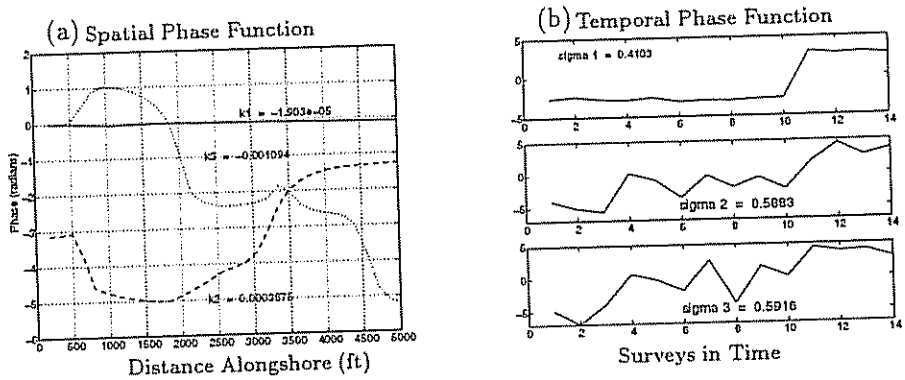

Figure 4.14: (a) Spatial phase function for alongshore location north of Indian River Inlet. The solid, dashed, and dotted lines correspond to the first, second, and third functions, respectively. (b) Temporal phase function for the same location.

in both real and imaginary combinations, the real part of each combination is shown on the left, while the imaginary combination is shown on the right. The results can be separated into the two portions as:

$$Ae^{(i\sigma\, t-\epsilon)} = A\cos(\sigma\, t-\epsilon) + i\, A\sin(\sigma\, t-\epsilon) \tag{4.6}$$

Both the real (A cos $(\sigma t - \epsilon)$) and imaginary (A sin $(\sigma t - \epsilon)$) plots contain both the amplitude (A) and phase component (cos or sin). The top panel shows the combination A1O1, which is defined as the product of the first eigenvector in the alongshore direction (A) and the first eigenvector in the cross-shore direction (O). This combination represents the mean bathymetry. Note how the real part is characterized by the erosion located at nearshore region of the inlet entrance. The middle panel shows the A1O3 combination, corresponding to the product of the first alongshore eigenvector and the third cross-shore eigenvector. This combination has a significant impact in the shoreline area where bypassing modifies the bathymetry. The lower panel, which contains the A3O3 combination (same nomenclature as before), is the most intriguing. A large "bump" appears on the real portion of the bathymetry, while the imaginary portion depicts a wave-like phase rotation. This imaginary "hot

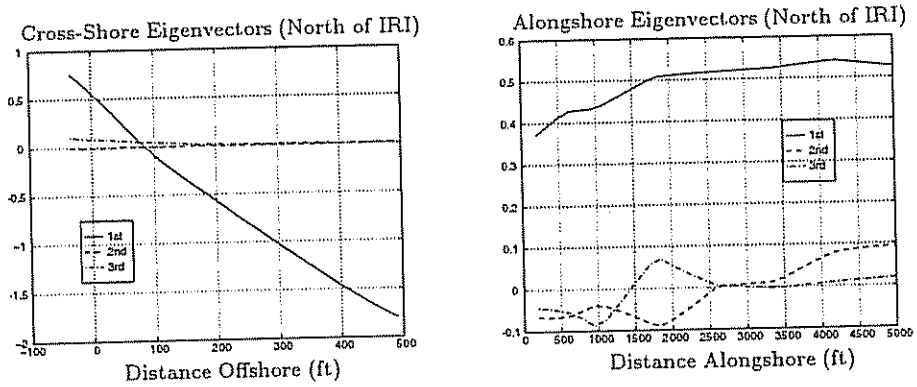

Figure 4.15: The real portion of cross-shore and alongshore eigenvectors computed from 3-mode CPCA.

spot" of movement indicates that the feature is in motion. Notice that the magnitude of the "imaginary" bathymetry decreases as we proceed offshore. Therefore, as noted in the two-dimensional analysis, the alongshore movement is strongest in the nearshore area and becomes weaker offshore.

The eigenvector combinations for the region extending 5000 feet south of the inlet and 400 feet offshore are shown in Figure 4.17. The nomenclature remains the same as for the combinations north of the inlet. Again, the top panel represents the mean bathymetry and shows a build up of sediment in the area adjacent to the southern jetty. The A2O3 and A2O1 combinations both illustrate changes that are occurring in the neighborhood of the inlet entrance. The difference between the two is that the imaginary portion of A203 identifies more of a movement in the alongshore direction, while the imaginary portion of A201 identifies more of a movement in the cross-shore direction. This may mean that, after bypassing occurs, the large eduction hole left behind recovers by receiving sediment from both the alongshore and offshore elements of the bathymetry.

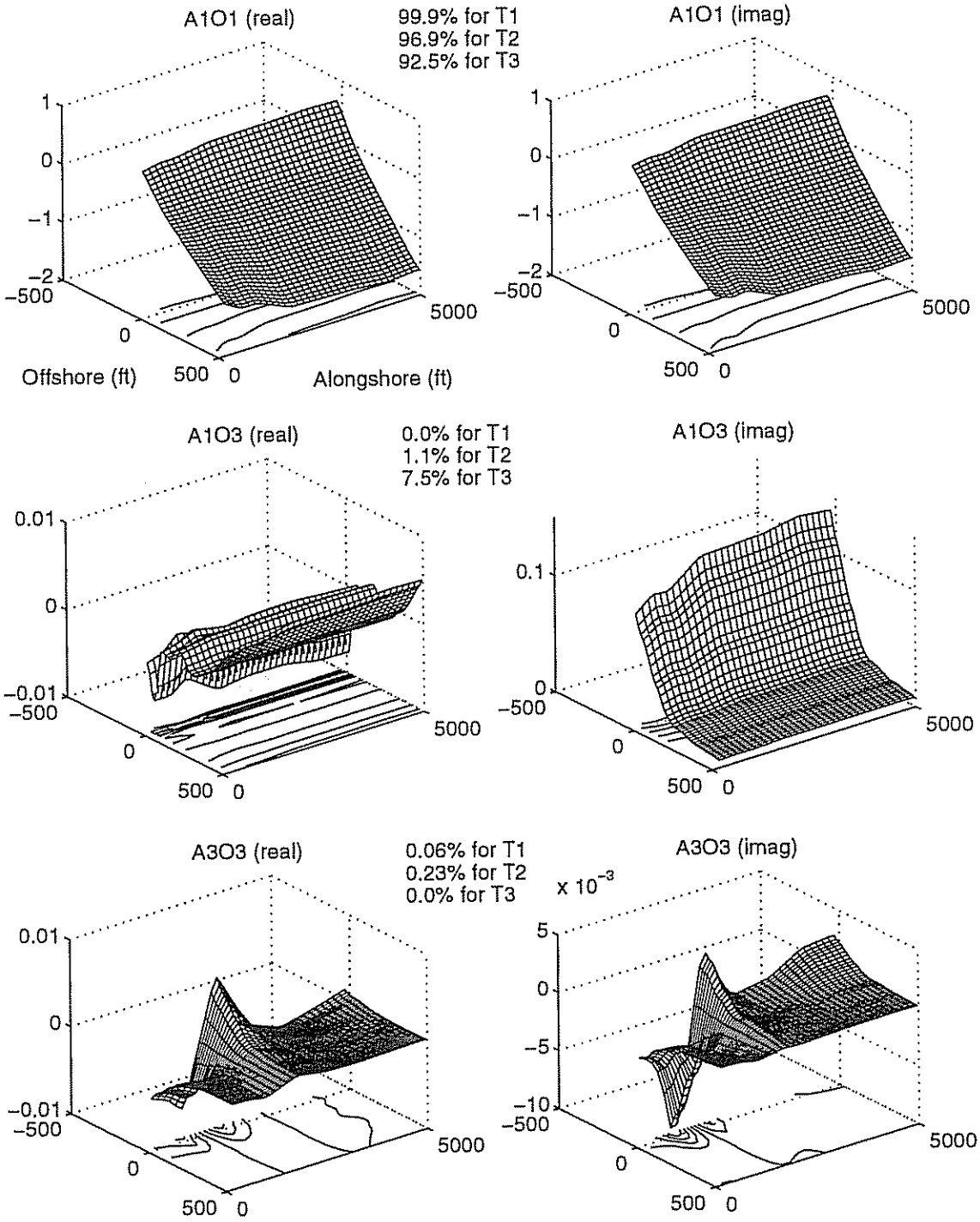

Figure 4.16: Eigenvector combinations north of Indian River Inlet. The numbers (or core matrix values) included represent the percent of variance captured by each eigenvector combination for a given temporal component.

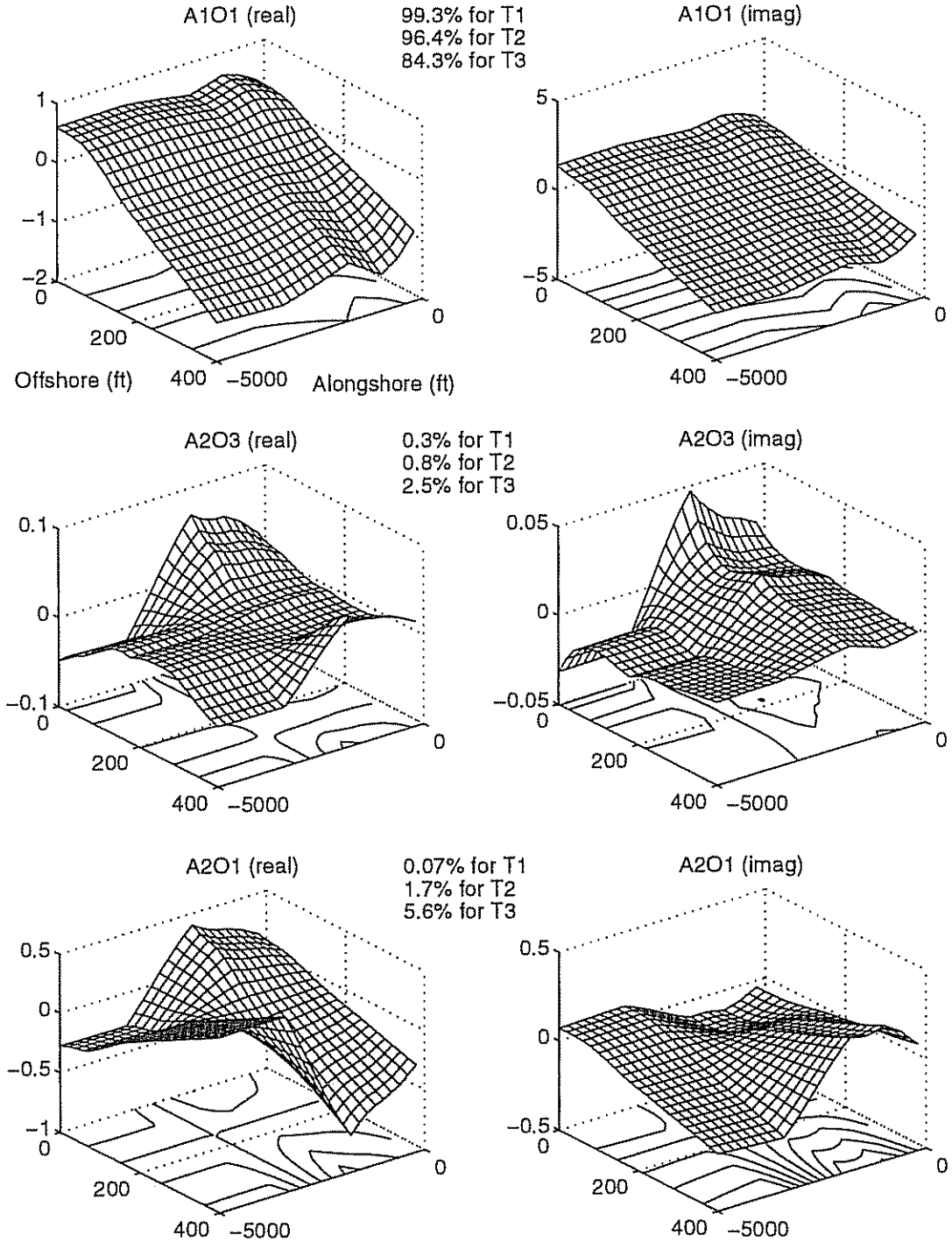

Figure 4.17: Eigenvector combinations south of Indian River Inlet. The numbers (or core matrix values) included represent the percent of variance captured by each eigenvector combination for a given temporal component.

Chapter 5

DEWEY BEACH FILL

As shown in Figure 1.1, Dewey Beach lies north of Indian River Inlet and directly south of Silver Lake, from which it extends southward for approximately one mile. In the past, the area has experienced major flooding, erosion, and wave attack causing damage to many shoreline structures. From 1992 to 1996, the region was declared a National Disaster Area by the President of the United States (U.S. Army Corps of Engineers, 1996). The northern portion of Dewey Beach is backed by a headland formation, described in Chapter 2. Much of the northern shore has been stabilized by a system of bulkheads. The southern portion however, is located on a narrow strip of land between the Atlantic Ocean and Rehoboth Bay. The region is essentially a barrier island, which is extremely vulnerable to storm damage. The town of Dewey Beach has become an overflow development of Rehoboth Beach, which is Delaware's largest resort area. Dewey Beach is a highly developed area with a mix of residential and commercial neighborhoods. The permanent population is 204, but can soar to 35,000 on a typical holiday weekend (U.S. Army Corps of Engineers, 1996). This chapter examines the largest and most recent beach nourishment on the Delaware coast; a beachfill of 592,878 yd^3 placed at Dewey Beach in the summer of 1994.

5.1 Field Data

The majority of the sediment (578,874 yd^3) for the beachfill was taken from the Hen and Chicken Shoal located approximately two to three miles offshore of

the Rehoboth Beach area. The remaining amount was "trucked" in to complete the nourishment. Monitoring profile locations were established every 500 feet, as shown in Figure 5.1. The fill extended approximately 6500 feet alongshore ranging from Collins Street in the south (S 20+00) to the south end of Silver Lake in the north (N 35+00). The data set was collected from May of 1991 to January of 1996. For each profile line, a total of nine to eleven surveys were taken over the five year period. Therefore, when generating a complete bathymetric grid, analysis required elimination of some surveys. Four of the surveys were taken after the beach nourishment, the remaining were pre-nourishment surveys. The survey dates and nomenclature are presented in Table 5.1. Again, survey points were taken randomly during each survey, thus requiring linear interpolation in both the alongshore and cross-shore directions for much of the analysis.

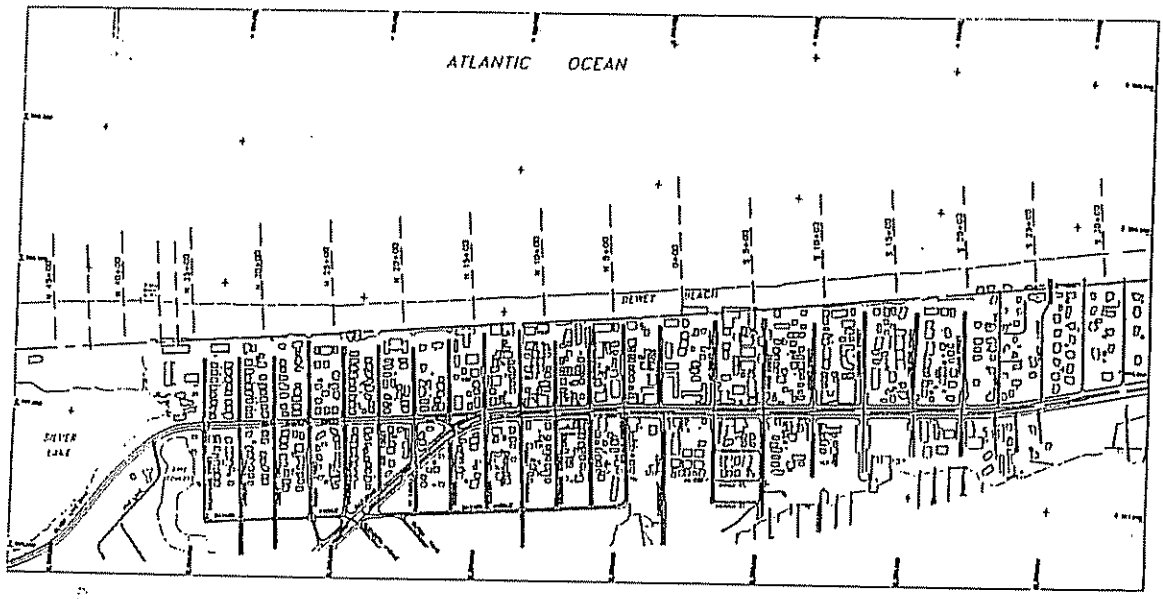

Figure 5.1: Dewey Beach layout and location of monitoring profiles (U.S. Army Corps of Engineers, 1996).

After interpolation, profile envelopes were computed for each profile station.

Table 5.1: Survey Dates for Dewey Beach

Survey Label	Date	Survey Label	Date
101	5/22/91	108	3/8/94
103	2/19/92	110	8/12/94
104	10/29/92	111	12/27/94
105	12/18/92	112	4/6/95
106	7/27/93	115	1/26/96
107	2/10/94		

The envelopes for stations N20+00 and S15+00 are shown in Figure 5.2. The results provide elevation variation bounds and the limits of recent shoreline locations. As shown, the surveys never seem to reach a depth of closure offshore. Most likely a result of an inaccurate survey method, the surveys not only fail to converge, but also exhibit high variations at distances far offshore. This is consistent throughout all profile stations. The beach fill placement is visible in both envelope plots as a large increase in beach width (approximately 150 feet) and elevation (approximately 10 feet).

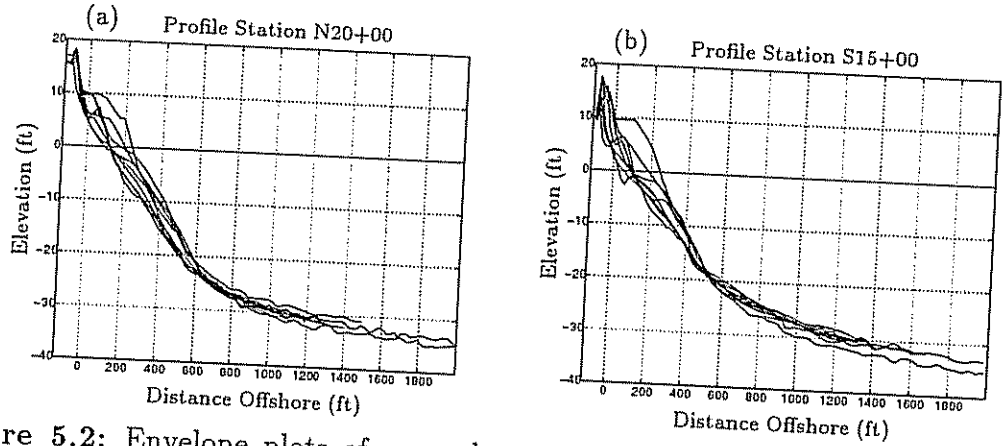

Figure 5.2: Envelope plots of cross-shore profile stations for the Dewey Beach region. (a) Profile station N20+00 (north of St. Louis St.). (b) Profile station S15+00 (north of Van Dyke Ave.).

Similar envelope plots can be generated for lines in the alongshore direction

at a fixed distance from the baseline. Figure 5.3 shows alongshore lines that are 120 ft and 400 ft from the baseline. The water line corresponds to the zero elevation mark. The variation in the alongshore direction is quite random, which is expected. Again, as in the cross-shore envelopes, the first post-nourishment survey is obvious. The plots show an elevation increase of eight feet at the 120 foot alongshore line and four feet at the 400 foot alongshore line. One interesting trend, evident in all the alongshore profile lines, is the accretion that occurs towards the northern region of the survey area. Coastal and Ocean Engineering and Research (1983) found there was accretion on the northern end of Dewey Beach at a rate of 2.9 feet/year and erosion on the southern end at a rate of 2.4 feet/year. A possible explanation is that the predominant littoral drift moves sediment from the fill region to the north. An extensive groin field at Rehoboth Beach then impedes the sediment flow, causing an accumulation of sediment in the northern region of the study area. Dewey Beach also may be an area where wave energy is concentrated because of the existing offshore bathymetry. Mild wave conditions may exist in the north, while larger waves result in a "hot spot" of erosion in the south.

Combining the cross-shore and alongshore lines, we can generate a complete bathymetric survey. Figure 5.4 shows pre- and post-nourishment bathymetric surveys for the Dewey Beach area. The effect of the nourishment is evident in the post-nourishment survey as a large increase in total area. The large bump appearing in the survey is most likely a survey error. The accretion at the north end of the region is apparent in the pre-nourishment bathymetry of Figure 5.4a. The remaining bathymetric surveys are presented in Appendix B.

5.2 Shoreline Change

As in the previous chapter, the change in shoreline position is calculated to quantify beach behavior and allow for comparison of pre- and post-nourishment. A minimal amount of historical information is available for the Dewey Beach area.

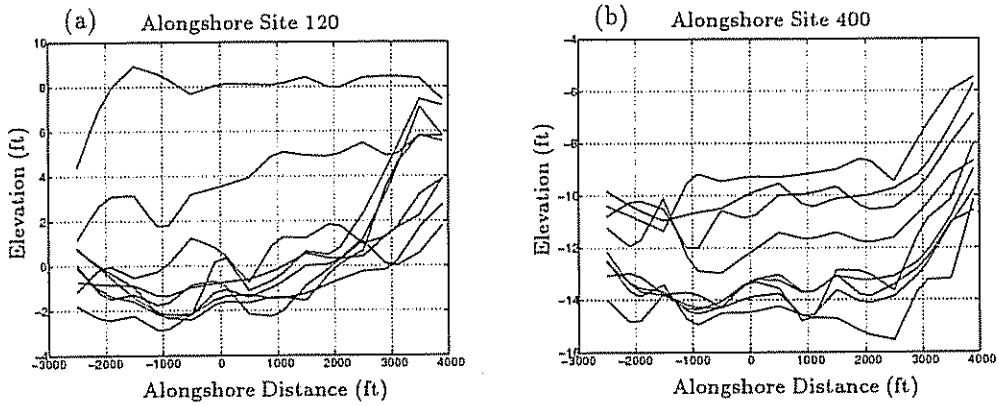

Figure 5.3: Envelope plots of alongshore lines for the Dewey Beach region (negative alongshore distance are south of station 0+00). (a) Alongshore line 120 (120 feet from baseline). (b) Alongshore line 400 (400 feet from baseline).

Previous measurements of the area are scattered and it is difficult to determine trends.

The cumulative shoreline change over the study period is shown in Figure 5.5 (north of station 0+00) and Figure 5.6 (south of station 0+00). The cumulative shoreline change is measured relative to the position of the shoreline at May of 1991. The figures illustrate the shoreline behavior through time at the various stations along Dewey Beach. The discontinuity in some of the time series indicate dates when surveys were not taken.

After July of 1993, a shoreline retreat of approximately 75 feet was apparent. The beach nourishment was visible in all the northern stations and for the first five stations south of station 0+00N. The beach fill quickly spread as the extreme wave climate during the winter season of 1994 acted on the coast. Station 5+00N actually showed an increase during this period, possibly due to the spreading out effect. The shoreline recovered substantially over the next survey period, but was approximately 50 feet short of the original post-nourishment position. Notice, however, that the

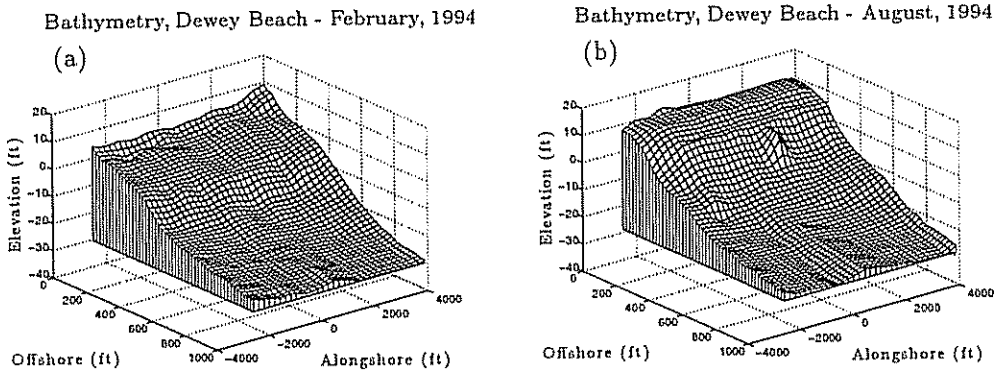

Figure 5.4: Bathymetric surveys for the Dewey Beach region (negative alongshore numbers indicate regions to the south of the center profile station). (a) Pre-nourishment survey of February 1994. (b) Post-nourishment survey of August 1994.

stations further north showed a retreat of only 25 feet over the first two survey periods. Also, the stations to the south of the original fill (30+00S to 50+00S) showed no reaction to the nourishment. This is a strong indication that sediment "spreading" was predominantly to the north. As shown, the large seasonal changes (approximate shoreline position changes of 50 to 100 feet is evident after beach nourishment) that occur at Dewey Beach are the same order or higher than the yearly changes. Therefore, it is difficult to determine trends in the data and may be somewhat responsible for the lack of historical information on the area. Although the fill shows a rapid dispersion, it is important to remember that the measurements are taken a brief time after fill placement. Typically, the initial adjustment of the nourishment occurs at a greatly enhanced rate, which would produce a beachfill lifetime of only a few years. This is certainly not the case. It is too early to determine the exact lifetime of the beach fill, but an approximation can be determined as shall be shown in the next section.

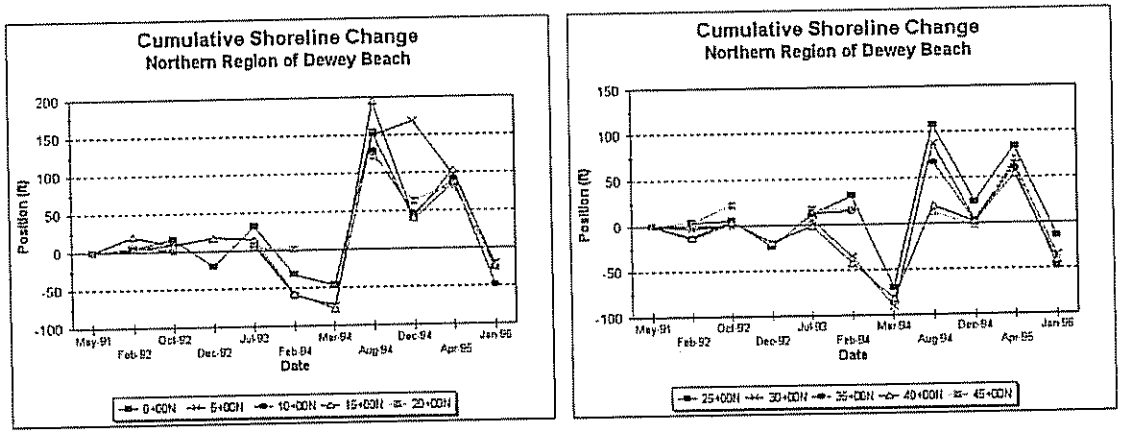

Figure 5.5: Cumulative shoreline plots for the region north of station 0+00N at Dewey Beach. Shoreline positions are shown relative to the shoreline position of May 1991 for each station.

5.3 Volume Change

As in the previous chapter, the volume changes for the areas between profile stations were determined. Recall that the net change in sand between two profiles is equal to the change in depth over the area.

$$\int\int \left(\frac{\partial h}{\partial t}\right) dx dy \Delta t \tag{5.1}$$

where,

h = depth

dx = width of vertical volume element

dy = alongshore volume element

The volume changes computed for stations south of 0+00 are shown in Table 5.2, while the volume changes for stations north of 0+00 are shown in Table 5.3.

As previously stated, most of the profile lines never converge to a depth of closure. The data also contain possible errors in measurement. Hence, the actual value of the volume change is not as important as the trend the change exhibits.

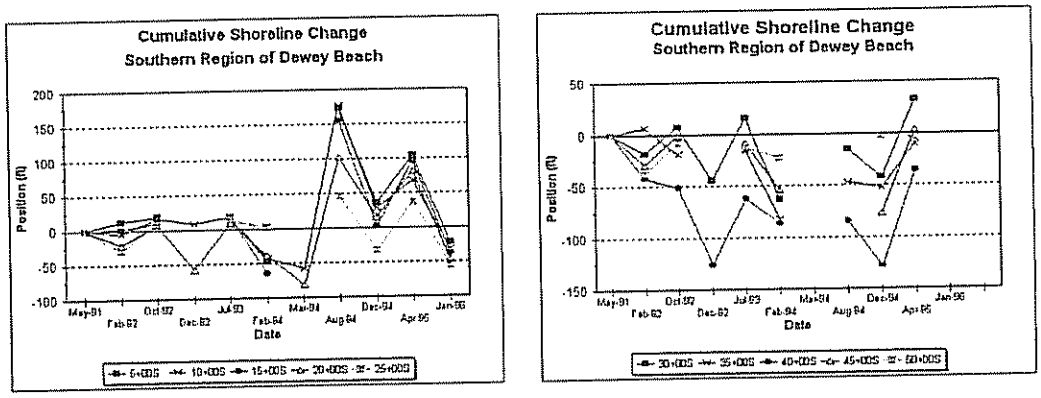

Figure 5.6: Cumulative shoreline plots for the region south of station 0+00N at Dewey Beach. Shoreline positions are shown relative to the shoreline position of May 1991 for each station.

The sum of all the volume change "cells" is shown in Figure 5.7. The figure contains both the immediate and cumulative volume changes for the Dewey Beach region. The results are very similar to the changes that are occurring at the shoreline.

An approximation of the beachfill lifetime can be calculated by using the following formula presented in Strine (1991).

$$\text{Lifetime} = \frac{\text{V}}{\text{EL}} \tag{5.2}$$

where,

V = total volume of fill (yd^3)

E = volumetric erosion rate per foot of beach ($yd^3/ft/yr$)

L = length of beach fill (ft)

From before, V=592,878 yd^3 and L=6500 ft. The volumetric erosion rate of the Dewey Beach region is determined from the calculated volume change. By looking at the volume changes of the pre-nourishment period (May of 1991 to February of 1994), an estimate of the erosion rate can be computed. A total of 311,267 yd^3 was

Table 5.2: Volume Change Summary, Profiles South of Station 0+00

Survey Period	Profile 0+00 - 5+00	Profile 5+00 - 10+00	Profile 10+00 - 15+00	Profile 15+00 - 20+00	Profile 20+00 - 25+00	Profile 25+00 - 30+00	Profile 30+00 - 40+00
101-103	-2494	-8128	-17240	-23075	-21967	-29428	-91570
103-104	-1728	450	2792	2228	3038	6892	12376
104-106	2780	-3409	-6202	-5239	-5993	-11550	-40388
106-107	-5255	-4899	-8669	-16042	-15060	-2964	19343
107-110	63198	64444	72383	678226	43608	2401	-45098
110-111	-14484	-16010	-29166	-29271	-13691	5657	39320
111-112	-2027	-164	9327	29314	23075	14416	21019
112-115	-45319	-47411	-53947	-70882	-61281	-4999	98361

Note: All values are given in yd^3 where negative values (-) indicate erosion.

lost from the study area over the pre-nourishment period. Therefore, for the entire 8000 foot region of volume calculations, the volumetric erosion per foot of beach was 14.3 $yd^3/ft/yr$. Since volume changes are measured for only a little under 3 years, this may or may not be an accurate estimate. Utilizing the simple formula above, the lifetime of the beachfill is estimated to be 6.4 years.

5.4 2-D CPCA Applied to Dewey Beach

2-mode CPCA can be applied to a cross-shore or an alongshore line. The analysis in the previous chapter used 2-mode CPCA to examine a alongshore line at a fixed distance from the baseline. Here, 2-mode CPCA is applied to an alongshore "line" of fixed depth. The fixed depth, in this case, is the zero foot depth, or the shoreline. The plan view of the shoreline as it evolves through the study period is shown in Figure 5.8. The strange lumps evident in the shorelines of August 1994 and December 1994 are assumed to be errors in measurement. A sudden increase in shoreline position of over 100 feet is illogical. Once again, the beachfill is apparent in the August 1994 shoreline position.

Table 5.3: Volume Change Summary, Profiles North of Station 0+00

Survey Period	Profile 0+00 - 5+00	Profile 5+00 - 10+00	Profile 10+00 - 15+00	Profile 15+00 - 20+00	Profile 20+00 - 25+00	Profile 25+00 - 30+00	Profile 35+00 - 40+00
101-103	-1715	3889	1569	-1399	7454	6338	14205
103-104	-2983	-3994	-3358	-2204	-5334	-5180	-2211
104-106	1688	1227	2337	2020	3748	3651	6239
106-107	-9012	-15098	-13743	-8167	-4728	-7971	-18129
107-110	76971	82218	82096	76699	64724	64414	113465
110-111	-29952	-30541	-26879	-25535	-19936	-19681	-30925
111-112	139	8429	6439	2313	1163	1378	-4371
112-115	-38559	-37393	-37561	-33141	-26297	-24614	-34191

Note: All values are given in yd^3 where negative values (-) indicate erosion.

The resulting eigenvectors from the analysis are shown in Figure 5.9. The results are plotted in the same format as in previous chapters. The mean eigenvector shows a slight "tilting" of the vectors to the north (or slight imaginary part) as well as an increase in amplitude. This does not indicate movement (as the temporal phase is shown to be constant), however the increase in amplitude indicates a seaward advance of the shoreline position in the north. The second and third components contain more of the total variance than the alongshore line examined at Indian River Inlet. So, a greater percent of the shoreline is in motion for this case. Although difficult to see because of the lack of alongshore spatial resolution, both the second and third eigenvectors contain movement illustrated by vector rotation. The spatial and temporal phase functions are shown in Figure 5.10. The second component, which displayed a choppy motion at best, is actually a result of the two large lumps assumed to be errors. The spatial phase function for the second component is relatively constant until the region where the large lump is present. The temporal phase function behaves similarly around the time of the erroneous surveys. The spatial wavenumber is negative for the second component. Therefore, indicating

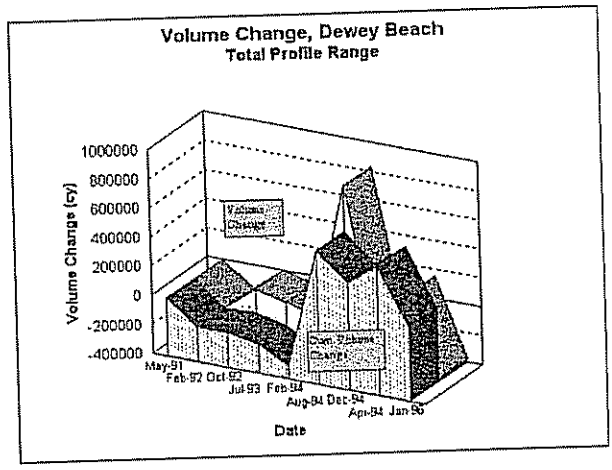

Figure 5.7: Volume changes for the Dewey Beach region. The rear bar shows volume change between surveys while the front bar shows the cumulative volume change.

the movement is to the south, which is easily verified from Figure 5.8. The second component is considered meaningless in this case. However, the third component is rendered more meaningful. The motion, especially in the northern region, can be identified as moving north. The speed of the movement can be simply calculated from the approximated values of the wavenumber and frequency as 2.35 ft/day to the north.

5.5 3-D CPCA applied to Dewey Beach

3-mode CPCA was also applied to the nearshore region (ranging from the baseline to 400 feet offshore) of Dewey Beach. This section presents some of the more important eigenvector combinations for the region. Figure 5.11 shows the real bathymetries for the eigenvector combinations A1O1 and A1O2 (same nomenclature as previous chapter). The A1O1 combination is representative of the mean bathymetry, with core matrix percentages of 98.2%, 98.5%, and 92.6% for each

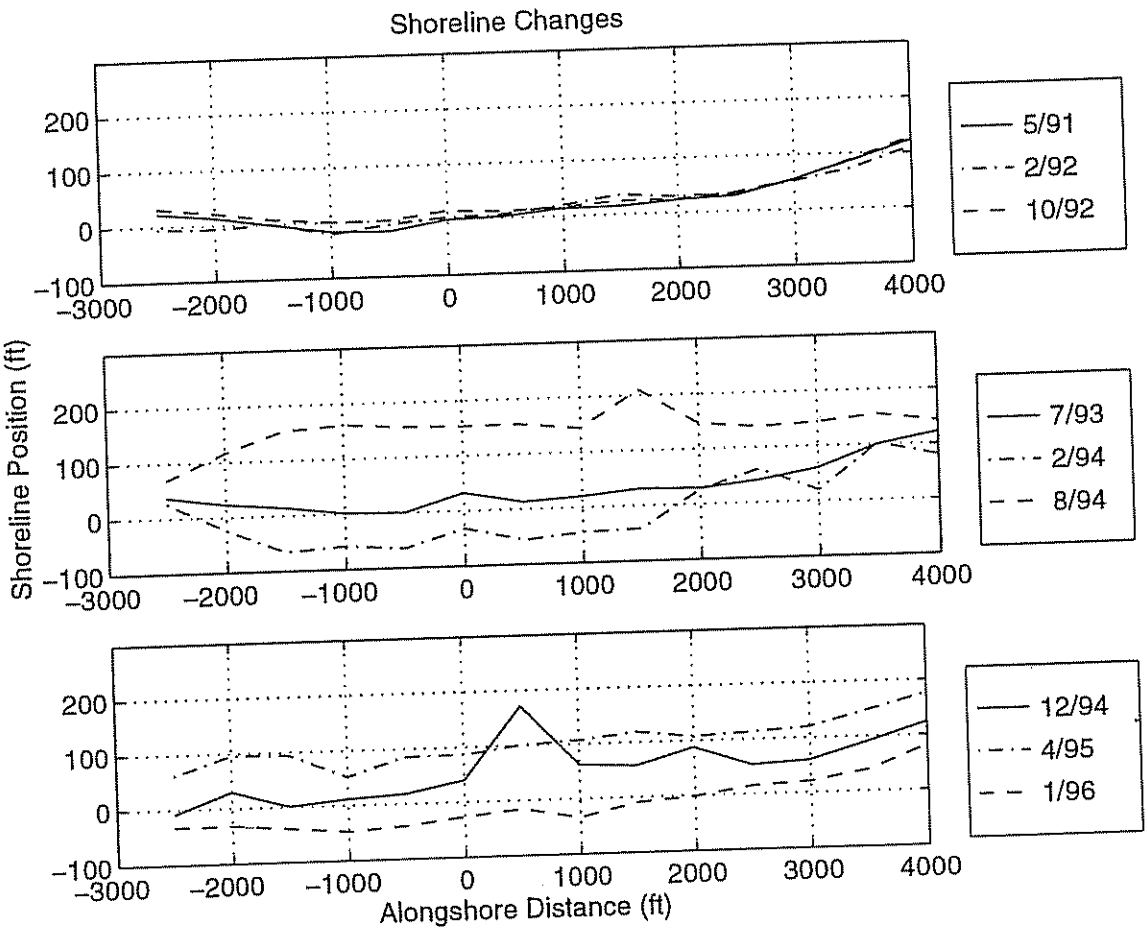

Figure 5.8: Plan view of the Dewey Beach shoreline as it evolves through time.

respective temporal component. The A1O2 combination, with core matrix percentages of 0.17%, 0.36%, and 5.8%, extracts the beachfill from the data matrix. This is an expected, yet impressive, result. By adding the two combinations, A1O2 modifies the mean bathymetry (A1O1) by superimposing the beachfill. Neither of these two combinations have significant imaginary parts and together they capture most of the variation for the area.

Figure 5.12 shows the eigenvector combination A1O3. The combination is

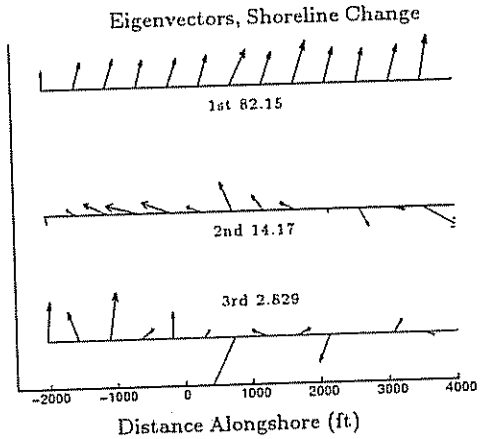

Figure 5.9: Eigenvectors computed by 2-mode CPCA for the Dewey Beach shoreline. The numbers correspond to the percent of total variance contained in each component.

interpreted as the offshore adjustment of the beachfill and captured approximately 0.2% to 2.0% of the variance for each temporal component. After fill placement, the bathymetry must re-adjust to its equilibrium slope resulting in a significant amount of sediment being carried offshore. The real portion (Figure 5.12a) modifies the mean as a protuberance, while the imaginary portion (Figure 5.12b) represents the movement offshore.

The cross-shore changes tend to dominate over alongshore movement in the region due to the immediate adjustment of the massive beach nourishment. However, Figure 5.13 presents the eigenvector combination A2O2, which was the only alongshore modification that captured a sizable portion of the total variance (ranging from 1.0 to 1.67%). A larger alteration occurs in the northern section of Dewey Beach. This corresponds to the previous sections that infer this is an area of accretion. The imaginary portion shows an indication of some type of movement, but would not demonstrate a consistent "spinning" motion if plotted with in vector format. It is not consistent across the range and difficult to interpret.

The changes identified by 3-mode CPCA are primarily influenced by the

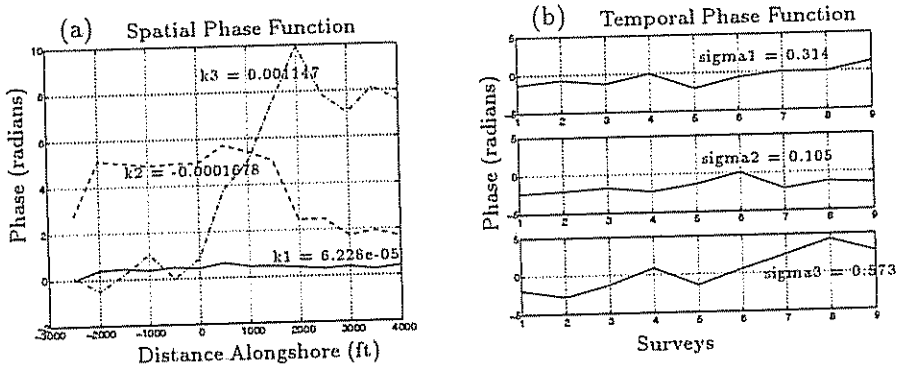

Figure 5.10: (a) Spatial phase functions of the first three components for the Dewey Beach shoreline. The numbers correspond to the wavenumber of each component. (b) Temporal phase functions of the same components. The numbers correspond to the instantaneous frequency of each component.

changes occurring in the bathymetry after the large beach nourishment episode. Combination A1O2 clearly identifies the addition of sediment to the bathymetry caused by the beach nourishment. The combination exhibits only minor fluctuations in the alongshore direction (since A1 represents the mean alongshore shape of the bathymetry). Combination A103 represents the offshore adjustment of the beach nourishment as a "bar" of sediment is moved offshore. The real portion of A1O3 exhibits a decrease in sediment in the nearshore region (0 to 150 feet from the baseline) and an increase in sediment farther offshore (200 to 300 feet from the baseline). The bathymetry is returning to its pre-nourishment slope and sediment is transported (indicated by the imaginary portion of A1O3) in the offshore direction. Combination A2O2 is the only combination exhibiting significant fluctuations in the alongshore direction,

Although three-dimensional analysis is a powerful tool, physical interpretation can be difficult due to the complex changes of a bathymetry and the limited spatial resolution in beach profile data sets. The analysis of the Dewey Beach nourishment contains only three surveys (approximately one and a half years) after the

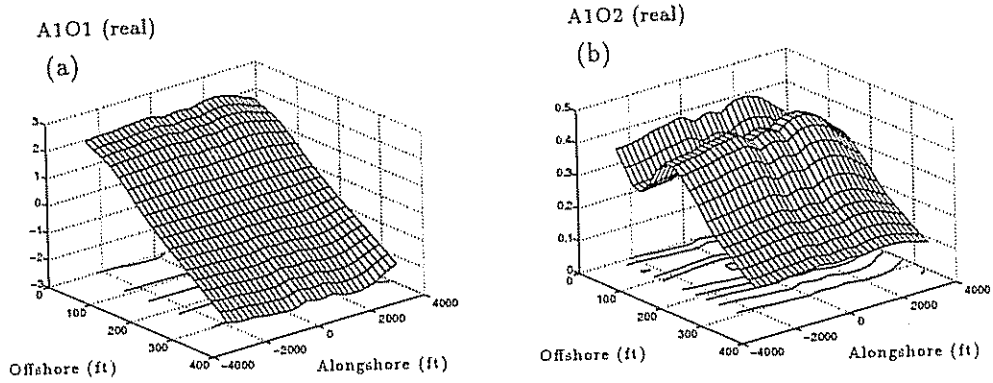

Figure 5.11: (a) The real portion of eigenvector combination A1O1 for Dewey Beach. This combination represents the mean bathymetry of the region. (b) The real portion of eigenvector combination A1O2. This combination represents the modification to the mean bathymetry by the beachfill.

initial placement of the fill. The lack of temporal measurement may explain the identification of strong changes occurring in the on/offshore direction as the bathymetry returns to an equilibrium shape, as well as the insignificant movement in the alongshore direction as the spreading out effect is not yet dominant for a majority of the bathymetry. Thus, if more post-nourishment surveys were included into the analysis, we would expect to see an increase in alongshore movement identified by 3-mode CPCA.

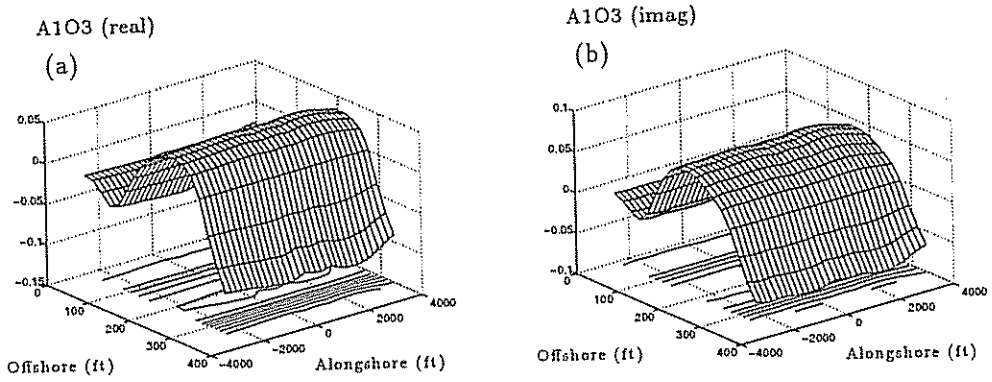

Figure 5.12: Eigenvector combination A1O3 for Dewey Beach. This combination illustrates the offshore adjustment of the beachfill. (a) The real portion (b) The imaginary portion.

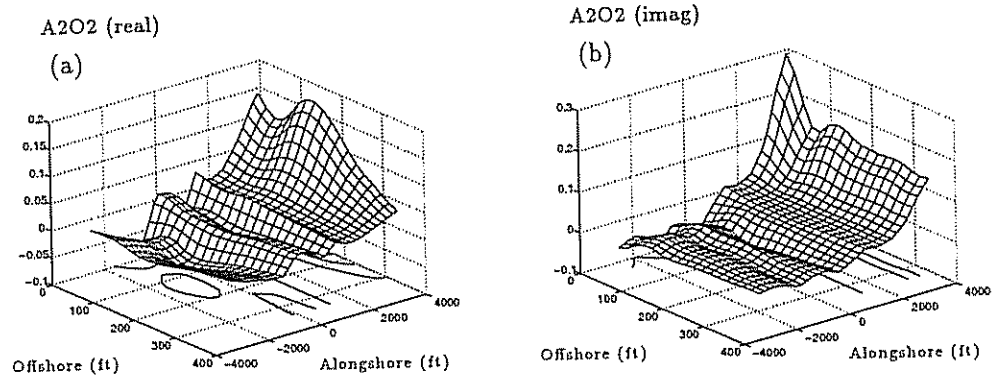

Figure 5.13: Eigenvector combination A2O2 for Dewey Beach. (a) The real portion (b) The imaginary portion.

Chapter 6

BETHANY BEACH FILL

As shown in Figure 1.1, Bethany Beach is located south of Indian River Inlet in another headland region of the Delaware coast. The beach, which is very narrow, extends for approximately 0.9 miles of the coast. Bulkheads constructed in the area have been rendered inadequate. Erosion has been a problem since the 19th century, when, between 1840 and 1929, the shoreline eroded at an average rate of four feet per year resulting in a total loss of over 300 feet of beach (Maurmeyer, 1985). Between 1934 and 1943, the State of Delaware constructed nine groins which have been effective at accumulating sand during normal wave activity. From 1938 to 1977, the overall rate of accretion was 0.2 to 0.8 feet per year (Dick and Dalrymple, 1983). Additional groins were constructed in the 1970's, however, severe erosion still occurs during even moderate storm events due to lack of sediment supply (U.S. Army Corps of Engineers, 1971). In fact, the U.S. Army Corps (1956) estimated that the average annual loss of beach material is 15,000 m^3, and in 1971, a total of 52,000 m^3! Therefore, there is concern that the shoreline is facing eminent danger and, in recent years, numerous beach nourishment projects have been placed in the Bethany Beach vicinity. This chapter investigates the recent behavior of Bethany Beach and the surrounding area.

6.1 Field Data

Delaware's DNREC has established 32 profile stations (with station 0+00 located at the south end of Bethany Beach) in the Bethany Beach neighborhood

spanning a total distance of 14,600 feet. Spaced at approximately 500 feet, this range covers the Bethany Beach, Sea Colony, Middlesex Beach, and South Bethany coastline (see Figure 6.1). Station nomenclature is the same as in previous chapters (i.e. 5+00N is a profile line located 500 ft north of the alongshore origin, 0+00). A total of 17 surveys were measured from June 1989 to March 1995. During this time, various beachfills were placed along the coast. A summary of the fill placement is provided in Table 6.1. As in the other areas, survey points were taken randomly during each survey, thus requiring linear interpolation in both the alongshore and cross-shore directions for much of the analysis.

Table 6.1: Bethany Beach and Vicinity Beach Fill Quantities

Year	Location	Amount (yd^3)
1989	Bethany Beach	284,500
1989	Sea Colony	132,600
1989	Middlesex Beach	63,700
1989	South Bethany	231,600
1992	Bethany Beach	219,735
1992	South Bethany	192,750
1994	Bethany Beach	184,452
1994	South Bethany	98,420

Profile envelopes were computed for both alongshore and cross-shore directions as in the previous chapter. The results for alongshore sites 136 and 356 feet from the baseline are shown in Figure 6.2. Both locations show high variability in the alongshore direction. Large erosion areas are evident at approximately 2250 ft north (Bethany Beach) and 4500 ft south (Middlesex/South Bethany) of the alongshore origin.

These erosion "chutes" are also evident in the bathymetric surveys in Figure 6.3. (Note: when generating bathymetric surveys, offshore distance was sacrificed in order to preserve the largest alongshore distance and temporal period.

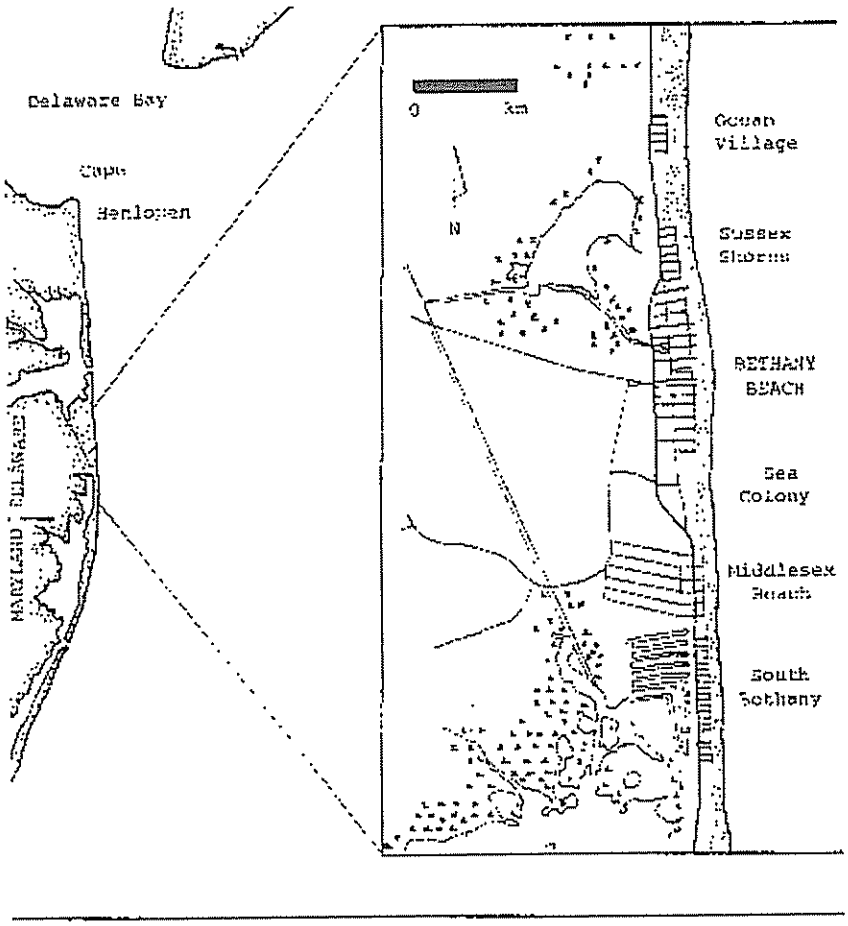

Figure 6.1: Locality map of Bethany Beach and surrounding communities (Dick and Dalrymple, 1983).

Therefore, bathymetric surveys only extend approximately 375 feet offshore).

Figure 6.3a shows a bathymetric picture soon after the beach nourishments of 1989. In that year, a total of 712,400 yd^3 of sediment was placed across the region (Table 6.1). The erosional features in the two areas of concern already show signs of reappearing. Figure 6.3b shows the bathymetry eight months later. In this short time period, the erosion chutes have strongly re-formed. Much of the sediment seems to have been transported to the center and outer portions of the bathymetry. At times, the chute to the south disappears, however the chute in the north is always

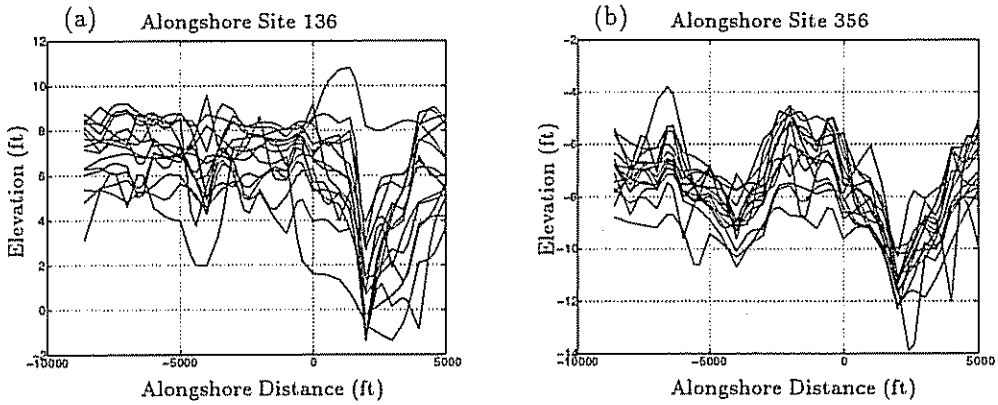

Figure 6.2: Envelope plots of alongshore lines for the Bethany Beach region. (a) Alongshore line 136 (136 feet from baseline). (b) Alongshore line 356 (356 feet from baseline).

present (Appendix B). The erosion chutes may be due to rip channels that quickly move sediment offshore, but is unlikely considering the large width of the channel, the expansive spacing between them, and the fact that they seem to be permanent. Typically, the spacing of rip channels discovered in nature is much smaller. Most likely these areas are caused by a lack of the groin field's influence or concentration of wave energy producing increased erosion. Note that ensuing nourishment episodes, in 1992 and 1994, occur in the two heavy erosion locations.

6.2 Shoreline Change

Cumulative shoreline changes for all the profile stations north and south of the origin from May 1989 to March 1995 are shown in Figure 6.4, Figure 6.5, and Figure 6.6. Gaps in the data indicate dates a survey was not taken. The shoreline increased significantly (75-100 feet) for all profile stations after the extensive beach nourishment project of 1989. The shoreline retreated after the initial fill and, after two and a half years, the shoreline has approximately returned to its original position at Bethany Beach (stations north of origin) and South Bethany (approximately

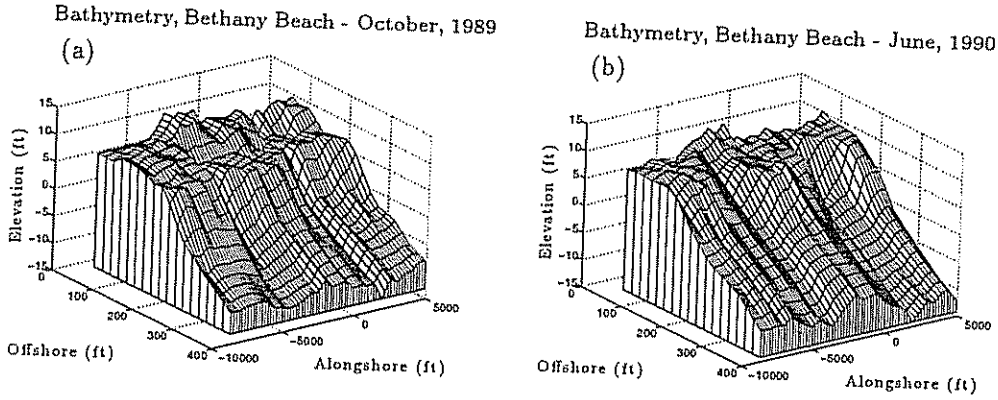

Figure 6.3: Bathymetric surveys for the Bethany Beach region (negative alongshore numbers indicate regions to the south of the center profile station). (a) Post-nourishment survey of October 1989. (b) Survey of June 1990.

stations 40+00S to 75+00S). The additional fills (of 1992 and 1994) were also visible at those two locations. Seasonal changes were not as significant as at Dewey Beach, rendering general trends in the data easier to perceive. Recession rates were evaluated in between the initial nourishment and the nourishment of 1992. The shoreline was broken into profile stations exhibiting similar recession rates. Table 6.2 shows the rates for the various sub-sections. Considering the recession rates are computed immediately following a fill, the actual values are certainly enhanced. However, the variation of the rates alongshore indicates areas where increased erosion is occurring.

Table 6.2: Recession Rates for Bethany Beach Following 1989 Nourishment.

Profile Sub-Section	Recession Rate (ft/yr)
0+00N - 5+00N	6.7
10+00N - 20+00N	16.7
25+00N - 35+00N	22.4
40+00N - 45+00N	5.5
5+00S - 25+00S	9.23
30+00S - 45+00S	12.7
50+00S - 75+00S	33.7

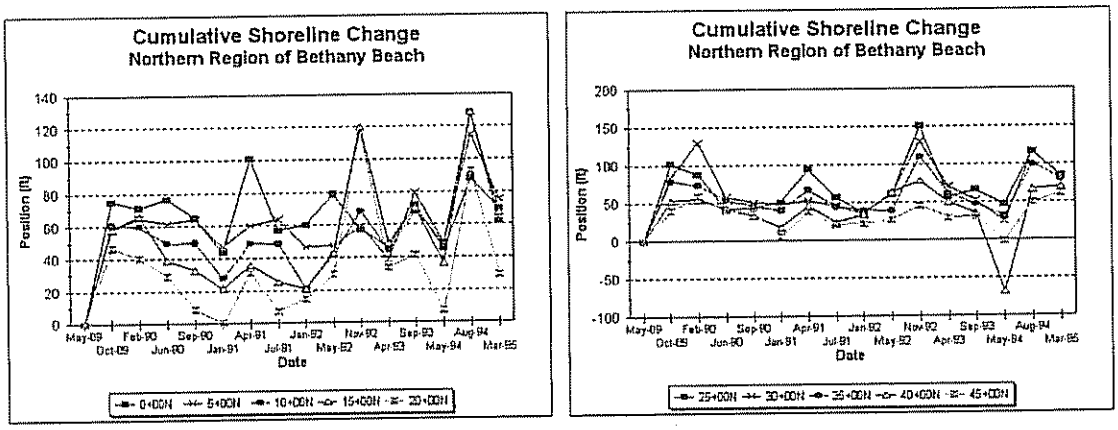

Figure 6.4: Cumulative shoreline plots for the region north of station 0+00N at Bethany Beach. Shoreline positions are shown relative to the shoreline position of May 1989 for each station.

6.3 2-D CPCA Applied to Bethany Beach

In this section, the two-mode CPCA model is applied to the Bethany Beach shoreline. The plan view of the shoreline as it evolves over the study period is shown in Figure 6.7. The initial fill was immediately evident in the shoreline position of October 1989. The shoreline retreated quickly and maintained a relatively constant position through much of the time period. Again, the two increased erosion areas are evident throughout the plots.

The eigenvectors produced from the analysis are shown in Figure 6.8. The mean shoreline (top panel) is characterized by considerable amplitude variations, which relate to the two high erosion locations. The mean, which is entirely real, accounts for 87% of the total variance and has no motion is associated with it. The second component (middle panel) accounts for 7.5% of the variance and shows a partially organized pattern of movement. The third component (bottom panel), although containing 2% of the variance, shows no consistent motion.

The spatial and temporal phase functions are shown in Figure 6.9. Using the computed wave number and frequency results, the second component is found

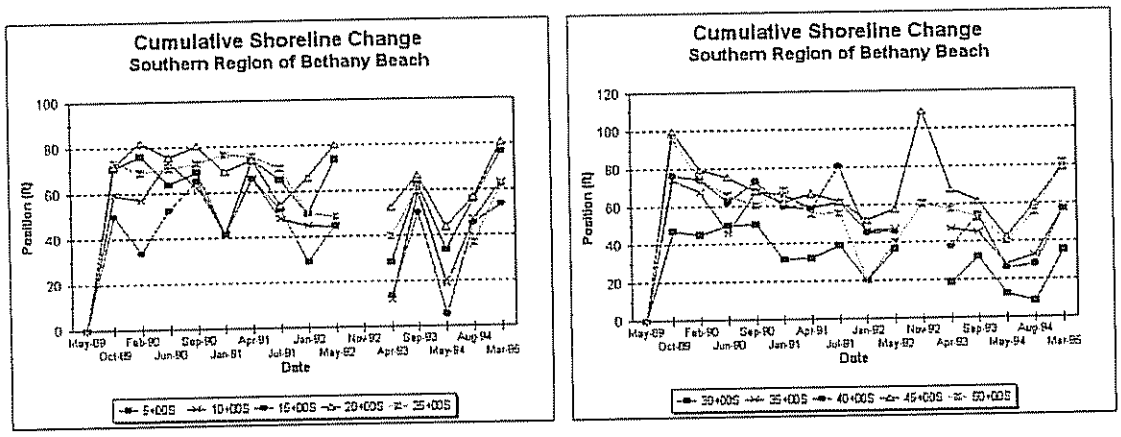

Figure 6.5: Cumulative shoreline plots for the region south (5+00S to 50+00S) of station 0+00N at Bethany Beach. Shoreline positions are shown relative to the shoreline position of May 1989 for each station.

to have a speed of 7.25 feet per day to the north. This result may not be entirely accurate because of the lack of continuity in rotation of the second component.

6.4 3-D CPCA Applied to Bethany Beach

The three-mode analysis proved to be less beneficial for Bethany Beach than for the previous areas. The analysis did not resolve any consistent progressive movement. Two eigenvector combinations (A1O1 and A2O2) captured over 99% of the variance for all time components. Also, only the real portion of each component had any significance. Figure 6.10 shows the real portion of each combination. The A1O1 combination, representing 94.2%, 92.7%, and 95% of the total variance for each respective time component, is shown in Figure 6.10a. The combination obviously represents the mean bathymetry and illustrates the power of CPCA to separate out all pertubations from the mean. The combination is remarkably smooth compared to the actual bathymetries in Appendix A. The A2O2 combination, representing 5.7%, 6.5%, and 5.0% for each respective time component, is shown in Figure 6.10b. This combination represents the erosional channels prevalent within the bathymetry. The

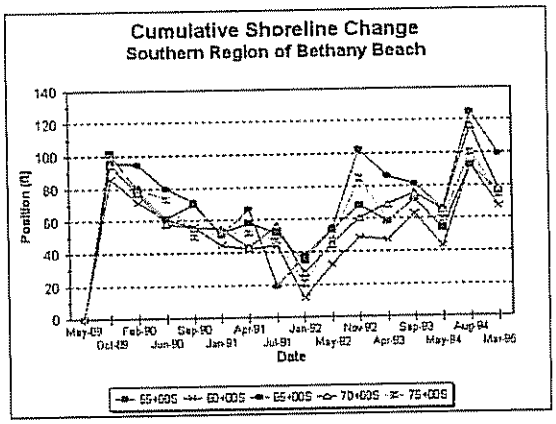

Figure 6.6: Cumulative shoreline plots for the region south (55+00S to 75+00S) of station 0+00N at Bethany Beach. Shoreline positions are shown relative to the shoreline position of May 1989 for each station.

summation of the two gives a reasonable estimate of the Bethany Beach bathymetry.

The dominant features in the Bethany Beach area is certianly the two erosional channels within the bathymetry. As a result of the non-periodic beach nourishment episodes (presented in Table 6.1), physical interpretation of the three-mode analysis became difficult. CPCA struggled to identify any organized pattern of movement within the bathymetry, except for the reformation of the two "chutes" after each nourishment. These unusual and unexplained features dominated the analysis and may have suppressed, if any existed at all, other consistent fluctuations in the region. The channels were identified as a standing motion (no imaginary portion was evident in combination A2O2) due to the intermittent nourishments and subsequent, relatively quick, reformation of the features.

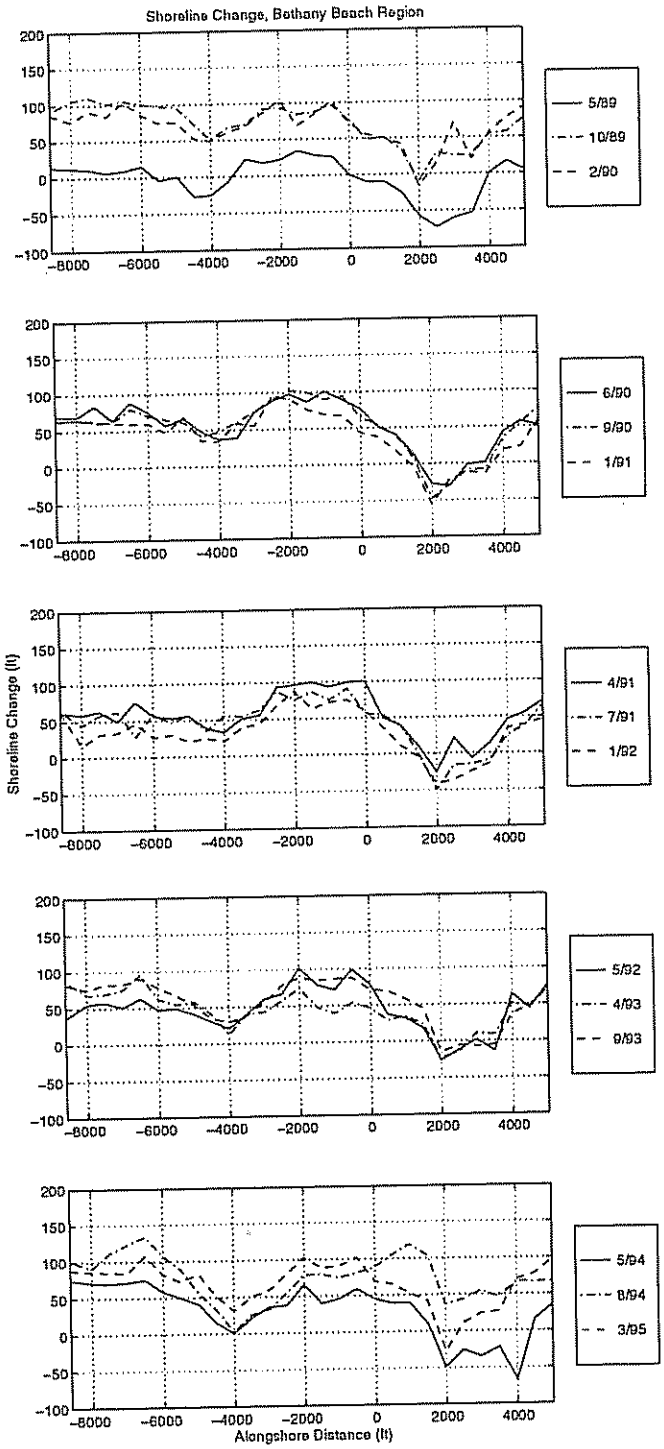

Figure 6.7: Plan view of the Bethany Beach shoreline as it evolves through time.

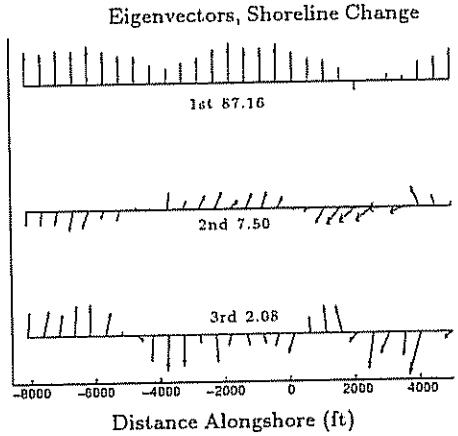

Figure 6.8: Eigenvectors computed by 2-mode CPCA for the Bethany Beach shoreline. The numbers correspond to the percent of total variance contained in each component.

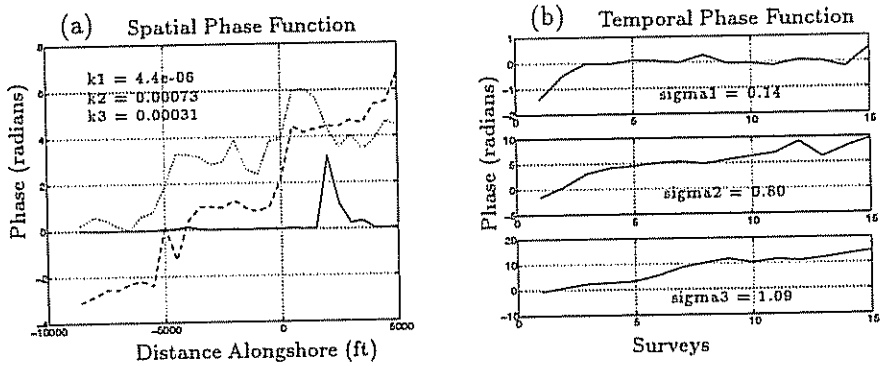

Figure 6.9: (a) Spatial phase functions of the first three components for the Bethany Beach shoreline. The numbers correspond to the wave number of each component. (b) Temporal phase functions of the same components. The numbers correspond to the instantaneous frequency of each component.

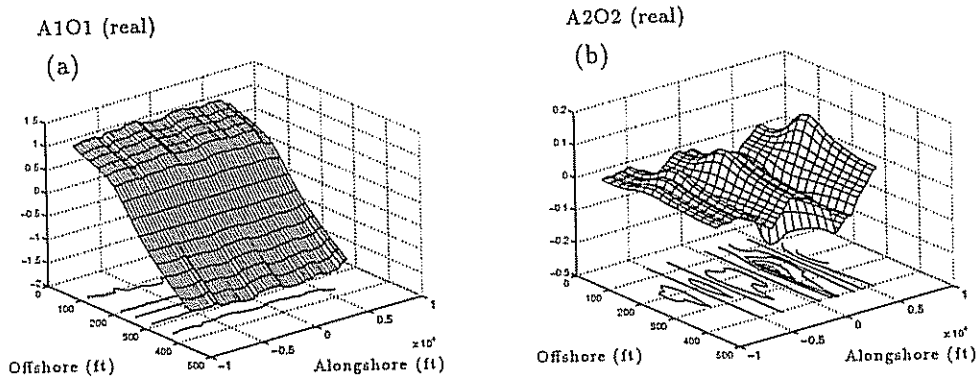

Figure 6.10: (a) The real portion of eigenvector combination A1O1 for Bethany Beach. This combination represents the mean bathymetry of the region. (b) The real portion of eigenvector combination A2O2. This combination represents the erosional channels prevalent in the bathymetry.

Chapter 7

CUMULATIVE SHORELINE

Having focused on specific areas along the Delaware coast in previous chapters, this chapter undertakes a general investigation of the entire coastline. Utilizing avialable data, shoreline changes, volume changes, and an integrated sediment budget are calculated. The hope is to obtain a solid understanding of the historic trends as well as possible future trends for the Delaware coast. Through a large scale examination of the coast, comparisons and contrasts can be made between major stretches of the coast.

7.1 Field Data

Beach profile data were obtained from the Line Reference Points (LRP) system established by the U.S. Army Corps of Engineers. The profiles extend from Cape Henlopen to the Delaware-Maryland state border. The Corps of Engineers used the LRP profiles as a system of locations seperated into seven (7) reaches within the range. Figure 7.1 presents the locations of the profile lines and the various reaches. An initial LRP survey was taken in 1964, and then abandoned until 1982. From 1982 until 1994, more frequent monitoring has occured. Approximately one (1) to two (2) surveys were taken every year for most LRP sites.

7.2 Shoreline Change

Shoreline change analysis is utilized to examine shoreline changes in time and to determine if the beach is stable, retreating, or accreting. The Corps of Engineers

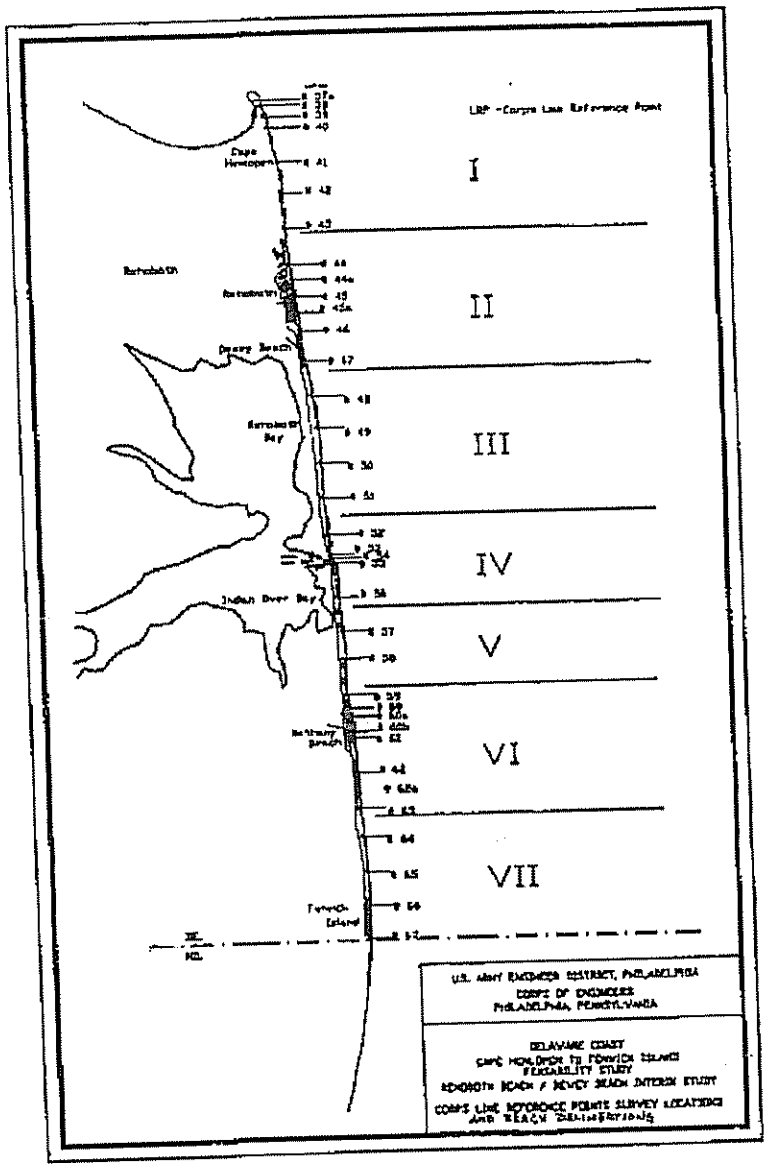

Figure 7.1: U.S. Army Corps of Engineers Line Reference Points survey locations (U.S. Army Corps of Engineers, 1996).

(1996) conducted a historic shoreline change analysis on the LRP profiles to establish reasonable estimate of long-term rates of change. By calculating the shoreline position for each survey from 1962 forward, the Corps performed a linear regression analysis for each profile station. The results are presented in Table 7.1. The analysis uncovers some expected results, such as accretion at Cape Henlopen (due to dominant northward littoral drift) and erosion at Dewey Beach and North of Indian River Inlet. However, some of the results are unexpected, for example the erosion South of Indian River Inlet. Variability, both spacially and temporally, is indicated by the flucuating rates within each reach and throughout the study area. This also indicates potential for sediment movement along the coast.

Utilizing the regression analysis developed by the U.S. Army Corps, this study conducts a similar shoreline regression analysis. However, here the shoreline position measured in 1962 is discarded, while two (2) additional surveys in measured in 1994 are added. The hope is to provide a more accurate representation of shoreline change rates by including only both frequent and recent measurements. Therefore, the regression analysis looks at LRP surveys from 1982 until 1994. Figure 7.2 shows an example of the analysis for the LRP site number 39, located at Cape Henlopen. Data points represent the measured shoreline position at each survey and the solid line is the linear fit through the data. As expected, the linear fit line indicates an advance in position at the approximate rate of 0.93 ft/yr. Cape Henlopen is considered an area of accretion, which the shoreline position verifies. Regression analysis for the remaining LRP sites are presented in Appendix C. Table 7.2 presents the results from the shoreline regression analysis for the LRP sites with adequate data.

Again, the results show various flucuations along the coast indicating a potential for movement of sediment. The results presented here do show less variability

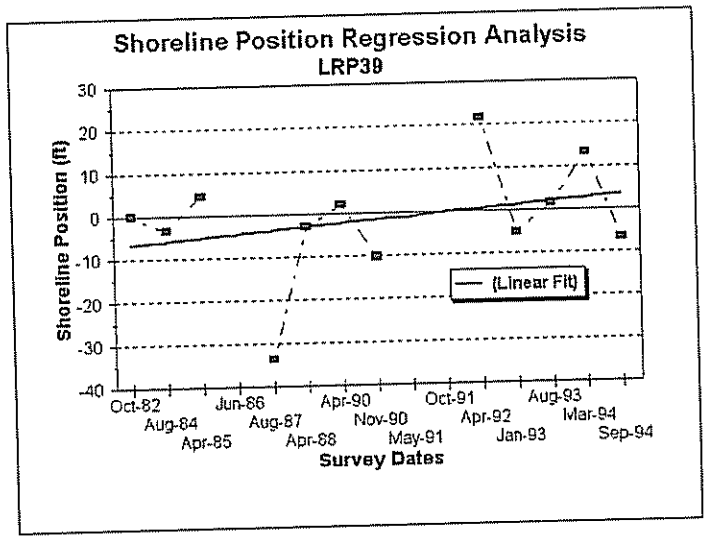

Figure 7.2: Shoreline regression analysis for LRP site 39 (Cape Henlopen). Shoreline position measurements are taken from October 1982 to September 1994.

than those presented by the U.S. Army Corps of Engineers (1996). Erosion dominates in the LRP sites north of Indian River Inlet, while significant erosion occurs in only one profile line (LRP 55) south of the inlet! Recent shoreline trends indicate erosion, on a long-term scale, is no longer occurring in the southern portion of the Delaware Atlantic coastline. The introduction of massive beach nourishment programs and increased structural intervention may have stabilized the area. Certainly the large accreational rate exhibited at Fenwick Island and the Delaware/Maryland State line is due to the beach nourishment efforts along that stretch of coastline. Also, recall the southern region of Dewey Beach exhibited higher erosion than the north (Chapter 5). Both analyses verify the increased erosion in the southern stretch of the Dewey Beach region.

7.3 Volume Change

The volume change of a profile may be a more accurate method of describing an individual profile's behavior (depending on the accuracy of the surveys). In this section, profile volume changes are computed at each LRP site by breaking the profile into "vertical slices" with vertical bounds at both ends of the profile. Volume changes can then be computed for successive surveys of each profile line by finding changes in elevation and cross-sectional area.

Each survey is linearly interpolated into a series of uniformly spaced elevations. Boundaries are established at both starting and ending distances. Selecting boundaries that remain within the actual domain for each survey is obviously important. The region between the boundaries can then be digitized using a selected interval. Once all the surveys of one profile have been digitized, it is possible to compute the elevation change at each digitized distance between a survey. The incremental change in cross-sectional area can also be computed by averaging adjacent elevation changes and then multiplied by the unit beach width to compute incremental volumes, which are summed to obtain a "net" profile change. This is then interpreted as the total material added or removed from the surveyed area. Cumulative changes in net volume, relative to the first survey, are also found for each profile.

Figure 7.3 presents the volume changes for LRP site 39. The plot shows the net profile volume change (thick solid line) as well as "above datum" (solid line) and "below datum" (dashed line) volume changes. The above and below datum changes are calculated based on the vertical bounds at the end of the computational area and using a horizontal bound at the datum intercept. The datum is defined as the mean sea level (MSL) for the analysis. As in the shoreline change results, the volume change indicates accretion at Cape Henlopen. Again, gaps in the data indicate periods when no survey was measured. The results for the remaining LRP

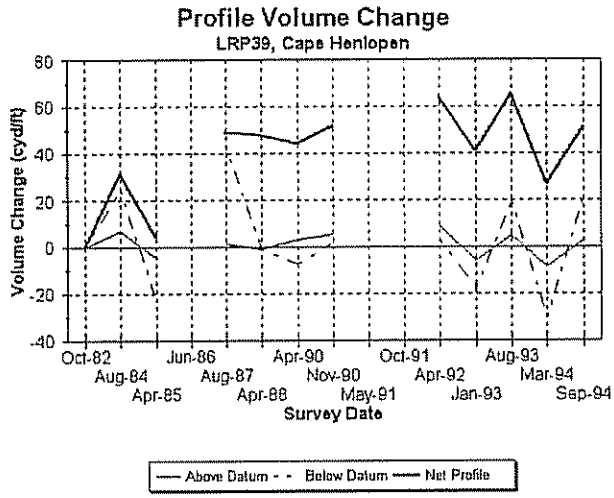

Figure 7.3: Volume changes for LRP site 39 (Cape Henlopen)

locations are presented in Appendix D. Unlike the shoreline analysis, many areas north of the inlet indicate accretion.

7.4 Sediment Budget

As presented in Chapter 4, a sediment budget was conducted for the northern region of the Delaware coast implementing Indian River Inlet as a natural divisional point. Unlike the volume change presented in the previous section, not all of the surveys could be utilized. A consistent distance offshore was required to complete a reasonable attempt at a coastwide sediment budget. Therefore, the sediment budget suffers by the loss of both profile stations along the coast and measurements in time. Another major constraint in the analysis is the extremely large distance between profile sites. Therefore, any mild change occurring at a profile site is multiplied by the distance extending to the next profile site, which in cases was over 10,000 feet. In essence, the minimized spatial resolution alongshore can result in massive errors in sediment quantity. The result of the analysis, which included all known bypassing and nourishment episodes, indicated an increase in total volume of approximately

10 million cubic yards north of Indian River Inlet. This result is only an order of magnitude approximation.

Table 7.1: Delaware Atlantic Coast Profile Trends (U.S. Army Corps of Engineers, 1996).

Profile	Approximate Location	Regression Shoreline Change Rate (ft/yr)
LRP39	Cape Henlopen	3.23
LRP40	Cape Henlopen	3.03
LRP41	Cape Henlopen St. Park	-5.49
LRP42	Cape Henlopen St. Park	-4.58
LRP43	Cape Henlopen St. Park	-9.62
LRP44a/44b	Whiskey and Deauville	-2.89
LRP45/45a	Rehoboth Beach	-0.73
LRP46	North End - Dewey Beach	-1.50
LRP47	Dewey Beach	-4.59
LRP48	South End - Dewey Beach	-6.12
LRP49	Key Box Road	-8.83
LRP50	Delaware Seashore St. Park	-6.92
LRP51	Delaware Seashore St. Park	-4.63
LRP52	Delaware Seashore St. Park	-5.90
LRP53	North of Indian River Inlet	-4.52
LRP54	North of Indian River Inlet	-7.05
LRP55	South of Indian River Inlet	-6.91
LRP56	South of Indian River Inlet	-3.02
LRP57	State Park	-1.30
LRP58	State Park	-1.52
LRP59	North End - Bethany Beach	2.83
LRP60	Bethany Beach	-0.096
LRP60a/60b	Bethany Beach	1.74
LRP61	South Bethany	2.75
LRP62	South Bethany	-1.73
LRP63	Fenwick Is. St. Park	-4.27
LRP64	Fenwick Is. St. Park	-5.23
LRP65	Fenwick Is. St. Park	-2.31
LRP66	Fenwick Is.	1.08
LRP67	DE-MD State Line	1.22

Note: Negative values (-) indicate erosion.

Table 7.2: Delaware Atlantic Coast Recent Shoreline Trends.

Profile	Approximate Location	Regression Shoreline Change Rate (ft/yr)
LRP39	Cape Henlopen	0.93
LRP42	Cape Henlopen St. Park	-5.37
LRP44a	Whiskey and Deauville	2.68
LRP44b	Whiskey and Deauville	-1.95
LRP45	Rehoboth Beach	-4.28
LRP45a	Rehoboth Beach	-2.64
LRP46	North End - Dewey Beach	-2.92
LRP47	Dewey Beach	-2.95
LRP48	South End - Dewey Beach	-7.23
LRP50	Delaware Seashore St. Park	-2.68
LRP51	Delaware Seashore St. Park	-1.34
LRP52	Delaware Seashore St. Park	-3.15
LRP53	North of Indian River Inlet	-4.53
LRP55	South of Indian River Inlet	-4.62
LRP56	South of Indian River Inlet	2.47
LRP57	State Park	2.58
LRP59	North End - Bethany Beach	5.83
LRP60b	Bethany Beach	6.88
LRP62	South Bethany	2.18
LRP63	Fenwick Is. St. Park	-0.03
LRP65	Fenwick Is. St. Park	2.14
LRP66	Fenwick Is.	7.37
LRP67	DE-MD State Line	11.17

Note: Negative values (-) indicate erosion.

Chapter 8

CONCLUSIONS

Over the years, a number of studies and reports have been written describing various aspects of the Delaware coastline. However, data collected over the last decade has not been examined. This work has analyzed many large sets of recent data to gain a better understanding of not only the Delaware Atlantic coast and specific features along the shore, but also profile analysis in general. Implementation of a broad range of tools, including introduction of CPCA, is applied in order to comprehensively analyze the profile data.

Long-term coastal processes and the overall wave climate were examined for the Delaware region to provide a background understanding. The relative sea-level change was found to be rising at approximately 1.0 foot per century. The wave climate indicated strong seasonal effects. Significant increases in wave height, and consequently wave power, greatly influence the behavior in the coastal zone.

Principal component analysis has been applied in numerous fields to explore spatial and temporal relations within a data set with the ability to express complicated variations in a few modes. Initial expansion of the tool into a complex form showed impresssive results (Liang and Seymour, 1991; Kroonenberg and DeLeeuw, 1980). CPCA was shown the ability to identify both standing and progressive movement, not just standing oscillations. Could then CPCA identify a moving form, or sand wave, initialized by a bypassing or beach nourishment? Could CPCA be expanded to three-dimensions to identify movement in multiple directions?

An in-depth analysis of the profiles in the Indian River Inlet, Delaware region has been accomplished by using standard analysis tools and CPCA. Early returns of the sand bypassing system seem to be positive. The shoreline analysis reveals that the north shore has been stabilized by the bypassing and the south shore recovers quickly from the eduction process. The inlet, as well as the sand bypassing system, show an influence extending approximately 3,500 feet on both the north and south shoreline positions. The volume changes and sediment budget indicate sand is moving to the north at a rate of 104,000 yd^3 per year. Therefore, efforts should be made to bypass a minimum of 100,000 yd^3 per year in order to sufficiently nourish the north shore. A sediment supply is readily available from the south, indicated by the quick closure of cavities left by the eductor and the stability of the southern shoreline position. Even-odd analysis performed on Indian River Inlet revealed a significant background erosion in the region and an inlet influence of 1 mile on both the north and south shorelines. Although accreation was evident in the summer season, erosion occurred during the remainder of the year. Background erosion accounted for an average retreat of approximately 7.5 feet per year. Generally, sand moves quickly to the north as evident from both the shoreline variation and CPCA analysis. Initally, the goal was to determine if we could identify the large quantities of sand bypassed across Indian River Inlet as moving forms, or sand waves that travel alongshore and eventually disperse to extinction. CPCA has shown to identify movement, as well as its speed, frequency, and direction, for the regions of Indian River Inlet. North of the inlet, a feature was found moving to the north at the rate of 5.5 feet per day with an amplitude of approximately 2.5 feet. Three-mode CPCA indicated a stronger progressive northward movement in the nearshore region, which became weaker offshore. Three-mode CPCA also indicated that eduction holes left from bypassing were nourished from both the alongshore and offshore directions.

Dewey Beach, which has become a growing tourist getaway, requires intermittent beach nourishments. Chapter 5 investigated the most recent, as well as largest, beachfill placed at Dewey Beach in the summer of 1994. Examination of the Dewey Beach shoreline positions indicated an extremely strong seasonal effect. Alongshore profile lines at Dewey Beach showed heightened erosion in the south when compared to the north. Utilizing volumetric changes, the estimated lifetime of the Dewey Beach nourishment of 1994 is approximately 6.4 years. A further extension of CPCA was utilized as two-mode CPCA was applied to the shoreline, rather than a specific distance from the baseline. A moving feature was identified to be moving at approximately 2.35 feet per day to the north. Three-mode CPCA for the region exhibits a significant movement in the on/offshore direction as the immediate influence of the nourishment results in the quick movement of sediment offshore. Alongshore movement was also depicted in the three-mode analysis for the Dewey Beach area, however, it was not as consistent or stout as identified in the two-mode analysis.

Bethany Beach is also undergoing a constant fight against the advancing ocean, therefore, necessitating scheduled beach nourishments. Shoreline recession rates indicate erosion of 5.5 to 33.7 feet per year following the beachfill of 1989. Two-mode CPCA, again applied to the shoreline position, revealed a inconsistent movement of approximately 7.5 feet per day to the north. Three-mode CPCA depicted the two odd erosional channels at Bethany Beach as a standing motion, constantly filling and reforming, during and after, each nourishment episode.

Utilizing available data, the entire stretch of Delaware Atlantic coastline was also evaluated. Since 1982, the shorelines south of Indian River Inlet have indicated accreation rather than erosion, indicating recent preventive measures have been beneficial. Overall erosion is still evident while north of Indian River Inlet, except at Cape Henlopen, the ever-growing spit at the northern extent of the coastline.

CPCA has been shown the potential to be an extremely powerful tool, however, future work needs to be undertaken a more finely sampled data set. CPCA has shown to identify movement, as well as its speed, frequency, and direction, in both two- and three-dimensional realms. With continued development, application, and understanding, CPCA can become unmatched in the ability to analyze bathymetric changes.

Beach profiles can provide a breadth of information about the nearshore coastal environment. Regular, maintained measurement programs should be established to monitor coastlines across the world, especially places with no historical data. Without any historical measurements of the coastlines, what information could we apply to potential erosion problems of today? What will future generations rely on? A well sampled and accurate bathymetry is unparalleled in characterizing the nature of a coastal environment.

REFERENCES

Aubrey, D. G. (1979). "Seasonal Patterns of Onshore/Offshore Sediment Movement." *J. of Geophys. Res.*, 84, 10, 6347-6354.

Barnett, T. P. (1983). "Interaction of the Monsoon and Pacific Trade Wind Systems at Interannual Time Scale. Part I: The equatorial zone." *Mon. Weather Review*, 111, 756-773.

Berek, E. P. and R. G. Dean (1982). "Field Investigation of Longshore Transport Distribution." *Proc. 18th Intl. Coastal Engineering Conf.*, ASCE, Cape Town, 1620-1639.

Clausner, J., Gebert, J., Watson, K., and A. Rambo (1992). "Sand Bypassing at Indian River Inlet, Delaware." The CERCular, Coatal Engineering Research Center, Vol CERC-92-1, 6 pp.

Coastal and Ocean Engineering and Research, Inc. (1983). "Sediment Budget and Sand Bypassing System Parameters for Delaware's Atlantic Coast." COER Inc., Newark, Delaware.

Dalrymple, R. A., Dean R. G., and R. Henry (1976). "Coastal Engineering Assesment of Delaware's Beach Erosion." (unpublished: University of Delaware, Newark, Delaware 19716).

Dalrymple, R. A. and D. W. Mann (1985). "A Coastal Engineering Assesment of Fenwick Island, Delaware." Ocean Engineering Technical Report No. CE-54, University of Delaware, Newark, Delaware, 19716.

Delaware State Highway Department (1956). "Beach Erosion - Delaware Bay and Atlantic Ocean." 1956 Report and Recommendations.

Dick, J. E. and R. A. Dalrymple (1983). "Coastal Engineering Study of Bethany Beach, Delaware." Ocean Engineering Research Report No. CE 83-38, University of Delaware, Newark, Delaware 19716.

Dick, J. E. and R. A. Dalrymple (1984). "Coastal Changes at Bethany Beach, Delaware." *Proc. 19th Intl. Conf. Coastal Engr.*, ASCE, Houston, 1650-1667.

Gebert, J., Watson, K., and A. Rambo (1992). "57 Years of Coastal Engineering Practice at a Problem Inlet: Indian River Inlet, Delaware." *Coastal Eng. Practice*, ASCE, 1-17.

Horel, J. D. (1984). "Complex Principal Component Analysis: Theory and Examples." *J. Climate Appl. Meteor.*, 23, 1660-1673.

Jensen, R. E. (1983). *Atlantic Coast Hindcast, Shallow-water, Significant Wave Information*, U.S. Army Engineer Waterways Experiment Station, Vicksburg, Mississippi.

Kraft, J. C. and C. J. John (1976). "The Geological Structure of the Shorelines of Delaware." University of Delaware, Newark Col. of Marine Studies, Sea Grant, Report No. DEL-SG-14-76.

Kroonenberg, P. M. and J. DeLeeuw (1980). "Principal Components Analysis of Three-Mode Data by Means of Alternating Least Squares Algorithms." *Psychometrika*, 45, 69-97.

Kroonenberg, P. M. (1985). "User's Guide to Tuckals3." Department of Education, University of Leiden, Leiden, Netherlands.

Lanan, G. A. and R. A. Dalrymple (1977). "A Coastal Engineering Study of Indian River Inlet, Delaware." University of Delaware, Newark Col. of Marine Studies, Sea Grant, Report No. DEL-SG-5-77.

Liang, G. and R. J. Seymour (1991). "Complex Principal Component Analysis of Wave-like Sand Motions." *Coastal Sediments '91*, ASCE, 2175-2186.

Liang, G., White T. E., and R. J. Seymour (1992). "Complex Principal Component Analysis of Seasonal Variation in Nearshore Bathymetry." *Proc. 23rd Intl. Coastal Eng. Conf.*, ASCE, 2242-2250.

Losada, M. A., Medina R., Vidal, C., and I. J. Losada (1992). "Temporal and Spatial Cross-shore Distributions of Sediment at 'El Puntal' Spit, Santander, Spain." *Proc. 23rd Intl. Coastal Eng. Conf.*, ACSE, 2251-2263.

Maurmeyer, E. M. and L. W. Carey (1985). *Striking a Balance: A Guide to Coastal Processes and Beach Management in Delaware*, Department of Natural Resources and Environmental Control, Dover, Delaware.

Medina, R., Losada, M. A., Dalrymple, R. A., and A. Roldan (1991). "Cross-shore Sediment Transport Determined by EOF Method." *Coastal Sediments '91*, ASCE, 2160-2174.

Medina, R., Vidal, C., Losada, M. A., A. J. Roldan (1992). "Three-Mode Principal Component Analysis of Bathymetric Data, Applied to 'Playa de Castilla' (Huelva, Spain)." *Proc. 23rd Intl. Coastal Eng. Conf.*, ASCE, 2265-2278.

Preisendorfer, R. W. (1988). *Principal Component Analysis in Meteorology and Oceanograhpy*, Elsevier Science Publishing Company, New York, New York.

Strine, M. A. (1991). "A Probabilistic Prediction of Beach Nourishment Project Lifetimes." *Master's Thesis*, University of Delaware, Newark, Delaware 19716.

Thompson, W. W. and R. A. Dalrymple (1976). "A History of Indian River Inlet, Delaware." *Shore and Beach*, Vol. 7, 24-31.

Tucker, L. R. (1966). "Some Mathematical Notes on Three-Mode Factor Analysis." *Psychometrika*, 31, 279-311.

U.S. Army Corps of Engineers (1956). "Delaware Coast from Kitts Hummock to Fenwick Island, Beach Erosion Control Study." U.S. Army Corps of Engineers, Philadelphia, Pennsylvania, 47 pp.

U.S. Army Corps of Engineers (1968). "Beach Erosion Control and Hurricane Protection Along the Delaware Coast." House Document lk216, 85th Congress.

U.S. Army Corps of Engineers (1971). "The National Shoreline Study: Regional Inventory Report, North Atlantic Region, Vol. I." U.S. Army Corps of Engineers, New York, New York, 120 pp.

U.S. Army Corps of Engineers, Philadelphia District (1984). "General Design Memorandum Sand Bypass Plant: Indian River Inlet, Delaware." U.S. Army Corps of Engineers, Philadelphia, Pennsylvania.

U.S. Army Corps of Engineers, Philadelphia District (1994). "Indian River Inlet and Bay." (unpublished: U.S. Army Corps of Engineers, Philadelphia District, Philadelphia, Pennsylvania 19107).

U.S. Army Corps of Engineers, Philadelphia District (1996). "Rehoboth Beach/Dewey Beach Interim Feasibility Study: Final Feasibility Report and Final Environmental Impact Statement." U.S. Army Corps of Engineers, Philadelphia, Pennsylvania, 146 pp. and appendicies A-G.

Wallace, J. M. and R. E. Dickinson (1972). "Empirical Orthogonal Representation of Time Series in the Frequency Domain, Part I. Theoretical Considerations." *J. Appl. Meteorology*, 11, 887-892.

Watson, K. D., Clausner, J. E., and R. D. Henry (1993). "Beach Response to Sand Bypassing at Indian River Inlet, Delaware." *Coastal Technology*, ASCE, Hilton Head S.C.

Winant, C. D., Inman, D. L., and C. E. Nordstrom (1975). "Description of Seasonal Beach Changes using Empirical Eigenfunctions." *J. Geophy. Res.*, 80, 15, 1979-1986.

Appendix A

MONTHLY WAVE AVERAGES

This Appendix presents the monthly average of significant wave height, dominant wave period, and wave power. The various gaps that appear in the plots are the result of periods when no data are available.

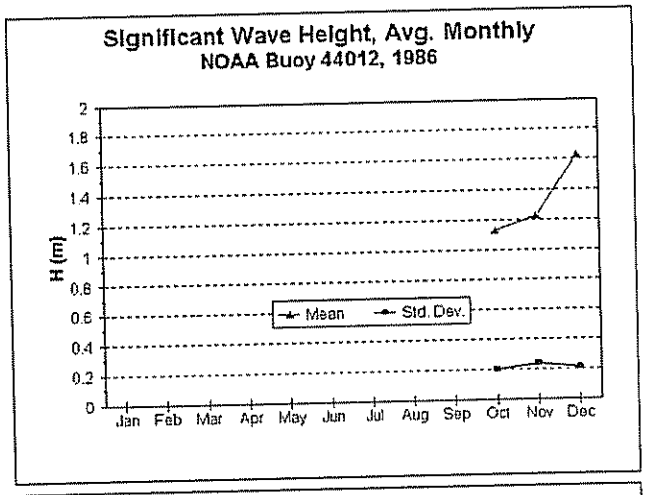
Significant Wave Height, Avg. Monthly
NOAA Buoy 44012, 1986
H (m)
2
1.8
1.6
1.4
1.2
1
0.8
0.6
0.4
0.2
0
Mean
Std. Dev.
Jan Feb Mar Apr May Jun Jul Aug Sep Oct Nov Dec

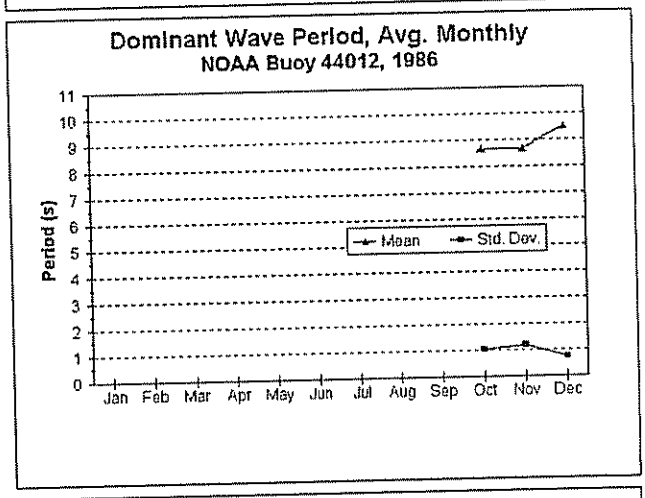
Dominant Wave Period, Avg. Monthly
NOAA Buoy 44012, 1986
Period (s)
11
10
9
8
7
6
5
4
3
2
1
0
Mean
Std. Dev.
Jan Feb Mar Apr May Jun Jul Aug Sep Oct Nov Dec

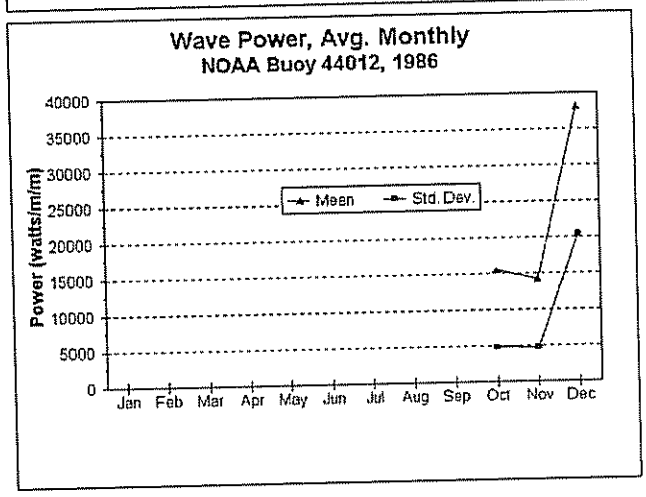
Wave Power, Avg. Monthly
NOAA Buoy 44012, 1986
Power (watts/m/m)
40000
35000
30000
25000
20000
15000
10000
5000
0
Mean
Std. Dev.
Jan Feb Mar Apr May Jun Jul Aug Sep Oct Nov Dec

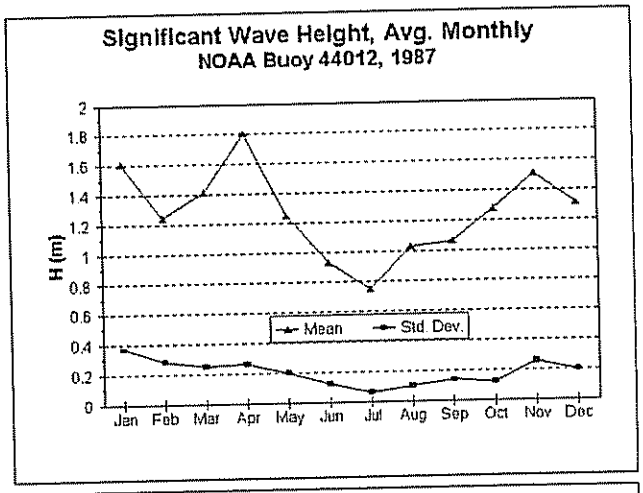
Significant Wave Height, Avg. Monthly
NOAA Buoy 44012, 1987
H (m)
2
1.8
1.6
1.4
1.2
1
0.8
0.6
0.4
0.2
0
Mean
Std. Dev.
Jan Feb Mar Apr May Jun Jul Aug Sep Oct Nov Dec

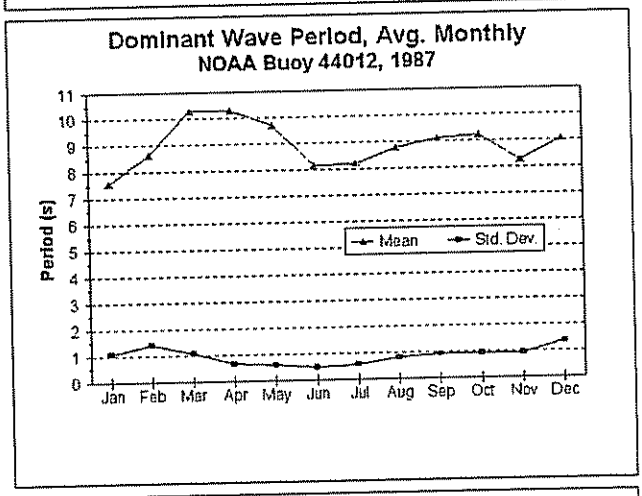
Dominant Wave Period, Avg. Monthly
NOAA Buoy 44012, 1987
Period (s)
11
10
9
8
7
6
5
4
3
2
1
0
Mean
Std. Dev.
Jan Feb Mar Apr May Jun Jul Aug Sep Oct Nov Dec

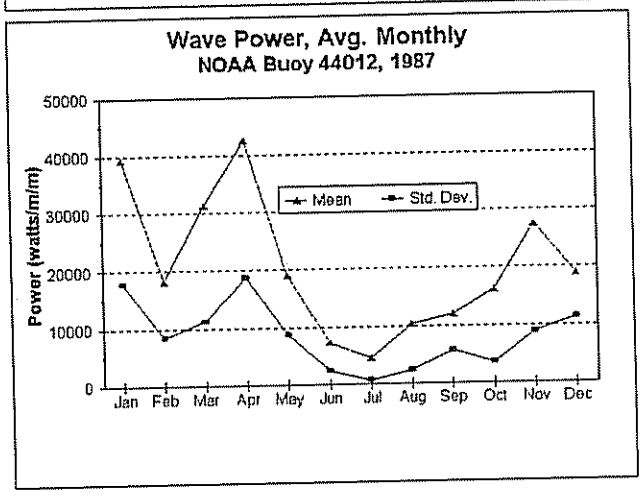
Wave Power, Avg. Monthly
NOAA Buoy 44012, 1987
Power (watts/m/m)
50000
40000
30000
20000
10000
0
Mean
Std. Dev.
Jan Feb Mar Apr May Jun Jul Aug Sep Oct Nov Dec

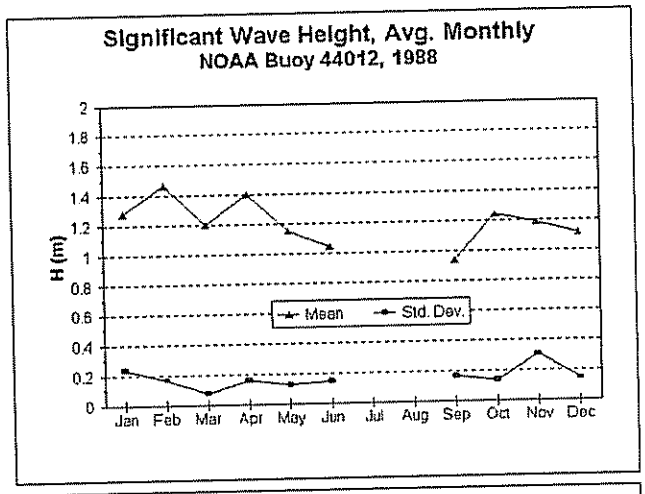
Significant Wave Height, Avg. Monthly
NOAA Buoy 44012, 1988
H (m)
2
1.8
1.6
1.4
1.2
1
0.8
0.6
0.4
0.2
0
Mean
Std. Dev.
Jan Feb Mar Apr May Jun Jul Aug Sep Oct Nov Dec

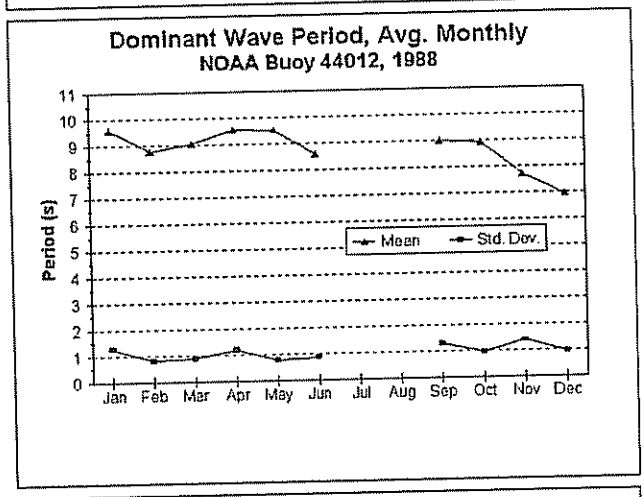
Dominant Wave Period, Avg. Monthly
NOAA Buoy 44012, 1988
Period (s)
11
10
9
8
7
6
5
4
3
2
1
0
Mean
Std. Dev.
Jan Feb Mar Apr May Jun Jul Aug Sep Oct Nov Dec

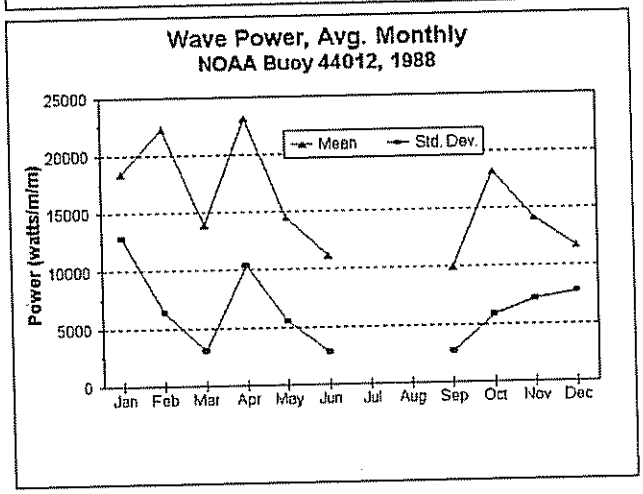
Wave Power, Avg. Monthly
NOAA Buoy 44012, 1988
Power (watts/m/m)
25000
20000
15000
10000
5000
0
Mean
Std. Dev.
Jan Feb Mar Apr May Jun Jul Aug Sep Oct Nov Dec

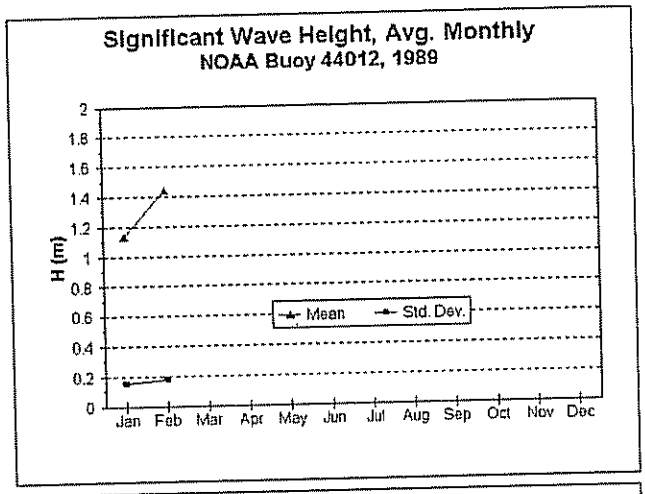
Significant Wave Height, Avg. Monthly
NOAA Buoy 44012, 1989
H (m)
2
1.8
1.6
1.4
1.2
1
0.8
0.6
0.4
0.2
0
Mean
Std. Dev.
Jan Feb Mar Apr May Jun Jul Aug Sep Oct Nov Dec

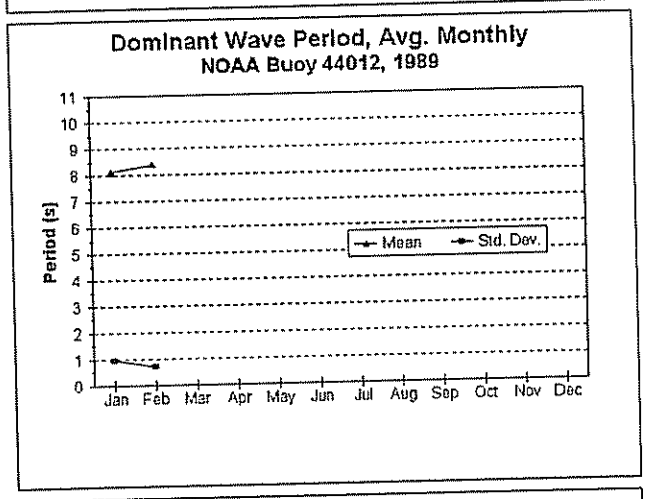
Dominant Wave Period, Avg. Monthly
NOAA Buoy 44012, 1989
Period (s)
11
10
9
8
7
6
5
4
3
2
1
0
Mean
Std. Dev.
Jan Feb Mar Apr May Jun Jul Aug Sep Oct Nov Dec

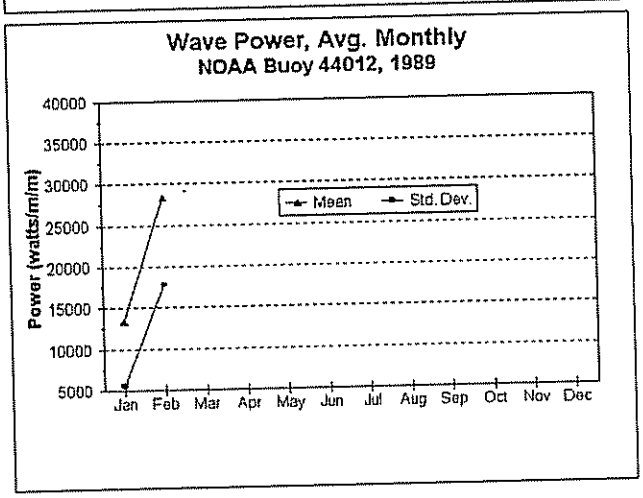
Wave Power, Avg. Monthly
NOAA Buoy 44012, 1989
Power (watts/m/m)
40000
35000
30000
25000
20000
15000
10000
5000
Mean
Std. Dev.
Jan Feb Mar Apr May Jun Jul Aug Sep Oct Nov Dec

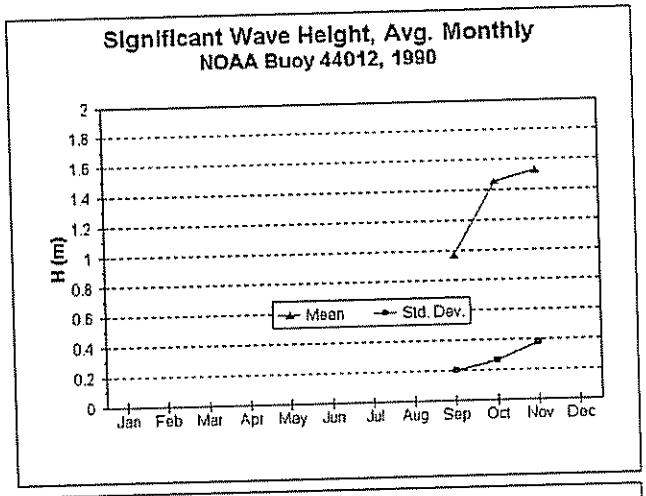
Significant Wave Height, Avg. Monthly
NOAA Buoy 44012, 1990
H (m)
2
1.8
1.6
1.4
1.2
1
0.8
0.6
0.4
0.2
0
Mean
Std. Dev.
Jan Feb Mar Apr May Jun Jul Aug Sep Oct Nov Dec

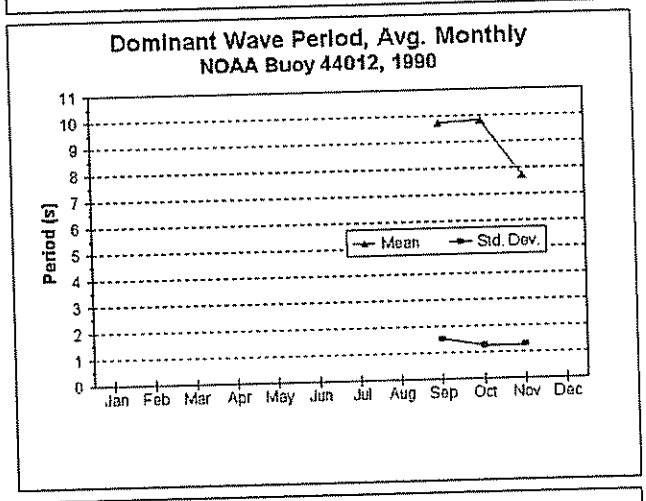
Dominant Wave Period, Avg. Monthly
NOAA Buoy 44012, 1990
Period (s)
11
10
9
8
7
6
5
4
3
2
1
0
Mean
Std. Dev.
Jan Feb Mar Apr May Jun Jul Aug Sep Oct Nov Dec

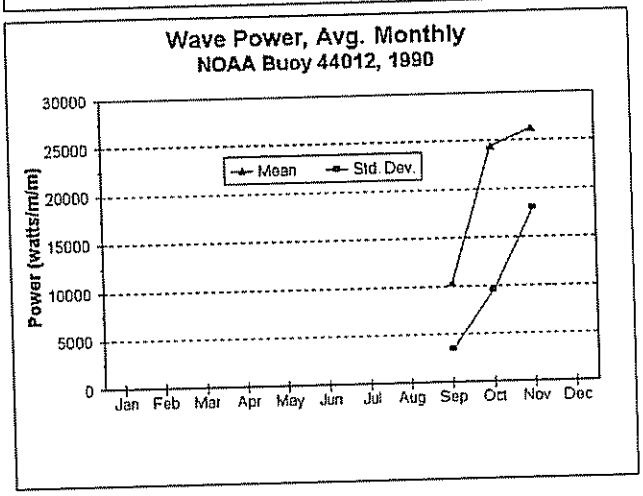
Wave Power, Avg. Monthly
NOAA Buoy 44012, 1990
Power (watts/m/m)
30000
25000
20000
15000
10000
5000
0
Mean
Std. Dev.
Jan Feb Mar Apr May Jun Jul Aug Sep Oct Nov Dec

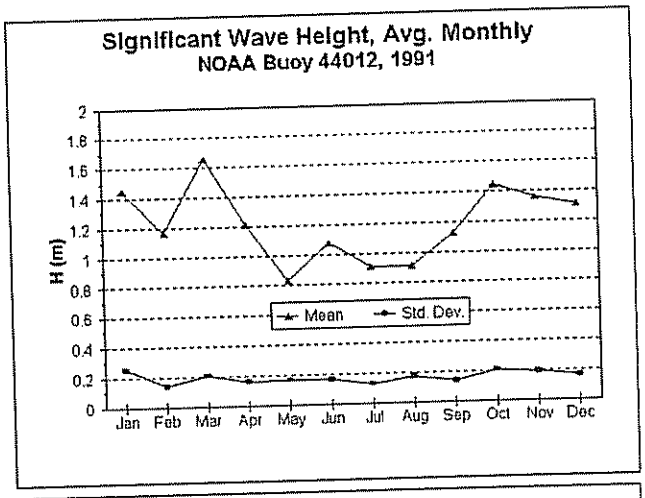
Significant Wave Height, Avg. Monthly
NOAA Buoy 44012, 1991
H (m)
2
1.8
1.6
1.4
1.2
1
0.8
0.6
0.4
0.2
0
Mean
Std. Dev.
Jan Feb Mar Apr May Jun Jul Aug Sep Oct Nov Dec

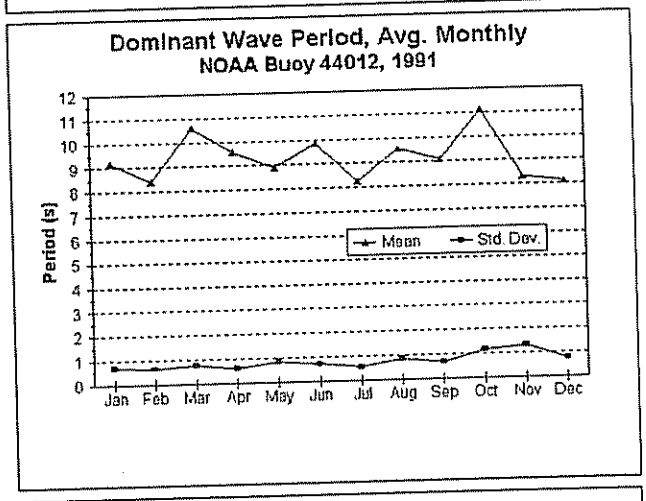
Dominant Wave Period, Avg. Monthly
NOAA Buoy 44012, 1991
Period (s)
12
11
10
9
8
7
6
5
4
3
2
1
0
Mean
Std. Dev.
Jan Feb Mar Apr May Jun Jul Aug Sep Oct Nov Dec

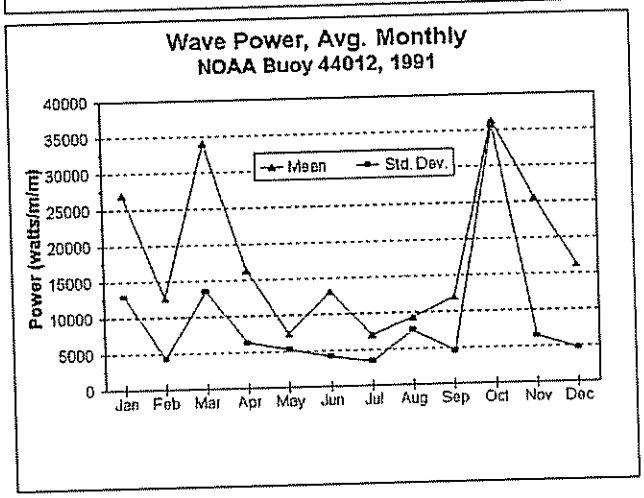
Wave Power, Avg. Monthly
NOAA Buoy 44012, 1991
Power (watts/m/m)
40000
35000
30000
25000
20000
15000
10000
5000
0
Mean
Std. Dev.
Jan Feb Mar Apr May Jun Jul Aug Sep Oct Nov Dec

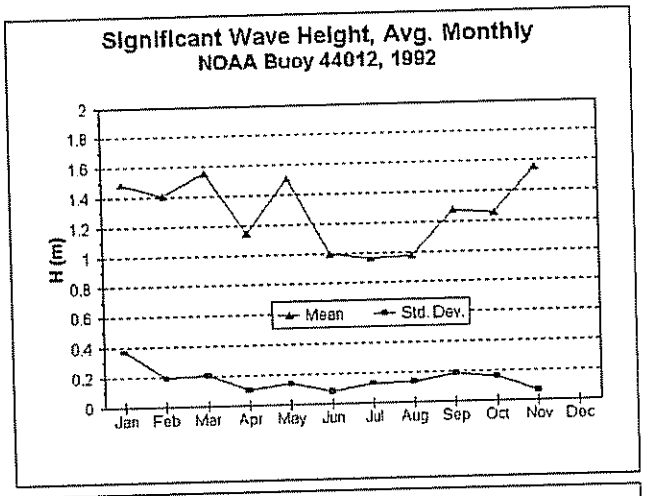
Significant Wave Height, Avg. Monthly
NOAA Buoy 44012, 1992
H (m)
2
1.8
1.6
1.4
1.2
1
0.8
0.6
0.4
0.2
0
Mean
Std. Dev.
Jan Feb Mar Apr May Jun Jul Aug Sep Oct Nov Dec

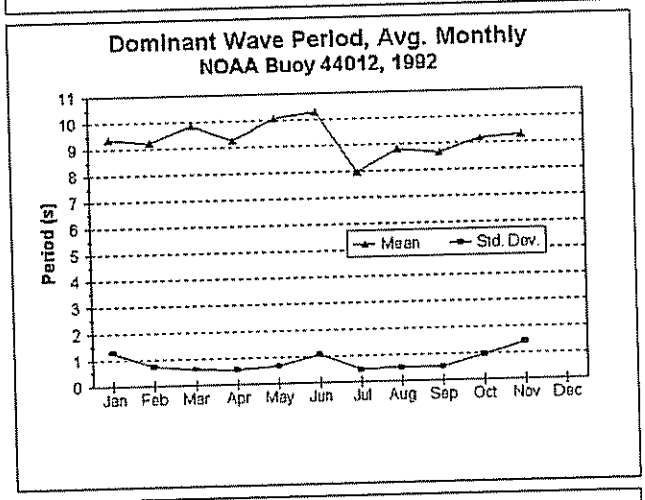
Dominant Wave Period, Avg. Monthly
NOAA Buoy 44012, 1992
Period (s)
11
10
9
8
7
6
5
4
3
2
1
0
Mean
Std. Dev.
Jan Feb Mar Apr May Jun Jul Aug Sep Oct Nov Dec

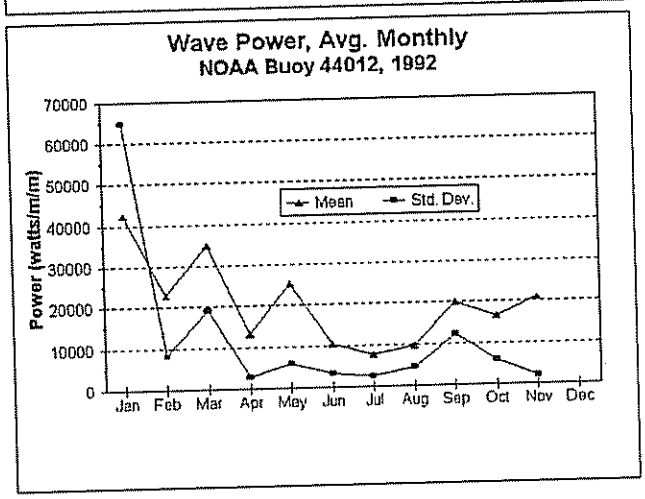
Wave Power, Avg. Monthly
NOAA Buoy 44012, 1992
Power (watts/m/m)
70000
60000
50000
40000
30000
20000
10000
0
Mean
Std. Dev.
Jan Feb Mar Apr May Jun Jul Aug Sep Oct Nov Dec

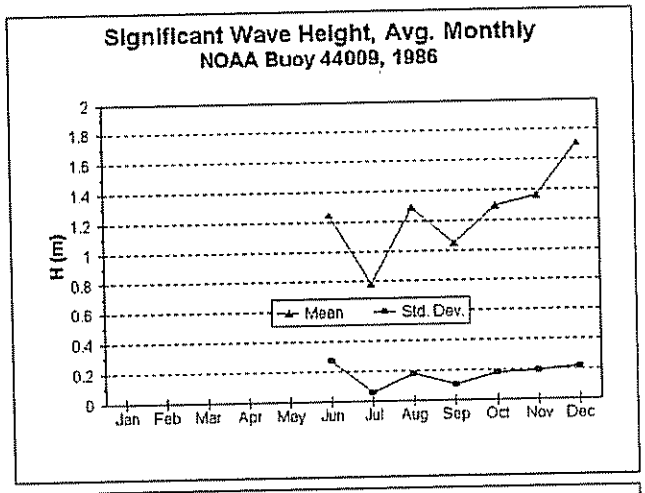
Significant Wave Height, Avg. Monthly
NOAA Buoy 44009, 1986
H (m)
2
1.8
1.6
1.4
1.2
1
0.8
0.6
0.4
0.2
0
Mean
Std. Dev.
Jan Feb Mar Apr May Jun Jul Aug Sep Oct Nov Dec

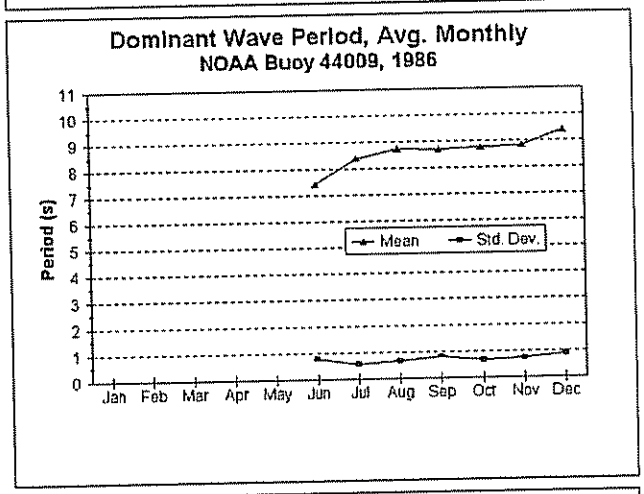
Dominant Wave Period, Avg. Monthly
NOAA Buoy 44009, 1986
Period (s)
11
10
9
8
7
6
5
4
3
2
1
0
Mean
Std. Dev.
Jan Feb Mar Apr May Jun Jul Aug Sep Oct Nov Dec

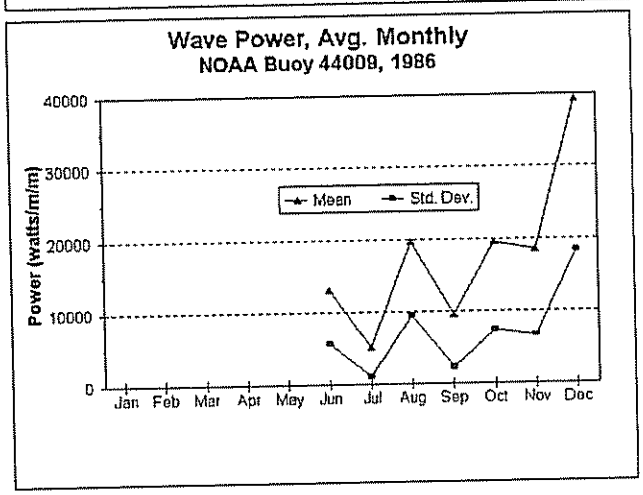
Wave Power, Avg. Monthly
NOAA Buoy 44009, 1986
Power (watts/m/m)
40000
30000
20000
10000
0
Mean
Std. Dev.
Jan Feb Mar Apr May Jun Jul Aug Sep Oct Nov Dec

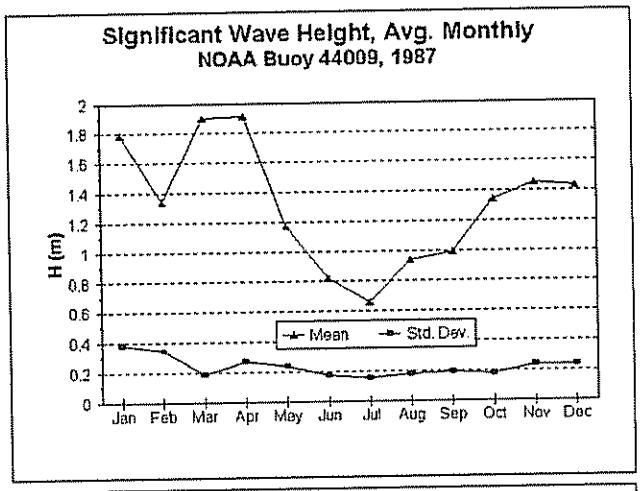
Significant Wave Height, Avg. Monthly
NOAA Buoy 44009, 1987
H (m)
2
1.8
1.6
1.4
1.2
1
0.8
0.6
0.4
0.2
0
Mean
Std. Dev.
Jan Feb Mar Apr May Jun Jul Aug Sep Oct Nov Dec

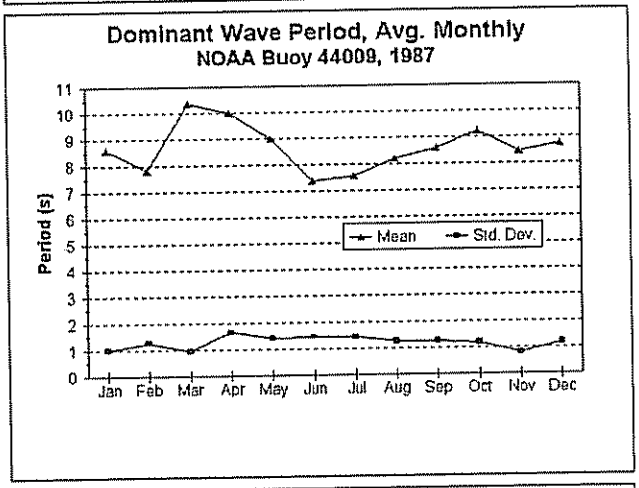
Dominant Wave Period, Avg. Monthly
NOAA Buoy 44009, 1987
Period (s)
11
10
9
8
7
6
5
4
3
2
1
0
Mean
Std. Dev.
Jan Feb Mar Apr May Jun Jul Aug Sep Oct Nov Dec

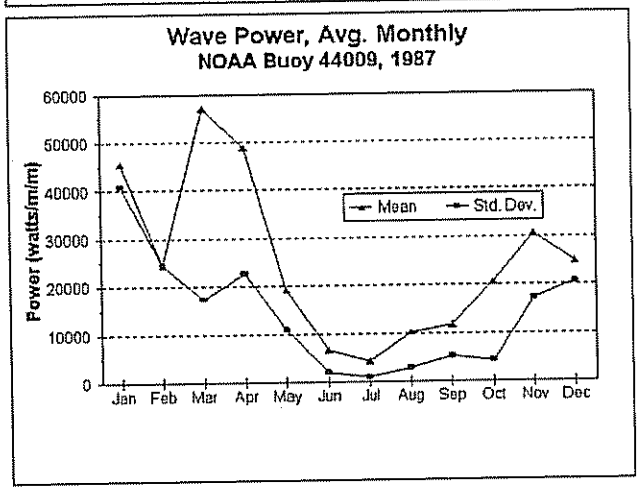
Wave Power, Avg. Monthly
NOAA Buoy 44009, 1987
Power (watts/m/m)
60000
50000
40000
30000
20000
10000
0
Mean
Std. Dev.
Jan Feb Mar Apr May Jun Jul Aug Sep Oct Nov Dec

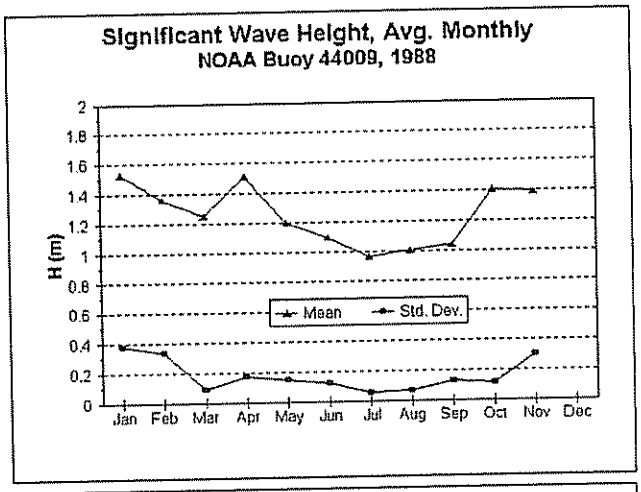
Significant Wave Height, Avg. Monthly
NOAA Buoy 44009, 1988
H (m)
2
1.8
1.6
1.4
1.2
1
0.8
0.6
0.4
0.2
0
Mean
Std. Dev.
Jan Feb Mar Apr May Jun Jul Aug Sep Oct Nov Dec

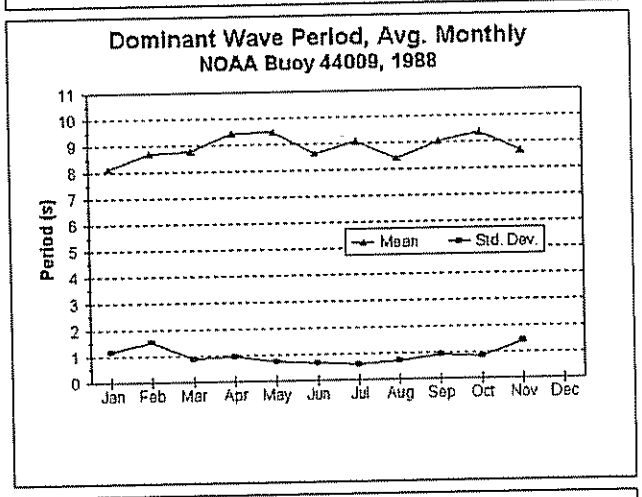
Dominant Wave Period, Avg. Monthly
NOAA Buoy 44009, 1988
Period (s)
11
10
9
8
7
6
5
4
3
2
1
0
Mean
Std. Dev.
Jan Feb Mar Apr May Jun Jul Aug Sep Oct Nov Dec

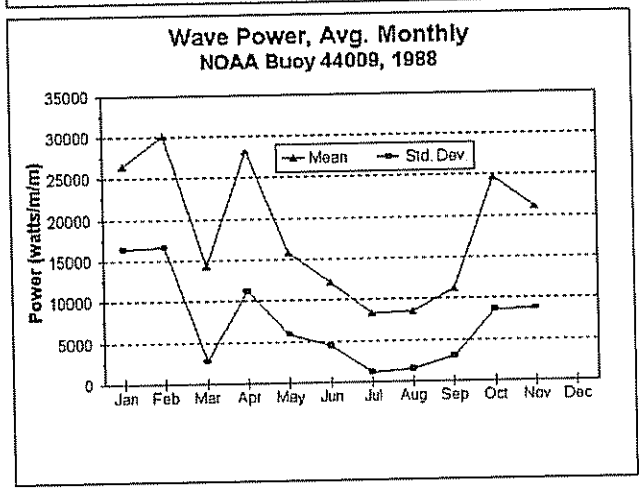
Wave Power, Avg. Monthly
NOAA Buoy 44009, 1988
Power (watts/m/m)
35000
30000
25000
20000
15000
10000
5000
0
Mean
Std. Dev.
Jan Feb Mar Apr May Jun Jul Aug Sep Oct Nov Dec

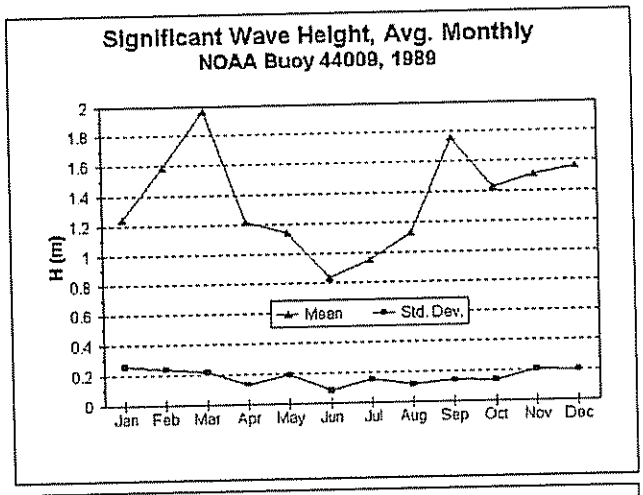
Significant Wave Height, Avg. Monthly
NOAA Buoy 44009, 1989
H (m)
2
1.8
1.6
1.4
1.2
1
0.8
0.6
0.4
0.2
0
Mean
Std. Dev.
Jan Feb Mar Apr May Jun Jul Aug Sep Oct Nov Dec

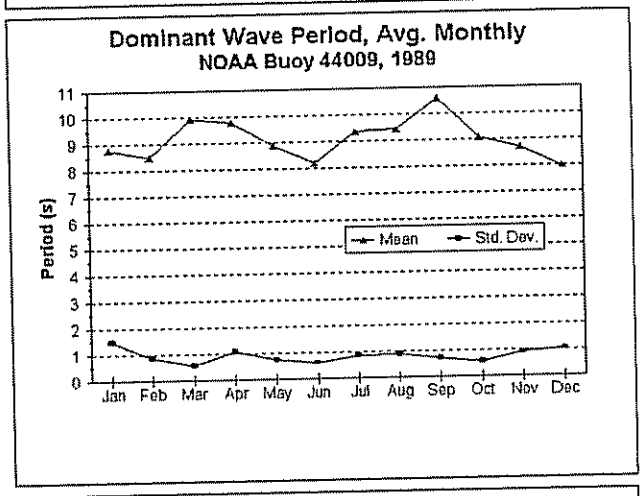
Dominant Wave Period, Avg. Monthly
NOAA Buoy 44009, 1989
Period (s)
11
10
9
8
7
6
5
4
3
2
1
0
Mean
Std. Dev.
Jan Feb Mar Apr May Jun Jul Aug Sep Oct Nov Dec

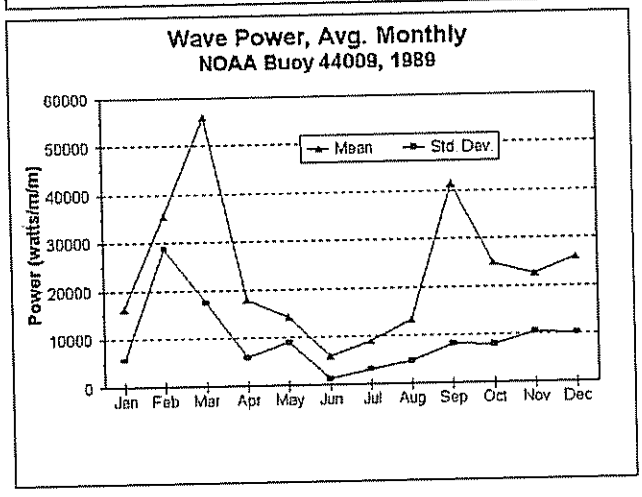
Wave Power, Avg. Monthly
NOAA Buoy 44009, 1989
Power (watts/m/m)
60000
50000
40000
30000
20000
10000
0
Mean
Std. Dev.
Jan Feb Mar Apr May Jun Jul Aug Sep Oct Nov Dec

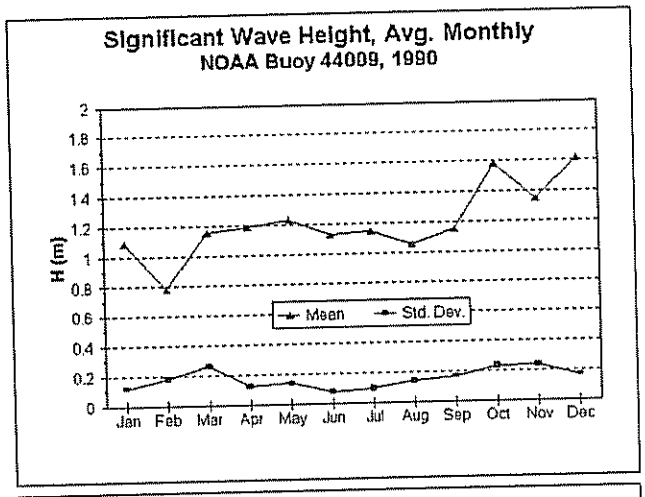
Significant Wave Height, Avg. Monthly
NOAA Buoy 44009, 1990
H (m)
2
1.8
1.6
1.4
1.2
1
0.8
0.6
0.4
0.2
0
Mean
Std. Dev.
Jan Feb Mar Apr May Jun Jul Aug Sep Oct Nov Dec

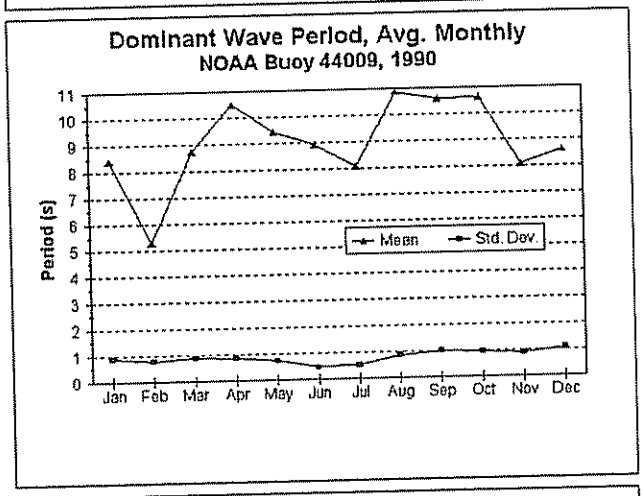
Dominant Wave Period, Avg. Monthly
NOAA Buoy 44009, 1990
Period (s)
11
10
9
8
7
6
5
4
3
2
1
0
Mean
Std. Dev.
Jan Feb Mar Apr May Jun Jul Aug Sep Oct Nov Dec

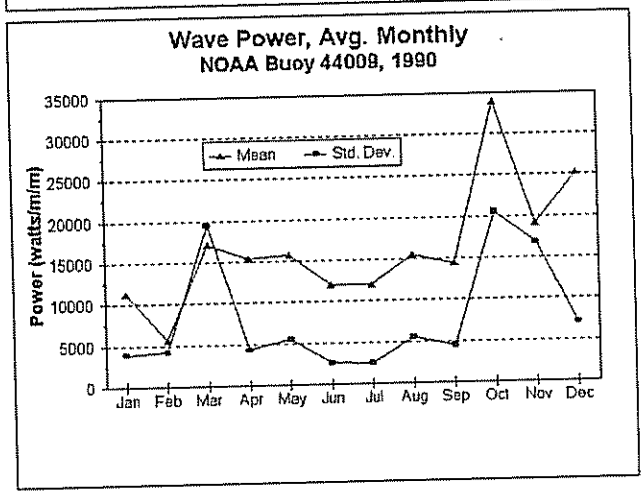
Wave Power, Avg. Monthly
NOAA Buoy 44009, 1990
Power (watts/m/m)
35000
30000
25000
20000
15000
10000
5000
0
Mean
Std. Dev.
Jan Feb Mar Apr May Jun Jul Aug Sep Oct Nov Dec

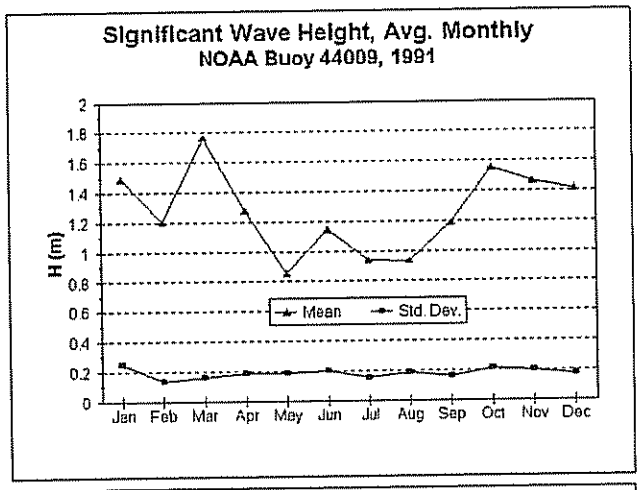
Significant Wave Height, Avg. Monthly
NOAA Buoy 44009, 1991
H (m)
2
1.8
1.6
1.4
1.2
1
0.8
0.6
0.4
0.2
0
Mean
Std. Dev.
Jan Feb Mar Apr May Jun Jul Aug Sep Oct Nov Dec

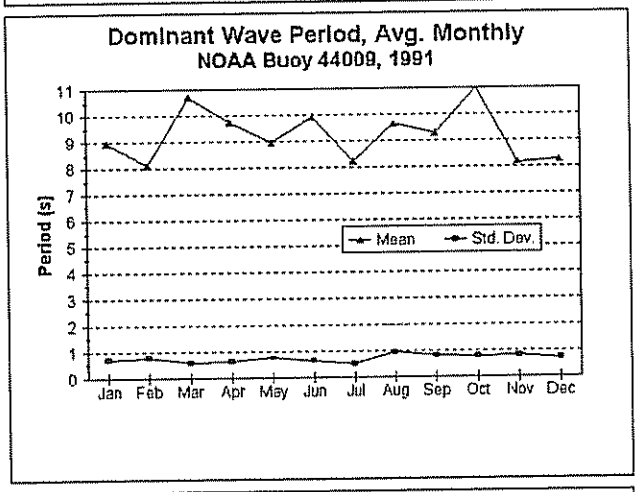
Dominant Wave Period, Avg. Monthly
NOAA Buoy 44009, 1991
Period (s)
11
10
9
8
7
6
5
4
3
2
1
0
Mean
Std. Dev.
Jan Feb Mar Apr May Jun Jul Aug Sep Oct Nov Dec

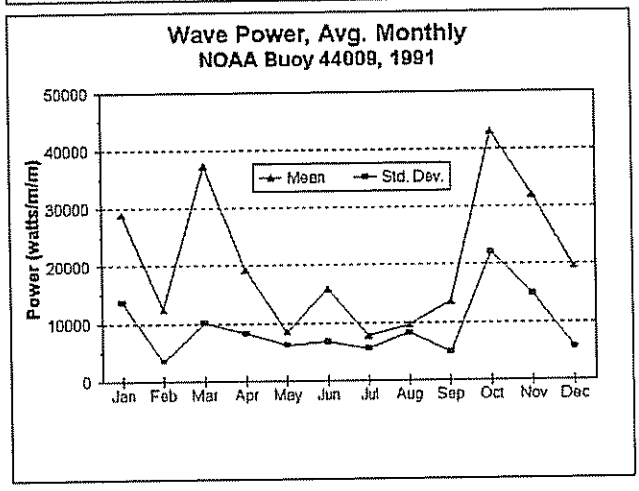
Wave Power, Avg. Monthly
NOAA Buoy 44009, 1991
Power (watts/m/m)
50000
40000
30000
20000
10000
0
Mean
Std. Dev.
Jan Feb Mar Apr May Jun Jul Aug Sep Oct Nov Dec

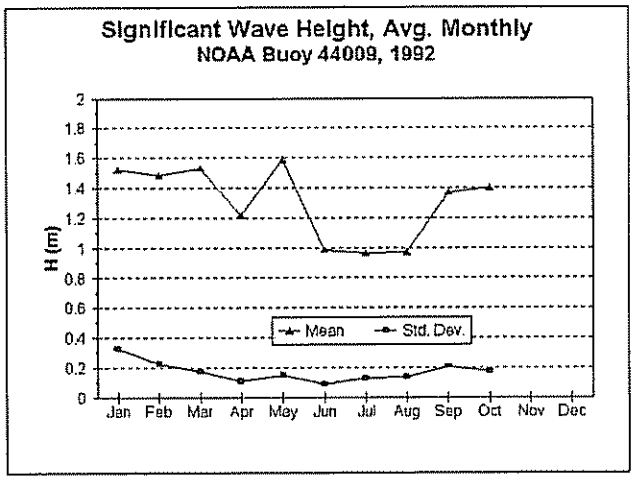
Significant Wave Height, Avg. Monthly
NOAA Buoy 44009, 1992
H (m)
2
1.8
1.6
1.4
1.2
1
0.8
0.6
0.4
0.2
0
Mean
Std. Dev.
Jan Feb Mar Apr May Jun Jul Aug Sep Oct Nov Dec

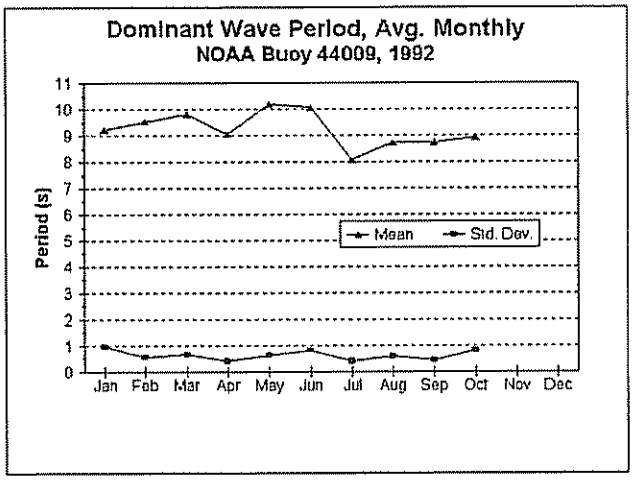
Dominant Wave Period, Avg. Monthly
NOAA Buoy 44009, 1992
Period (s)
11
10
9
8
7
6
5
4
3
2
1
0
Mean
Std. Dev.
Jan Feb Mar Apr May Jun Jul Aug Sep Oct Nov Dec

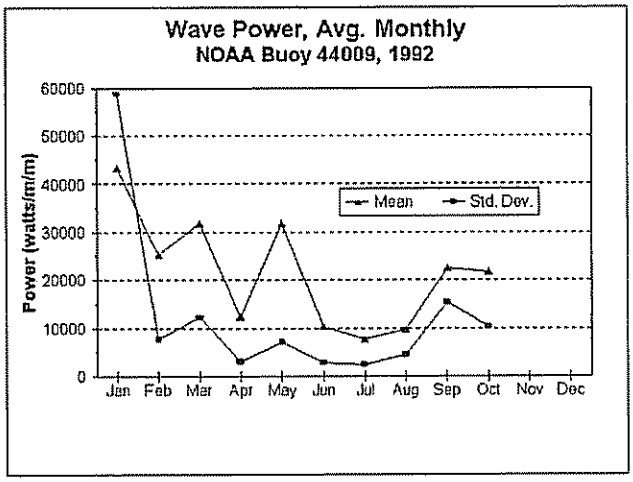
Wave Power, Avg. Monthly
NOAA Buoy 44009, 1992
Power (watts/m/m)
60000
50000
40000
30000
20000
10000
0
Mean
Std. Dev.
Jan Feb Mar Apr May Jun Jul Aug Sep Oct Nov Dec

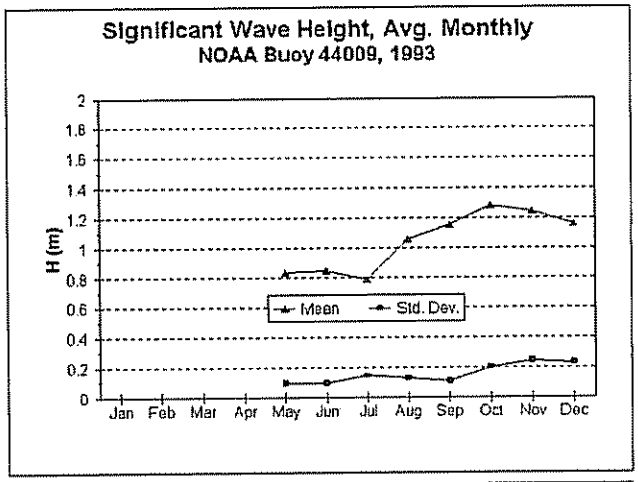
Significant Wave Height, Avg. Monthly
NOAA Buoy 44009, 1993
H (m)
2
1.8
1.6
1.4
1.2
1
0.8
0.6
0.4
0.2
0
Mean
Std. Dev.
Jan Feb Mar Apr May Jun Jul Aug Sep Oct Nov Dec

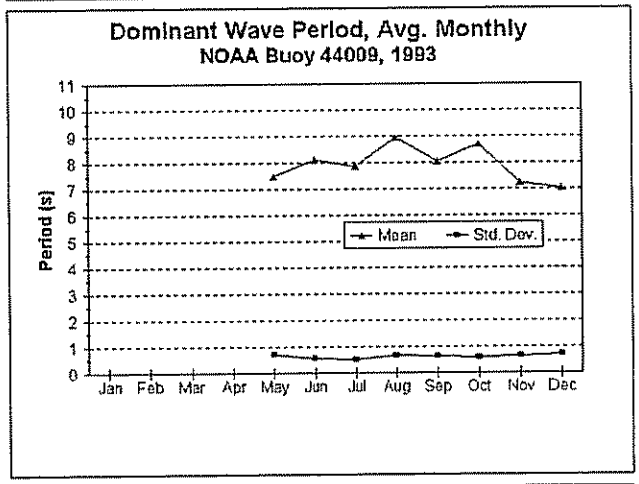
Dominant Wave Period, Avg. Monthly
NOAA Buoy 44009, 1993
Period (s)
11
10
9
8
7
6
5
4
3
2
1
0
Mean
Std. Dev.
Jan Feb Mar Apr May Jun Jul Aug Sep Oct Nov Dec

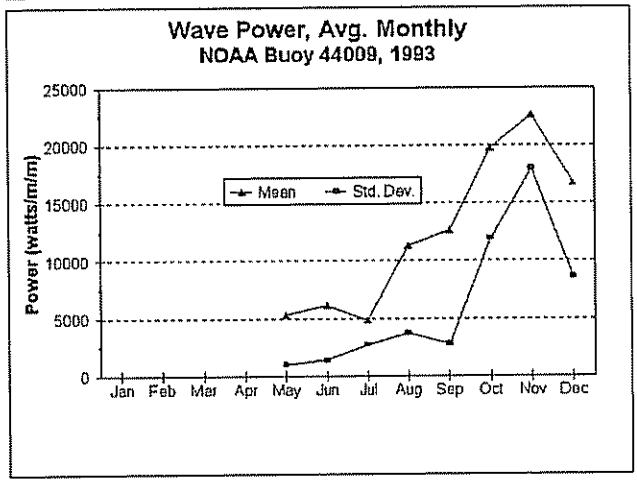
Wave Power, Avg. Monthly
NOAA Buoy 44009, 1993
Power (watts/m/m)
25000
20000
15000
10000
5000
0
Mean
Std. Dev.
Jan Feb Mar Apr May Jun Jul Aug Sep Oct Nov Dec

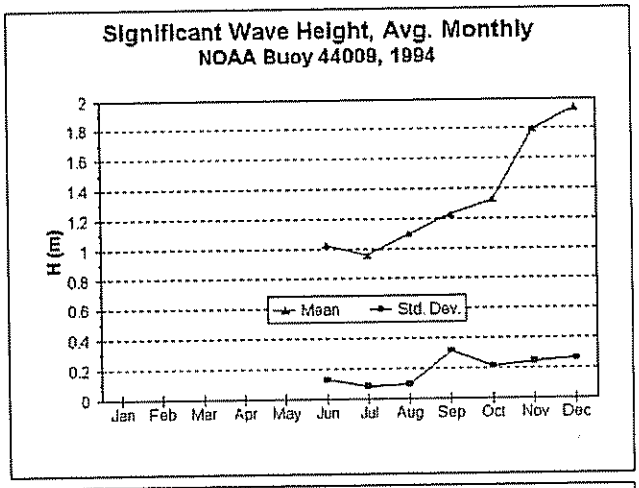
Significant Wave Height, Avg. Monthly
NOAA Buoy 44009, 1994
H (m)
2
1.8
1.6
1.4
1.2
1
0.8
0.6
0.4
0.2
0
Mean
Std. Dev.
Jan Feb Mar Apr May Jun Jul Aug Sep Oct Nov Dec

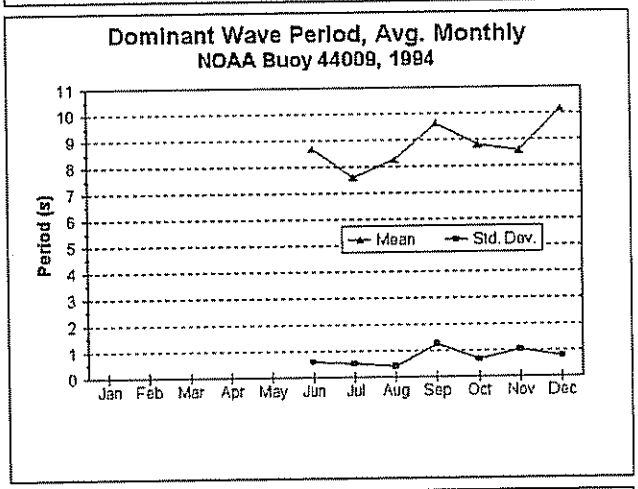
Dominant Wave Period, Avg. Monthly
NOAA Buoy 44009, 1994
Period (s)
11
10
9
8
7
6
5
4
3
2
1
0
Mean
Std. Dev.
Jan Feb Mar Apr May Jun Jul Aug Sep Oct Nov Dec

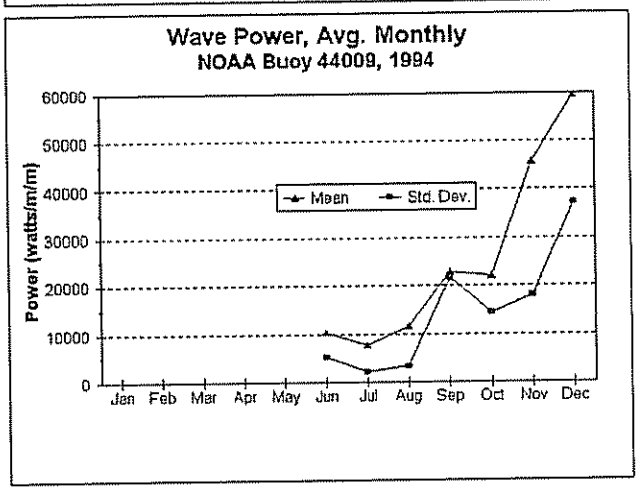
Wave Power, Avg. Monthly
NOAA Buoy 44009, 1994
Power (watts/m/m)
60000
50000
40000
30000
20000
10000
0
Mean
Std. Dev.
Jan Feb Mar Apr May Jun Jul Aug Sep Oct Nov Dec

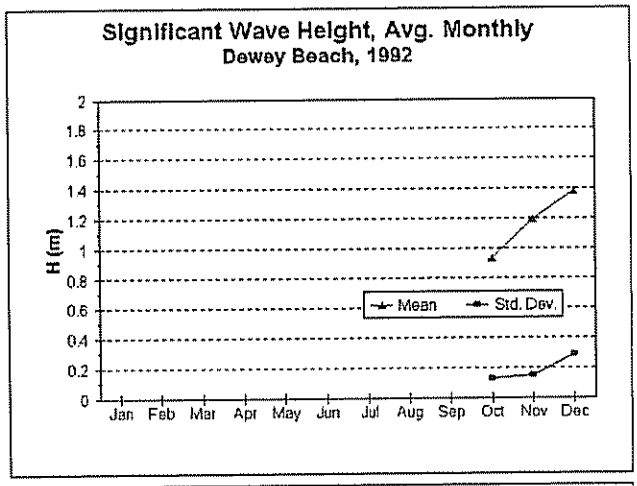
Significant Wave Height, Avg. Monthly
Dewey Beach, 1992
H (m)
2
1.8
1.6
1.4
1.2
1
0.8
0.6
0.4
0.2
0
Mean
Std. Dev.
Jan Feb Mar Apr May Jun Jul Aug Sep Oct Nov Dec

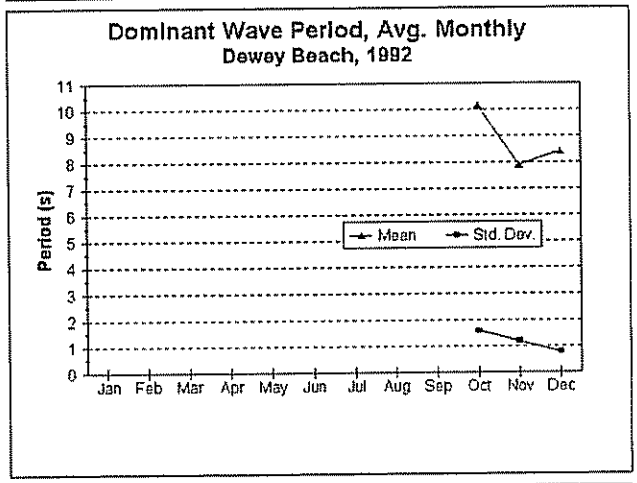
Dominant Wave Period, Avg. Monthly
Dewey Beach, 1992
Period (s)
11
10
9
8
7
6
5
4
3
2
1
0
Mean
Std. Dev.
Jan Feb Mar Apr May Jun Jul Aug Sep Oct Nov Dec

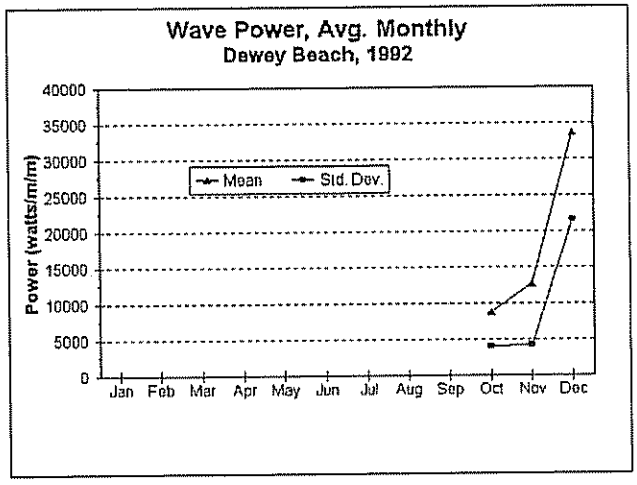
Wave Power, Avg. Monthly
Dewey Beach, 1992
Power (watts/m/m)
40000
35000
30000
25000
20000
15000
10000
5000
0
Mean
Std. Dev.
Jan Feb Mar Apr May Jun Jul Aug Sep Oct Nov Dec

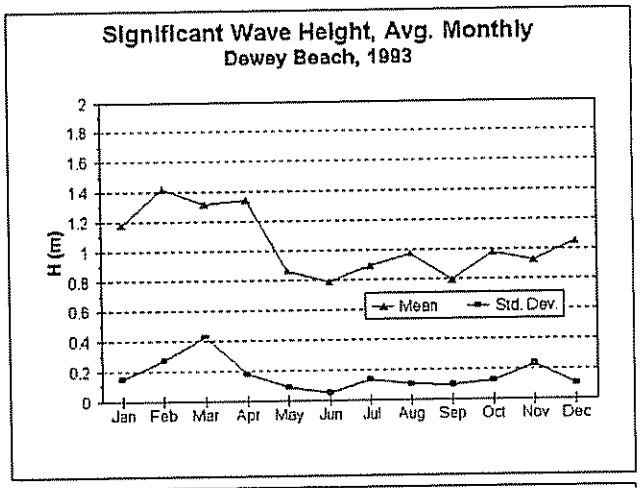
Significant Wave Height, Avg. Monthly
Dewey Beach, 1993
H (m)
2
1.8
1.6
1.4
1.2
1
0.8
0.6
0.4
0.2
0
Mean
Std. Dev.
Jan Feb Mar Apr May Jun Jul Aug Sep Oct Nov Dec

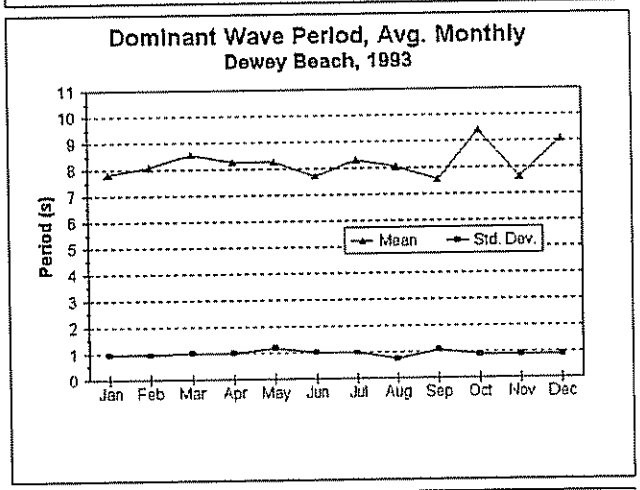
Dominant Wave Period, Avg. Monthly
Dewey Beach, 1993
Period (s)
11
10
9
8
7
6
5
4
3
2
1
0
Mean
Std. Dev.
Jan Feb Mar Apr May Jun Jul Aug Sep Oct Nov Dec

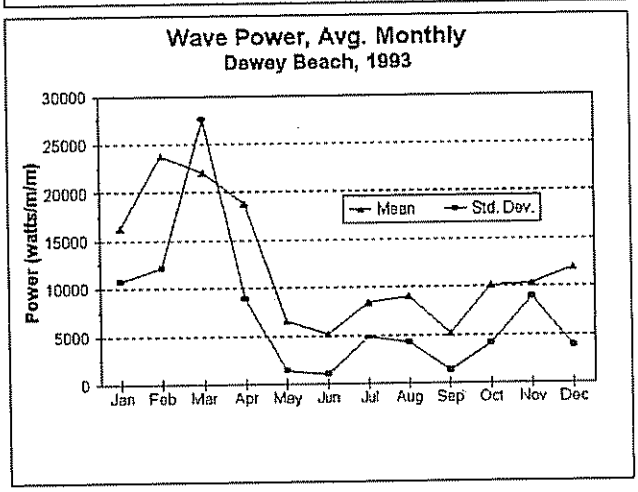
Wave Power, Avg. Monthly
Dewey Beach, 1993
Power (watts/m/m)
30000
25000
20000
15000
10000
5000
0
Mean
Std. Dev.
Jan Feb Mar Apr May Jun Jul Aug Sep Oct Nov Dec

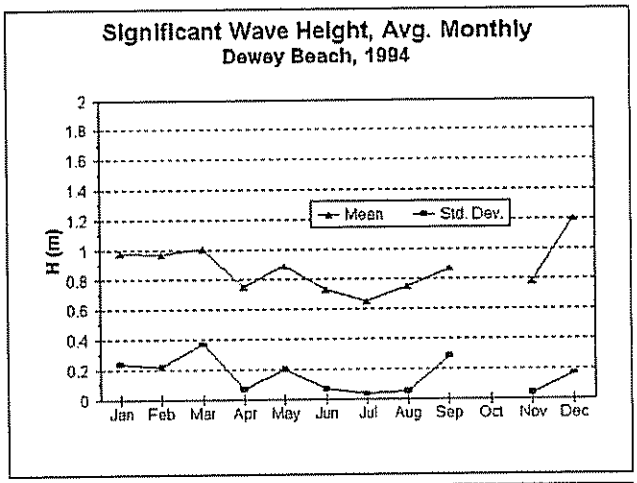
Significant Wave Height, Avg. Monthly
Dewey Beach, 1994
H (m)
2
1.8
1.6
1.4
1.2
1
0.8
0.6
0.4
0.2
0
Mean
Std. Dev.
Jan Feb Mar Apr May Jun Jul Aug Sep Oct Nov Dec

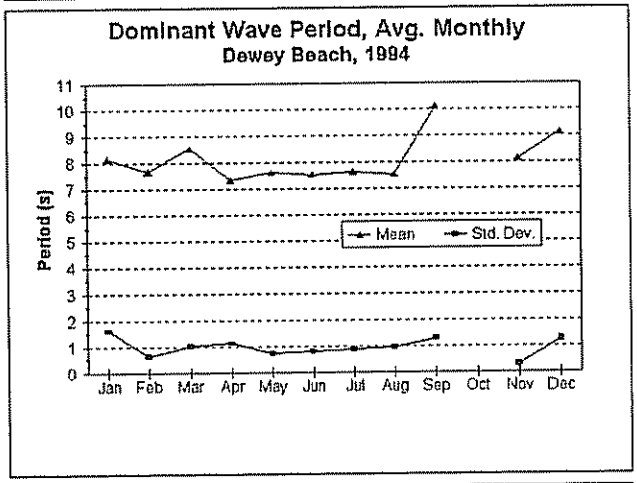
Dominant Wave Period, Avg. Monthly
Dewey Beach, 1994
Period (s)
11
10
9
8
7
6
5
4
3
2
1
0
Mean
Std. Dev.
Jan Feb Mar Apr May Jun Jul Aug Sep Oct Nov Dec

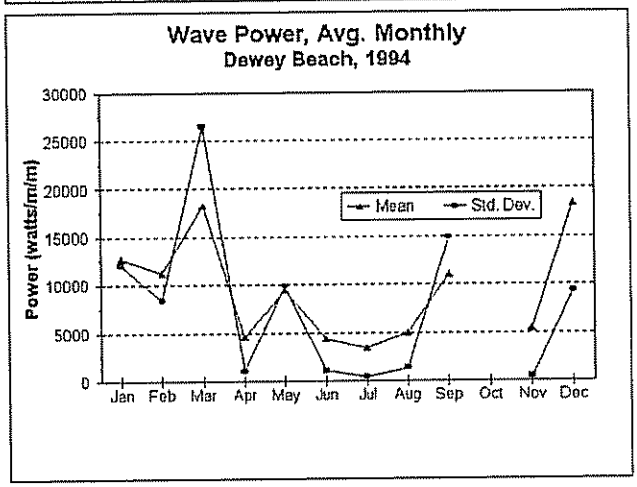
Wave Power, Avg. Monthly
Dewey Beach, 1994
Power (watts/m/m)
30000
25000
20000
15000
10000
5000
0
Mean
Std. Dev.
Jan Feb Mar Apr May Jun Jul Aug Sep Oct Nov Dec

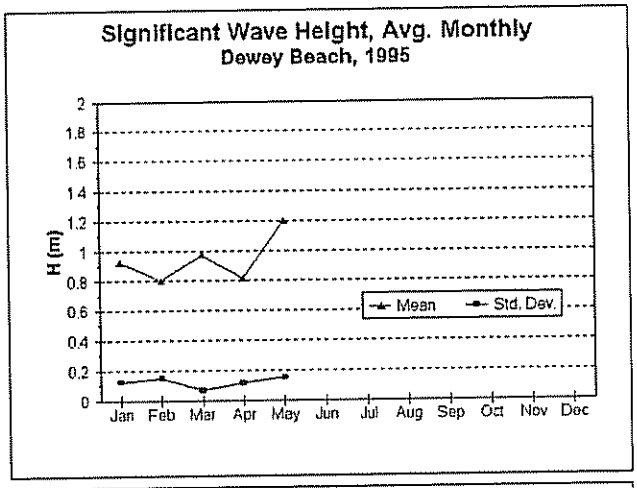
Significant Wave Height, Avg. Monthly
Dewey Beach, 1995
H (m)
2
1.8
1.6
1.4
1.2
1
0.8
0.6
0.4
0.2
0
Mean
Std. Dev.
Jan Feb Mar Apr May Jun Jul Aug Sep Oct Nov Dec

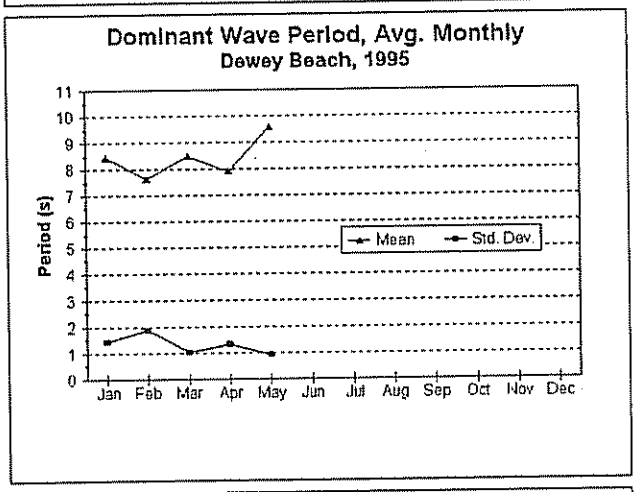
Dominant Wave Period, Avg. Monthly
Dewey Beach, 1995
Period (s)
11
10
9
8
7
6
5
4
3
2
1
0
Mean
Std. Dev.
Jan Feb Mar Apr May Jun Jul Aug Sep Oct Nov Dec

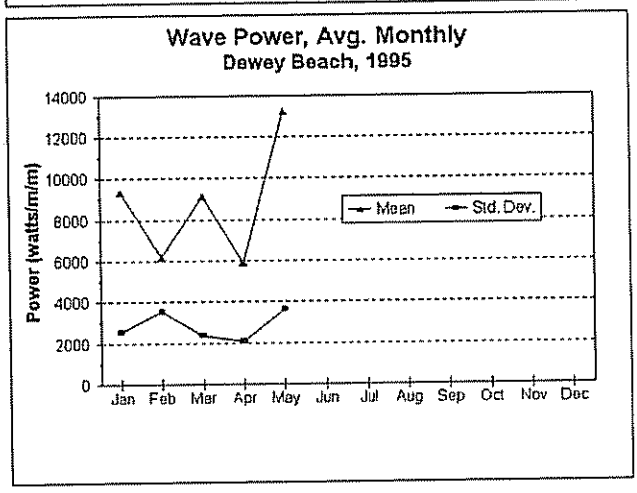
Wave Power, Avg. Monthly
Dewey Beach, 1995
Power (watts/m/m)
14000
12000
10000
8000
6000
4000
2000
0
Mean
Std. Dev.
Jan Feb Mar Apr May Jun Jul Aug Sep Oct Nov Dec

Appendix B

BATHYMETRIC SURVEYS OF INDIAN RIVER INLET, DEWEY BEACH, AND BETHANY BEACH AREAS

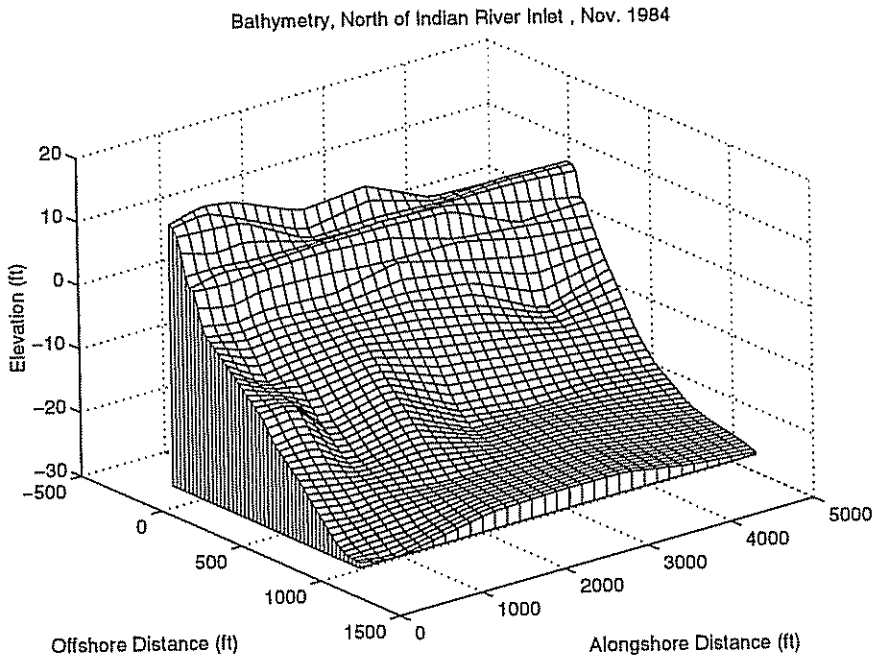
Bathymetry, North of Indian River Inlet , Nov. 1984
Elevation (ft)
20
10
0
-10
-20
-30
-500
0
500
1000
1500
Offshore Distance (ft)
0
1000
2000
3000
4000
5000
Alongshore Distance (ft)

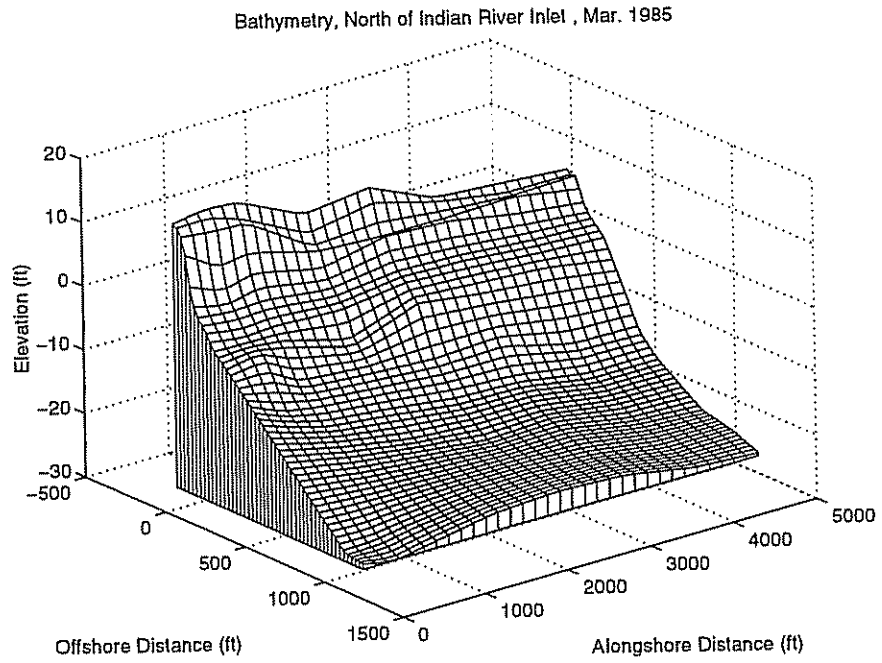
Bathymetry, North of Indian River Inlet , Mar. 1985
Elevation (ft)
20
10
0
-10
-20
-30
-500
0
500
1000
1500
Offshore Distance (ft)
0
1000
2000
3000
4000
5000
Alongshore Distance (ft)

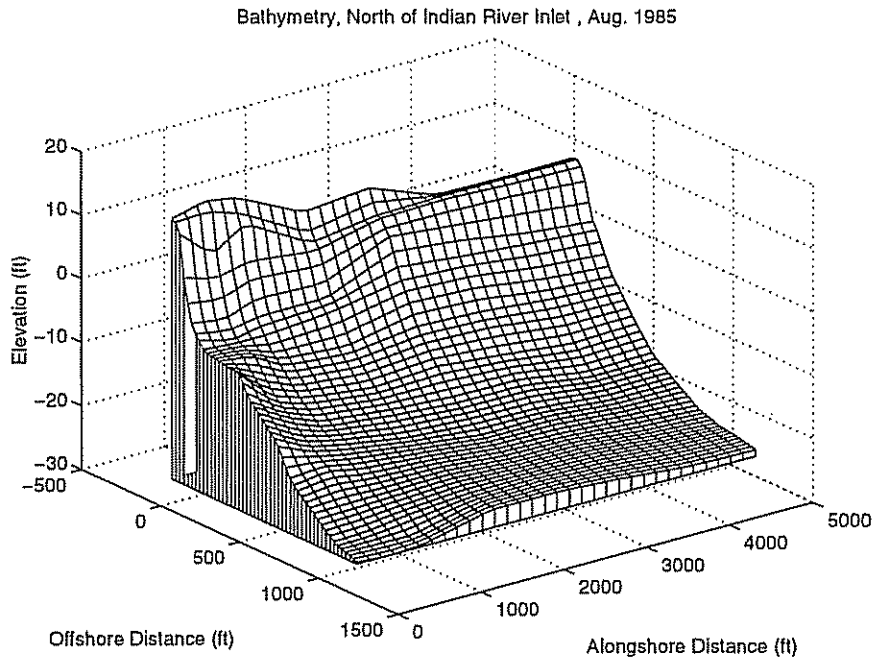
Bathymetry, North of Indian River Inlet , Aug. 1985
Elevation (ft)
20
10
0
−10
−20
−30
−500
0
500
1000
1500
Offshore Distance (ft)
0
1000
2000
3000
4000
5000
Alongshore Distance (ft)

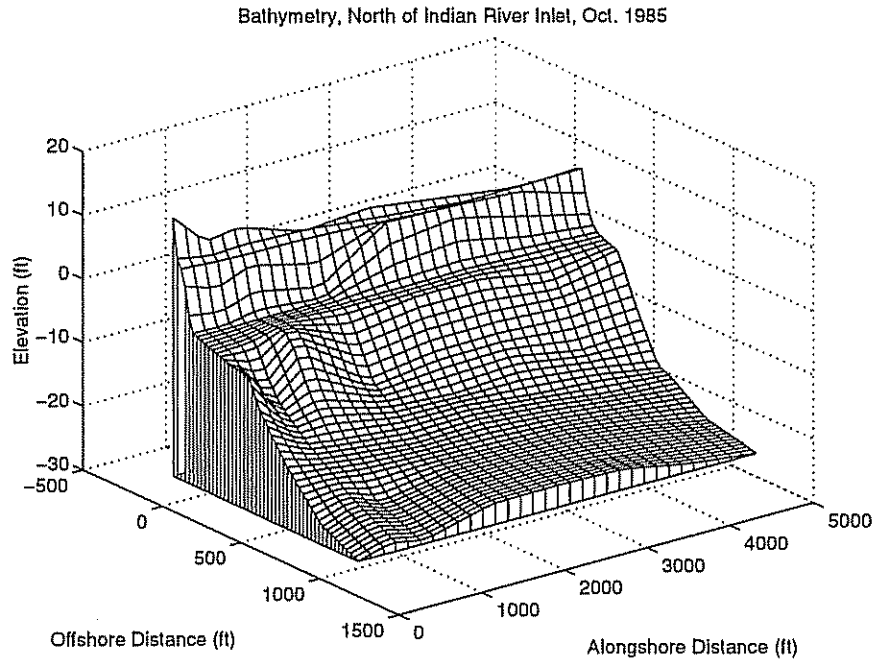
Bathymetry, North of Indian River Inlet, Oct. 1985
Elevation (ft)
20
10
0
−10
−20
−30
−500
0
500
1000
1500
Offshore Distance (ft)
0
1000
2000
3000
4000
5000
Alongshore Distance (ft)

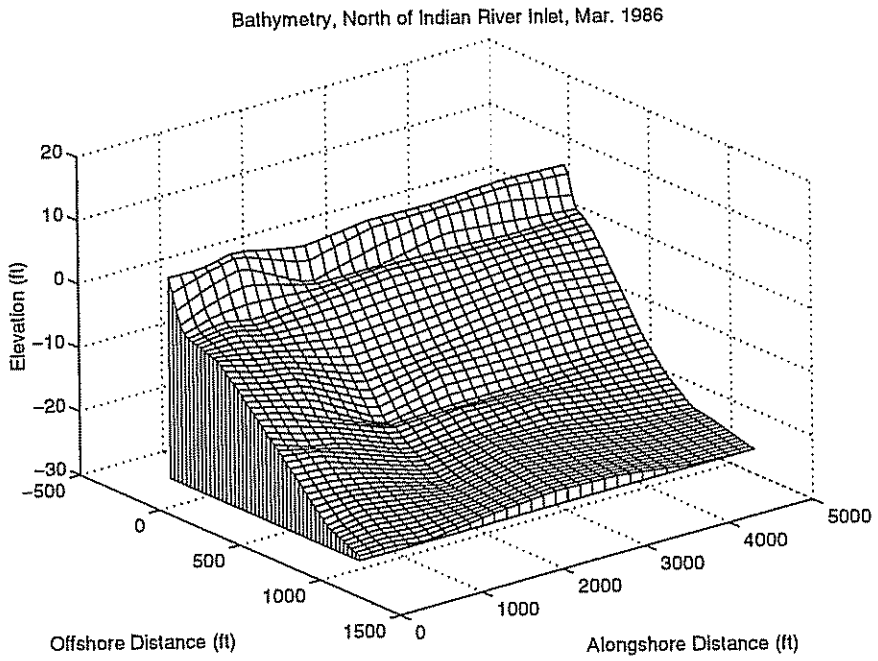
Bathymetry, North of Indian River Inlet, Mar. 1986
Elevation (ft)
20
10
0
−10
−20
−30
−500
0
500
1000
1500
Offshore Distance (ft)
0
1000
2000
3000
4000
5000
Alongshore Distance (ft)

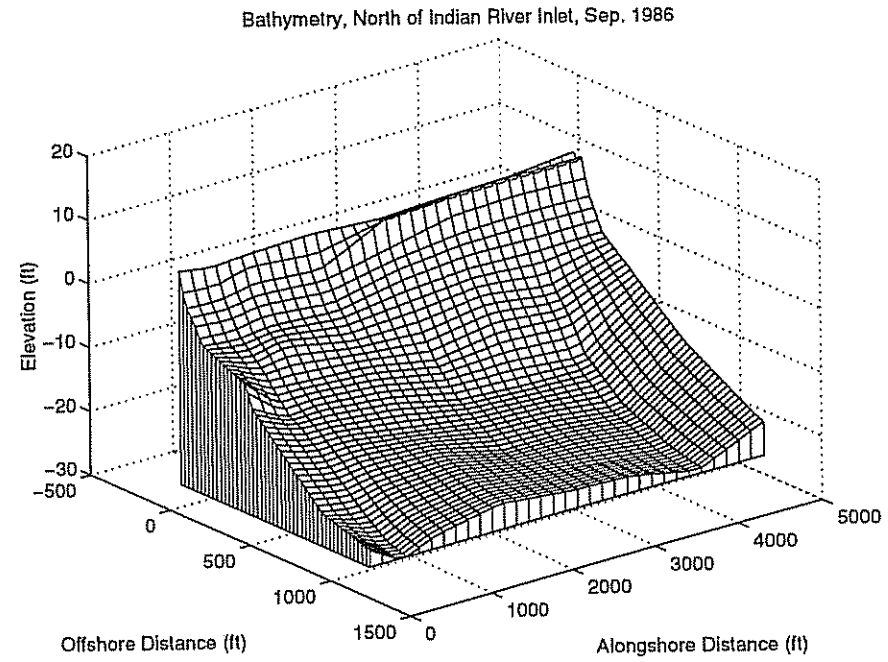
Bathymetry, North of Indian River Inlet, Sep. 1986
Elevation (ft)
20
10
0
−10
−20
−30
−500
0
500
1000
1500
Offshore Distance (ft)
0
1000
2000
3000
4000
5000
Alongshore Distance (ft)

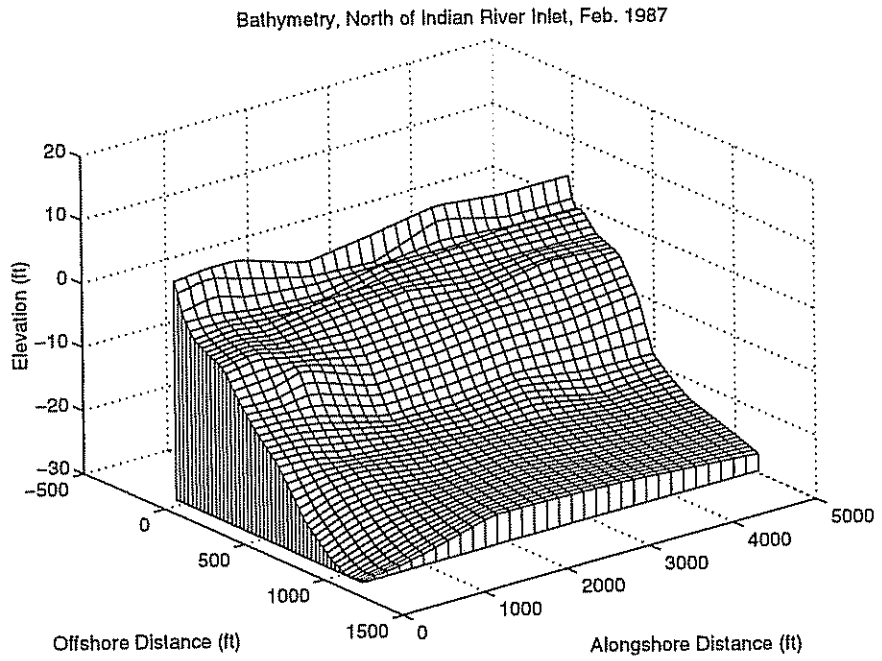
Bathymetry, North of Indian River Inlet, Feb. 1987
Elevation (ft)
20
10
0
−10
−20
−30
−500
0
500
1000
1500
Offshore Distance (ft)
0
1000
2000
3000
4000
5000
Alongshore Distance (ft)

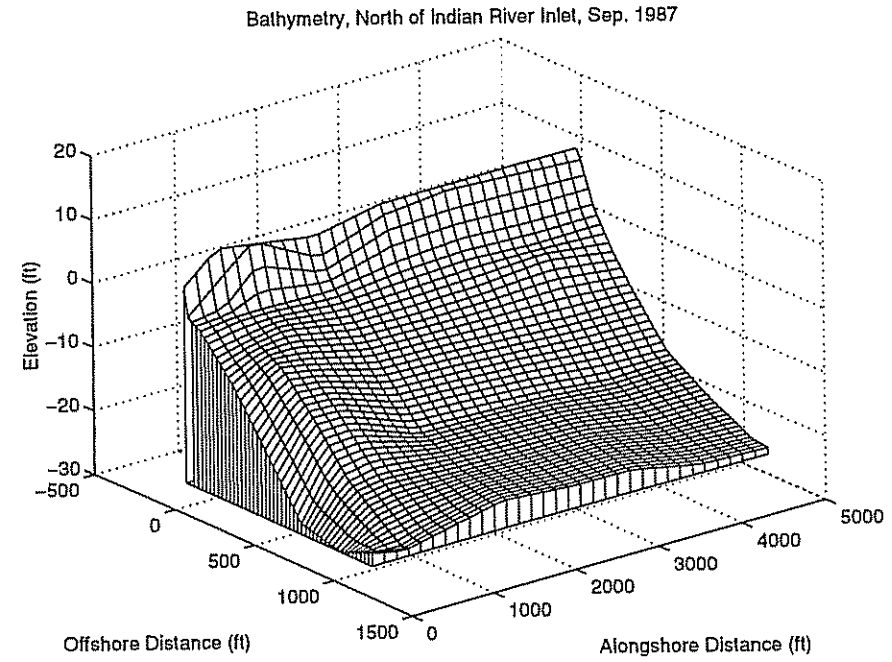
Bathymetry, North of Indian River Inlet, Sep. 1987
Elevation (ft)
20
10
0
−10
−20
−30
−500
0
500
1000
1500
Offshore Distance (ft)
0
1000
2000
3000
4000
5000
Alongshore Distance (ft)

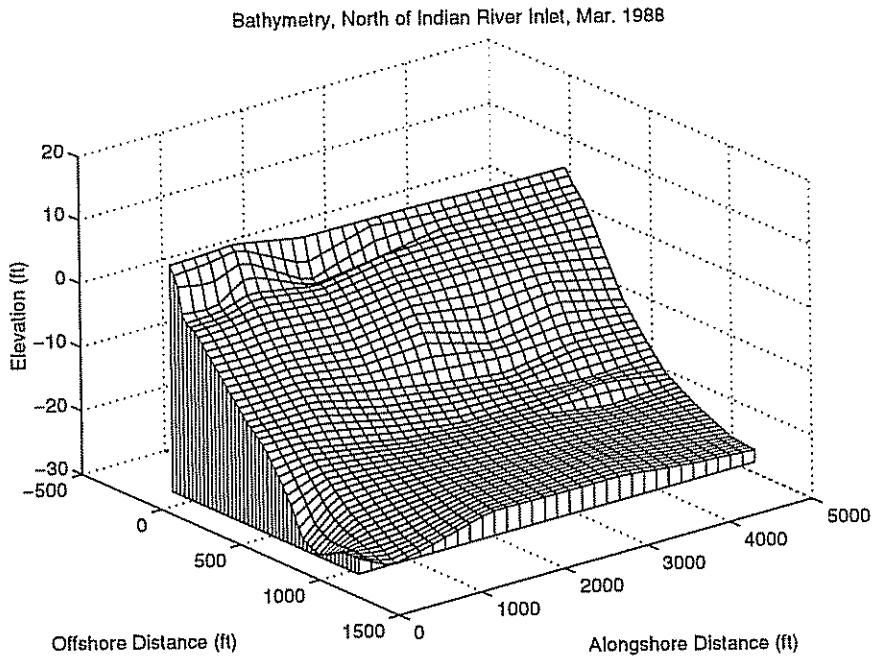
Bathymetry, North of Indian River Inlet, Mar. 1988
Elevation (ft)
20
10
0
−10
−20
−30
−500
0
500
1000
1500
Offshore Distance (ft)
0
1000
2000
3000
4000
5000
Alongshore Distance (ft)

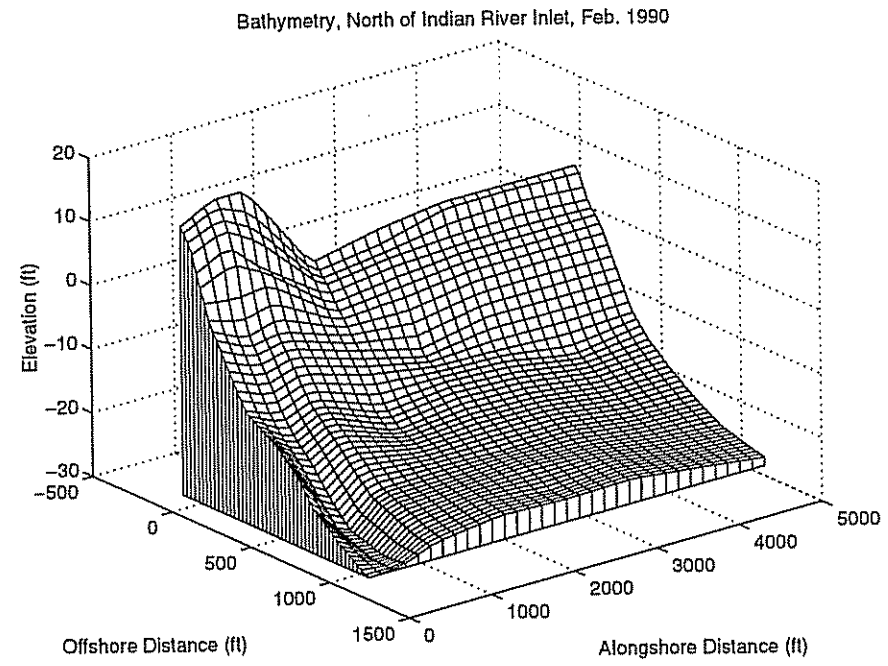
Bathymetry, North of Indian River Inlet, Feb. 1990
Elevation (ft)
20
10
0
−10
−20
−30
−500
0
500
1000
1500
Offshore Distance (ft)
0
1000
2000
3000
4000
5000
Alongshore Distance (ft)

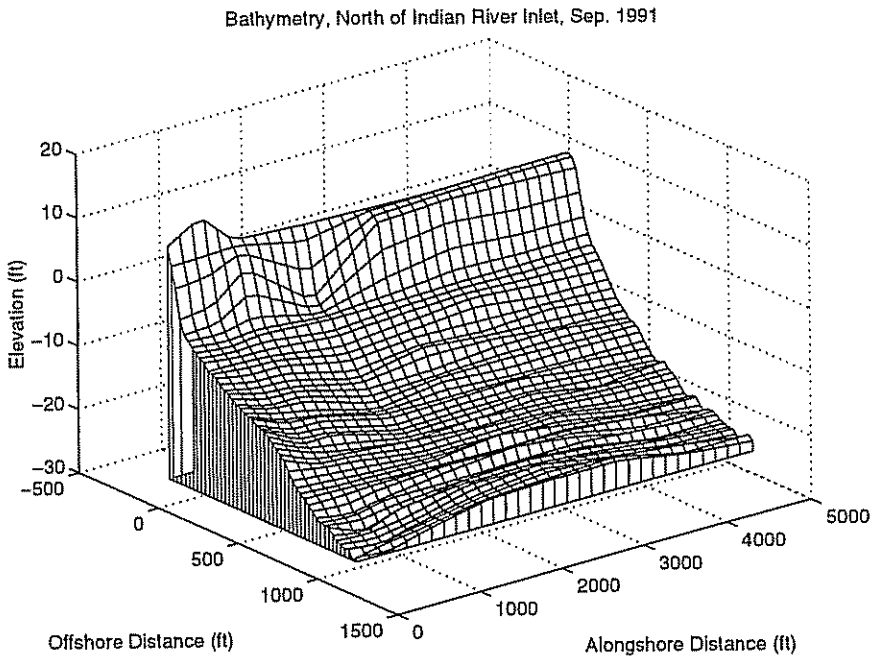
Bathymetry, North of Indian River Inlet, Sep. 1991
Elevation (ft)
20
10
0
−10
−20
−30
−500
0
500
1000
1500
Offshore Distance (ft)
0
1000
2000
3000
4000
5000
Alongshore Distance (ft)

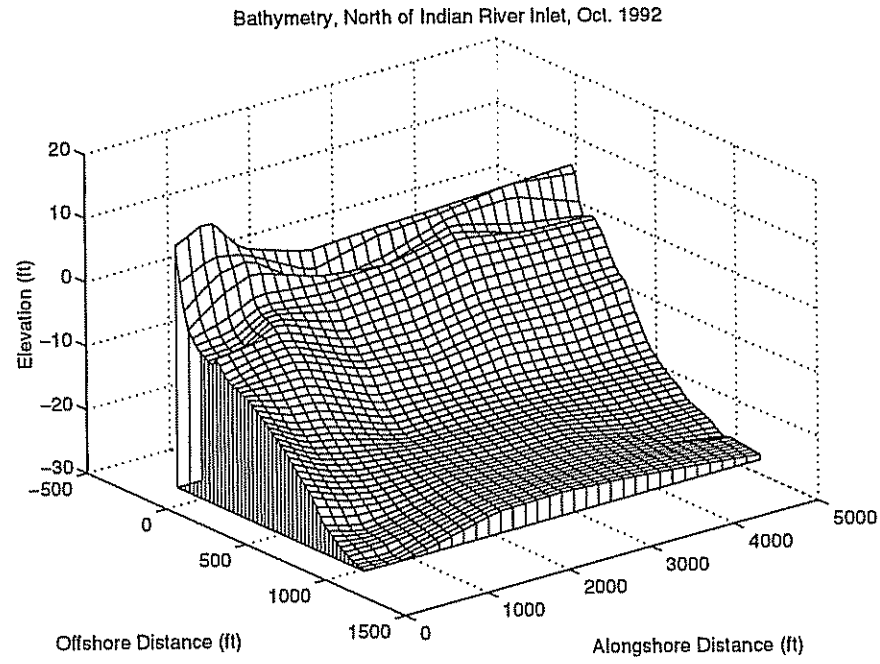
Bathymetry, North of Indian River Inlet, Oct. 1992
Elevation (ft)
20
10
0
−10
−20
−30
−500
0
500
1000
1500
Offshore Distance (ft)
0
1000
2000
3000
4000
5000
Alongshore Distance (ft)

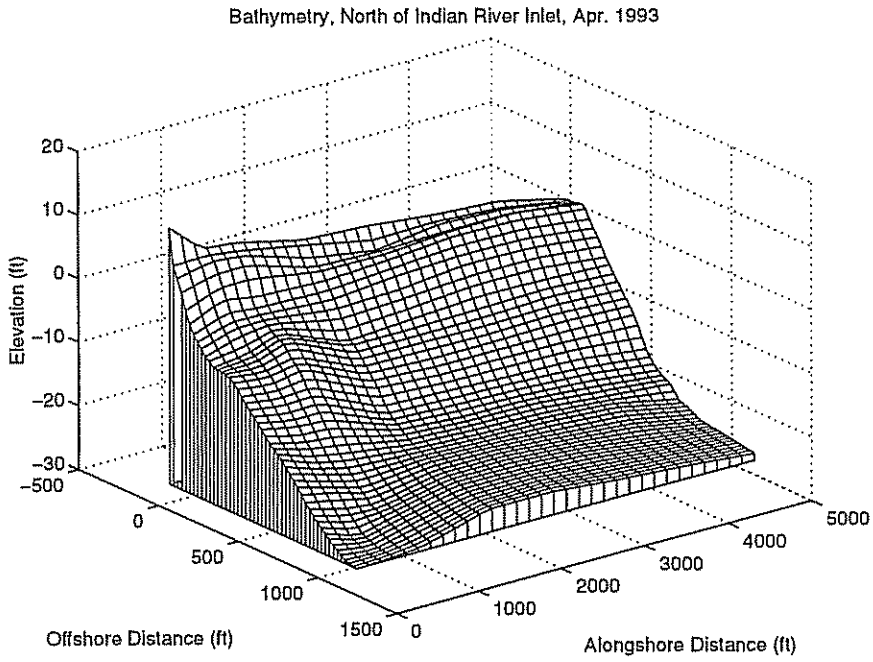
Bathymetry, North of Indian River Inlet, Apr. 1993
Elevation (ft)
20
10
0
−10
−20
−30
−500
0
500
1000
1500
Offshore Distance (ft)
0
1000
2000
3000
4000
5000
Alongshore Distance (ft)

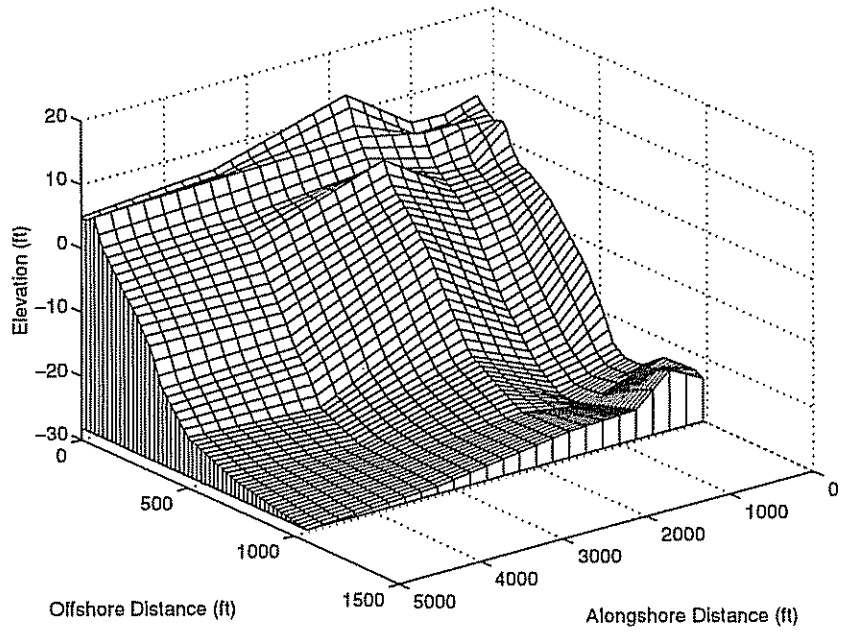
Bathymetry, South of Indian River Inlet, Mar. 1985
Elevation (ft)
20
10
0
−10
−20
−30
0
500
1000
1500
Offshore Distance (ft)
0
1000
2000
3000
4000
5000
Alongshore Distance (ft)

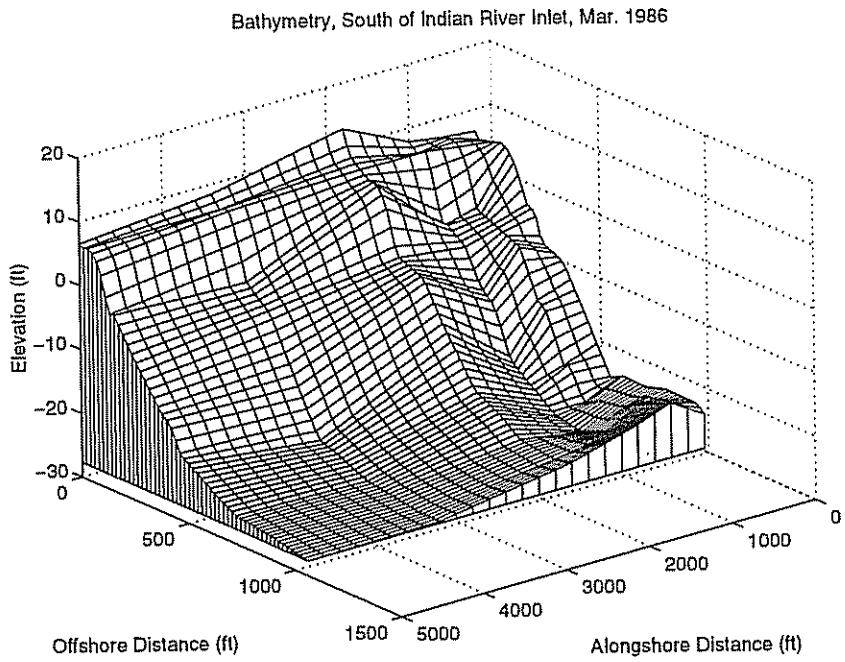
Bathymetry, South of Indian River Inlet, Mar. 1986
Elevation (ft)
20
10
0
−10
−20
−30
0
500
1000
1500
Offshore Distance (ft)
0
1000
2000
3000
4000
5000
Alongshore Distance (ft)

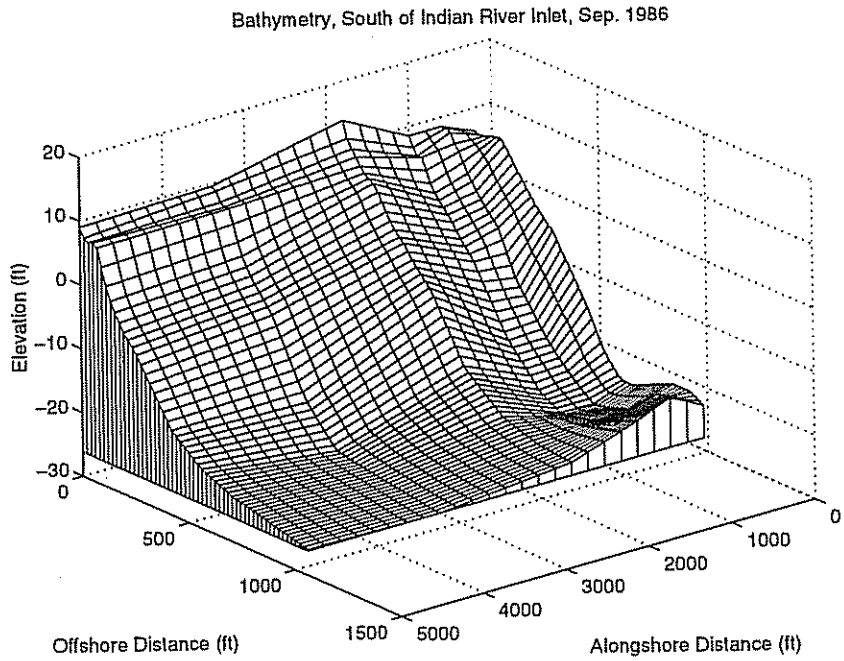
Bathymetry, South of Indian River Inlet, Sep. 1986
Elevation (ft)
20
10
0
−10
−20
−30
0
500
1000
1500
Offshore Distance (ft)
0
1000
2000
3000
4000
5000
Alongshore Distance (ft)

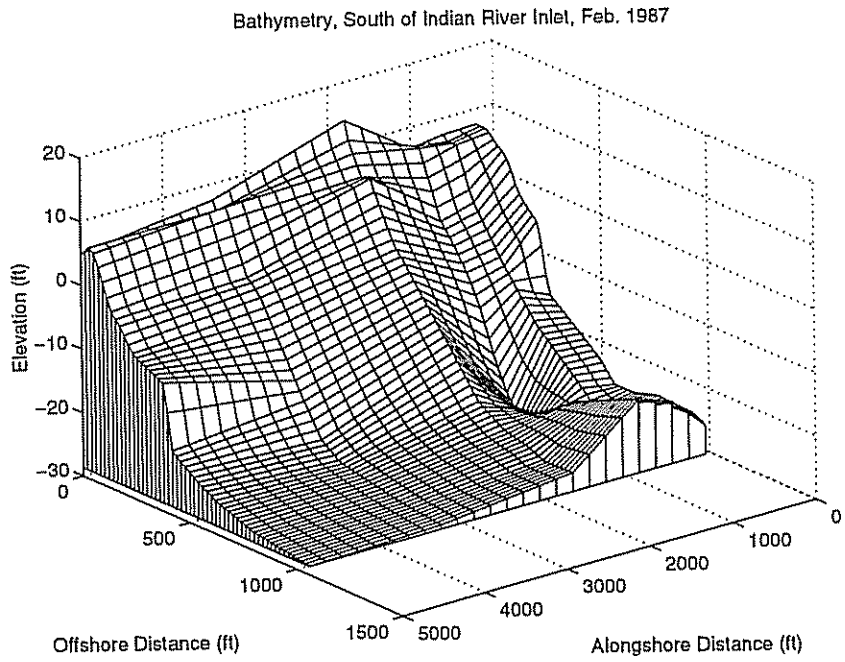
Bathymetry, South of Indian River Inlet, Feb. 1987
Elevation (ft)
20
10
0
−10
−20
−30
0
500
1000
1500
Offshore Distance (ft)
0
1000
2000
3000
4000
5000
Alongshore Distance (ft)

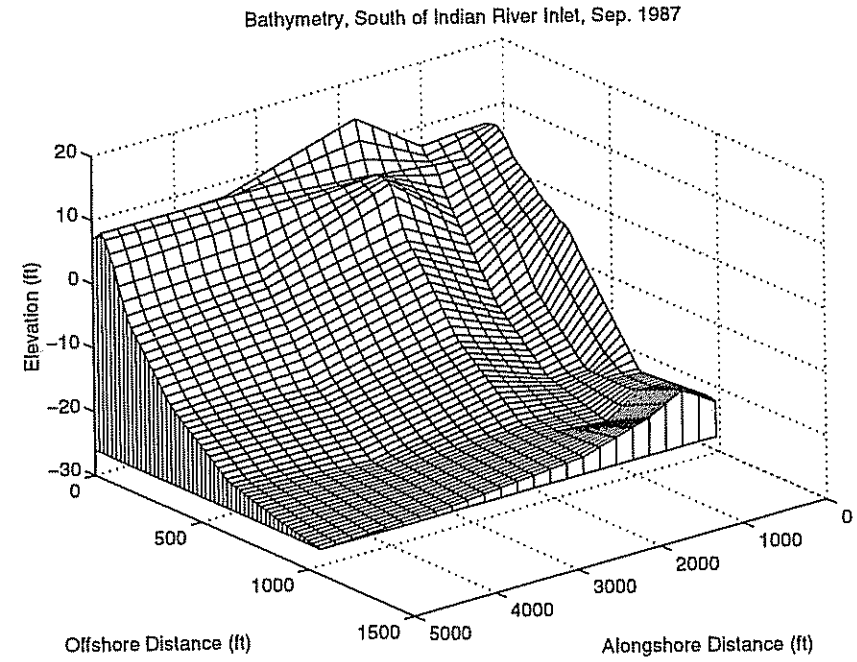
Bathymetry, South of Indian River Inlet, Sep. 1987
Elevation (ft)
20
10
0
−10
−20
−30
0
500
1000
1500
Offshore Distance (ft)
0
1000
2000
3000
4000
5000
Alongshore Distance (ft)

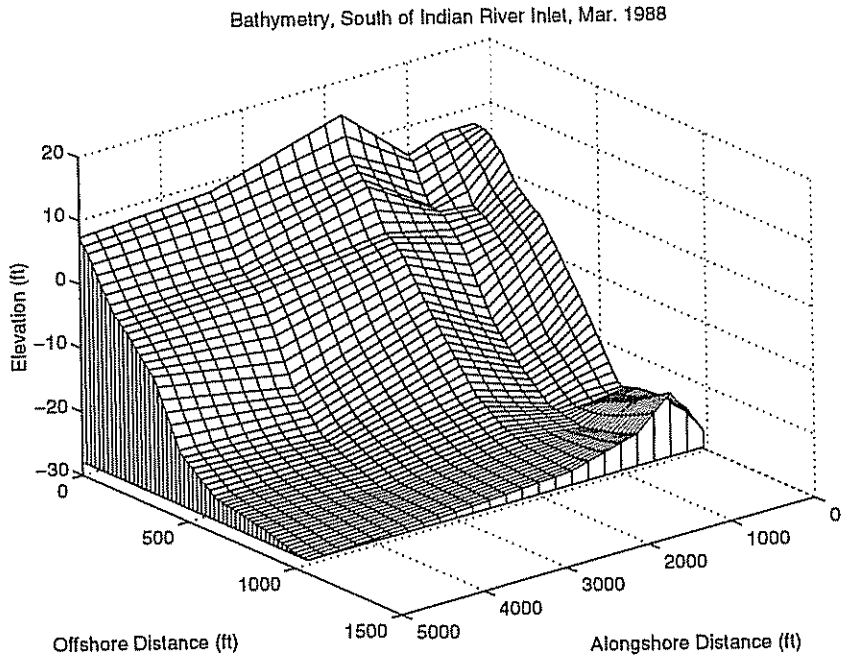
Bathymetry, South of Indian River Inlet, Mar. 1988
Elevation (ft)
20
10
0
−10
−20
−30
0
500
1000
1500
Offshore Distance (ft)
0
1000
2000
3000
4000
5000
Alongshore Distance (ft)

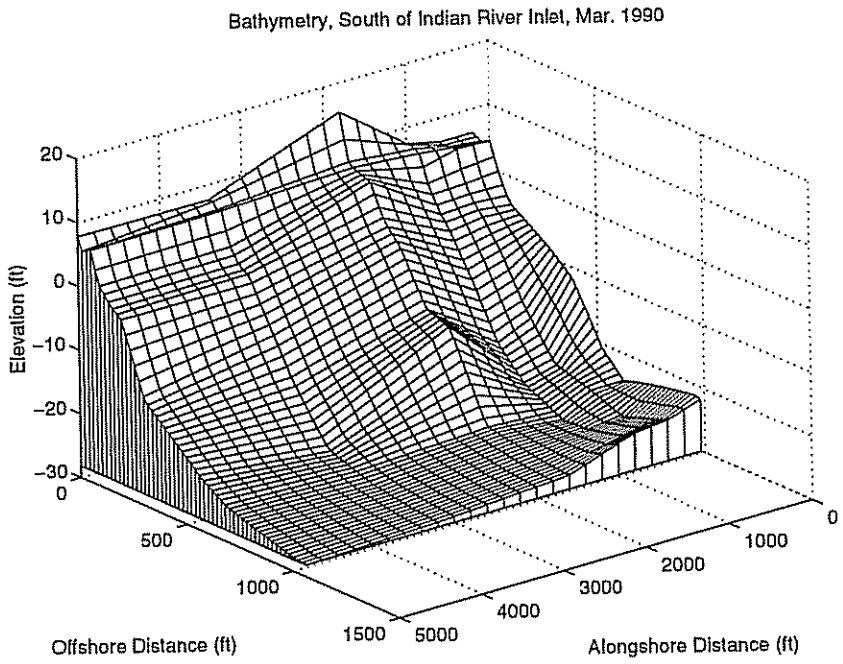
Bathymetry, South of Indian River Inlet, Mar. 1990
Elevation (ft)
20
10
0
−10
−20
−30
0
500
1000
1500
Offshore Distance (ft)
0
1000
2000
3000
4000
5000
Alongshore Distance (ft)

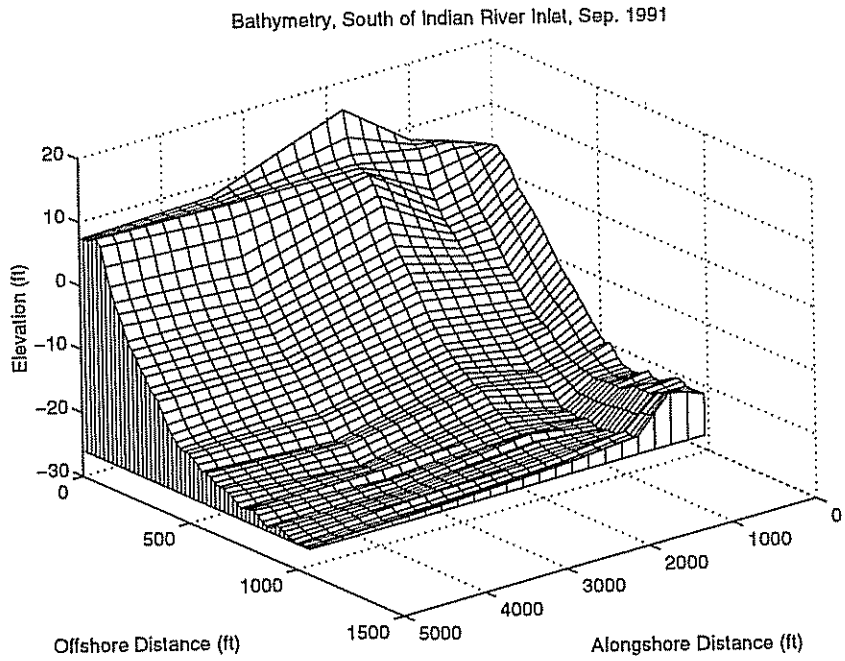
Bathymetry, South of Indian River Inlet, Sep. 1991
Elevation (ft)
20
10
0
-10
-20
-30
0
500
1000
1500
Offshore Distance (ft)
0
1000
2000
3000
4000
5000
Alongshore Distance (ft)

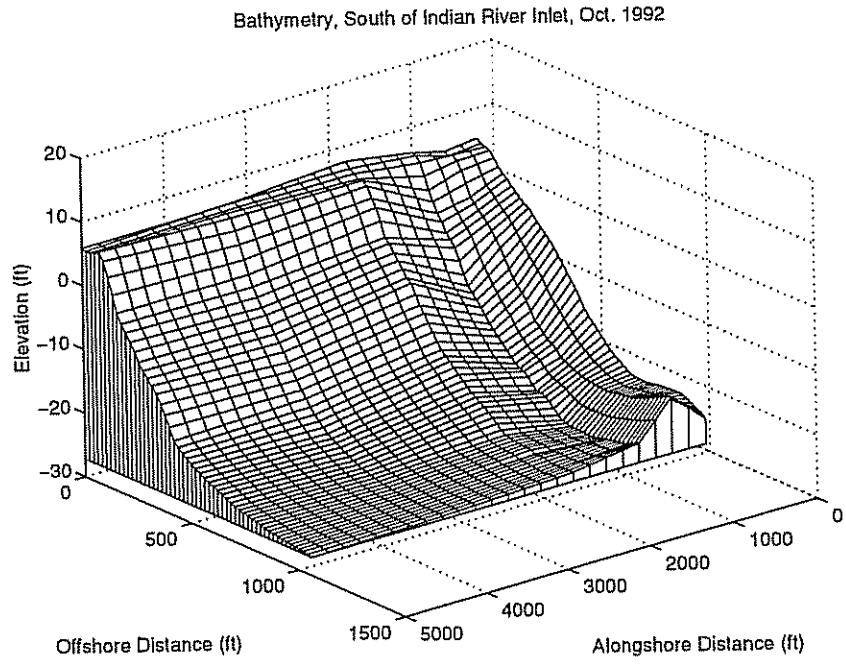
Bathymetry, South of Indian River Inlet, Oct. 1992
Elevation (ft)
20
10
0
-10
-20
-30
0
500
1000
1500
Offshore Distance (ft)
0
1000
2000
3000
4000
5000
Alongshore Distance (ft)

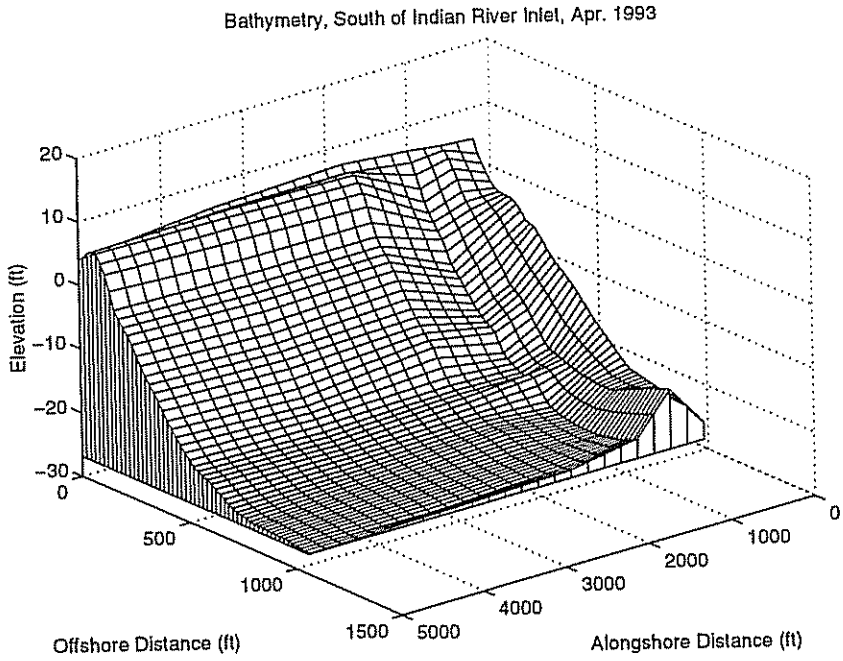
Bathymetry, South of Indian River Inlet, Apr. 1993
Elevation (ft)
20
10
0
−10
−20
−30
0
500
1000
1500
Offshore Distance (ft)
0
1000
2000
3000
4000
5000
Alongshore Distance (ft)

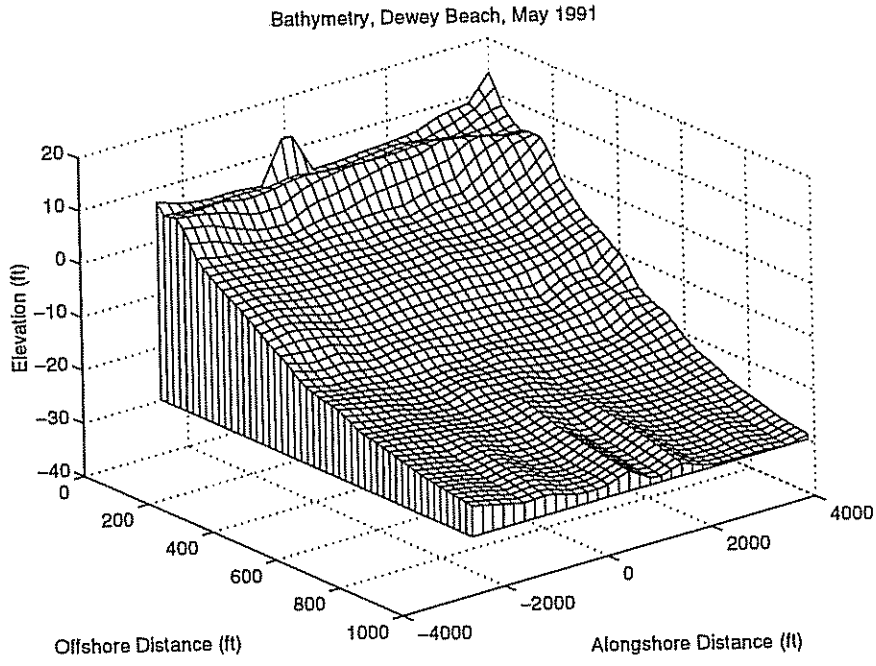
Bathymetry, Dewey Beach, May 1991
Elevation (ft)
20
10
0
−10
−20
−30
−40
0
200
400
600
800
1000
Offshore Distance (ft)
4000
2000
0
−2000
−4000
Alongshore Distance (ft)

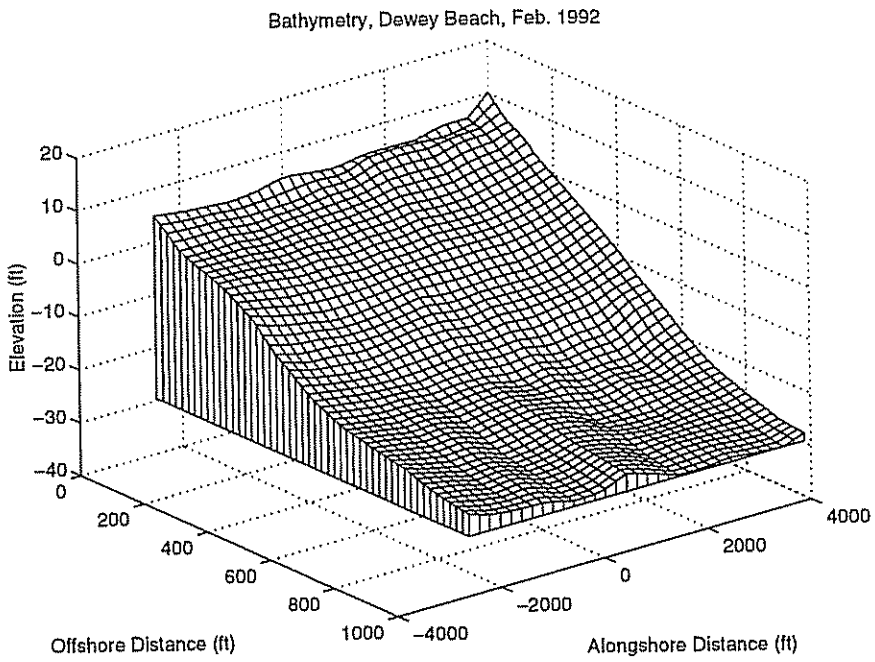
Bathymetry, Dewey Beach, Feb. 1992
Elevation (ft)
20
10
0
−10
−20
−30
−40
0
200
400
600
800
1000
Offshore Distance (ft)
−4000
−2000
0
2000
4000
Alongshore Distance (ft)

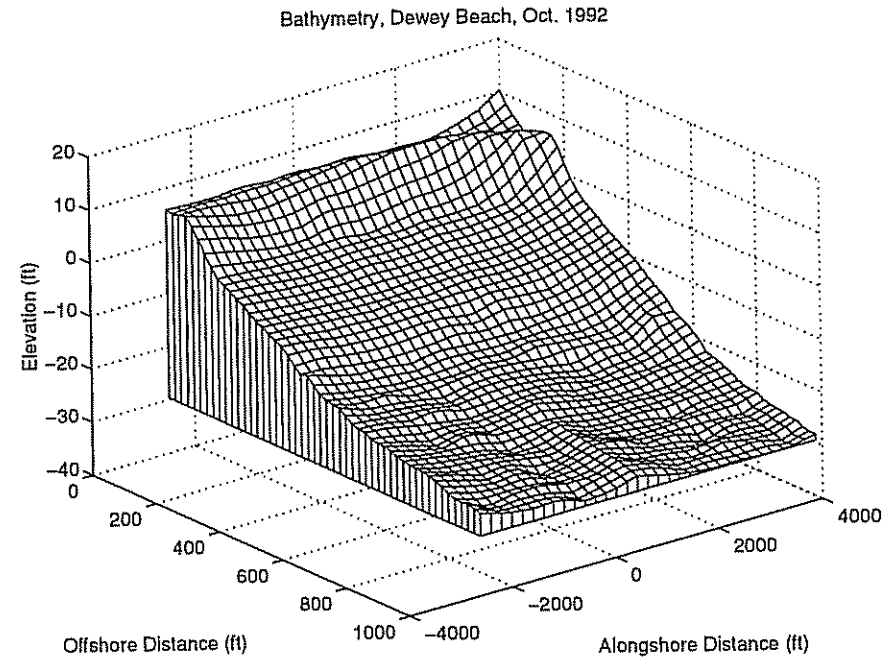
Bathymetry, Dewey Beach, Oct. 1992
Elevation (ft)
20
10
0
−10
−20
−30
−40
0
200
400
600
800
1000
Offshore Distance (ft)
−4000
−2000
0
2000
4000
Alongshore Distance (ft)

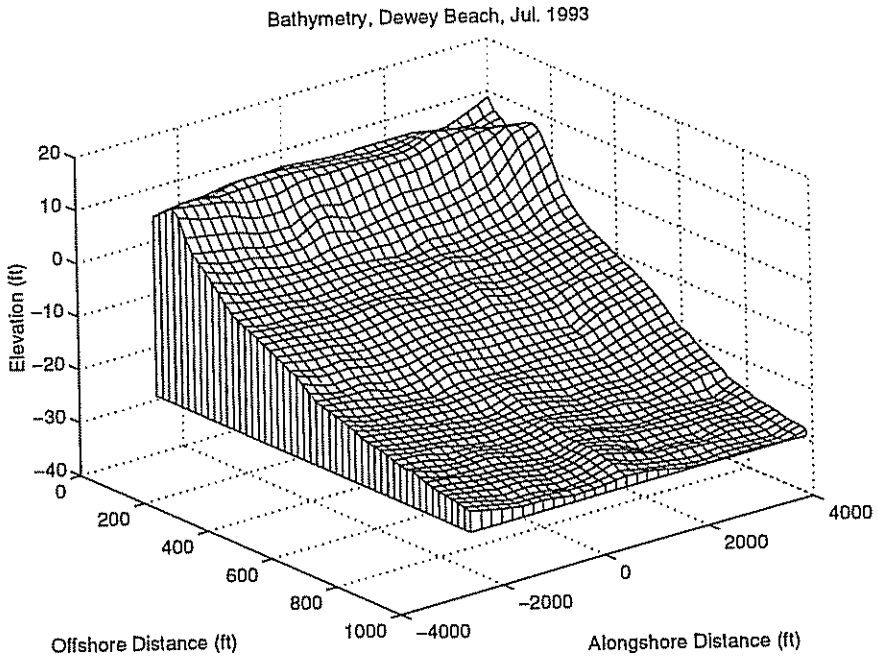
Bathymetry, Dewey Beach, Jul. 1993
Elevation (ft)
20
10
0
−10
−20
−30
−40
0
200
400
600
800
1000
Offshore Distance (ft)
−4000
−2000
0
2000
4000
Alongshore Distance (ft)

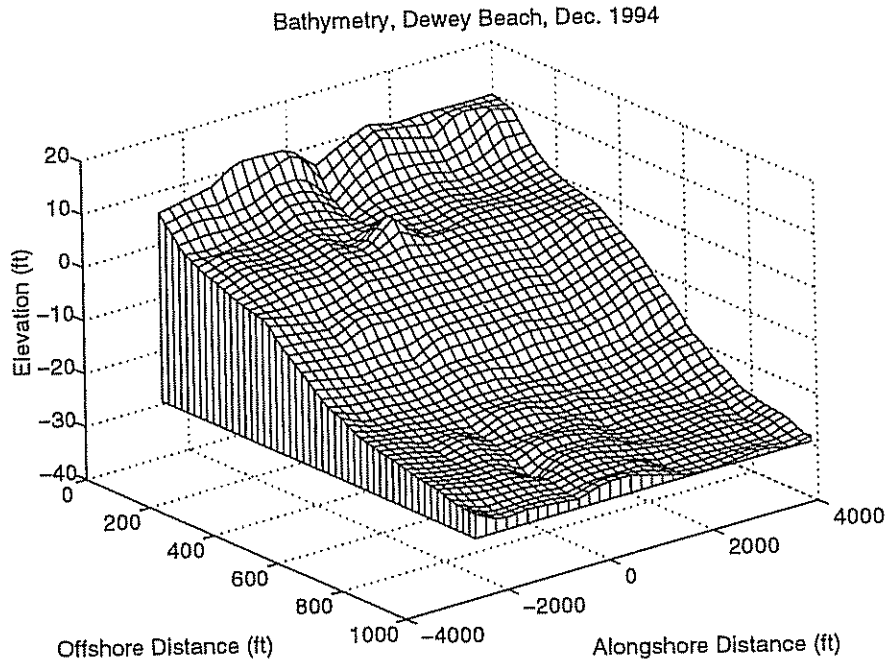
Bathymetry, Dewey Beach, Dec. 1994
Elevation (ft)
20
10
0
−10
−20
−30
−40
0
200
400
600
800
1000
Offshore Distance (ft)
−4000
−2000
0
2000
4000
Alongshore Distance (ft)

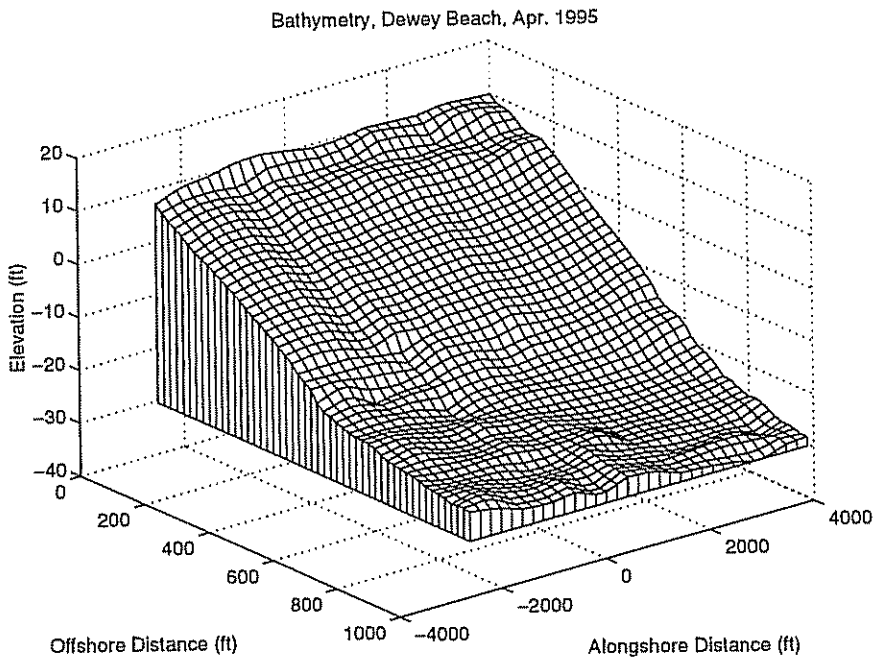
Bathymetry, Dewey Beach, Apr. 1995
Elevation (ft)
20
10
0
−10
−20
−30
−40
0
200
400
600
800
1000
Offshore Distance (ft)
−4000
−2000
0
2000
4000
Alongshore Distance (ft)

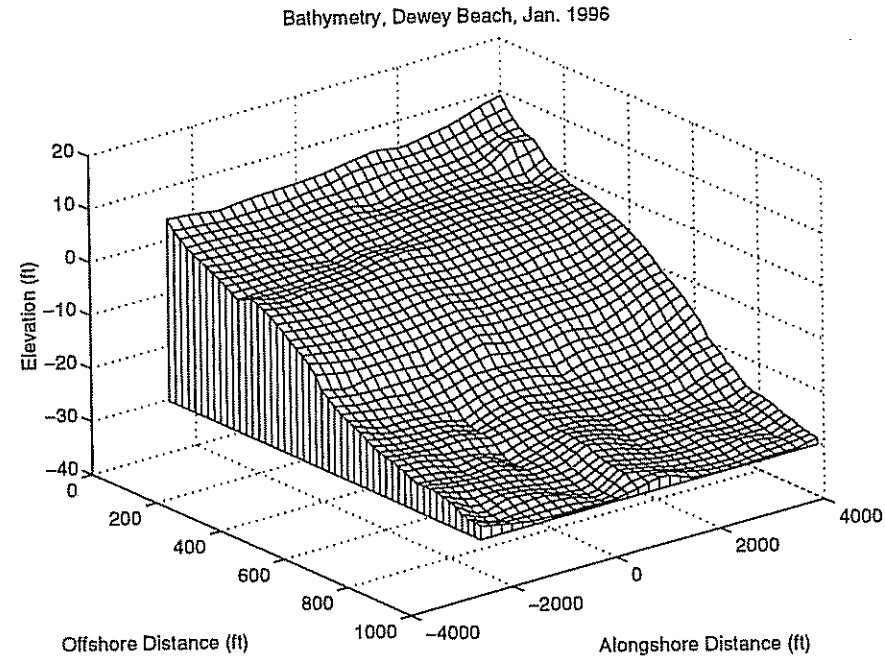
Bathymetry, Dewey Beach, Jan. 1996
Elevation (ft)
20
10
0
−10
−20
−30
−40
0
200
400
600
800
1000
Offshore Distance (ft)
−4000
−2000
0
2000
4000
Alongshore Distance (ft)

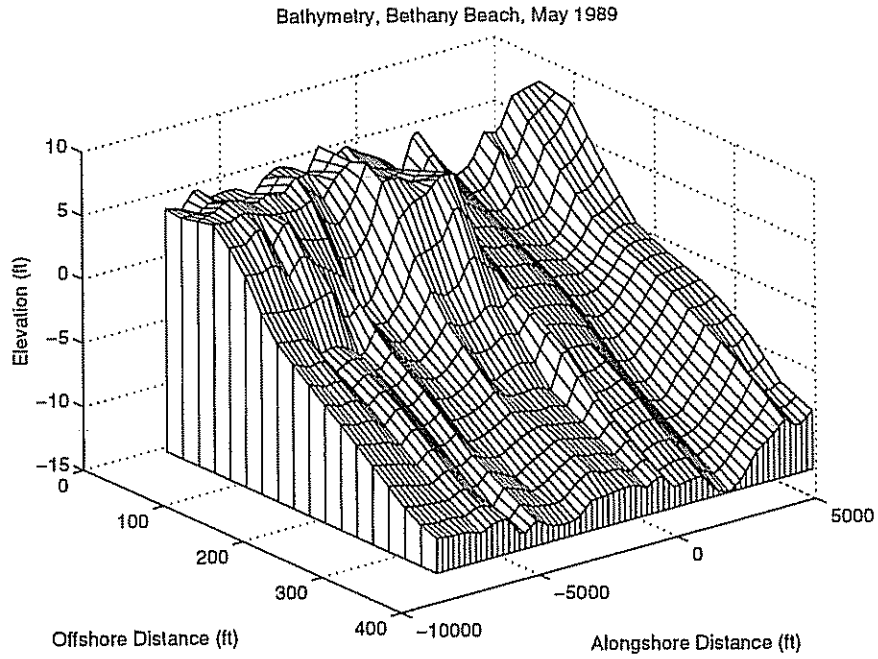
Bathymetry, Bethany Beach, May 1989
Elevation (ft)
10
5
0
−5
−10
−15
0
100
200
300
400
Offshore Distance (ft)
−10000
−5000
0
5000
Alongshore Distance (ft)

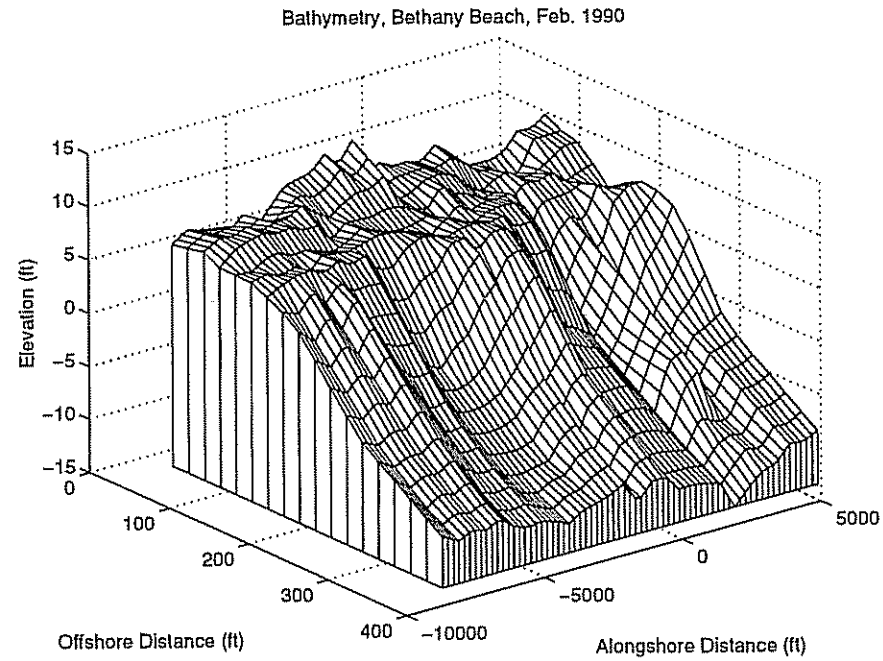
Bathymetry, Bethany Beach, Feb. 1990
Elevation (ft)
15
10
5
0
−5
−10
−15
0
100
200
300
400
Offshore Distance (ft)
−10000
−5000
0
5000
Alongshore Distance (ft)

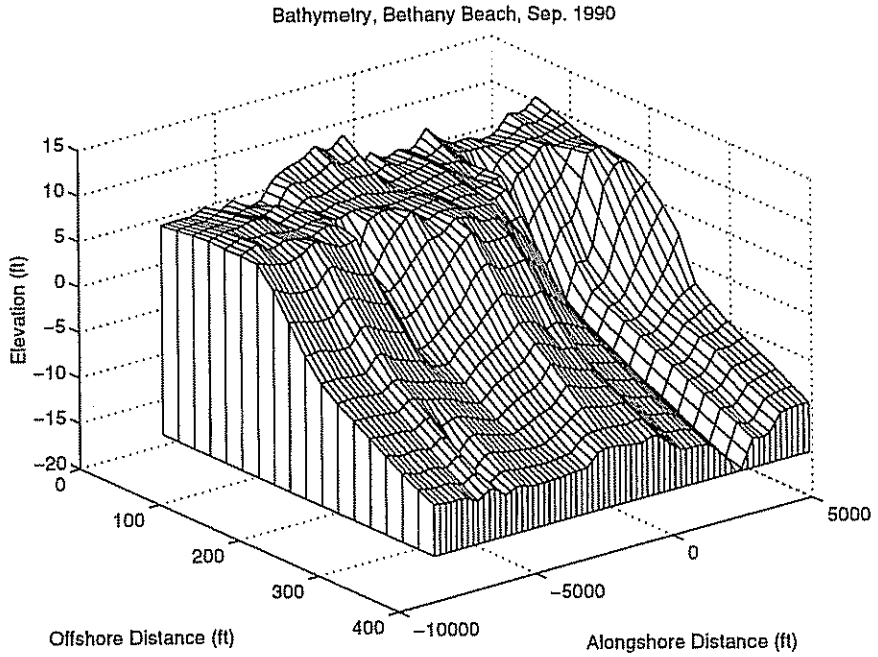
Bathymetry, Bethany Beach, Sep. 1990
Elevation (ft)
15
10
5
0
-5
-10
-15
-20
0
100
200
300
400
Offshore Distance (ft)
-10000
-5000
0
5000
Alongshore Distance (ft)

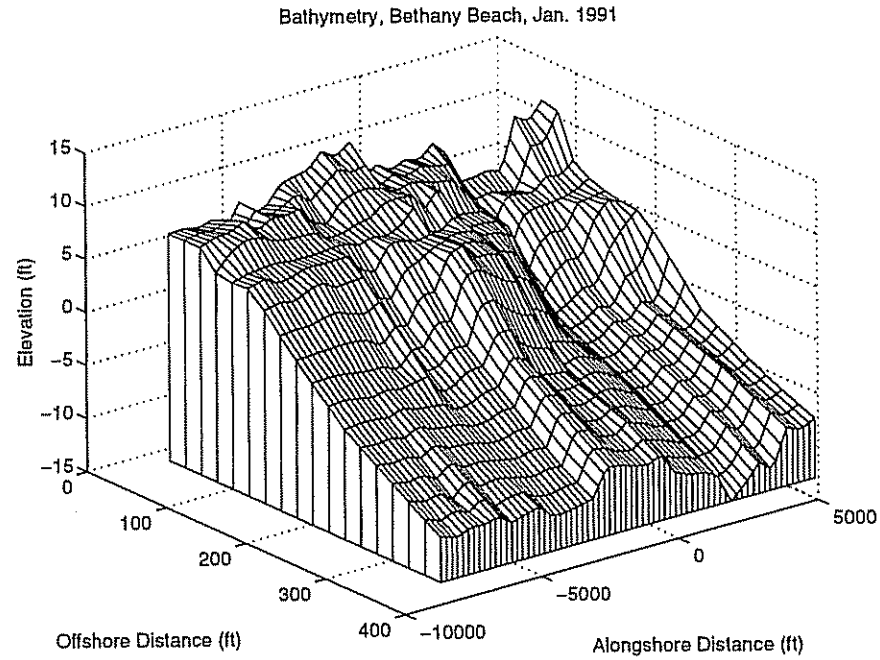
Bathymetry, Bethany Beach, Jan. 1991
Elevation (ft)
15
10
5
0
-5
-10
-15
0
100
200
300
400
Offshore Distance (ft)
-10000
-5000
0
5000
Alongshore Distance (ft)

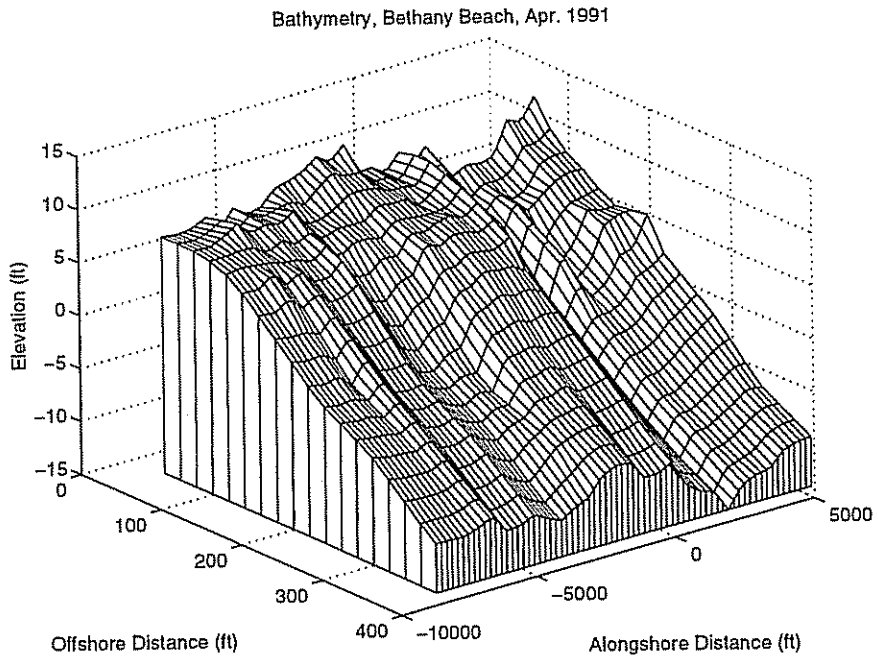
Bathymetry, Bethany Beach, Apr. 1991
Elevation (ft)
15
10
5
0
−5
−10
−15
0
100
200
300
400
Offshore Distance (ft)
−10000
−5000
0
5000
Alongshore Distance (ft)

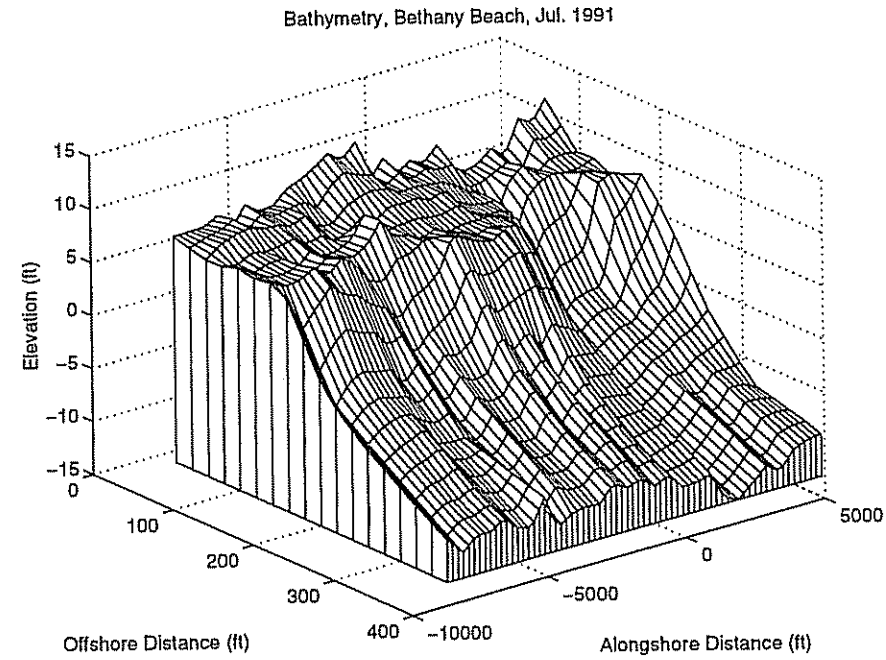
Bathymetry, Bethany Beach, Jul. 1991
Elevation (ft)
15
10
5
0
−5
−10
−15
0
100
200
300
400
Offshore Distance (ft)
−10000
−5000
0
5000
Alongshore Distance (ft)

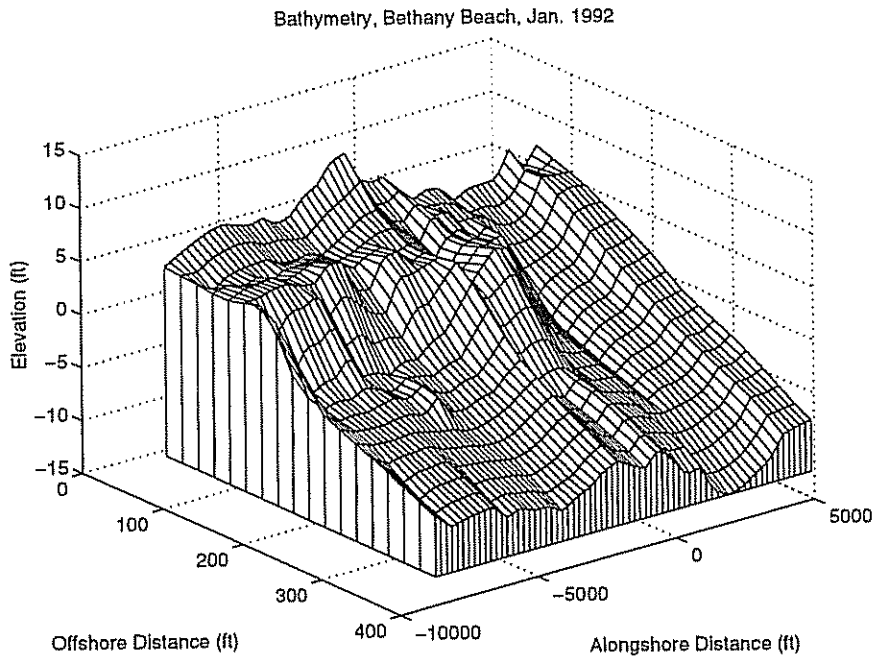
Bathymetry, Bethany Beach, Jan. 1992
Elevation (ft)
15
10
5
0
−5
−10
−15
0
100
200
300
400
Offshore Distance (ft)
−10000
−5000
0
5000
Alongshore Distance (ft)

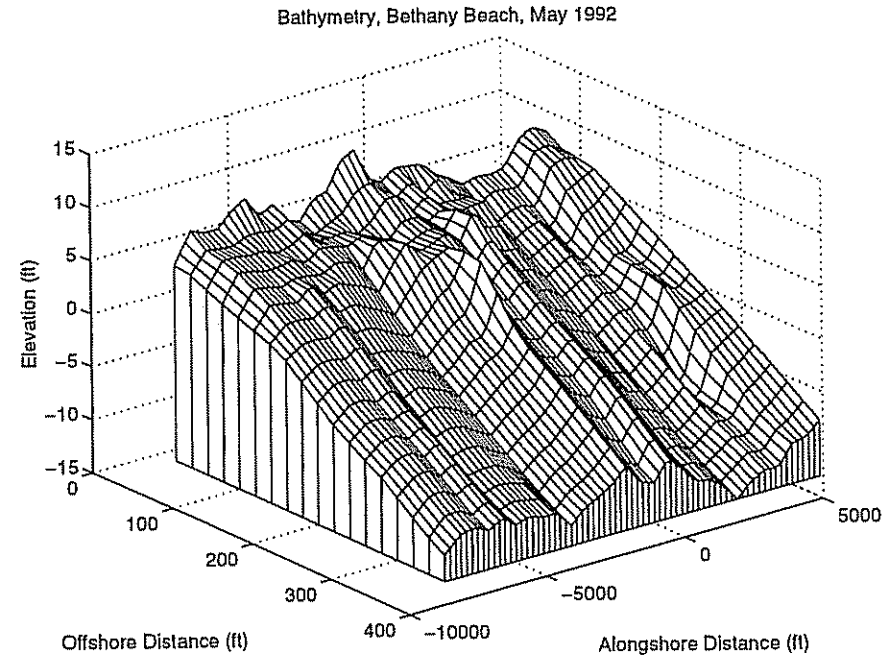
Bathymetry, Bethany Beach, May 1992
Elevation (ft)
15
10
5
0
−5
−10
−15
0
100
200
300
400
Offshore Distance (ft)
−10000
−5000
0
5000
Alongshore Distance (ft)

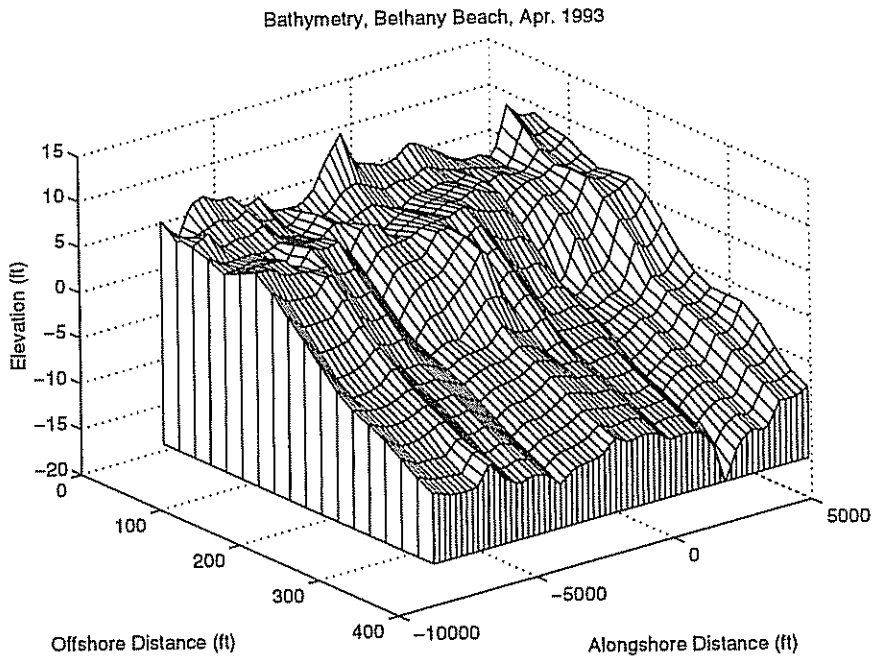
Bathymetry, Bethany Beach, Apr. 1993
Elevation (ft)
15
10
5
0
−5
−10
−15
−20
0
100
200
300
400
Offshore Distance (ft)
−10000
−5000
0
5000
Alongshore Distance (ft)

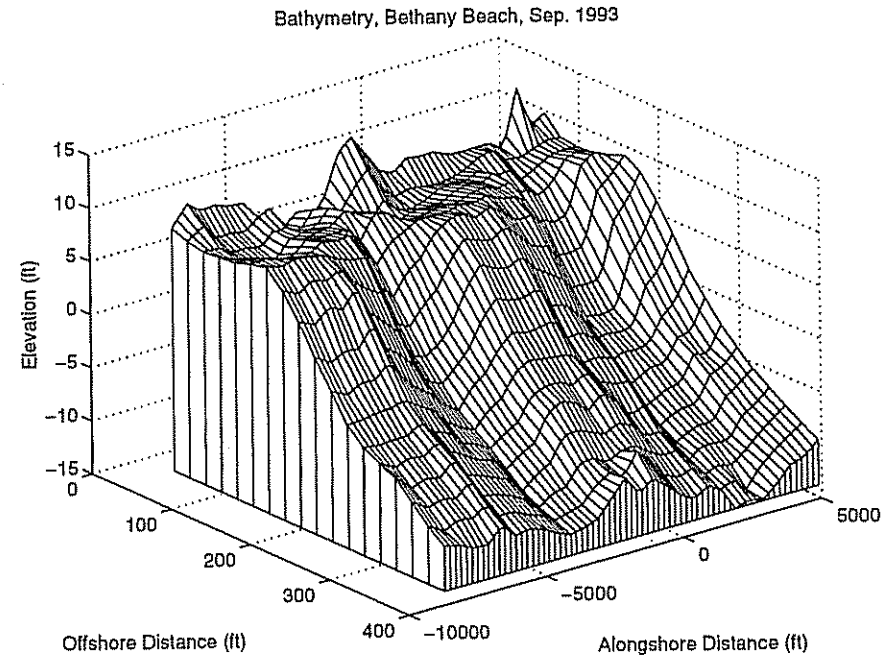
Bathymetry, Bethany Beach, Sep. 1993
Elevation (ft)
15
10
5
0
−5
−10
−15
0
100
200
300
400
Offshore Distance (ft)
−10000
−5000
0
5000
Alongshore Distance (ft)

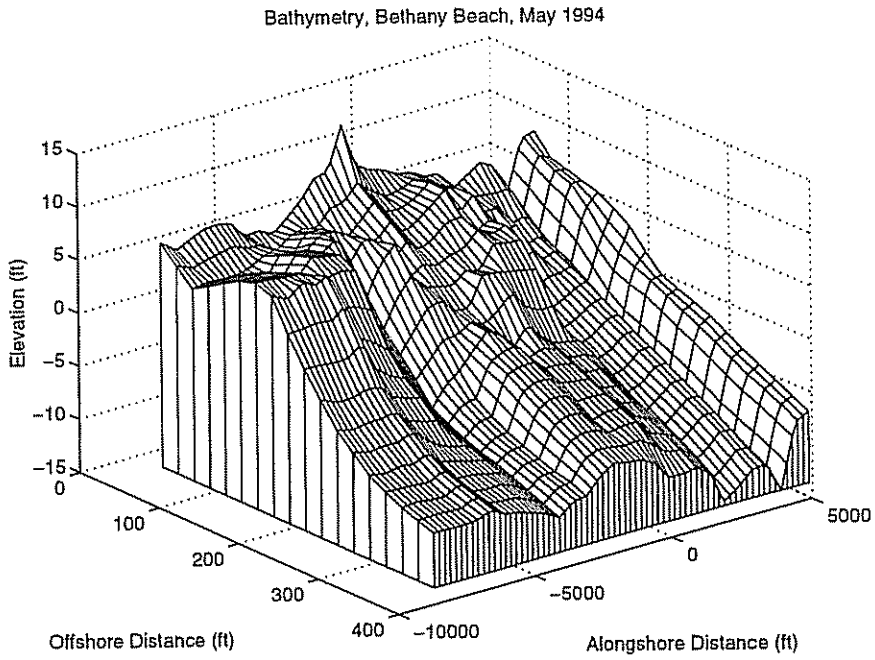
Bathymetry, Bethany Beach, May 1994
Elevation (ft)
15
10
5
0
−5
−10
−15
0
100
200
300
400
Offshore Distance (ft)
−10000
−5000
0
5000
Alongshore Distance (ft)

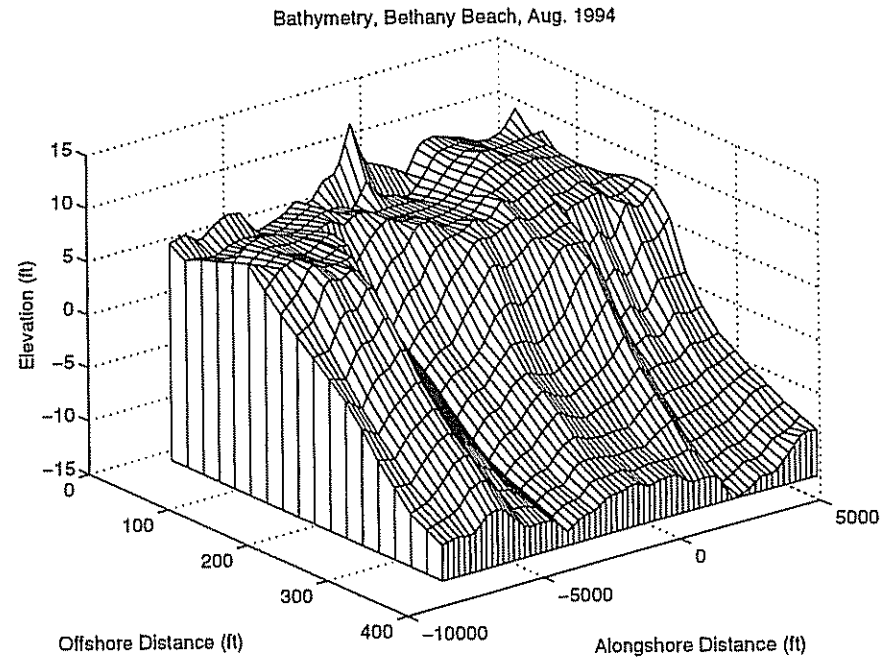
Bathymetry, Bethany Beach, Aug. 1994
Elevation (ft)
15
10
5
0
−5
−10
−15
0
100
200
300
400
Offshore Distance (ft)
−10000
−5000
0
5000
Alongshore Distance (ft)

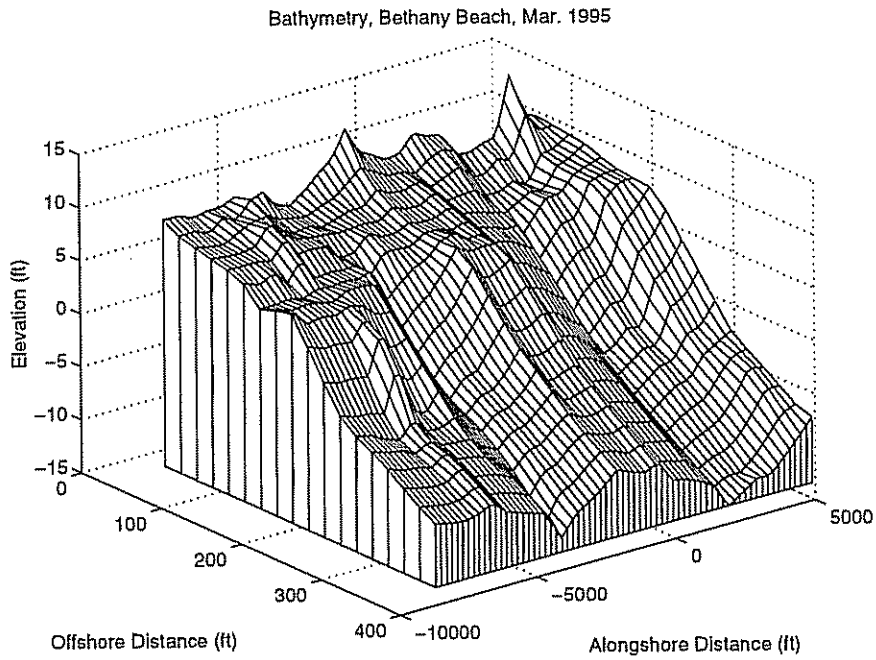
Bathymetry, Bethany Beach, Mar. 1995
Elevation (ft)
15
10
5
0
−5
−10
−15
0
100
200
300
400
Offshore Distance (ft)
−10000
−5000
0
5000
Alongshore Distance (ft)

Appendix C

LRP SITES - SHORELINE REGRESSION ANALYSIS RESULTS

This Appendix presents the results from the shoreline regression analysis performed on the LRP sites. The sites are shown in Figure 7.1. A linear regression line is fit to the shoreline position to indicate shoreline recession or accreation over the last 12 years.

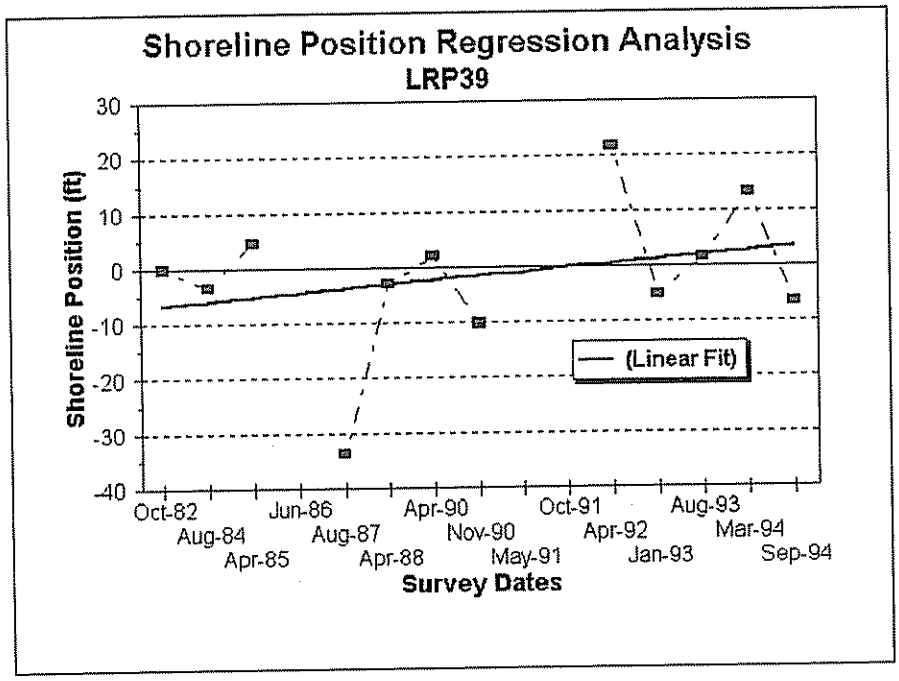
Shoreline Position Regression Analysis
LRP39
Shoreline Position (ft)
30
20
10
0
-10
-20
-30
-40
(Linear Fit)
Oct-82
Aug-84
Apr-85
Jun-86
Aug-87
Apr-88
Apr-90
Nov-90
May-91
Oct-91
Apr-92
Jan-93
Aug-93
Mar-94
Sep-94
Survey Dates

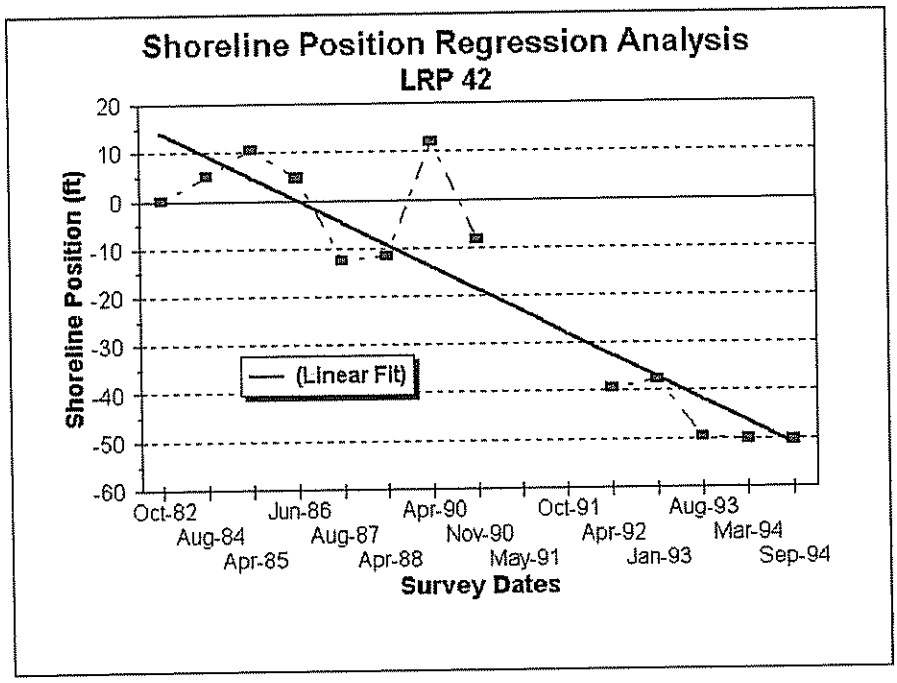
Shoreline Position Regression Analysis
LRP 42
Shoreline Position (ft)
20
10
0
-10
-20
-30
-40
-50
-60
(Linear Fit)
Oct-82
Aug-84
Apr-85
Jun-86
Aug-87
Apr-88
Apr-90
Nov-90
May-91
Oct-91
Apr-92
Jan-93
Aug-93
Mar-94
Sep-94
Survey Dates

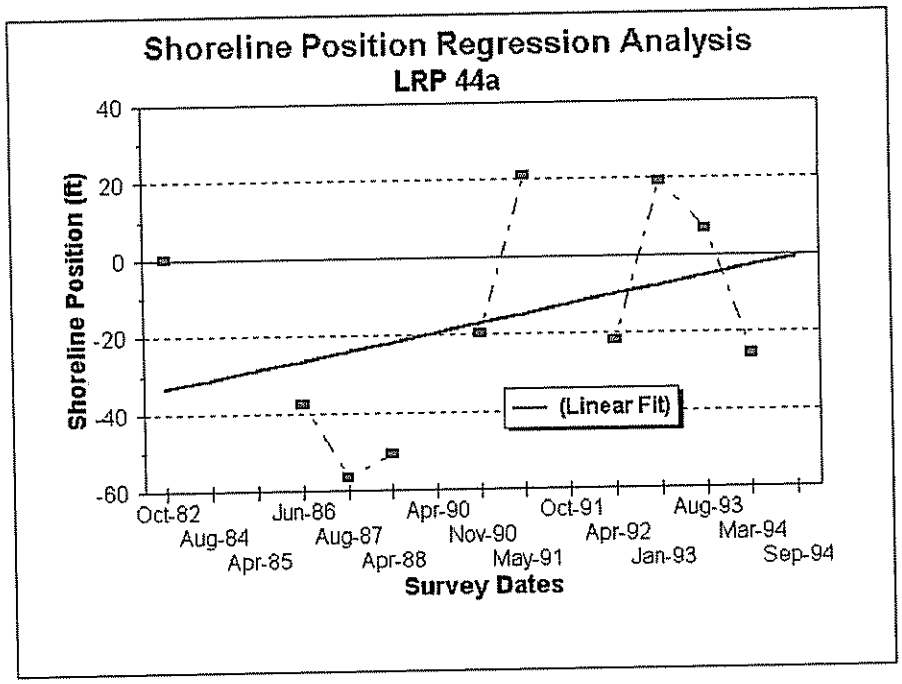
Shoreline Position Regression Analysis
LRP 44a
Shoreline Position (ft)
40
20
0
-20
-40
-60
(Linear Fit)
Oct-82
Aug-84
Apr-85
Jun-86
Aug-87
Apr-88
Apr-90
Nov-90
May-91
Oct-91
Apr-92
Jan-93
Aug-93
Mar-94
Sep-94
Survey Dates

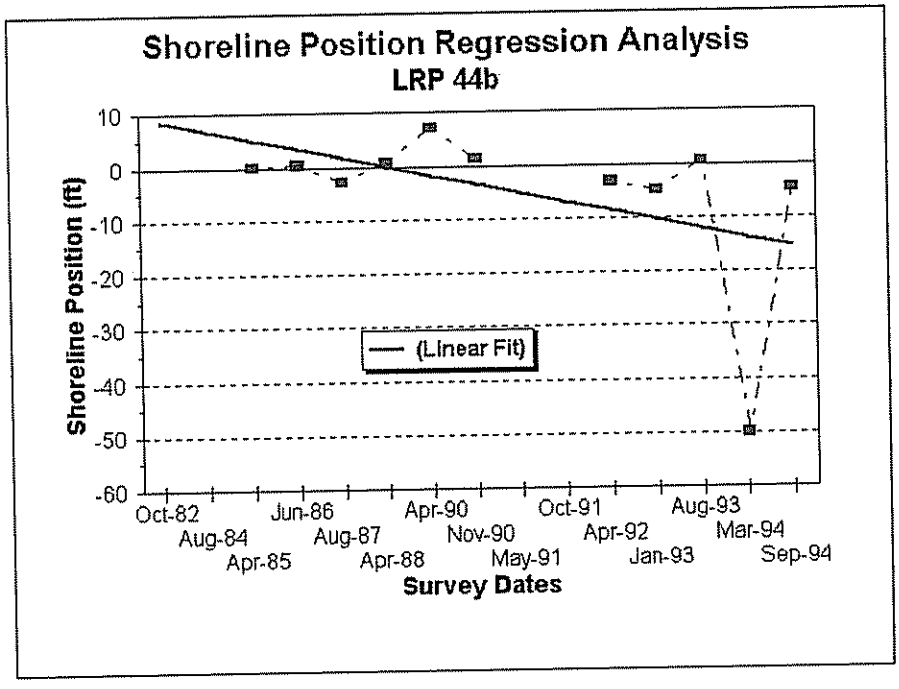
Shoreline Position Regression Analysis
LRP 44b
Shoreline Position (ft)
10
0
-10
-20
-30
-40
-50
-60
(Linear Fit)
Oct-82
Aug-84
Apr-85
Jun-86
Aug-87
Apr-88
Apr-90
Nov-90
May-91
Oct-91
Apr-92
Jan-93
Aug-93
Mar-94
Sep-94
Survey Dates

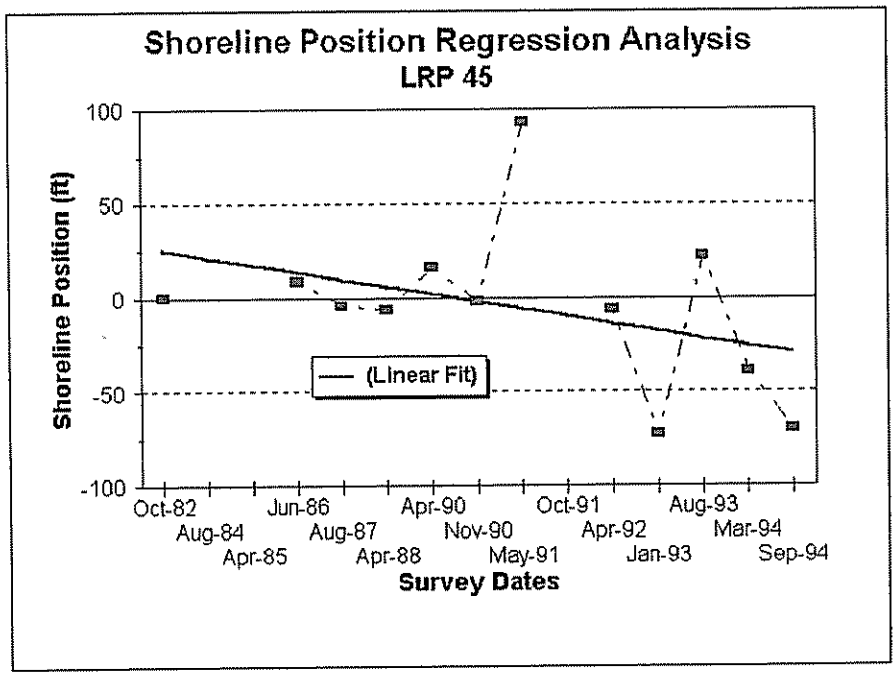
Shoreline Position Regression Analysis
LRP 45
Shoreline Position (ft)
100
50
0
-50
-100
(Linear Fit)
Oct-82
Aug-84
Apr-85
Jun-86
Aug-87
Apr-88
Apr-90
Nov-90
May-91
Oct-91
Apr-92
Jan-93
Aug-93
Mar-94
Sep-94
Survey Dates

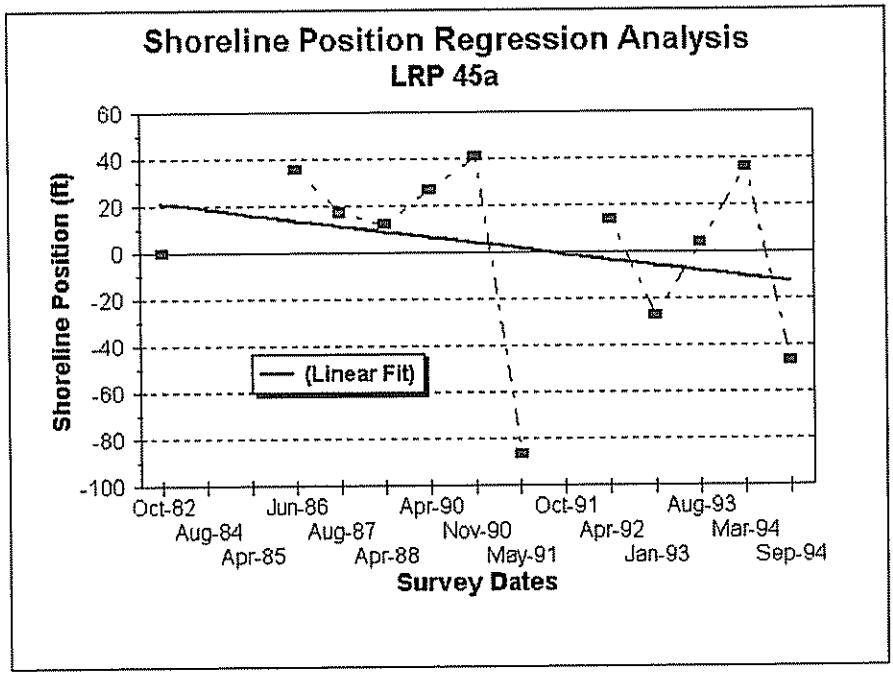
Shoreline Position Regression Analysis
LRP 45a
Shoreline Position (ft)
60
40
20
0
-20
-40
-60
-80
-100
(Linear Fit)
Oct-82
Aug-84
Apr-85
Jun-86
Aug-87
Apr-88
Apr-90
Nov-90
May-91
Oct-91
Apr-92
Jan-93
Aug-93
Mar-94
Sep-94
Survey Dates

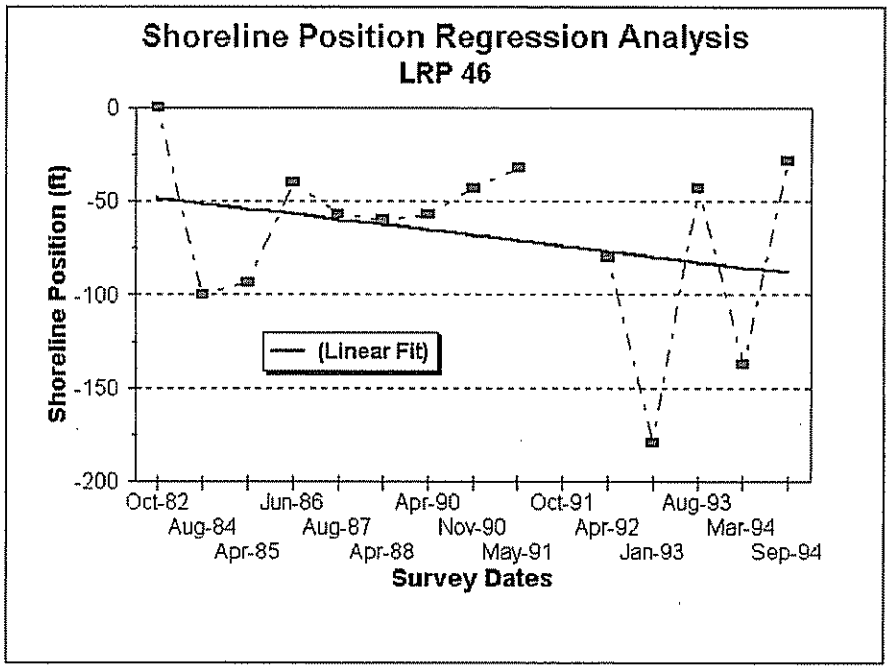
Shoreline Position Regression Analysis
LRP 46
Shoreline Position (ft)
0
-50
-100
-150
-200
(Linear Fit)
Oct-82
Aug-84
Apr-85
Jun-86
Aug-87
Apr-88
Apr-90
Nov-90
May-91
Oct-91
Apr-92
Jan-93
Aug-93
Mar-94
Sep-94
Survey Dates

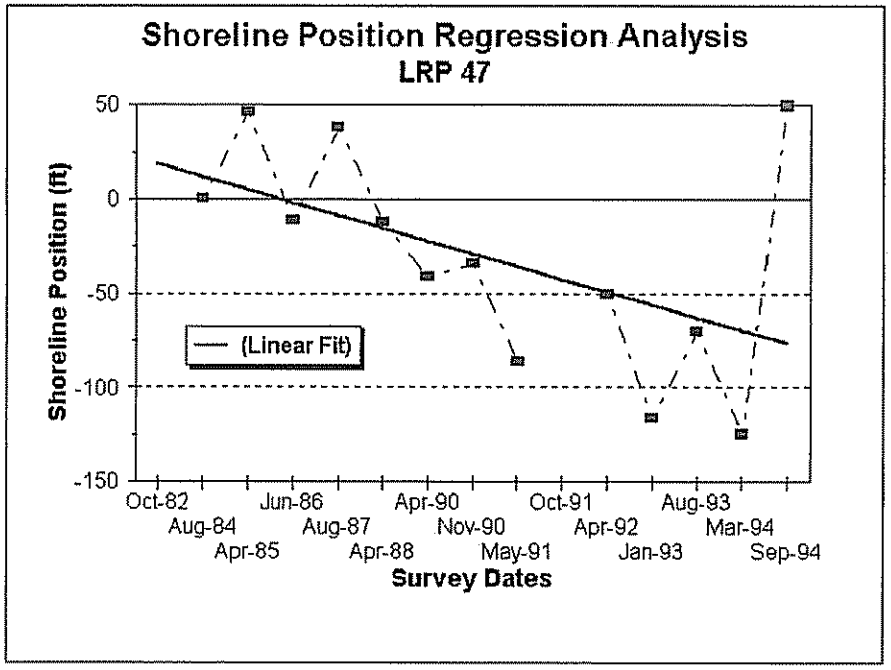
Shoreline Position Regression Analysis
LRP 47
Shoreline Position (ft)
50
0
-50
-100
-150
(Linear Fit)
Oct-82
Aug-84
Apr-85
Jun-86
Aug-87
Apr-88
Apr-90
Nov-90
May-91
Oct-91
Apr-92
Jan-93
Aug-93
Mar-94
Sep-94
Survey Dates

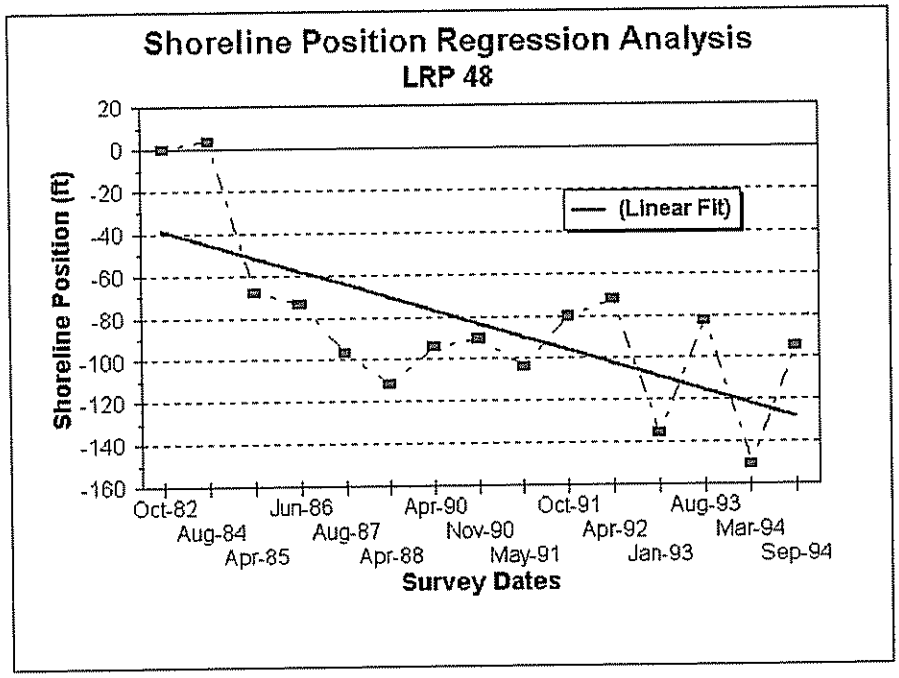
Shoreline Position Regression Analysis
LRP 48
Shoreline Position (ft)
20
0
-20
-40
-60
-80
-100
-120
-140
-160
(Linear Fit)
Oct-82
Aug-84
Apr-85
Jun-86
Aug-87
Apr-88
Apr-90
Nov-90
May-91
Oct-91
Apr-92
Jan-93
Aug-93
Mar-94
Sep-94
Survey Dates

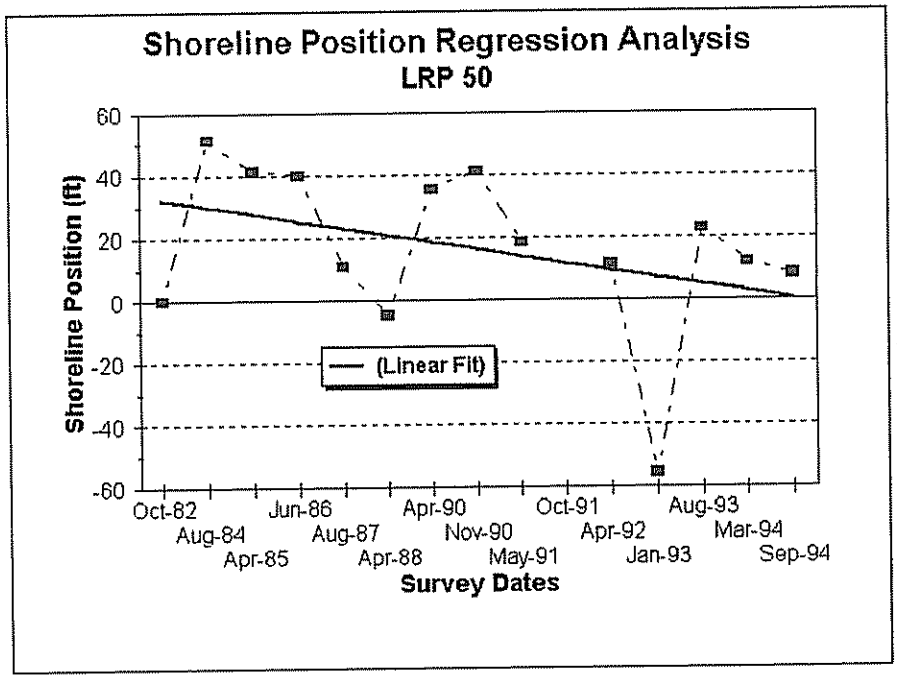
Shoreline Position Regression Analysis
LRP 50
Shoreline Position (ft)
60
40
20
0
-20
-40
-60
(Linear Fit)
Oct-82
Aug-84
Apr-85
Jun-86
Aug-87
Apr-88
Apr-90
Nov-90
May-91
Oct-91
Apr-92
Jan-93
Aug-93
Mar-94
Sep-94
Survey Dates

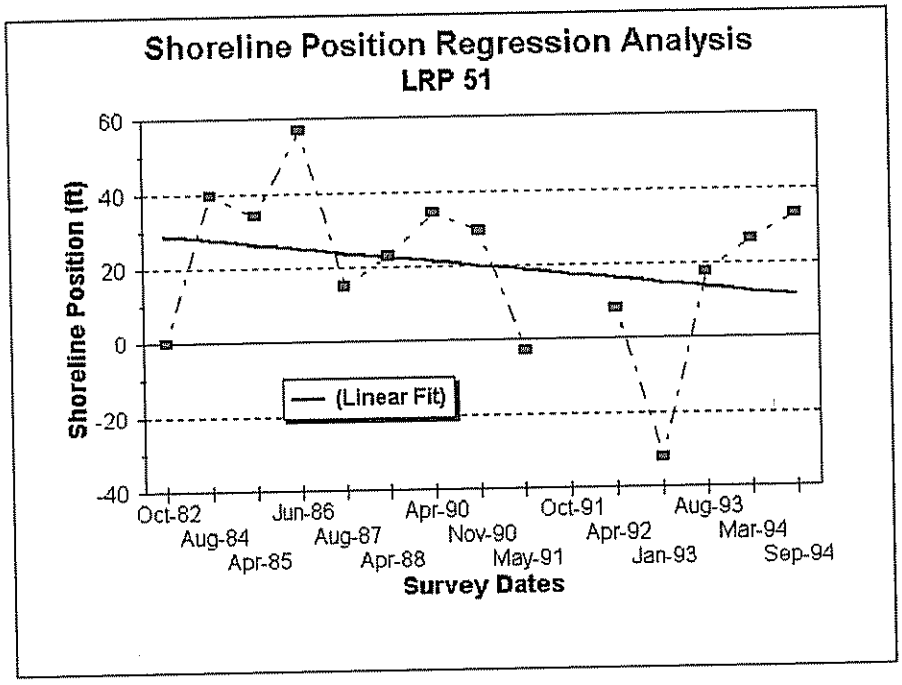
Shoreline Position Regression Analysis
LRP 51
Shoreline Position (ft)
60
40
20
0
-20
-40
(Linear Fit)
Oct-82
Aug-84
Apr-85
Jun-86
Aug-87
Apr-88
Apr-90
Nov-90
May-91
Oct-91
Apr-92
Jan-93
Aug-93
Mar-94
Sep-94
Survey Dates

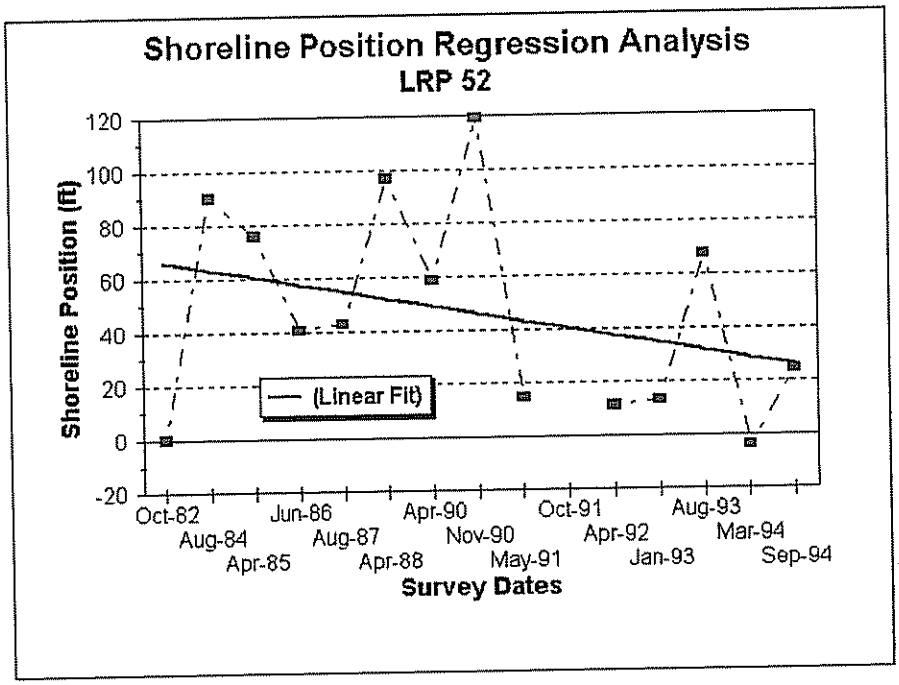
Shoreline Position Regression Analysis
LRP 52
Shoreline Position (ft)
120
100
80
60
40
20
0
-20
(Linear Fit)
Oct-82
Aug-84
Apr-85
Jun-86
Aug-87
Apr-88
Apr-90
Nov-90
May-91
Oct-91
Apr-92
Jan-93
Aug-93
Mar-94
Sep-94
Survey Dates

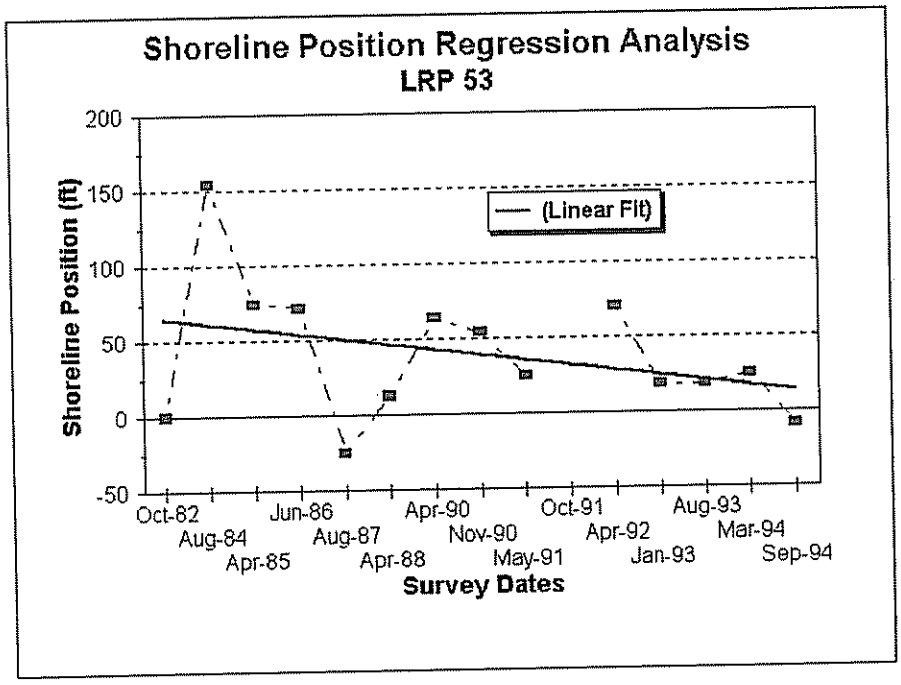
Shoreline Position Regression Analysis
LRP 53
Shoreline Position (ft)
200
150
100
50
0
-50
(Linear Fit)
Oct-82
Aug-84
Apr-85
Jun-86
Aug-87
Apr-88
Apr-90
Nov-90
May-91
Oct-91
Apr-92
Jan-93
Aug-93
Mar-94
Sep-94
Survey Dates

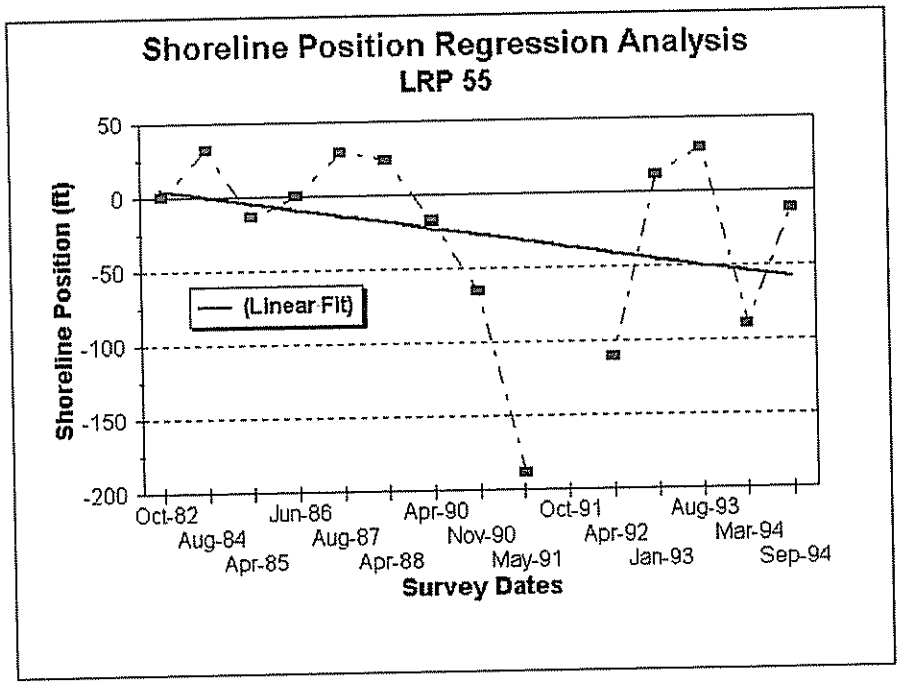
Shoreline Position Regression Analysis
LRP 55
Shoreline Position (ft)
50
0
-50
-100
-150
-200
(Linear Fit)
Oct-82
Aug-84
Apr-85
Jun-86
Aug-87
Apr-88
Apr-90
Nov-90
May-91
Oct-91
Apr-92
Jan-93
Aug-93
Mar-94
Sep-94
Survey Dates

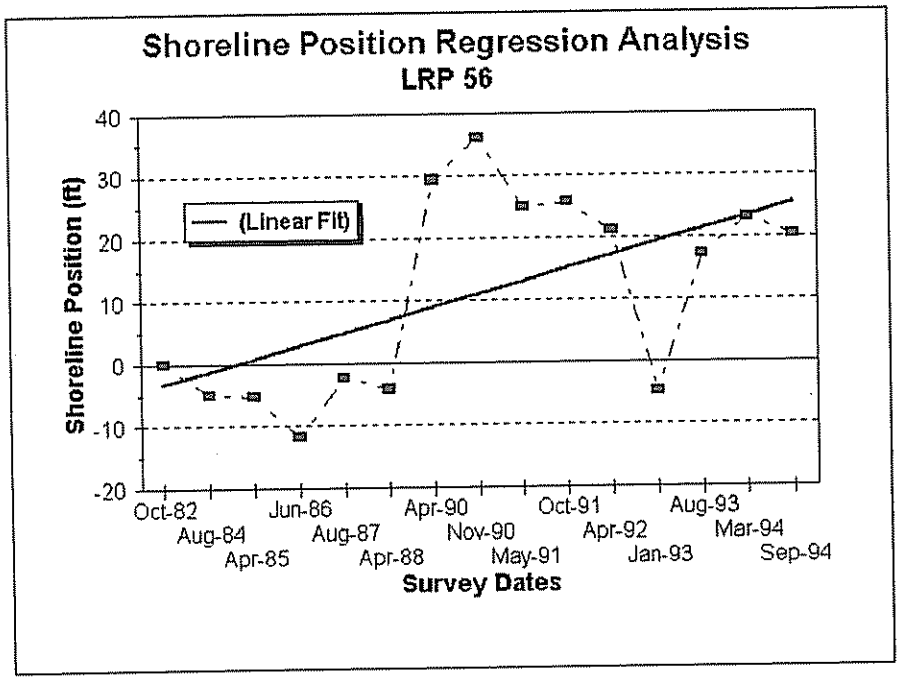
Shoreline Position Regression Analysis
LRP 56
Shoreline Position (ft)
40
30
20
10
0
-10
-20
(Linear Fit)
Oct-82
Aug-84
Apr-85
Jun-86
Aug-87
Apr-88
Apr-90
Nov-90
May-91
Oct-91
Apr-92
Jan-93
Aug-93
Mar-94
Sep-94
Survey Dates

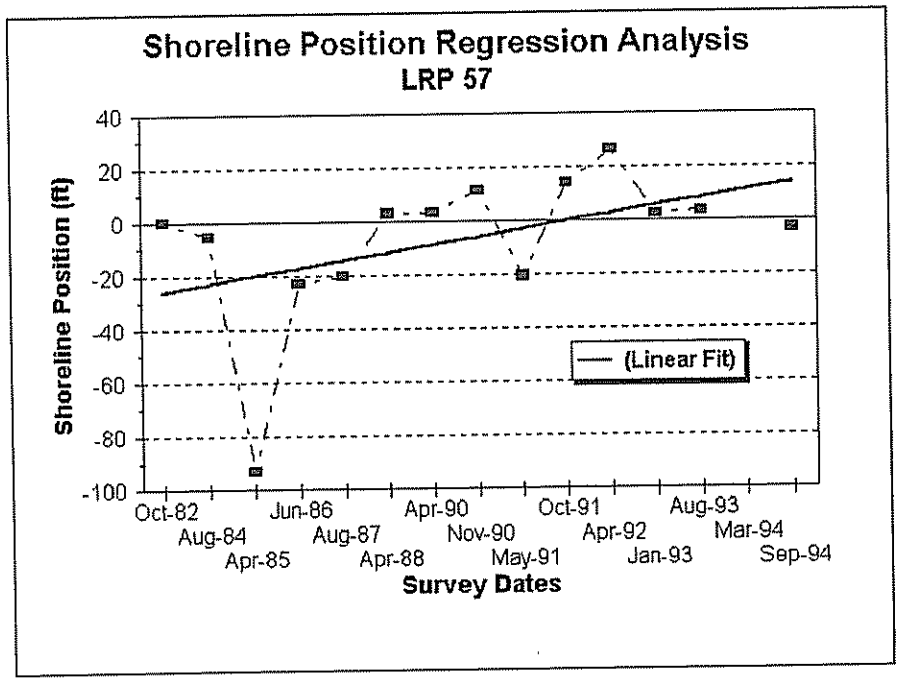
Shoreline Position Regression Analysis
LRP 57
Shoreline Position (ft)
40
20
0
-20
-40
-60
-80
-100
(Linear Fit)
Oct-82
Aug-84
Apr-85
Jun-86
Aug-87
Apr-88
Apr-90
Nov-90
May-91
Oct-91
Apr-92
Jan-93
Aug-93
Mar-94
Sep-94
Survey Dates

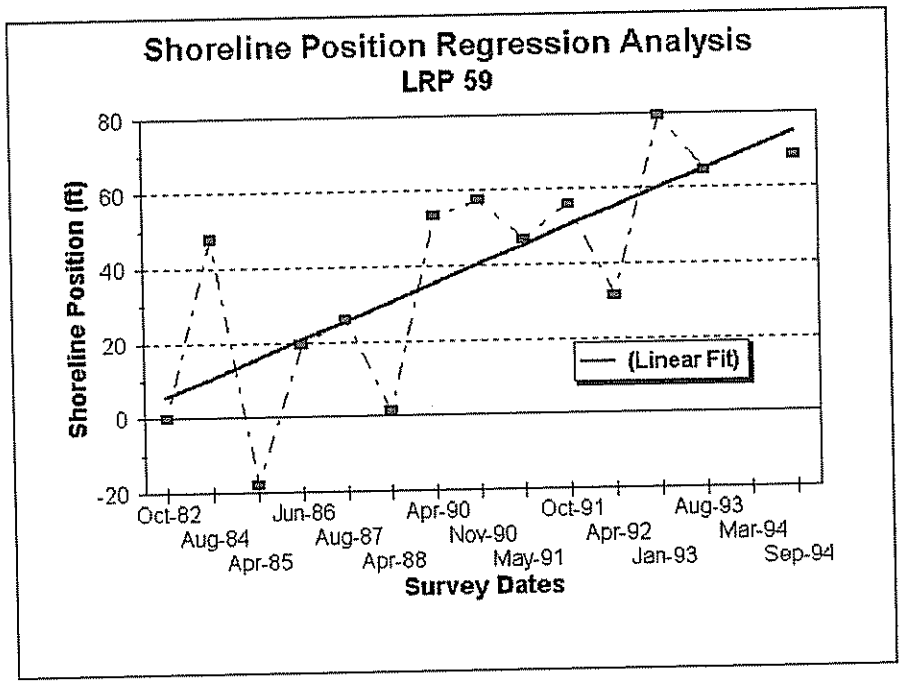
Shoreline Position Regression Analysis
LRP 59
Shoreline Position (ft)
80
60
40
20
0
-20
(Linear Fit)
Oct-82
Aug-84
Apr-85
Jun-86
Aug-87
Apr-88
Apr-90
Nov-90
May-91
Oct-91
Apr-92
Jan-93
Aug-93
Mar-94
Sep-94
Survey Dates

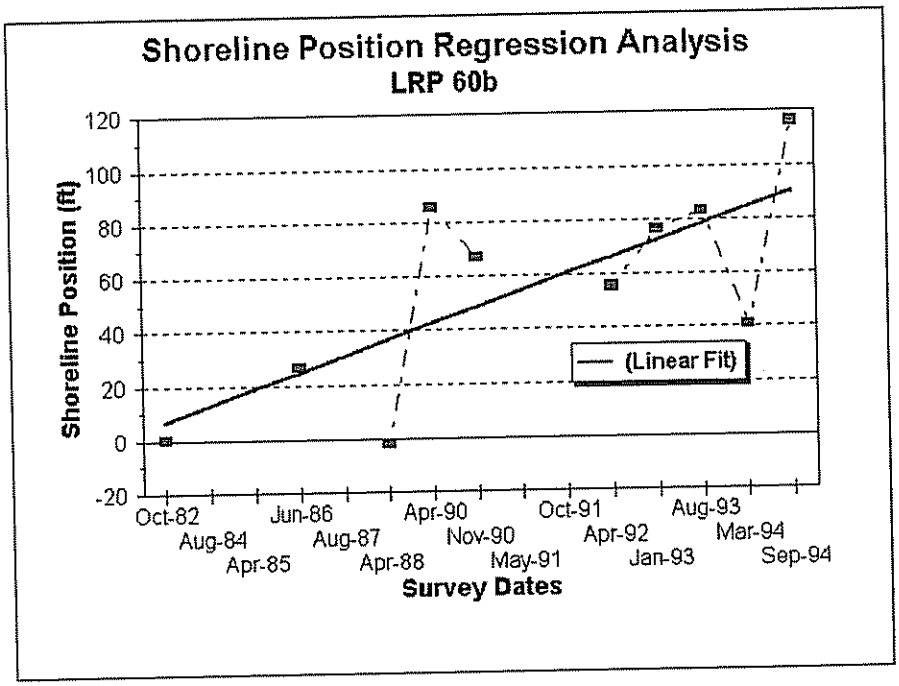
Shoreline Position Regression Analysis
LRP 60b
Shoreline Position (ft)
120
100
80
60
40
20
0
-20
(Linear Fit)
Oct-82
Aug-84
Apr-85
Jun-86
Aug-87
Apr-88
Apr-90
Nov-90
May-91
Oct-91
Apr-92
Jan-93
Aug-93
Mar-94
Sep-94
Survey Dates

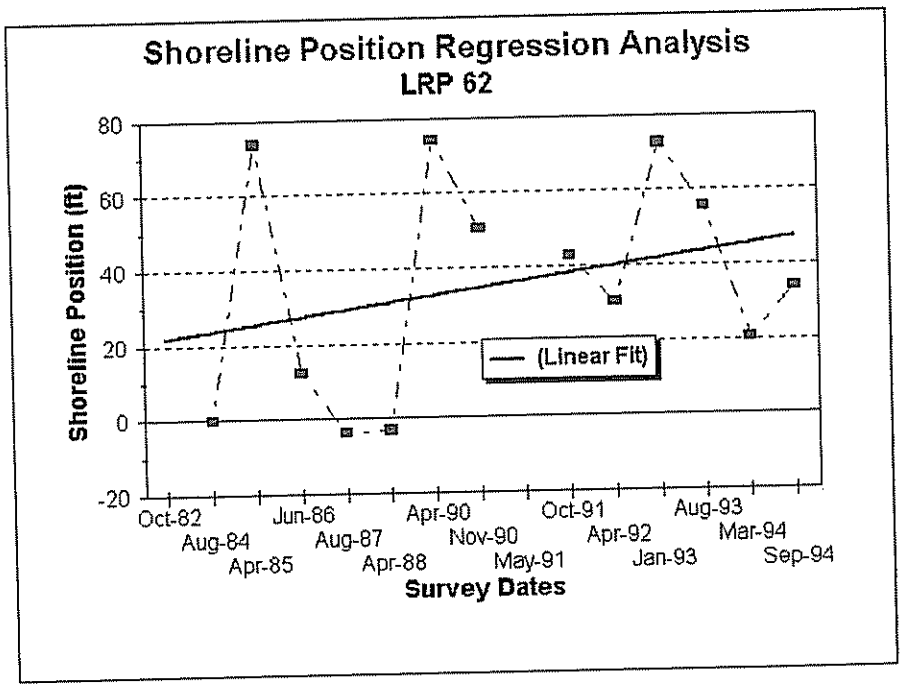
Shoreline Position Regression Analysis
LRP 62
Shoreline Position (ft)
80
60
40
20
0
-20
(Linear Fit)
Oct-82
Aug-84
Apr-85
Jun-86
Aug-87
Apr-88
Apr-90
Nov-90
May-91
Oct-91
Apr-92
Jan-93
Aug-93
Mar-94
Sep-94
Survey Dates

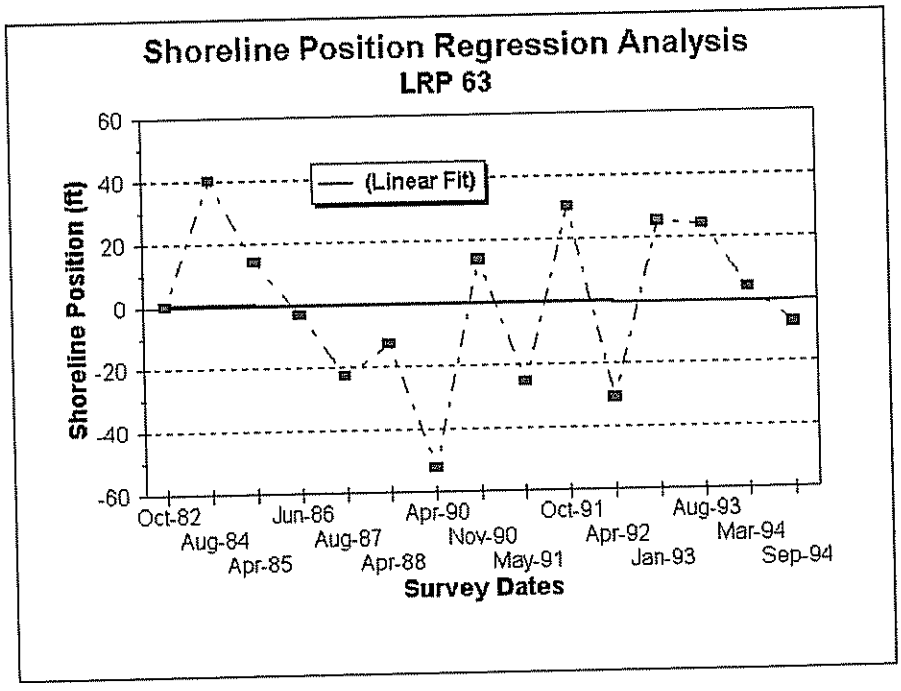
Shoreline Position Regression Analysis
LRP 63
Shoreline Position (ft)
60
40
20
0
-20
-40
-60
(Linear Fit)
Oct-82
Aug-84
Apr-85
Jun-86
Aug-87
Apr-88
Apr-90
Nov-90
May-91
Oct-91
Apr-92
Jan-93
Aug-93
Mar-94
Sep-94
Survey Dates

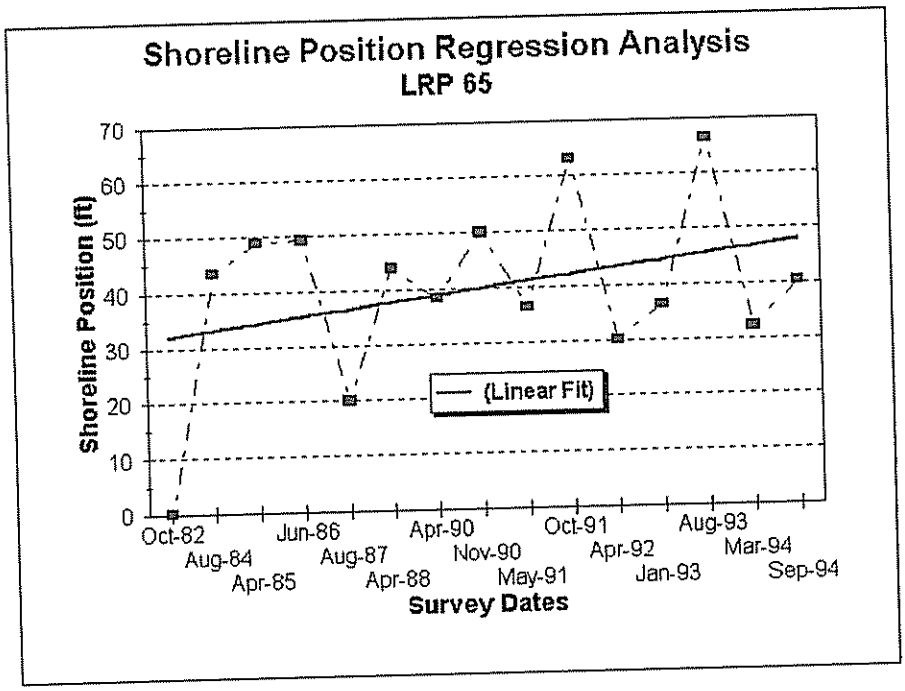
Shoreline Position Regression Analysis
LRP 65
Shoreline Position (ft)
70
60
50
40
30
20
10
0
(Linear Fit)
Oct-82
Aug-84
Apr-85
Jun-86
Aug-87
Apr-88
Apr-90
Nov-90
May-91
Oct-91
Apr-92
Jan-93
Aug-93
Mar-94
Sep-94
Survey Dates

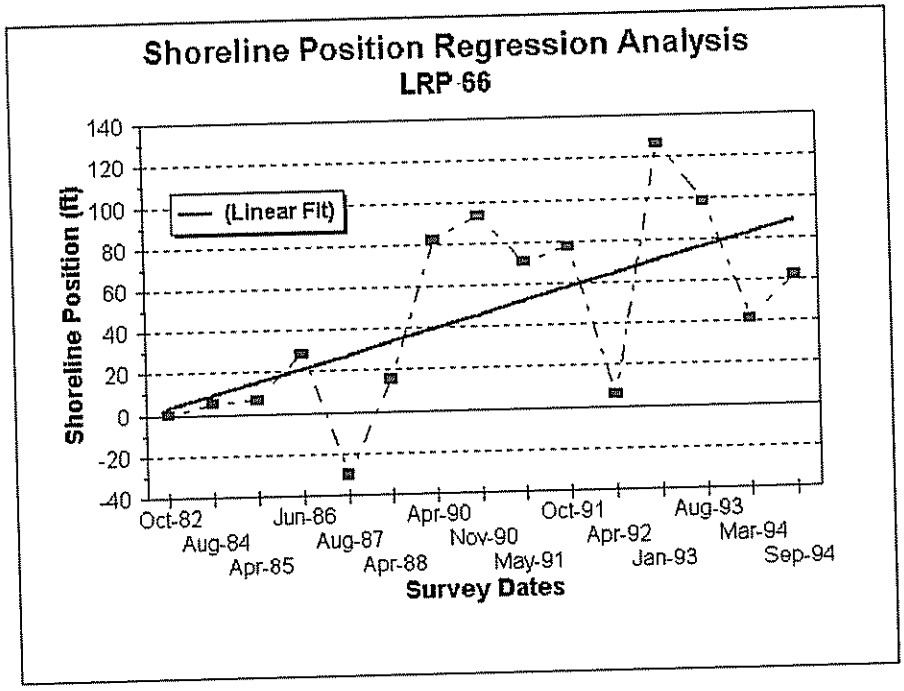
Shoreline Position Regression Analysis
LRP 66
Shoreline Position (ft)
140
120
100
80
60
40
20
0
-20
-40
(Linear Fit)
Oct-82
Aug-84
Apr-85
Jun-86
Aug-87
Apr-88
Apr-90
Nov-90
May-91
Oct-91
Apr-92
Jan-93
Aug-93
Mar-94
Sep-94
Survey Dates

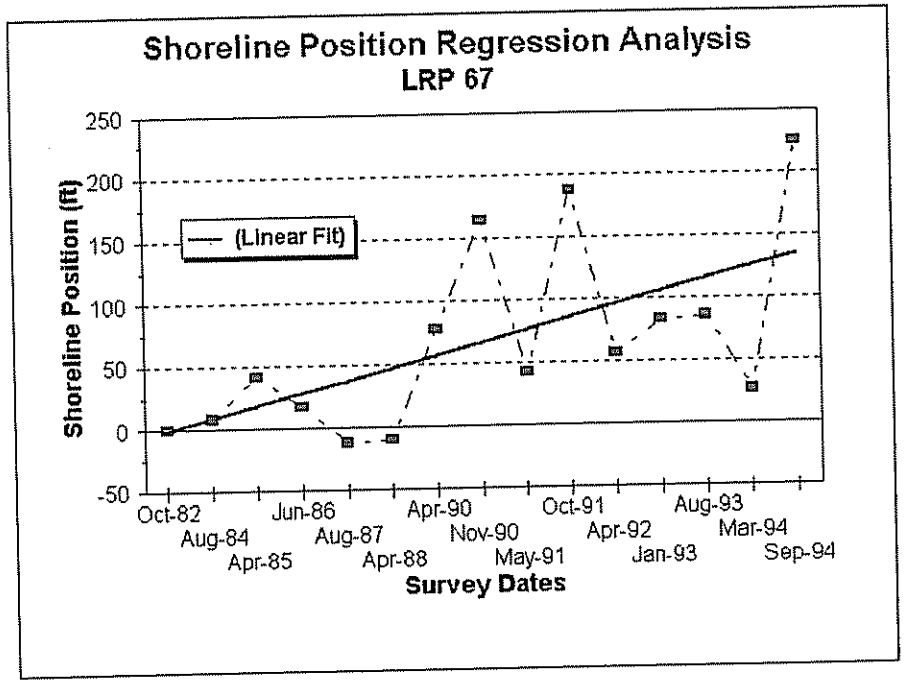
Shoreline Position Regression Analysis
LRP 67
Shoreline Position (ft)
250
200
150
100
50
0
-50
(Linear Fit)
Oct-82
Aug-84
Apr-85
Jun-86
Aug-87
Apr-88
Apr-90
Nov-90
May-91
Oct-91
Apr-92
Jan-93
Aug-93
Mar-94
Sep-94
Survey Dates

Appendix D

LRP SITES - PROFILE VOLUME CHANGES

This Appendix presents cumulative volume changes for most of the LRP profile stations along Delaware's Atlantic coast. The datum used is Mean Sea Level (MSL). Plots show volume changes for the portion of the profile above the datum, the portion of the profile below the datum, and the cumulative net volume change.

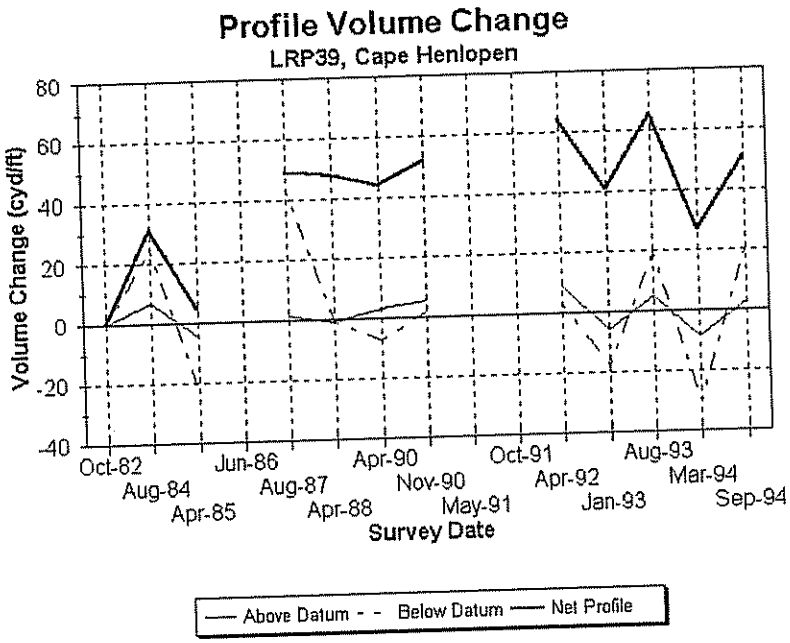
Profile Volume Change
LRP39, Cape Henlopen
Volume Change (cyd/ft)
80
60
40
20
0
-20
-40
Oct-82
Aug-84
Apr-85
Jun-86
Aug-87
Apr-88
Apr-90
Nov-90
May-91
Oct-91
Apr-92
Jan-93
Aug-93
Mar-94
Sep-94
Survey Date
Above Datum
Below Datum
Net Profile

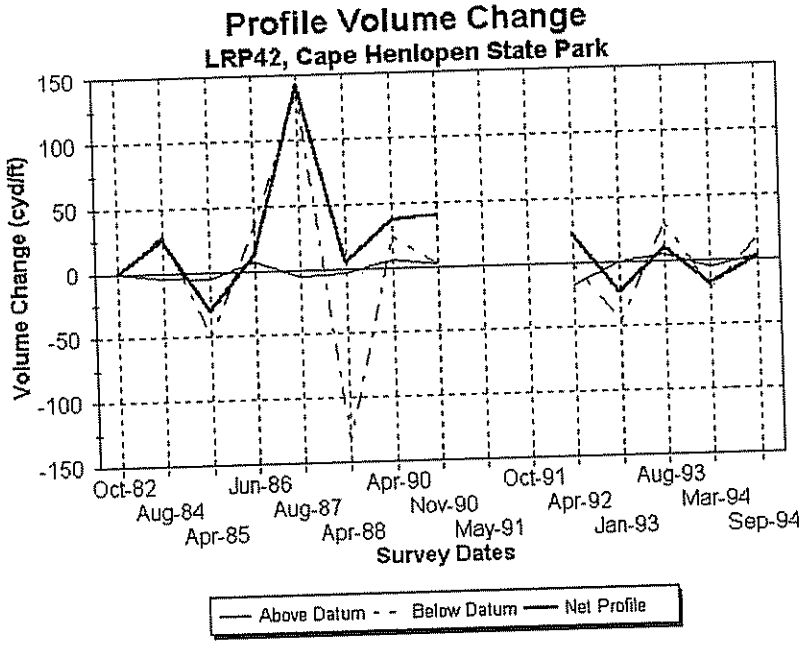
Profile Volume Change
LRP42, Cape Henlopen State Park
Volume Change (cyd/ft)
150
100
50
0
-50
-100
-150
Oct-82
Aug-84
Apr-85
Jun-86
Aug-87
Apr-88
Apr-90
Nov-90
May-91
Oct-91
Apr-92
Jan-93
Aug-93
Mar-94
Sep-94
Survey Dates
Above Datum
Below Datum
Net Profile

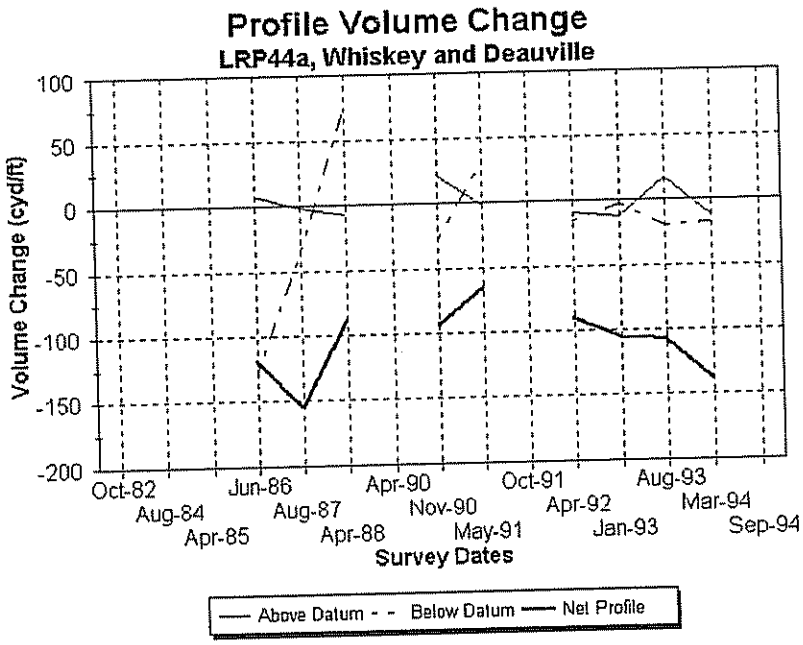
Profile Volume Change
LRP44a, Whiskey and Deauville
Volume Change (cyd/ft)
100
50
0
-50
-100
-150
-200
Oct-82
Aug-84
Apr-85
Jun-86
Aug-87
Apr-88
Apr-90
Nov-90
May-91
Oct-91
Apr-92
Jan-93
Aug-93
Mar-94
Sep-94
Survey Dates
Above Datum
Below Datum
Net Profile

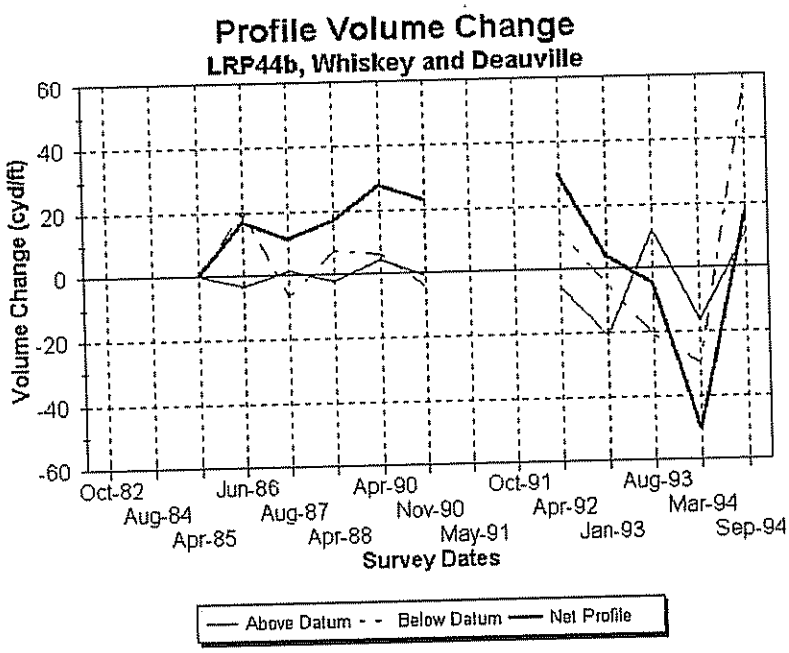
Profile Volume Change
LRP44b, Whiskey and Deauville
Volume Change (cyd/ft)
60
40
20
0
-20
-40
-60
Oct-82
Aug-84
Apr-85
Jun-86
Aug-87
Apr-88
Apr-90
Nov-90
May-91
Oct-91
Apr-92
Jan-93
Aug-93
Mar-94
Sep-94
Survey Dates
Above Datum
Below Datum
Net Profile

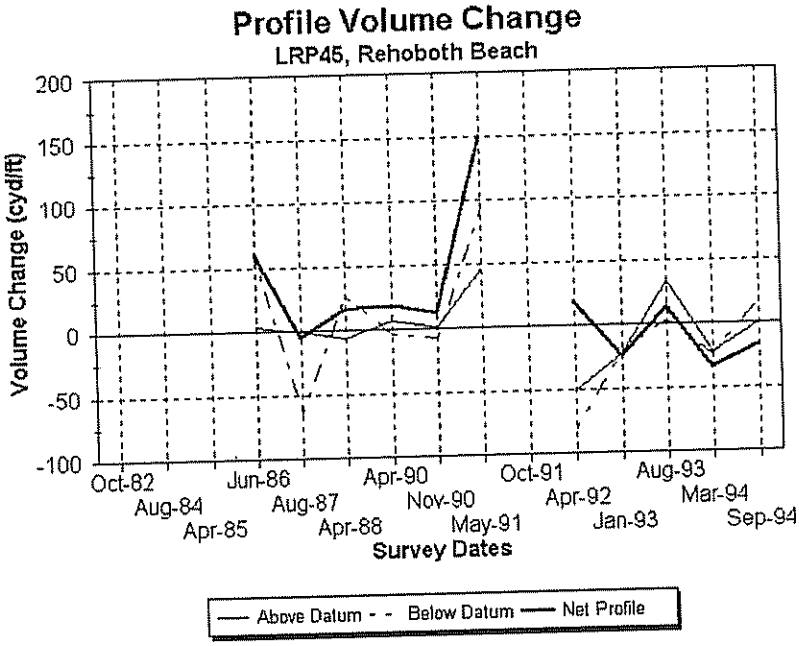
Profile Volume Change
LRP45, Rehoboth Beach
Volume Change (cy/dft)
200
150
100
50
0
-50
-100
Oct-82
Aug-84
Apr-85
Jun-86
Aug-87
Apr-88
Apr-90
Nov-90
May-91
Oct-91
Apr-92
Jan-93
Aug-93
Mar-94
Sep-94
Survey Dates
Above Datum
Below Datum
Net Profile

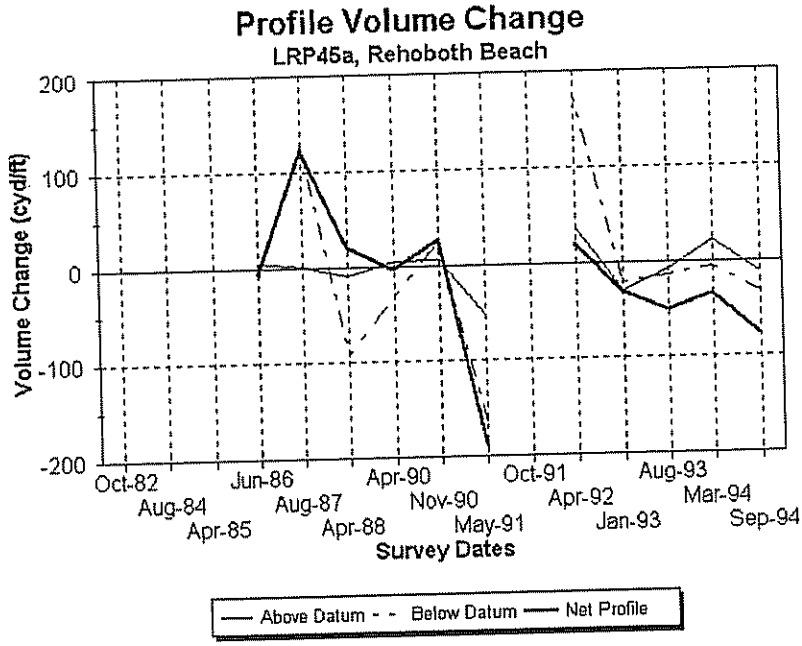
Profile Volume Change
LRP45a, Rehoboth Beach
Volume Change (cy/dft)
200
100
0
-100
-200
Oct-82
Aug-84
Apr-85
Jun-86
Aug-87
Apr-88
Apr-90
Nov-90
May-91
Oct-91
Apr-92
Jan-93
Aug-93
Mar-94
Sep-94
Survey Dates
Above Datum
Below Datum
Net Profile

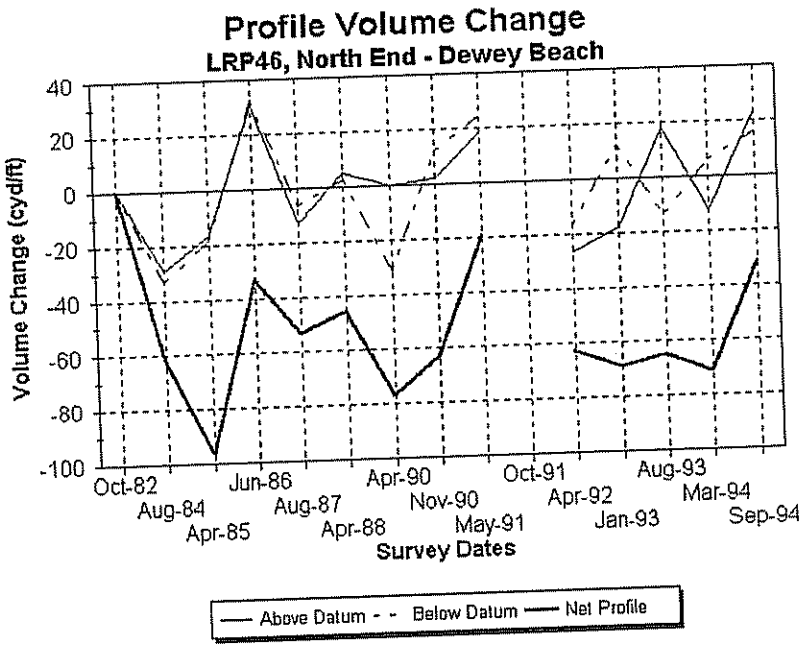
Profile Volume Change
LRP46, North End - Dewey Beach
Volume Change (cyd/ft)
40
20
0
-20
-40
-60
-80
-100
Oct-82
Aug-84
Apr-85
Jun-86
Aug-87
Apr-88
Apr-90
Nov-90
May-91
Oct-91
Apr-92
Jan-93
Aug-93
Mar-94
Sep-94
Survey Dates
Above Datum
Below Datum
Net Profile

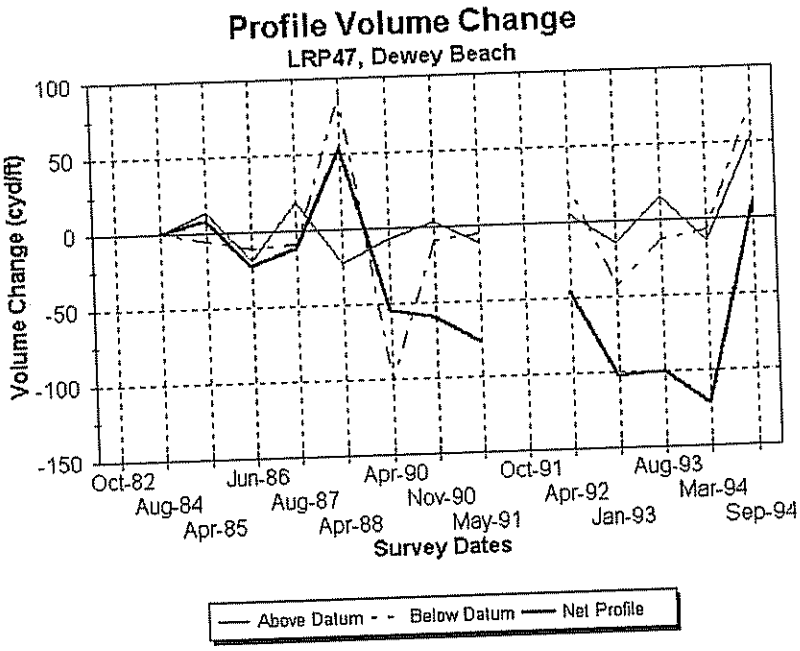
Profile Volume Change
LRP47, Dewey Beach
Volume Change (cyd/ft)
100
50
0
-50
-100
-150
Oct-82
Aug-84
Apr-85
Jun-86
Aug-87
Apr-88
Apr-90
Nov-90
May-91
Oct-91
Apr-92
Jan-93
Aug-93
Mar-94
Sep-94
Survey Dates
Above Datum
Below Datum
Net Profile

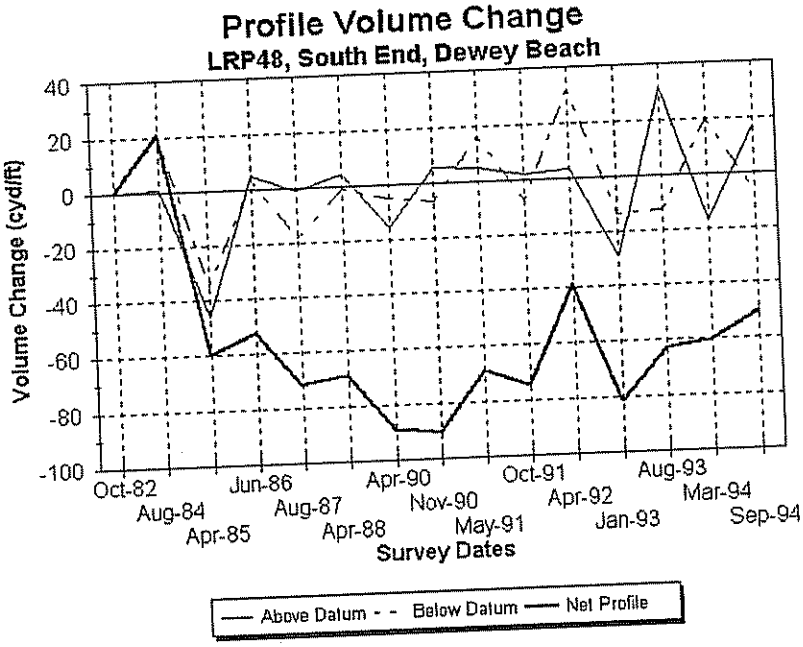
Profile Volume Change
LRP48, South End, Dewey Beach
Volume Change (cyd/ft)
40
20
0
-20
-40
-60
-80
-100
Oct-82
Aug-84
Apr-85
Jun-86
Aug-87
Apr-88
Apr-90
Nov-90
May-91
Oct-91
Apr-92
Jan-93
Aug-93
Mar-94
Sep-94
Survey Dates
Above Datum
Below Datum
Net Profile

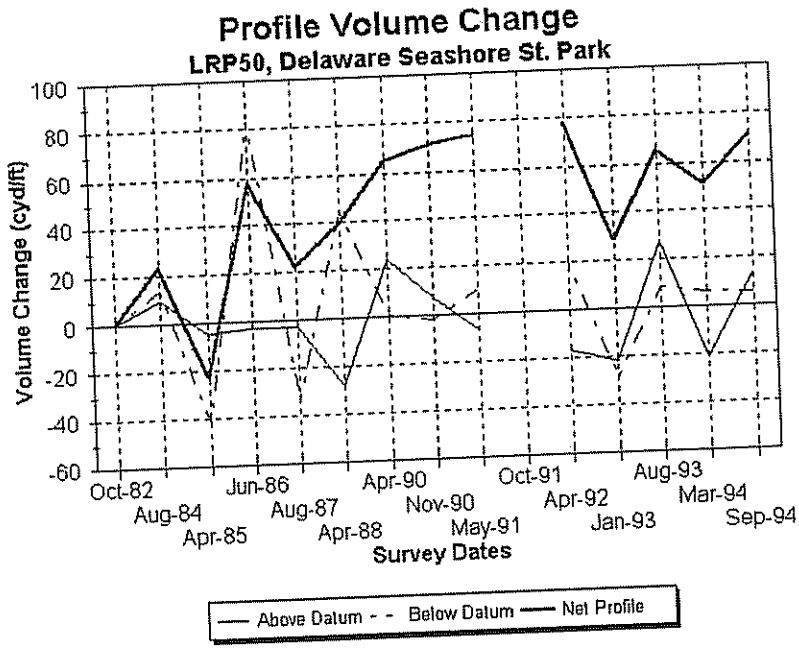
Profile Volume Change
LRP50, Delaware Seashore St. Park
Volume Change (cyd/ft)
100
80
60
40
20
0
-20
-40
-60
Oct-82
Aug-84
Apr-85
Jun-86
Aug-87
Apr-88
Apr-90
Nov-90
May-91
Oct-91
Apr-92
Jan-93
Aug-93
Mar-94
Sep-94
Survey Dates
Above Datum
Below Datum
Net Profile

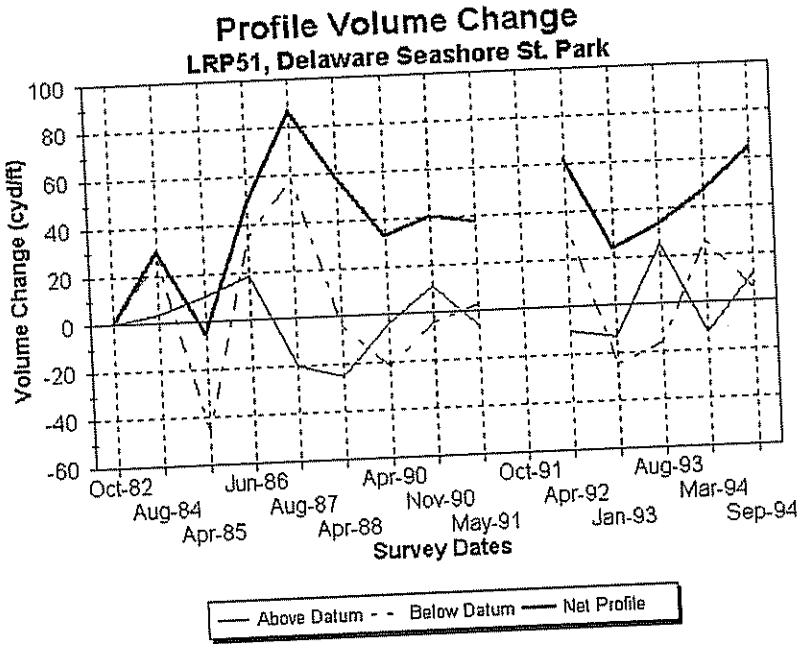
Profile Volume Change
LRP51, Delaware Seashore St. Park
Volume Change (cyd/ft)
100
80
60
40
20
0
-20
-40
-60
Oct-82
Aug-84
Apr-85
Jun-86
Aug-87
Apr-88
Apr-90
Nov-90
May-91
Oct-91
Apr-92
Jan-93
Aug-93
Mar-94
Sep-94
Survey Dates
Above Datum
Below Datum
Net Profile

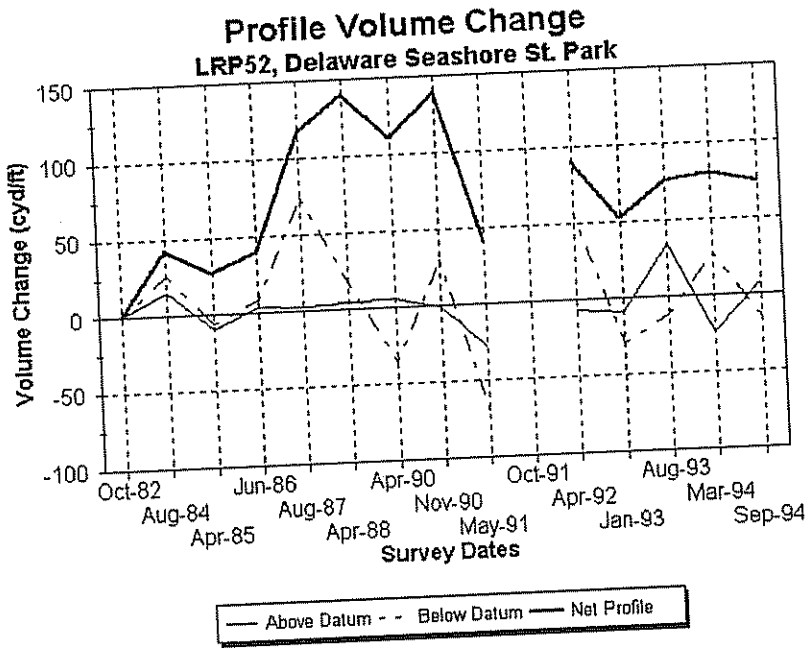
Profile Volume Change
LRP52, Delaware Seashore St. Park
Volume Change (cyd/ft)
150
100
50
0
-50
-100
Oct-82
Aug-84
Apr-85
Jun-86
Aug-87
Apr-88
Apr-90
Nov-90
May-91
Oct-91
Apr-92
Jan-93
Aug-93
Mar-94
Sep-94
Survey Dates
Above Datum
Below Datum
Net Profile

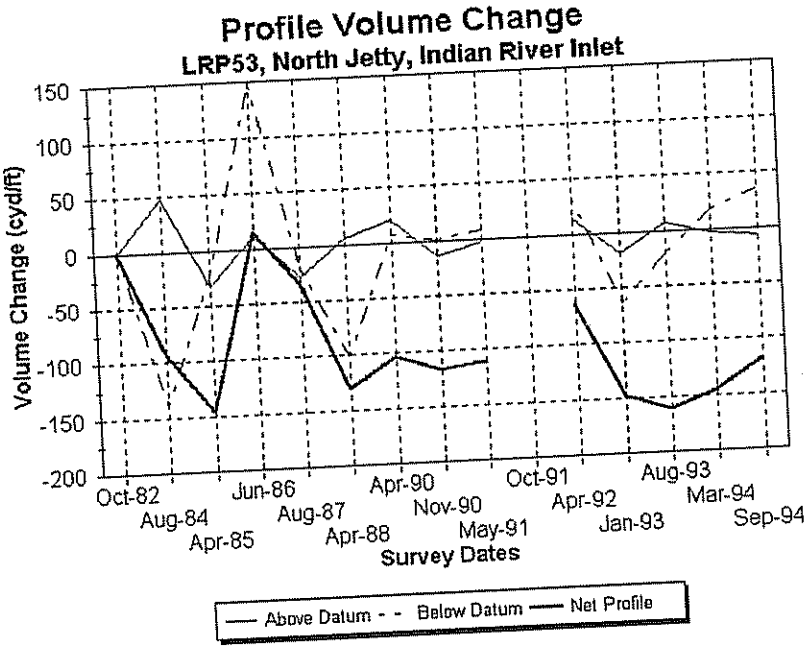
Profile Volume Change
LRP53, North Jetty, Indian River Inlet
Volume Change (cyd/ft)
150
100
50
0
-50
-100
-150
-200
Oct-82
Aug-84
Apr-85
Jun-86
Aug-87
Apr-88
Apr-90
Nov-90
May-91
Oct-91
Apr-92
Jan-93
Aug-93
Mar-94
Sep-94
Survey Dates
Above Datum
Below Datum
Net Profile

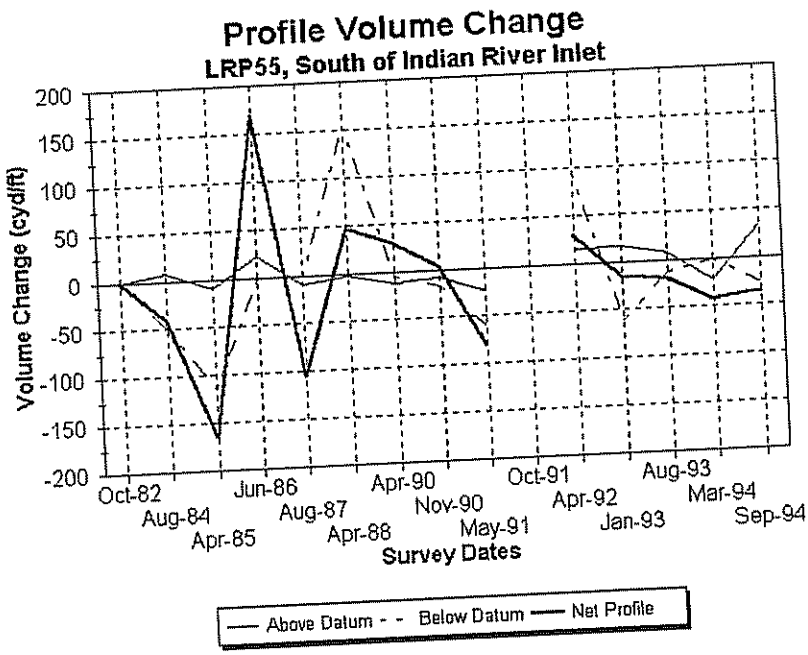
Profile Volume Change
LRP55, South of Indian River Inlet
Volume Change (cyd/ft)
200
150
100
50
0
-50
-100
-150
-200
Oct-82
Aug-84
Apr-85
Jun-86
Aug-87
Apr-88
Apr-90
Nov-90
May-91
Oct-91
Apr-92
Jan-93
Aug-93
Mar-94
Sep-94
Survey Dates
Above Datum
Below Datum
Net Profile

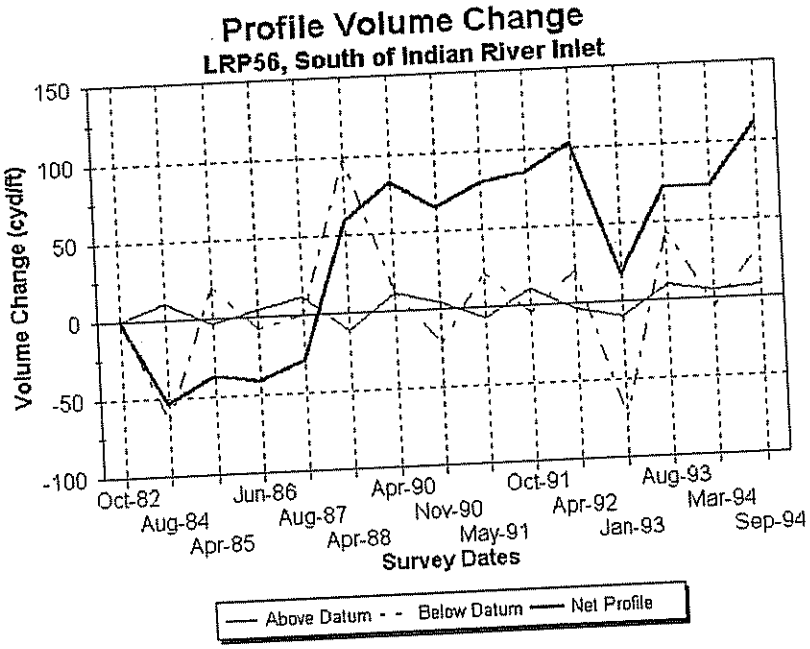
Profile Volume Change
LRP56, South of Indian River Inlet
Volume Change (cyd/ft)
150
100
50
0
-50
-100
Oct-82
Aug-84
Apr-85
Jun-86
Aug-87
Apr-88
Apr-90
Nov-90
May-91
Oct-91
Apr-92
Jan-93
Aug-93
Mar-94
Sep-94
Survey Dates
Above Datum
Below Datum
Net Profile

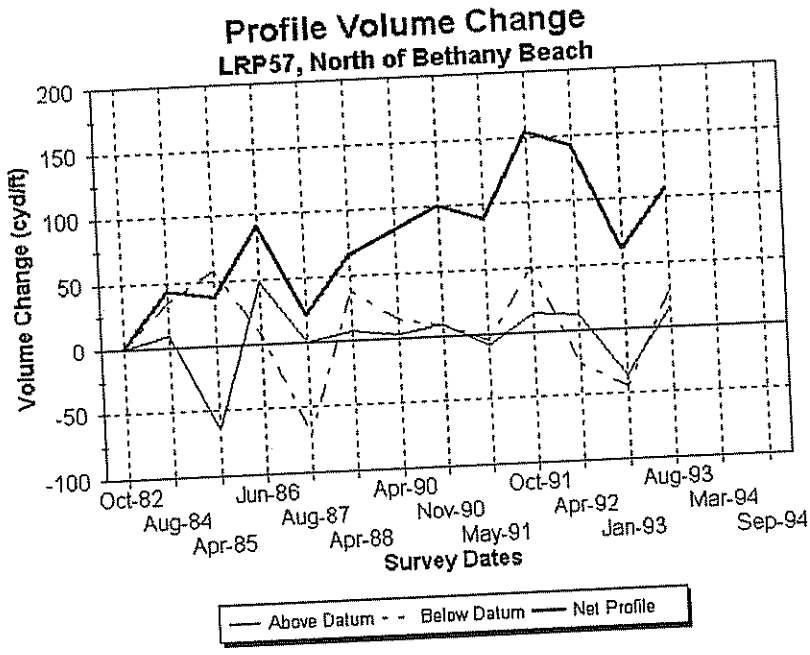
Profile Volume Change
LRP57, North of Bethany Beach
Volume Change (cyd/ft)
200
150
100
50
0
-50
-100
Oct-82
Aug-84
Apr-85
Jun-86
Aug-87
Apr-88
Apr-90
Nov-90
May-91
Oct-91
Apr-92
Jan-93
Aug-93
Mar-94
Sep-94
Survey Dates
Above Datum
Below Datum
Net Profile

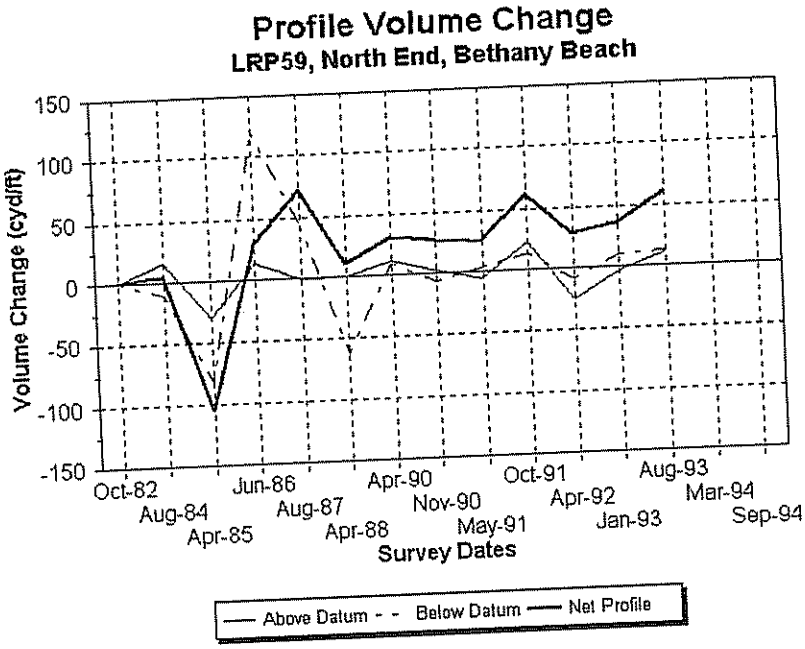
Profile Volume Change
LRP59, North End, Bethany Beach
Volume Change (cydiff)
150
100
50
0
-50
-100
-150
Oct-82
Aug-84
Apr-85
Jun-86
Aug-87
Apr-88
Apr-90
Nov-90
May-91
Oct-91
Apr-92
Jan-93
Aug-93
Mar-94
Sep-94
Survey Dates
Above Datum
Below Datum
Net Profile

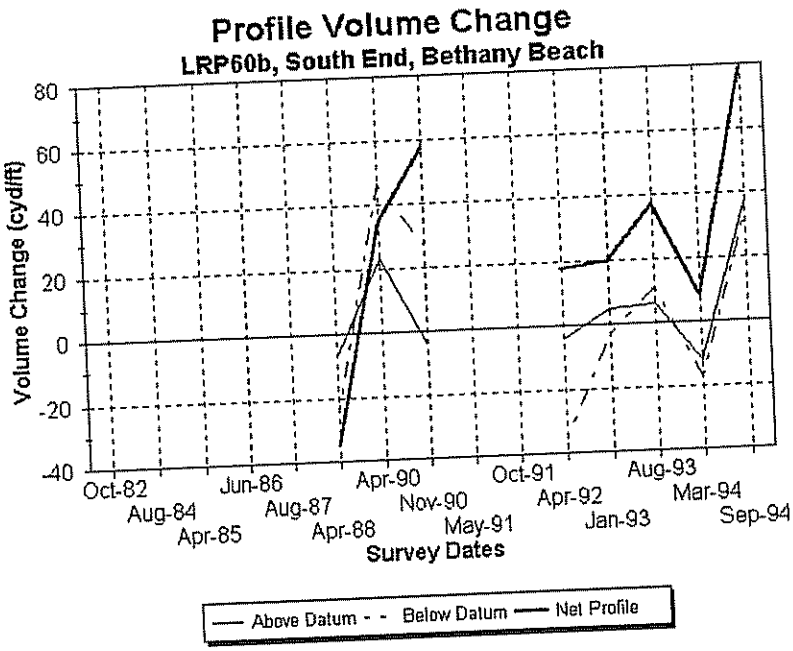
Profile Volume Change
LRP60b, South End, Bethany Beach
Volume Change (cydiff)
80
60
40
20
0
-20
-40
Oct-82
Aug-84
Apr-85
Jun-86
Aug-87
Apr-88
Apr-90
Nov-90
May-91
Oct-91
Apr-92
Jan-93
Aug-93
Mar-94
Sep-94
Survey Dates
Above Datum
Below Datum
Net Profile

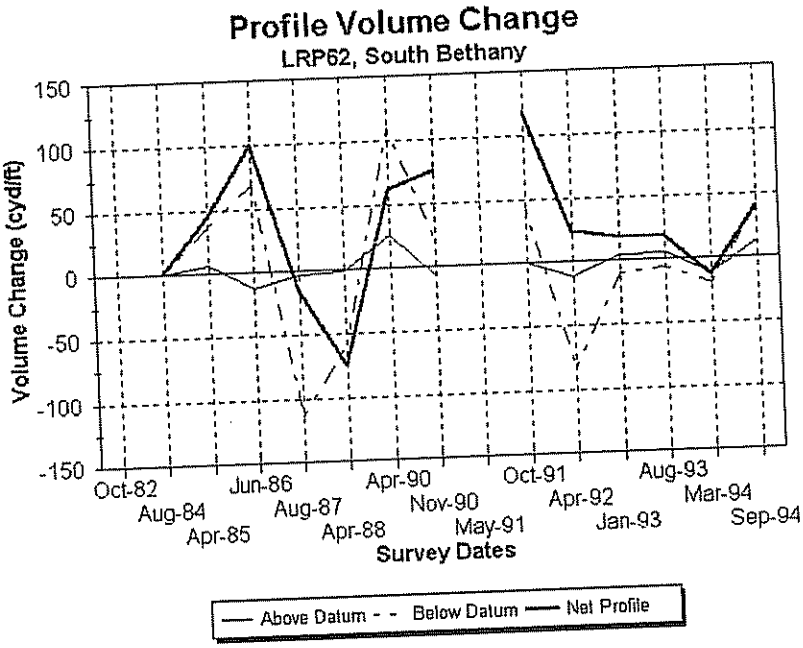
Profile Volume Change
LRP62, South Bethany
Volume Change (cydiff)
150
100
50
0
-50
-100
-150
Oct-82
Aug-84
Apr-85
Jun-86
Aug-87
Apr-88
Apr-90
Nov-90
May-91
Oct-91
Apr-92
Jan-93
Aug-93
Mar-94
Sep-94
Survey Dates
Above Datum
Below Datum
Net Profile

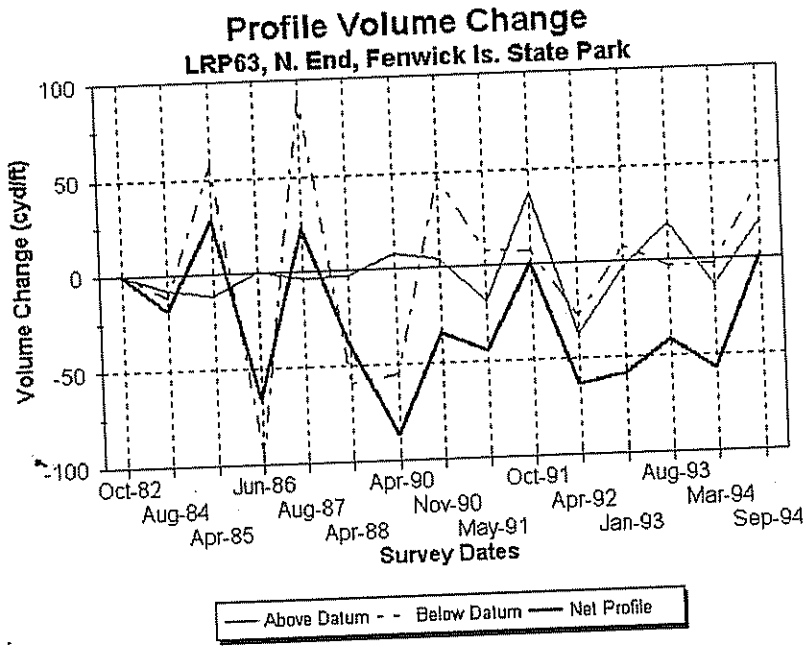
Profile Volume Change
LRP63, N. End, Fenwick Is. State Park
Volume Change (cydiff)
100
50
0
-50
-100
Oct-82
Aug-84
Apr-85
Jun-86
Aug-87
Apr-88
Apr-90
Nov-90
May-91
Oct-91
Apr-92
Jan-93
Aug-93
Mar-94
Sep-94
Survey Dates
Above Datum
Below Datum
Net Profile

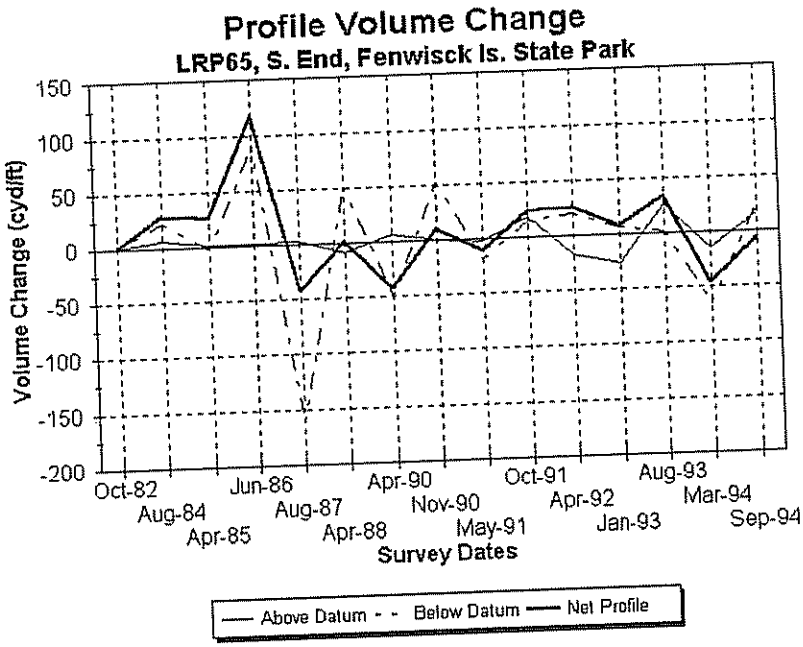
Profile Volume Change
LRP65, S. End, Fenwisck Is. State Park
Volume Change (cydift)
150
100
50
0
-50
-100
-150
-200
Oct-82
Aug-84
Apr-85
Jun-86
Aug-87
Apr-88
Apr-90
Nov-90
May-91
Oct-91
Apr-92
Jan-93
Aug-93
Mar-94
Sep-94
Survey Dates
Above Datum
Below Datum
Net Profile

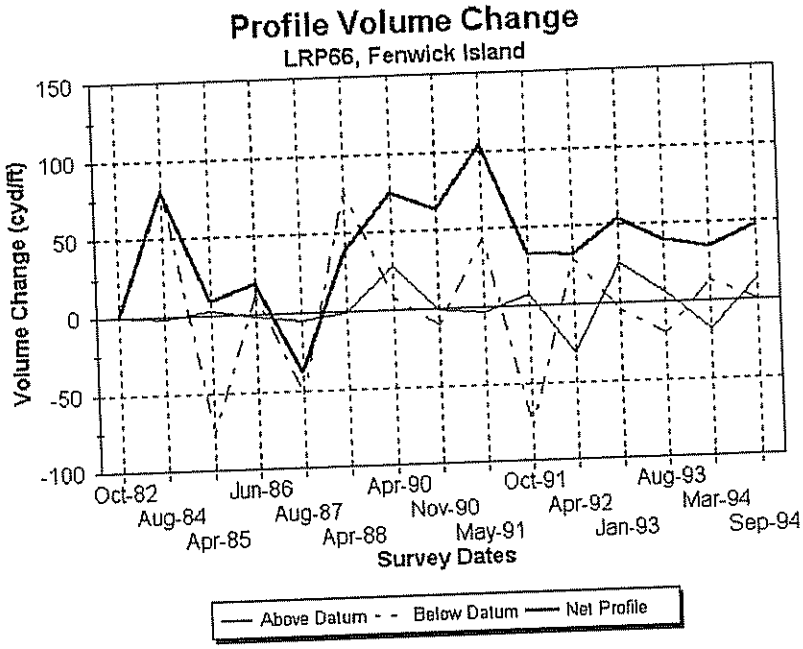
Profile Volume Change
LRP66, Fenwick Island
Volume Change (cydift)
150
100
50
0
-50
-100
Oct-82
Aug-84
Apr-85
Jun-86
Aug-87
Apr-88
Apr-90
Nov-90
May-91
Oct-91
Apr-92
Jan-93
Aug-93
Mar-94
Sep-94
Survey Dates
Above Datum
Below Datum
Net Profile

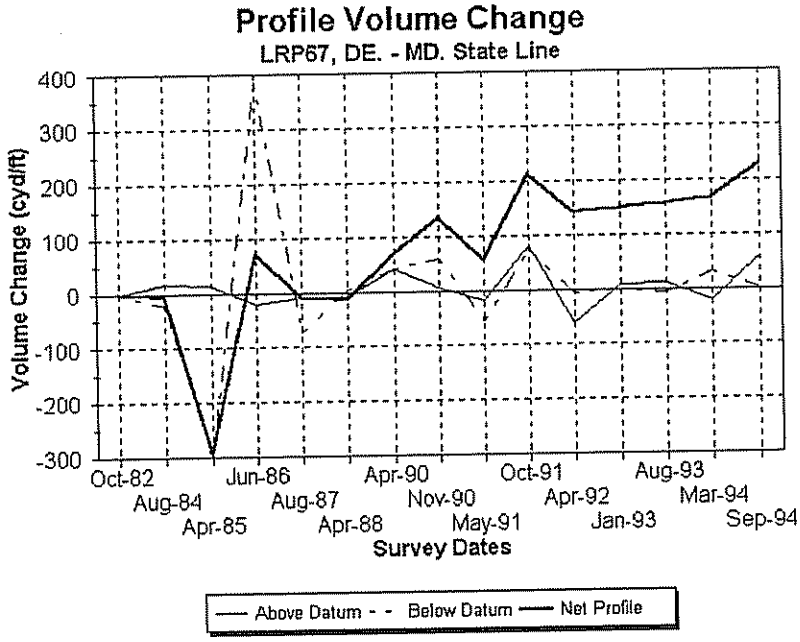
Profile Volume Change
LRP67, DE. - MD. State Line
Volume Change (cyd/ft)
400
300
200
100
0
-100
-200
-300
Oct-82
Aug-84
Apr-85
Jun-86
Aug-87
Apr-88
Apr-90
Nov-90
May-91
Oct-91
Apr-92
Jan-93
Aug-93
Mar-94
Sep-94
Survey Dates
Above Datum
Below Datum
Net Profile